We would like to thank the reviewers for their thorough reading of the paper and their very helpful comments: the paper is improved because of the review process. The reviewer comments are in black, and our responses in red. At the bottom of the response, the manuscript is attached, with track changes in red.

Reviewer #1:

This manuscript is a broad community review of natural aerosol variability and its uncertainty in the Earth system. It synthesizes Earth system model estimates and paleoclimate proxy archives for dust, biomass-burning, volcanic, and marine aerosols across the Last Glacial Maximum and the preindustrial-to-present transition. The paper is timely, comprehensive, and well referenced. It will be a valuable resource for both the paleoclimate and aerosol-modeling communities. I recommend publication after the authors address the points below.

Thank you for your constructive comments.

General Comments:

1. One strong claim is that models get the dust feedback 10–100× too small compared to data-based estimates, and the abstract leads with it. I suggest adding two cautions, ideally in the abstract. First, this compares a feedback, not a forcing. The data-based number comes from dividing the LGM-to-PI dust change by the temperature change. But that dust change had many causes besides temperature (ice sheets, dust sources, winds, vegetation), so calling all of it a temperature feedback may make it look too big. As the authors note (lines 2007–2009), the gap might instead mean models are missing human-made dust sources. Second, the data-based number leans mainly on one group's work (chiefly Kok et al., 2018 and 2023). A gap this large would be more convincing with independent estimates from other groups. Flagging both points up front would keep readers from assuming the models are simply wrong by 100×.

Excellent points. We modify the abstract, the relevant section and the conclusions to reflect these comments.

The second reviewer also highlighted this statement as not being a main part of the review, so we rephrased this point to downgrade the claim in the abstract:

Line 72: Abstract: “Available comparisons suggest that model-data comparisons of feedbacks can highlight gaps and poorly simulated processes in the models.”

Line 2282: “Model estimates of the changes in dust deposition over the historical period are one or two orders of magnitude too small compared to the limited model-data based estimates (Table 6), suggesting that our models may not yet be able to effectively simulate these feedbacks (for example, due to warming-induced changes in vegetation and dust source extent) or else that models are missing anthropogenic dust sources.”

Line 2347: Conclusions: “It is important to recognize that Earth system responses in the Anthropocene may be quite different than during earlier paleo periods, especially because of land use changes and the dependence of the sensitivity of clouds to the aerosol perturbation upon the original, unperturbed aerosol composition and load (e.g., Carslaw et al., 2013). Dust illustrates this problem: the limited inferred sensitivities of dust to climate based on observations differ substantially between current climate changes and LGM to PI changes (Kok et al, 2018; Table 6).”

2. Tables 4 and 5 are the quantitative core of the synthesis, but several entries are incomplete or garbled. In Table 4, the BVOC uncertainty reads “−0.3 ± 0.” and the DMS entry reads “−1.0+.−0.5”. The ± formatting is inconsistent across rows. The sea-spray citation cell is also hard to parse: it reads “Rap et al, 2013. Thornhill et al., 2021; 2013,Venugopal et al., 2025.” The separators switch between period, semicolon, and comma, and a stray “2013” has no author attached. In Table 5, the period labels are inconsistent and contain typos (“6kbp” vs “6bp”; “Last Millenial”). Please proofread both tables. Give every value a complete uncertainty, use one ± and citation format, and use one period label convention (e.g., “6 ka BP”).

   Good points. We reformat Tables 4 and 5 to make these points clear. We also consistently use +/- format. We note in the table caption that if the original paper did not include uncertainties we mark with a daggar.

3. Some assertions lack references. The clearest case is the four criteria for a “reliable” dust record (lines 599–602). These are stated as established, but no citation is given. Please add references, or state that this is the authors’ own framework. I suggest a general check of the background statements in Sections 1–2 for the same issue.

   We review the background statements and sections to be more clear when we are presenting our expert opinions versus established facts.

   In the beginning of the background section highlighted by the author we add some context—we think this is the most important.

   Line 206: “We recognize that some of these statements include expert assessment of the authors of this review, not established fact.”

   Line 623: “Here we discuss limitations and issues specific to dust proxies, in the view of the authors of this review.”

   657: “For the purposes of this review, a dust record is considered reliable when 1) it captures past dust dynamics,…”

4. The depth of coverage is uneven. Dust, fire, and volcanic aerosols are treated in detail. Nitrate, ammonium, marine organics, BVOCs, and anthropogenic aerosols (Sections 6.2–6.3) are covered only briefly. This is reasonable given the data, but please state it as a scope limitation. The review also focuses on the LGM and PI–PD. A short note on what these paleo constraints imply for future projections would strengthen the motivation.

Good point: we emphasize in the abstract and conclusions that the other aerosols and time periods are important but we do not have enough data to estimate their forcings.

Line 66: Abstract: "There is insufficient spatial coverage of paleo-data proxies to conduct observationally based estimates of radiative forcing for several potentially important aerosols (dimethyl sulfide, sea spray, Biogenic volatile organic carbon) and time periods (e.g. Pliocene, LIG, 6kbp, Last Millennium), which highlights remaining important uncertainties in estimating forcings in paleoclimates. We focus here on the Last Glacial Maximum and preindustrial time periods because those time periods have available data. These uncertainties reduce our ability to constrain the climate sensitivity using paleo-data proxies."

Line 2365: Conclusions: "In addition, for time periods besides preindustrial LGM, there are no available data-model syntheses, and thus we must assume large uncertainties in aerosol forcings until such estimates are available (Table 6).."

Finally, consider one summary figure that maps each aerosol type to its archives, the periods it can constrain, and its current forcing estimate.

Great idea. We modify Figure 7 so that it includes more information about our definition of good paleocoverage. We could not figure out away to add in different time periods.

Minor Comments:

Lines 193–194: The text first describes aerosols forming in the atmosphere (SO2 to sulfate). Please introduce the term "secondary aerosols" here, as the distinction is used later.

Line 213: Good point: "Some aerosols are formed in the atmosphere (e.g. conversion of the gas SO_2 into sulfate aerosols)—called secondary aerosols in contrast to primary aerosols which are emitted. The conversion process to secondary aerosols is included with different complexities in the different models."

Line 270: "millenial-scale" should be "millennial-scale".

Thank you. Corrected.

Line 1684: "Rap et al,. 2013" should be "Rap et al., 2013".

Thank you. Corrected.

Line 1739: "Moschos et al.,. 2022" should be "Moschos et al., 2022".

Thank you. Corrected.

Line 1741: "Tsigaridis and and Kanakidou, 2018" has a duplicated "and".

Thank you. Corrected.

Line 1811: "…for calculating radiative forcing,. The ladder…" has a stray ",.". Use a single period.

Thank you. Corrected.

Line 2060: "…is available.. Careful…" has a double period. Use one.

Thank you. Corrected.

Table 6 caption: It refers to "(Table 6: −2 to 0.1 W/m2)" inside Table 6. This value comes from Table 5, so the cross-reference should read "Table 5."

Thank you. Corrected.

Section references: Line 1769 says "Sections 3–6," but the Table 4 caption and line 1633 say "Sections 2–6." The aerosol sections are 3–6. Please make these consistent.

Thank you. Corrected.

Reviewer #2:

The manuscript is a review of the available data on natural aerosol variability, aerosol effective radiative forcing, and the uncertainties of both in the pre-industrial and paleo-time periods. It gives a thorough overview of the available proxies for mineral dust, biomass burning, volcanic emissions, and marine and other aerosols. It also provides a suggested 'roadmap' for dataset synergy going forward. It represents a substantial contribution to the field of atmospheric science and paleoclimate. My recommendation is for publication following minor revisions.

Thank you for your constructive criticism.

General comments

- More specific advice about combining uncertainties in section 7.3 would be very welcome. This is an essential section and currently feels short. Also, the abstract mentions 'regularised inversion approaches', but there isn't a lot of advice on how to regularise them.

We agree, but unfortunately there is not the literature to address this point, which is one of the areas of research that need more work. To highlight this we add:

Line 2096: In section 7.2 add at the end: "More studies using data assimilation after proxy calibration would provide guidance on the best practices for regularizing inversion approaches."

Line 2171: In section 7.3 we add at the end: “More studies need to address the best approach for addressing different uncertainties and adding them together.”

- The claim that modelled dust feedbacks are up to 100x lower than are consistent with the record is not the ‘headline’ result that the placement in the abstract suggests it is. The derivation from a range for instantaneous forcing divided by a range for the temperature change is not strong enough to hold up the claim that this ‘casts doubt on our ability to successfully model feedbacks in the current generation of Earth system models’. It’s also slightly off-angle from the main contribution of the paper as a review and roadmap. Also, the ranges for PI–PD dust changes quoted in the introduction are not the same as those section 3.1.1.

As the first reviewer also felt this statement was not a large part of the review, so we downgraded the abstract comment to:

“Available comparisons suggest that model-data comparisons of feedbacks can highlight gaps and poorly simulated processes in the models.”

We have also adjusted the relevant section in 3.1.1 such that it is now consistent with the increase in dust mentioned in the introduction.

Line 511: “Consistent with these drivers, numerous deposition records indicate long-term increases in dust flux over the historical period (McConnell et al., 2007b; Mulitza et al., 2010; Mahowald et al., 2010; Hooper and Marx, 2018). A recent proxy-constrained reconstruction estimated that global atmospheric dust loading increased by 55 ± 30% between the pre-industrial period (1841–1860) and 1981–2000 (Kok et al., 2023). However, this increase was not monotonic: dust loading peaked around the 1980s at approximately 75 ± 40% above pre-industrial levels. Dust subsequently declined, with a recent reconstruction of dust loading using satellite data and inverse modeling indicating a global decrease of 5 ± 4% per decade during 2003–2023 (Gupta et al., 2026).”

- It would be very helpful to see even a minimal worked example for the ladder for a specific aerosol type using real datasets. This reader also still came away uncertain as to how the obstacle of geographically limited proxies can be overcome to form global datasets.

  Good idea. We added the example of LGM dust throughout this framework as well as some more examples and text. So Section 7.2 is largely rewritten.

Line 1998: “To illustrate, we use the example of the Last Glacial Maximum dust cycle, which evolved over many years before the first synthesis of paleo-data generated aerosol radiative effects.”

Line 2041: “For the LGM dust cycle, different papers synthesized different proxies, for example Rea (1994) compiled marine sediment records, while Kohfeld and Harrison (2003) synthesized terrestrial sediment records.

It is also recommended to report not only the total uncertainty associated with individual records, but also uncertainties arising from different sources, including measurement and calibration processes, assumptions made to address missing information, and spatial representativeness (e.g., Cosentino et al., 2024). For example, two records using the same measurement techniques may share systematic uncertainties and therefore should not automatically be treated as having independent errors (e.g., Dolman et al., 2021). Identifying these sources would help avoid overconfidence in conclusions drawn from multiple records, whether in proxy synthesis or in data–model integration (e.g., Wahl et al., 2022; Okazaki et al., 2025).”

Line 2057: “Efforts to harmonize different measurements across different sizes and types can continue for years: for example for the LGM dust example, there are still papers trying to understand how best to treat different sources and sizes (Maher et al. 2010; Cosentino et al., 2024).

Harmonization should also assess the consistency of records that provide comparable environmental information across different datasets. For example, newly incorporated observations should be compared with nearby records, where available (Albani et al., 2015). Substantial discrepancies, whether in magnitude or in the inferred direction of change (e.g., increasing versus decreasing), should be documented and investigated to identify possible causes. Unresolved discrepancies should be clearly reported, and any exclusion of conflicting records should be justified, so that subsequent proxy synthesis and data-model integration efforts can evaluate the reliability of conflicting observations and determine how to account for them.”

Line 2070: “Because individual proxy records differ in spatial representativeness, temporal resolution, and sensitivity to environmental processes, synthesis should consider whether changes observed at individual sites reflect broader environmental patterns or local and regional variability. As an example, DIRTMAP created a new publicly available compilation of paleodust including more tracers of dust, including terrestrial, marine, and ice cores (Kohfeld and Harrison, 2001). Previous studies had looked only at the ice cores, which showed much larger changes than closer to the main source areas (e.g. Andersen and Genthon, 1996). These differences illustrate why records from a single region may not be representative of global changes, highlighting the importance of integrating observations across different regions to capture spatial heterogeneity. Such spatial patterns provide valuable observational constraints for model-based reconstructions of aerosol emissions.”

Line 2084: “The fourth step involves translating proxy measurements into physically meaningful aerosol metrics such as emission fluxes or atmospheric concentrations through physical model and data-model integration (e.g. see examples in Sections 3, 4 and 6). This is challenging because aerosol deposition reflects not only emissions but also atmospheric transport and removal processes. Care should therefore be taken not to attribute all model-observation

discrepancies to emission errors, as adjustments to emissions may compensate for biases in modeled transport or deposition. Comparing model performance across multiple observations can help identify discrepancies that cannot be explained by emission changes alone. Furthermore, using multiple models can help assess model uncertainty, although systematic biases shared across models may remain undetected (e.g., Kok et al., 2021).

For the LGM example, early modeling studies estimated dust emissions and evaluated simulated deposition against paleo-observations (e.g. Mahowald et al., 1999), while subsequent studies used inverse modeling to quantitatively constrain regional dust emissions from compiled deposition records (e.g., Albani et al., 2014). More studies using data assimilation after proxy calibration would provide guidance on the best practices for regularizing inversion approaches and assessing the robustness of reconstructed emissions."

Line 2081: "Fully integrated global reconstructions remain rare, but recent studies have begun linking proxy-constrained emission reconstructions to estimates of aerosol radiative forcing.

Early studies estimated LGM dust radiative forcing using modeled dust distributions (e.g., Claquin et al., 2003). Subsequent work incorporated multiple observational constraints, including dust deposition, particle size distributions, and provenance information, to improve dust simulations and their estimates of radiative forcing (e.g., Albani et al., 2014). More recently, proxy-constrained historical dust emission reconstructions have been used in eight Earth system models to quantify dust direct radiative forcing since the pre-industrial era (Leung et al., 2025; Haugvaldstad et al., 2026). However, systematically propagating uncertainties from proxy observations through emission reconstructions and atmospheric processes to radiative forcing remains a major challenge that requires further investigation."

Tables 4 and 5 mix instantaneous radiative effect, RF and ERF in the same columns. They both also seem incomplete. These two tables are central to the paper and need to be standardised for consistency and reviewed to ensure completeness.

We clarify the table headers for more consistency. Unfortunately, there is not sufficient literature to complete the table. We highlight this more in the paper to identify the important gaps.

Line 1886: Section 7.1: "Notice that for many aerosols there is not sufficient information in the Tables to be complete (Table 4 and 5). More studies of natural aerosols in the current climate (Table 4) and combined with paleo-data proxies are needed (Table 5). In addition, for several time periods that are being used for climate sensitivity studies (e.g. Sherwood et al., 2021) there are no aerosol syntheses, meaning they are subject to large uncertainties in their aerosol forcings (e.g. 6kbp, Last Millennial, Pliocene).

We also modify the abstract and conclusions as noted above to highlight these gaps.

Line 70: “We focus here on the Last Glacial Maximum and preindustrial time periods because those time periods have available data.”

Line 2367: “In addition, for time periods besides preindustrial LGM, there are no available data-model syntheses, and thus we must assume large uncertainties in aerosol forcings until such estimates are available (Table 6).”

Lines 191–192: ‘Aerosols are included in most ESMs so that their interactions with [...] varying sources and sinks [...] can be included’ – awkward phrasing to say that aerosols interact with their sources and sinks: rephrase.

We appreciate this and following editorial suggestions, as we agree they make the paper more readable.

Line 210: Rephrase: “Aerosols are included in most ESMs and thus their interactions with dynamics, varying sources and sinks, and radiation can be simulated (Szopa et al., 2021).”

Lines 317–321: This seems like two separate sentences, one ending at ‘escarpments’ and one beginning at ‘Post-depositional’.

Line 343: We rewrite as separate sentences: “In addition, loess-derived dust fluxes can deviate from actual atmospheric dust deposition rates due to several factors. Wind-blown material can become focused onto the surfaces of windward escarpments (e.g., Comola et al., 2019). Post-depositional slope processes in high-relief environments can rework the loess deposits (e.g., Volvakh et al., 2022). And the potential lack of surface roughness elements, such as vegetation, can reduce the surface retention of atmospherically deposited dust particles (e.g., Yan et al., 2011).”

Line 354: ‘Post-industrial’ sounds like a future scenario – rephrase as ‘present-day’.

Line 382We rephrase: “Recently a network of fire-scar sites was compiled for North American forests (Margolis et al., 2022) that allowed for broader inferences about fire–climate relationships (Margolis et al., 2025) and comparisons of relative area burned between pre-industrial and present day time periods (Parks et al., 2025).”

Lines 452–453: ‘yet many of these properties remain simplified or poorly constrained in paleoclimate simulations’ – this could be expanded on, especially given the constructive focus of this paper on the use of proxies to improve modelling.

Line 490: We rephrase: “These effects depend strongly on particle size, shape, mineralogy, mixing state, and surface coatings (Kok et al., 2017; Song et al., 2022; Huang et al., 2023; Gonçalves-Ageitos et al., 2023; Obiso et al., 2026), yet many of these properties remain simplified or poorly constrained in paleoclimate datasets. More collection of these attributes could help constrain model simulations. “

Lines 523–524: ‘Together with changes in surface albedo’ – the mention of surface albedo came unexpectedly. What proxies are there for albedo? This sentence seems to have been constructed with knowledge not available to the reader, at least this reader.

Line 577: We rephrase: “Radiative effects are very sensitive to surface albedo as well, which is not well known in past climates (Claquin et al., 2003; Potenza et al. 2016). Together optical properties and surface albedo changes imply that the dust radiative effect efficiency - the radiative effect of dust per unit mass or optical depth - differed from that in the present climate (Claquin et al., 2003; Potenza et al., 2016).”

Lines 705–706: ‘The predominantly organic matrix also contains only trace amounts of mineral material, sometimes below the detection limits for mineralogical characterization’ – again, confusing to someone in the aerosol modelling field not expert in proxies. Trace amounts of pre-existing mineral material sounds like the peat would be a good matrix for trapping mineral dust, not a disadvantageous one as the framing seems to suggest.

Line 765: We clarify: “The predominantly organic matrix also contains only trace amounts of mineral material, and these low concentrations can sometimes be below the detection limits for mineralogical characterization (Shotyk et al., 2023).”

Line 890: 1997 is not the usual threshold for the beginning of the satellite era – either say 1970s or specify why this specific year is chosen.

Line 953: We clarify: Simulation of spatially and temporally continuous global fire regimes pre satellite-era (pre-1997, when the satellites acquired sufficient temporal and spatial coverage of appropriate variables) requires the use of fire models.

Lines 901–917: reformat with a new line for each numbered heading, as this is a very long sentence on its own.

We modify as suggested.

Lines 1004–1005: ‘mixed contributions from both biomass burning and fossil fuel sources [...] particularly during the industrial era’ – do fossil fuel sources contribute prior to the industrial era? I would assume that this was limited to the industrial era. If not, briefly explain.

Fossil fuels have been burned since 2000BC in small quantities, so we think the sentence is accurate as stated.

Line 1233: ‘The impact of fire on dust likely changes the further back in time is explored’ – awkward, rephrase.

Line 1307: We rephrase: “The impact of fire on dust may change during different time periods, as fire regimes shifted in the colder, drier world of the Last Glacial Maximum (Figure 3).”

Line 1665: ‘emitted directly by humans’ → ‘emitted directly by human activity’; similarly line 1747 ‘while humans can directly emit’ → ‘while human activity can directly emit’

Thank you. We make these changes.

Lines 1779–1781: ‘One important issue is that paleoaerosol modelers calculate the effective radiative forcing, not just the instantaneous radiative forcing’ – please explain with an additional sentence or two why this is important.

Line 1867: We rephrase: “ One important issue is that paleoaerosol modelers should calculate the effective radiative forcing, not just the instantaneous radiative forcing, since effective radiative forcing is needed for climate sensitivity calculations. “

Technical comments:

There are a number of instances of unnecessarily italicised text (e.g. lines 202–206). There are also a few instances of extra spaces. There are also some instances of unnecessary bolding (e.g. line 1302) and one instance of unnecessary capitalisation (line 1353).

Thank you: we fix these.

A few inconsistencies naturally arise from having multiple authors. ‘Aeolian’ vs ‘eolian’ is one, also ‘paleo aerosol’, ‘paleo-aerosol’, ‘paleoaerosol’.

Yes, good point: we fix these.

Line 271: ‘complicated for the highly spatially’ → ‘complicated by the highly spatially’

Thank you: we fix this.

Line 367: Delete ‘Therefore’ at the beginning of the sentence – it doesn’t follow as a logical conclusion from the previous sentence.

Thank you: we fix this.

Lines 365–366: ‘Some corals provide highly indirect dust records because they reflect water column geochemistry rather while others record direct atmospheric deposition Eakin’ – delete one of ‘rather’ or ‘while’ and add parenthesis → ‘atmospheric deposition (Eakin’

Line 396: Sentence changed to: “Some corals provide highly indirect dust records because they reflect water column geochemistry, while others record direct atmospheric deposition (Eakin and Grottoli, 2006; Mukhopadhyay and Kreycik, 2008).”

Line 1176: ‘ice core black carbon, tree ring fire scars’ → ‘ice core black carbon, and tree ring fire scars’

Thank you: we fix this.

Line 1459: ‘temporally’ → ‘temporary’

Thank you: we fix this.

Line 2135: ‘ARE; ’ → ‘ARE: ’

Thank you: we fix this.

Figures and tables:

Table 1: ‘Fire scars’ should be capitalised for consistency.

Thank you: we fix this.

Table 2: While DMAR is defined in the glossary, it would be helpful to define it in-text also.

Thank you: we fix this.

Table 4: It should be noted what blank cells in this table mean, if they cannot be filled in (?). For example, the ‘Open Fires’ total ERF is not equal to just the ERFari, though the ERFaci is blank.

Thank you: we fix this and modify the header to be more clear:

Line 1893: “**Table 4:** Natural aerosol present day (PD) effective radiative effect (ERE) from Sections 3-6.

ERE ari= Effective Radiative Forcing, aerosol radiation interaction; ERE aci= aerosol cloud interaction. DMS=dimethyl sulfide, BVOC=biogenic volatile organic compounds. The ERE ari and ERE aci may be derived from separate studies as the ERE (and thus not add up) or may not be available for all species. If the paper does not include an uncertainty for the ERE value, we indicate with †.

“

Characterizing Natural Aerosol Variability and its Uncertainty in the Earth System

Natalie Mahowald[1], Hannah Liddy[2,3], Jennifer Marlon[4], Kostas Tsigaridis[2,3], Gisela Winckler[5], Douglas S. Hamilton[6], Jasper F. Kok[7], Michael Sigl[8], Jordan T. Abell[9], Adwoa Aboagye-Okyere[1], Joe Adabouk Amooli[10], Samuel Albani[11], Susanne Bauer[3], Emilie Beaudon[12], Hunter Brown[13], Nathan Chellman[14], Nicolás J. Cosentino[15,16,17], Nathalie F. Goodkin[18], Christopher H. Guiterman[19, 20], Stijn Hantson[21], Chengfei He[22], Aviva Intveld[23], Jed O. Kaplan[24], Jeremy M. Klavans[25], Fabrice Lambert[26], Haobo Liu[27,28], Marie-France Loutre[29], Joe McConnell[14], Zachary McGraw[30], Keren Mezuman[2,3], Ron Miller[3], Nicholas O'Mara[4], Maria Rosabelle Ong[18], Gavin A. Schmidt[3], Richard Vachula[31], Lily Wu[1], Bingqing Zhang[32]

Affiliations

[1] Department of Earth and Atmospheric Sciences, Cornell University, Ithaca, NY, USA

[2] Center for Climate Systems Research, Columbia University, New York, USA

[3] NASA Goddard Institute of Space Studies, New York, NY, USA

[4] School of the Environment, Yale University, New Haven, CT, USA

[5] Columbia Climate School and Lamont-Doherty Earth Observatory, Columbia University, New York, USA

[6] Marine, Earth, and Atmospheric Science, North Carolina State University, Raleigh, NC, USA

[7] Department of Atmospheric and Oceanic Sciences, University of California – Los Angeles, USA

[8] University of Bern, Bern, Switzerland

[9] Department of Earth and Environmental Sciences, Lehigh University, Bethlehem, PA, USA

[10] Lamont-Doherty Earth Observatory, Columbia University, New York, USA

[11] Department of Environmental and Earth Sciences, University of Milano-Bicocca, Milan, Italy

[12] School of Earth Sciences, The Ohio State University, Columbus, OH, USA

[13] University of Wyoming, Laramie, WY, USA

[14] Division of Hydrologic Sciences, Desert Research Institute, Reno, NV, USA

[15] Facultad de Ciencias Exactas y Naturales, Universidad de Buenos Aires, Buenos Aires, Argentina

[16] Centro de Investigaciones del Mar y la Atmósfera (CIMA, CONICET-UBA), Buenos Aires, Argentina

[17] Instituto Franco-Argentino de Estudios sobre el Clima y sus Impactos (IFAECI, IRL 3351, CNRS-CONICET-IRD-UBA), Buenos Aires, Argentina

[18] Department of Earth and Planetary Sciences, American Museum of Natural History, New York, NY, USA

[19] Cooperative Institute for Research in Environmental Sciences, University of Colorado, Boulder, Boulder, CO, USA

[20] NOAA's National Centers for Environmental Information, Boulder, CO, USA

[21] Universidad del Rosario, Bogotá, Colombia

[22] Department of Marine and Environmental Sciences, Marine Science Center, Northeastern University, Boston, MA, USA

Deleted: McGraw[10]

Deleted: Vachula[30]

Deleted: Zhang[31]

Formatted: Default Paragraph Font, Font color: Black

Formatted: Normal, Centered, Border: Top: (No border), Bottom: (No border), Left: (No border), Right: (No border), Between : (No border), Tab stops: 3.25", Centered + 6.5", Right, Position: Horizontal: Left, Relative to: Column, Vertical: In line, Relative to: Margin, Wrap Around

Formatted: Font color: Black

[23] Department of Earth and Environmental Sciences and Lamont-Doherty Earth Observatory, Columbia University, New York, USA

[24] Department of Earth, Energy, and Environment, University of Calgary, Calgary, Canada

[25] Rosenstiel School of Marine, Atmospheric, and Earth Sciences, University of Miami, Miami, FL, USA

[26] Geography Institute, Pontificia Universidad Católica de Chile, Santiago, Chile

[27] School of Earth and Atmospheric Sciences, Georgia Institute of Technology, Atlanta, GA, USA

[28] Department of Atmospheric and Oceanic Sciences, Peking University, Beijing, China

[29] Past Global Changes (PAGES), Hochschulstrasse 4, 3012 Bern, Switzerland

[30] Department of Meteorology and Geophysics, University of Vienna, Vienna, Austria

[31] Department of Geosciences, Auburn University, Auburn, AL, USA

[32] Department of the Geophysical Sciences, University of Chicago, Chicago, IL, USA

Correspondence: Natalie M. Mahowald mahowald@cornell.edu

Abstract

Aerosol radiative forcing represents the largest source of uncertainty for calculating present-day climate sensitivity. This uncertainty has been underestimated in climate models, as they have not adequately accounted for uncertainties in the emissions of aerosols prior to the satellite era. This is especially the case for natural aerosols, such as mineral dust and aerosols from biomass burning. In this paper, we take a step towards reducing this uncertainty by providing a roadmap for improved integration of proxy-based observational constraints on past aerosol variability with model simulations. We first review existing literature on the importance of natural aerosol radiative forcing during historical and paleo-time periods, with a focus on the Last Glacial Maximum and the preindustrial era (ca. 1850) to the present. We then compile existing paleo-data archives and describe their ability to constrain emissions of aerosols, highlighting existing gaps. Model-data combinations are available to estimate radiative effects for dust and volcanoes in several time periods, and for biomass burning for preindustrial to present day, but are not available for other aerosols. There is insufficient spatial coverage of paleo-data proxies to conduct observationally based estimates of radiative forcing for several potentially important aerosols (dimethyl sulfide, sea spray, Biogenic volatile organic carbon) and time periods (e.g. Pliocene, LIG, 6kbp, Last Millennium), which highlights remaining important uncertainties in estimating forcings in paleoclimates. We focus here on the Last Glacial Maximum and preindustrial time periods because those time periods have available data. These uncertainties reduce our ability to constrain the climate sensitivity using paleo-data proxies. Available comparisons suggest that model-data comparisons of feedbacks can highlight gaps and poorly simulated processes in the models. Finally, we propose a framework for integrating paleo-archives with models through harmonized datasets, proxy–model translation metrics, and regularized inversion approaches, and identify priority measurements needed to reduce uncertainty in both aerosol loading and radiative-effect efficiency across climate states.

1 Introduction

Modern climate change is predominantly caused by accumulation of CO_2 and other greenhouse gases in the atmosphere, but changes in aerosols are the main source of uncertainty in estimates of effective radiative forcing (Szopa et al., 2021). Aerosols influence climate through multiple pathways: they can reflect and absorb both incoming solar radiation and outgoing planetary radiation, as well as modulate clouds and atmospheric chemistry while in the atmosphere (Li, Carlson et al., 2022; Szopa et al., 2021). In addition, once deposited, aerosols can impact the biogeochemistry of land or ocean

Deleted: Geosciences, Auburn

Deleted: , Auburn, AL, USA

Deleted: [31]

Deleted: Modeled feedbacks of aerosols to climate ($W/m^2/^oC$) are 10-100× lower than model-data derived estimates for dust, casting doubt on our ability to successfully model feedbacks in the current generation of Earth system models.

Formatted: Default Paragraph Font, Font color: Black

Formatted: Normal, Centered, Border: Top: (No border), Bottom: (No border), Left: (No border), Right: (No border), Between : (No border), Tab stops: 3.25", Centered + 6.5", Right, Position: Horizontal: Left, Relative to: Column, Vertical: In line, Relative to: Margin, Wrap Around

Formatted: Font color: Black

ecosystems as well as the albedo of the surface beneath them (Mahowald et al., 2017; Szopa et al., 2021). Of these impacts, aerosol-cloud interactions are both the most important and most uncertain for modern climate (Szopa et al., 2021). Aerosol impacts in the present day are very uncertain because of the range of temporal, spatial, composition and size variability (Matsui et al., 2018; Li, Carlson et al., 2022; Szopa et al., 2021). The sensitivity of aerosol interactions with radiation and clouds depends on not only composition and size, but whether the aerosols are below, within or above the clouds (Li, Carlson et al., 2022; Quaas et al., 2020).

Most studies of anthropogenic aerosol radiative forcing define their estimates relative to a preindustrial baseline (PI; ca. 1850) and derive their uncertainties from the spread across models using similar PI aerosol emissions (Bellouin et al., 2020; Smith et al., 2021). However, the magnitude of PI-to-present-day (PD) anthropogenic aerosol radiative forcing depends critically on how the PI baseline atmospheric composition is specified (Carslaw et al., 2017). The pre-industrial is not however a very well defined concept (Hawkins et al., 2017) though, in practice, the community has settled on conditions around 1850 CE for most purposes. The IPCC uses a slightly earlier baseline (1750 CE) for some forcing calculations, while pre-industrial surface temperatures are often taken as the average of 1850-1900 due to the paucity of global data in earlier periods. Aerosol radiative forcing is defined as the difference in the radiative effects of changing aerosol loading between two time periods. Because there are no direct observations of the PI atmosphere, this baseline must be reconstructed from proxy records and modeling, introducing substantial uncertainty (Hamilton et al., 2014; Carslaw et al., 2018). Reducing this uncertainty is therefore essential: if PI aerosol loading is underestimated, the anthropogenic aerosols forcing inferred from PI-PD differences in aerosol radiative effects will be correspondingly overestimated (Hamilton et al. 2018; Wan et al. 2020; Mahowald et al. 2024).

Most studies of aerosol climate impacts have focused on directly emitted anthropogenic aerosols or immediate precursors, such as those emitted by industry, transport or residential sources (Szopa et al., 2021). However, many climatically important aerosols – including mineral dust, those arising from biomass burning, volcanic, and sea spray – are normally classified as "natural" because they arise primarily from natural processes (e.g., wind and fire) that can occur without direct human involvement (Carslaw et al., 2010). However, this classification should not be interpreted to mean that their emissions are independent of human influence in the Anthropocene. Dust emissions, for example, can be altered by land use, irrigation, construction, grazing, and water management (Ginoux et al., 2012; Webb and Pierre, 2018), while biomass-burning aerosol reflects both natural fire regimes and human ignition, suppression, industry, and land management (Bowman et al., 2011). Consequently, paleoclimate, historical, and modern records show that all aerosols are sensitive to both climate variability and human activities, including land use change (e.g. Charlson et al. 1987; Prospero and Lamb, 2003; van der Werf et al., 2008).

Thus, a major source of uncertainty in the PI baseline arises from limited constraints on natural aerosols (Carslaw et al., 2013). However, reconstructing natural aerosol loading prior to the modern observational era is challenging. Prior to ~1980 - and especially for the PI and earlier time periods - direct in situ measurements of atmospheric aerosols are limited or entirely unavailable, leaving deposition-based proxy records as the primary observational constraint (Albani et al., 2018). These proxy records suggest that natural aerosol sources may have varied substantially between the PI and PD, variability which is not fully captured in current models. For instance, studies based on the limited available proxy data have shown a substantial increase of 55 ± 30% in 'natural' dust aerosols from PI to PD, a change that Earth system models struggle to reproduce (Kok et al., 2023). Similarly, biomass burning PI-PD changes in the aerosol emission datasets implemented in the Coupled Model Intercomparison Project (CMIP) phase 6 Earth System Models (ESMs) are inconsistent with available ice core data constraints (Hamilton et al., 2018; Liu et al., 2021). These discrepancies are likely to cause an additional uncertainty in the estimates of radiative forcing between PI and PD on top of the multi-model range of aerosol forcing, which is currently considered as the largest uncertainty (Bellouin et al., 2020; Mahowald et al., 2024).

Further back in time, observational constraints on atmospheric aerosols and thus aerosol radiative forcing are even more limited. Deposition records exist for only a limited set of aerosol types, though

Formatted: Default Paragraph Font, Font color: Black

Formatted: Normal, Centered, Border: Top: (No border), Bottom: (No border), Left: (No border), Right: (No border), Between : (No border), Tab stops: 3.25", Centered + 6.5", Right, Position: Horizontal: Left, Relative to: Column, Vertical: In line, Relative to: Margin, Wrap Around

Formatted: Font color: Black

important compilations are available for specific types. For example, desert dust compilations drawing on ice cores, marine sediments, terrestrial deposits, and lake sediments (Maher et al., 2010; Albani et al., 2015; Lambert et al., 2015; Cosentino et al., 2024) have been used to constrain model estimates of dust emission rates and dust radiative forcing across the Last Glacial Maximum (LGM ~19.0-26.5 ka BP; Clark et al., 2009) and the Holocene, albeit with substantial uncertainties in dust sources, transports, sinks, and process representation (Mahowald et al., 2006; Albani et al., 2014, 2016). Global charcoal compilations likewise have a long history, with databases such as the Global Paleofire Database providing records of biomass burning variability across multiple time periods (Power et al., 2008; Marlon et al., 2016). Despite this foundation, quantitative assessments of how biomass burning aerosol forcing changed across various paleoclimate intervals remain at an early stage, which is notable given that aerosols from fires likely exert a larger global mean radiative effect than dust (Mahowald et al., 2024).

Observational and modelling capabilities are simultaneously advancing, enabling improved constraints on aerosol radiative forcing and therefore climate sensitivity. New proxies and analytical methods are expanding the range of aerosol types that paleoclimate archives can constrain, including biomass burning and other natural aerosols (Vachula et al., 2022a; Zuo et al., 2025; Ström et al., 2026). Parallel advances in proxy interpretation are refining the quantitative relationships between deposition records and the model-relevant metrics needed for aerosol radiative forcing estimates (Gilgen et al., 2018; Hennebelle et al., 2020; Miller et al., 2026). On the modeling side, fire models have advanced considerably since CMIP5, with CMIP6 ESMs showing improved simulations of global burned area, spatial patterns, and seasonal variability (Li et al., 2024). The integration of FireMIP into CMIP7 (Li et al., 2026) will now provide a coordinated framework for evaluating fire in fully coupled ESMs across historical and paleoclimate timescales, directly relevant to the proxy-model integration challenges discussed in this review.

The expansion of computational ability has led to many modeling studies seeking to isolate the climate impact of aerosols (e.g. Kay et al., 2015). Most of these studies used emission datasets which have more recently been shown to be inconsistent with the available paleo-data (Hamilton et al., 2018; Liu et al., 2021). In addition, recent studies have used paleo-time periods before the PI to improve estimates of the climate sensitivity (Sherwood et al., 2020). However, these analyses used estimates of aerosol radiative forcing uncertainties that were likely underestimated (Mahowald et al., 2024). Despite these advances, a coherent roadmap for constraining aerosol radiative forcing and its uncertainty across past climates - from the PI to the PD and across key paleoclimate periods of specific interest for the IPCC - remains lacking. In particular, there is no consistent roadmap for integrating proxy-based observational constraints with ESM simulations to quantify best estimates and uncertainties in natural aerosol radiative forcing.

This paper aims to address this gap by providing such a roadmap. The discussion is organized around the key time periods defined in the CMIP and PMIP (Paleoclimate Modelling Intercomparison Project) experimental design protocols:the historical period (1850 CE to present day), the preindustrial period (PI: ~1850 CE), the last millennium, the mid-Holocene (MH, ~6 ka BP), and the Last Glacial Maximum (LGM, 21 ka BP). Longer transient simulations spanning the Holocene (Braconnot et al., 2019; Hopcroft and Valdes, 2022) and the last deglaciation (He et al., 2021; Ivanovic et al., 2016) are also increasingly feasible and are considered where relevant.

Note that the ranges and uncertainties of radiative effects and forcing discussed here refer to the global averages. However, unlike for well-mixed gases, these uncertainties should not be interpreted as a measure of spatial dispersion around the global mean, since aerosols are highly heterogeneously distributed and their local radiative effects can be orders of magnitudes larger than the global average.

In this review, the background Section 2 discusses radiative effects and forcing and how these are derived from models, different types of paleo-data archives, and how to combine models with paleo-data proxies. Next, for each of the major natural aerosol types – mineral dust, biomass burning aerosols, volcanic emissions, and other natural aerosols – we assess the current state of ESM-based aerosol radiative forcing estimates alongside the proxy records and existing datasets that could constrain them. Particular attention is given to where the coupling between archives and models is most tractable and

Formatted: Default Paragraph Font, Font color: Black

Formatted: Normal, Centered, Border: Top: (No border), Bottom: (No border), Left: (No border), Right: (No border), Between : (No border), Tab stops: 3.25", Centered + 6.5", Right, Position: Horizontal: Left, Relative to: Column, Vertical: In line, Relative to: Margin, Wrap Around

Formatted: Font color: Black

where the largest uncertainties remain. Each section concludes with recommended future directions, with the aim of providing a consolidated roadmap for reducing uncertainty in natural aerosol radiative forcing across these past climates.

2 Background information

In this section we provide a brief overview of our definition of aerosol radiative forcing estimation in ESMs, and the potential of using information from natural archives to constrain the key variables that largely determine past variability in aerosol radiative forcing, namely aerosol loading and physicochemical properties. We also define terms used throughout the manuscript, and discuss challenges in combining paleo-data with models, propagating uncertainties, and identifying robust datasets. Specific uncertainties relative to individual aerosol species and/or aerosol source types (depending on how they are typically sourced in ESMs) are discussed in the subsequent sections. We recognize that some of these statements include expert assessment of the authors of this review, not established fact.

2.1 Aerosols in Earth system models and radiative forcing

Aerosols are included in most ESMs and thus their interactions with dynamics, varying sources and sinks, and radiation can be simulated (Szopa et al., 2021). Most recent models include aerosol-cloud interactions as well (Szopa et al., 2021). Aerosol or precursor sources can be prescribed (for example for industrial emissions) or calculated interactively (e.g. for dust or sea spray). Some aerosols are formed in the atmosphere (e.g. conversion of the gas SO_2 into sulfate aerosols)—called secondary aerosols in contrast to primary aerosols which are emitted. The conversion process to secondary aerosols is included with different complexities in the different models. Once emitted, the models use the winds, moist convective parameterization, boundary layer parameterizations and settling to calculate how the aerosols move around in the atmosphere. Aerosols are removed from the atmosphere by wet and dry deposition processes within the models.

Thanks to the embedded radiative transfer schemes, ESMs can simulate waveband-dependent radiative fluxes as a function of surface albedo and of the amount and spatial distribution of specific types of atmospheric trace gases, aerosols and clouds. By adding or removing a specific species, or a specific source, it is possible to estimate its direct (aerosol-radiation) and indirect (aerosol-cloud, biogeochemistry, snow darkening, atmospheric chemistry) Radiative Effects (RE), in terms of differences in radiative fluxes (e.g., at the surface or at the top of the atmosphere) instantaneously or after atmospheric adjustments. Accounting for these adjustments, which are assumed to be rapid compared to the duration of climate adjustment following the aerosol change, leads to the Effective Radiative Forcing (ERF) (Sherwood et al., 2015), the radiative imbalance at top-of-atmosphere that drives the climate perturbation needed to eventually restore equilibrium. By *tracking the temporal evolution of the amount and distribution of a given species and the resulting variations in radiative effects, we can define its Radiative Forcing (RF), as the change in radiative flux compared to a reference period* (Forster et al., 2021). In general, a radiative 'effect' refers to the radiative imbalance caused by the presence of a species, while 'forcing' refers to the radiative change corresponding to a change in aerosol species abundance over a given period.

Changes in natural aerosol loads may be due to anthropogenic activities, feedbacks linked to human-induced climate changes, or natural variability (e.g. in response to insolation-triggered climate changes in the past). Regardless of the causes of past aerosol changes, it may be pragmatically convenient to consider those as climate forcing agents, at least for the purpose of estimating RF, even when they are responding or feeding back to a more fundamental climate driver (Mahowald et al., 2024). Next, we focus on how natural archives can constrain past aerosol variability across different time scales and how to best use ESMs to estimate the corresponding RF (Carslaw et al., 2010).

Deleted: so that

Deleted: included

Deleted:), and this

Formatted: Subscript

Formatted: Font: Not Italic

Formatted: Font: Not Italic

Deleted:

Deleted:

Formatted: Default Paragraph Font, Font color: Black

Formatted: Normal, Centered, Border: Top: (No border), Bottom: (No border), Left: (No border), Right: (No border), Between : (No border), Tab stops: 3.25", Centered + 6.5", Right, Position: Horizontal: Left, Relative to: Column, Vertical: In line, Relative to: Margin, Wrap Around

Formatted: Font color: Black

2.2 Natural archives of past aerosol variability

Natural archives are unique environments that preserve information about past climatic and environmental conditions through their physical and chemical composition. When aerosol deposition is preserved within an environmental matrix, and the aerosols can be subsequently identified and isolated either through 1) direct measurements of aerosol particles, or 2) indirect measurement of aerosol proxies, we can extract useful information about past aerosol variability. Some archives can also serve as source proxies, such as fire scars in tree rings (Margolis et al., 2022).

Typically, the concentration of specific aerosol particles or aerosol proxies in the environmental matrix (AC: Aerosol Concentration, typically referred to as 'eolian content' in the dust community) is measured as a function of depth and placed in time by an established age model based on datable material in the archive. While time series of the AC provide first order estimates of aerosol deposition variability, they do not directly quantify the rate of change in aerosol deposition. Multiplying the accumulation rate of the archive's matrix (e.g. m s^{-1}) by the AC measurements (e.g. kg m^{-3}) provides an aerosol flux (e.g. kg m^{-2} s^{-1}, also called mass accumulation rate (MAR) in some communities), which represents the aerosol deposition flux as recorded by natural archives (Albani et al., 2015; Kohfeld and Harrison, 2001). A well-known example of an instance where divergence between AC and aerosol flux would produce contrasting conclusions is the LGM-to-Holocene ratio in dust recorded in the EPICA Dome C Antarctic ice core, where the AC ratio is ~50, whereas the corresponding dust flux ratio is ~25 (Lambert et al., 2008).

Different types of natural archives vary in their ability to preserve information about past aerosol variability (Table 1). In the following sections, we briefly summarize the archives commonly used to reconstruct past aerosol variability, and highlight their potential to preserve aerosols, associated methods for isolating ACs from the environmental matrix, their potential to record aerosol fluxes, their geographical distribution (i.e., where the archives are typically found), the spatial representativeness of the proxies they preserve, their temporal coverage, and their resolution. We present the archives in order of the quantity of aerosol proxies they can preserve, from the most to the least inclusive.

Table 1: Types of archive, and the aerosols types they can determine (PSD=particle size distribution, OC=organic carbon, BC=black carbon, REEs=rare earth elements, ss=sea salt, nss=non-sea salt)

	Aerosol types			
Archive	**Mineral dust**	**Fire emission product**	**Volcanic (sulfate, tephra)**	**Other**
Ice	PSD, nss-Ca, radiogenic isotopes, mineralogy, major and trace elements (including REEs)	OC, BC, biomarkers, NO_3, NH_4	S/SO_4, tephra	ss-Na, ss-S, biogenic S, N-species
Marine sediment	radiogenic isotopes, mineralogy, major and trace elements (including REEs), ^{232}Th, $^{4}He_{terr}$, PSD	Charcoal, biomarkers	tephra	
Lakes	PSD, radiogenic isotopes, mineralogy, major and trace elements(including REEs)	Charcoal, biomarkers	tephra	

Formatted: Font: Not Italic

Formatted: Font: Not Italic

Formatted: Font: Not Italic

Formatted Table

Formatted: Default Paragraph Font, Font color: Black

Formatted: Normal, Centered, Border: Top: (No border), Bottom: (No border), Left: (No border), Right: (No border), Between : (No border), Tab stops: 3.25", Centered + 6.5", Right, Position: Horizontal: Left, Relative to: Column, Vertical: In line, Relative to: Margin, Wrap Around

Formatted: Font color: Black

Loess and loess-paleosol sequences	Layer thickness, PSD, radiogenic isotopes, mineralogy, major and trace elements (including REEs)	Charcoal, biomarkers	tephra	
Peatlands	Radiogenic isotopes, mineralogy, major and trace elements (including REEs), PSD	Charcoal, biomarkers	tephra	
Corals	^{4}He			
Trees		Fire scars		
Speleothems	Major and trace elements	Biomarkers, trace and minor elements	S/SO_4	

2.2.1 Ice

Comprehensive records of aerosols directly related to radiative effects including dust, black and brown carbon, sea spray, volcanic and biogenic sulfate are archived in glacier ice (Lorius et al., 1990). Ice cores from high-elevation alpine glaciers (e.g., Thompson et al., 2006a), mid-latitude ice caps (e.g., Thompson et al., 2024), and the ice sheets (e.g., Lambert et al., 2008; Erhardt et al., 2022) have been used extensively to reconstruct past aerosol concentrations (AC) and depositional fluxes, as well as to infer natural and anthropogenic sources (e.g., McConnell et al., 2007a-b), source regions, and changes in those sources over time (Delmonte et al., 2008). State-of-the-art ice core records offer several advantages for paleo-aerosol research. They provide direct measurement of generally regional- to hemispheric-scale atmospheric and precipitation aerosol chemistry. A single ice core can yield a wide breadth of exactly co-registered records, not only of radiatively active aerosols but also a range of possible aerosol source tracers and climate indicators such as water isotopes, which are important for interpretation. Ice cores are also accurately dated, and their highest temporal resolution can reach seasonal to annual, extending over recent decades, centuries, or even millennia. However, there are important limitations. The two ice sheets that provide the most well-dated, multi-millennial to orbital-scale ice core records are located in polar regions far from major low- and mid-latitude aerosol emission sources (North Greenland Ice Core Project Members, 2004; EPICA Community, 2004; Gkinis et al., 2021, Royo-Garibaldi et al., 2024). Alpine glaciers, in contrast, generally consist of much younger (century to millennial-scale) ice and are restricted to a few high-elevation regions where aerosol flux estimates are complicated by the highly spatially variable snow accumulation rates and, for low-lying ice caps and glaciers in temperate regions, by seasonal melting (Lambert, 2025).

2.2.2 Marine sediment

Marine sediment cores are powerful paleoclimate archives because they provide an ubiquitous, continuous, high-resolution record of Earth history that can be well dated. Numerous proxies are available to assess the aerosols marine sediments contain. These include the multiple proxies used as tracers for the AC of lithogenic material (mineral dust). Commonly used dust proxies include 232-thorium (^{232}Th), an isotope of Th enriched in continental crust and negligible in background basaltic oceanic crust; terrigenous ^{4}He ($^{4}He_{terr}$), emitted during alpha decay of U and Th in a variety of minerals and negligible in volcanogenic material; and major and trace elements predominantly sourced from continental crust that display conservative behavior in the ocean, including Fe, Al, Ti, and Sc. For open-ocean sites distal to landmasses, these proxies primarily reflect aeolian supply, with known grain-size effects on ^{232}Th and $^{4}He_{terr}$ concentration minimized by the isolation of the fine fraction (<5 μm) (McGee et al., 2016; Kienast et al., 2016) after ~1000-2000 km of transport from the source (Serno et al., 2014). In

Deleted: fire

Deleted: millenial

Deleted: for

Formatted: Default Paragraph Font, Font color: Black

Formatted: Normal, Centered, Border: Top: (No border), Bottom: (No border), Left: (No border), Right: (No border), Between : (No border), Tab stops: 3.25", Centered + 6.5", Right, Position: Horizontal: Left, Relative to: Column, Vertical: In line, Relative to: Margin, Wrap Around

Formatted: Font color: Black

a few cases, charcoal records and volcanic ash (tephra) were also retrieved from marine sediment cores providing complementary information on fire activity and volcanism (Freundt et al., 2023; Marlon et al., 2016; Van Der Kaars and De Deckker, 2002). Fluxes of all aerosol constituents can be estimated through age model-based linear sedimentation rates, or more accurately through ^{230}Th- and extraterrestrial ^{3}He ($^{3}He_{ET}$)- normalization (Bacon and Anderson, 1982; Francois et al., 2004; McGee and Mukhopadhyay, 2013; Winckler et al, 2005, 2008; Abell et al, 2021). Depending on the deposition rate and length of the core, marine sediment records of aerosols can resolve centennial- to orbital-scale variability.

2.2.3 Lake sediment

Lakes generally host annual- to multi-millennial-scale archives of sediment, within which various aerosol proxies can be preserved (Marlon, 2020). Lakes integrate aerosol environmental and atmospheric signals through their sediments, capturing inputs from the surrounding watershed, the land area draining into the lake, as well as from the broader air-shed, the region of the atmosphere supplying aerosols and other airborne materials (Cohen, 2020). In terms of AC, lakes have provided the bulk of charcoal archives for fire history reconstructions (Power et al., 2008). Estimating atmospheric dust fluxes from lake sediment cores, however, is less straightforward due to the mixing of aeolian and fluvial sediment contributions (Arcusa et al., 2019) . Geomorphological variations can further influence the reliability of signals, and determining the spatial representativity of individual sites is often difficult (Muhs et al., 2003; Seelos et al., 2009). Moreover, sedimentation processes and subsequent preservation biases can affect the integrity of aerosol proxy records, particularly when examining changes on a range of timescales, so that the estimation of reliable fluxes is challenging (Vachula et al. 2022b).

2.2.4 Loess and loess-paleosol sequences

Loess is a continental deposit composed predominantly of silt-sized inorganic sediment, formed mostly by deposition of wind-blown dust (Smalley et al., 2011). Recent pedogenetic processes may create a soil at the top of loess profiles, while past pedogenesis may create buried paleosol layers (Kemp, 2001). To isolate the fraction of loess sediment mass that corresponds to dust (i.e., dust AC), it is important to quantify and correct for post-depositional, pedogenetic organic matter and carbonate contents, as well as for direct volcanic ash fall (Cosentino et al., 2024). The main strength of loess as a dust archive lies in its widespread continental distribution, usually close to dust sources (Li et al., 2020). However, there are important limitations. Dating methods for loess do not allow for decadal reconstructions of dust fluxes since the pre-industrial period, and are instead better suited for reconstructing dust fluxes during the last few million years, with typical millennial to multi-millennial resolutions. In addition, loess-derived dust fluxes can deviate from actual atmospheric dust deposition rates due to several factors. Wind-blown material can become focused onto the surfaces of windward escarpments (e.g., Comola et al., 2019). Post-depositional slope processes in high-relief environments can rework the loess deposits (e.g., Volvakh et al., 2022). And the potential lack of surface roughness elements, such as vegetation, can reduce the surface retention of atmospherically deposited dust particles (e.g., Yan et al., 2011). Thus, loess profiles that are considered good dust archives for quantitative reconstructions of dust fluxes are those accumulated in regional low-relief surfaces in semi-arid regions. The preservation of aerosols other than dust in loess has not been extensively explored. Only a few charcoal records, indicative of intensified fire activity rather than of intensified fire aerosols emissions, were retrieved from loess-paleosol sequences (Harrison et al., 2022; Tan et al., 2015).

2.2.5 Ombrotrophic peat

Peatlands are mostly found in tropical and high-latitude regions and can be divided into two sections: a lower minerotrophic and an upper ombrotrophic layer. The former is bathed into shallow groundwater which mixes dissolved ions and elements laterally throughout the system. In contrast, the latter receives nutrients exclusively from the atmosphere through precipitation and wet and dry deposition

Deleted:

Deleted:), post

Deleted: that

Deleted:), and

Formatted: Default Paragraph Font, Font color: Black

Formatted: Normal, Centered, Border: Top: (No border), Bottom: (No border), Left: (No border), Right: (No border), Between : (No border), Tab stops: 3.25", Centered + 6.5", Right, Position: Horizontal: Left, Relative to: Column, Vertical: In line, Relative to: Margin, Wrap Around

Formatted: Font color: Black

of aerosols (Dominguez et al., 2015). The upper ombrotrophic peat section is generally composed of over 90% organic material, while the inorganic material is mostly composed of deposited mineral dust (Shotyk et al., 2001). Dust concentrations (AC) can be measured either indirectly using geochemical elements measured through mass spectroscopy or X-ray fluorescence or directly, along with particle size distributions, using a Coulter Counter and optical methods (De Vleeschouwer et al., 2012). The ombrotrophic peat section is generally a few hundred to a couple thousand years old, never covering more than the Holocene. Peat cores are usually sampled at a 1 cm depth resolution, which can vary in time resolution between a few years for fast-growing peat, to multi-decadal resolution at slow-growth sites, allowing for the estimation of fluxes. Beyond dust, peatlands and other wetlands, including mires, marshes and swamps - are also important natural archives for charcoal and tephra, providing information on fire activity and volcanic deposition (Chambers et al., 1997; Hall, 2020; Marlon et al., 2016).

2.2.6 Tree-ring fire scars

Trees can record fire events as wounds from nonlethal cambial injury (Gutsell and Johnson 1996). The resulting scars are preserved in the tree-ring growth sequences of the tree, and can be dated with annual to seasonal precision following dendrochronological methods (Dieterich and Swetnam, 1984; Baisan and Swetnam, 1990). Fire scars therefore provide direct, precisely dated evidence of fire occurrence at a particular location (i.e., the individual tree) and time (year, and in some cases season, of growth). Generally, multiple trees are sampled at plot (<1 ha) to stand (10–50 ha) or watershed (100s–1000s ha) scales (Falk et al., 2011), allowing for inferences regarding the spread of fires among trees and stands (Niklasson and Granström, 2000; Farris et al., 2026). Recently a network of fire-scar sites was compiled for North American forests (Margolis et al., 2022) that allowed for broader inferences about fire–climate relationships (Margolis et al., 2025) and comparisons of relative area burned between pre-industrial and present day time periods (Parks et al., 2025). A limitation is that fire scars primarily record moderate- to low-severity fire, which may or may not have generated substantial aerosol emissions or widespread smoke transport. Dendroecologists, however, have derived multiple methods of dating and mapping historical high-severity fires in forest ecosystems that experienced it, including mesic, higher elevation and boreal forests (Héon et al., 2014; Tepley and Veblen, 2015). The temporal length of the tree-ring fire scar record is dependent on the tree species and their natural preservation *in situ*, which for many temperate forests spans 200-400 years (Margolis et al., 2022), with the exception of giant sequoia (*Sequoiadendron giganteum*) that preserves fire scars spanning 3,000 years (Swetnam, 1993). Fire scar sites sampled near sediment core locations have been used to reconstruct fire regimes through the Holocene (e.g., Allen et al., 2008; Swetnam et al., 2009; Higuera et al., 2021).

2.2.7 Corals

Some corals provide highly indirect dust records because they reflect water column geochemistry, while others record direct atmospheric deposition (Eakin and Grottoli, 2006; Mukhopadhyay and Kreycik, 2008). Any aeolian dust signal captured by corals is already modified by processes such as mixing with riverine and coastal inputs, dissolution, biological uptake, and diagenetic overprinting. The particle size distribution, mineralogical compositions, and isotopic fingerprint of dust are generally not preserved in corals, limiting their ability to resolve provenance or to infer transport mechanisms (Eakin and Grottoli, 2006). Despite these limitations, there has been one attempt to directly assess dust fluxes via corals (Mukhopadhyay and Kreycik, 2008). However, the applicability of this approach is limited to corals proximal to dust source regions yet distal to other areas of potential detrital inputs (i.e., rivers). Therefore, corals may provide localized insights into dust deposition, but their broader applicability as paleo-aerosol archives remains limited.

2.2.8 Speleothems

Deleted:) .

Deleted: post-Industrial

Deleted: rather

Deleted: Therefore, any

Formatted: Default Paragraph Font, Font color: Black

Formatted: Normal, Centered, Border: Top: (No border), Bottom: (No border), Left: (No border), Right: (No border), Between : (No border), Tab stops: 3.25", Centered + 6.5", Right, Position: Horizontal: Left, Relative to: Column, Vertical: In line, Relative to: Margin, Wrap Around

Formatted: Font color: Black

Speleothems are calcareous cave formations that serve as excellent terrestrial paleoclimate archives due to their minimal post-depositional alteration and capacity for absolute dating using high-precision uranium-series disequilibrium methods (Fairchild et al., 2006; Mason et al., 2022; Hua et al., 2012; Baker et al, 2021). Traditionally speleothems have been used for hydroclimate and environment reconstruction, but an emerging body of literature now positions them as a promising archive for paleo-aerosol deposition, including proxies for fire activity (Campbell et al., 2023) and dust input (Frumpkin and Stein, 2004; Cruz et al., 2021; Hess et al., 2024).

A range of fire-related biomarkers have been identified in speleothems, including lignin oxidation products (LOP), combustion-sensitive anhydrosugars (e.g., levoglucosan), polycyclic aromatic hydrocarbons (PAHs), or monosaccharide anhydrides (MA), and used to reconstruct fire activity and biomass burning in different regions of the world (Homann et al., 2022; McDonough et al., 2022; Homann et al., 2023). These compounds are introduced via dripwater and reflect a combination of atmospheric deposition, soil processes, and karst transport pathways. Therefore, distinguishing between an autochthonous (in-cave) or allochthonous (remote) origins or transport processes remains challenging for both fire- and dust-related aerosols. Despite these limitations, speleothems provide precisely dated, high-resolution terrestrial records that can capture localized to regional aerosol variability. As demand grows for improved constraints on terrestrial aerosol emission models, speleothems may offer another valuable terrestrial record of localized aerosol variability.

2.2.9 Proxy system models

Forward models, which forward-simulate the response of the climate system given a set of known initial climate and environment constraints, can help resolve outstanding questions such as absolute flux, size distribution and geochemical characterization (Sudarchikova et al., 2015; Evans et al., 2013). Proxy system models (PSM), are a type of forward model in which a synthetic proxy signal is produced by forward-simulating the geochemical processes which transmit the original atmospheric signal from the climate system into the archive proxy (Dee et al., 2015). They can help resolve outstanding questions unique to individual archives, such as the fraction of total accumulation that corresponds to a specific aerosol type, and any signal attenuation or post-deposition modification. To the best of our knowledge, no study has produced a PSM of a paleo-aerosol record; this is an unmet need in the existing literature.

3 Dust

Desert dust or mineral aerosols are entrained by strong winds in dry, unvegetated regions and consist of largely insoluble minerals.

3.1 Dust Modeling

ESMs represent the mineral dust cycle, comprising emission, transport, and removal. Dust emission is typically triggered when near-surface winds exceed a threshold speed that depends on soil characteristics including soil moisture, surface roughness, and vegetation cover (Marticorena and Bergametti, 1995; Gillette, 1974; Fécan et al., 1999; Zender et al., 2003, Kok et al., 2012, 2014; Okin, 2022; Leung et al., 2023). As a result, regions of prolific dust emission are generally arid areas with abundant loose sediments, low soil moisture, and sparse vegetation, which otherwise shields the surface from wind stress (Raupach et al., 1993). Models either prescribe dust source regions from geomorphic features such as topographic depressions where sediments accumulate (Prospero et al. 2002) or simulate dust source strength using more physically based emission schemes (Kok et al., 2014; Leung et al., 2023). Although these approaches reproduce the broad spatial patterns of the modern-day dust cycle, they remain sensitive to poorly constrained surface properties and unresolved sub-grid wind variability (Lunt et al., 2002; Cakmur et al., 2006; Leung et al., 2023).

Deleted:

Formatted: Default Paragraph Font, Font color: Black

Formatted: Normal, Centered, Border: Top: (No border), Bottom: (No border), Left: (No border), Right: (No border), Between : (No border), Tab stops: 3.25", Centered + 6.5", Right, Position: Horizontal: Left, Relative to: Column, Vertical: In line, Relative to: Margin, Wrap Around

Formatted: Font color: Black

Most ESMs assume an approximately invariant emitted dust size distribution, broadly consistent with modern observations (Kok, 2011a, 2011b; Meng et al., 2022). However, this assumption may not hold in past climates, particularly for glacial environments where sediment production processes like mechanical grinding may result in soil particle size distributions that differ substantially from those created by weathering in arid regions (Mahowald et al., 2006; Panta et al., 2025; Gonzalez-Romero et al., 2024). This uncertainty in the emitted dust size distribution for paleoclimates propagates directly into both the radiative effect produced per unit dust loading (Miller et al., 2006; Kok et al., 2017; Song et al., 2022) and into simulated transport and deposition, which strongly influences modeled dust distributions.

Downwind transport is limited by removal processes (Tegen and Fung 1994, Ginoux, 2003; van der Does et al., 2020; Meng et al., 2022). The majority of dust particles are washed out through collision with precipitation, both within and below a cloud (Dana and Hales 1976), or after nucleating cloud droplets and ice particles (Nenes et al., 2014; McGraw et al., 2020a; Froyd et al., 2022). Dust particles also return to the surface through gravity, while small-scale atmospheric mixing both enhances removal at the surface or conversely maintains particles aloft within the atmosphere (Rodakoviski et al. 2023). These dry processes preferentially remove super coarse particles (diameters > 10 um) (Miller et al., 2006). However, comparisons with in situ data indicate that many models underestimate the atmospheric lifetime of super coarse dust (Weinzierl et al., 2017; Adebiyi and Kok, 2020; Meng et al., 2022; Drakaki et al., 2022).

To represent the climatic impacts of dust, ESMs simulate its impacts on radiation (Miller et al. 2014), cloud formation (McGraw et al., 2020a), atmospheric chemistry (Detener et al. 1996) and nutrient delivery to remote ecosystems (Jickells et al. 2005). The direct radiative effects of dust depend sensitively on particle size and mineralogical composition, as well as on the albedo of the underlying surface (Tegen and Lacis, 1996; Sokolik and Toon, 1999; Kok et al., 2017; Song et al., 2022; Li, Mahowald et al., 2022; Obiso et al., 2024). The importance of accurately representing dust properties is underscored by a recent estimate of the global longwave (LW) dust direct radiative effect of $+0.25 \pm 0.06$ W m^{-2}, approximately twice what climate models account for (~0.13 W m^{-2}; Kok et al., 2026). This discrepancy arises primarily from underestimated coarse and super-coarse dust abundance and the neglect of LW scattering in models. In addition to direct effects, important indirect effects arise because mineral dust is the most globally abundant source of ice-nucleating particles, thereby influencing mixed-phase and cirrus cloud properties (DeMott et al., 2016; Kanji et al., 2017; McGraw et al., 2020a; Froyd et al., 2022), and because dust supplies key nutrients—primarily iron and phosphorus—to marine and terrestrial ecosystems, enhancing biological productivity and CO_2 uptake (Mahowald, 2011; Jickells et al., 2005). These effects depend strongly on particle size, shape, mineralogy, mixing state, and surface coatings (Kok et al., 2017; Song et al., 2022; Huang et al., 2023; Gonçalves-Ageitos et al., 2023; Obiso et al., 2026), yet many of these properties remain simplified or poorly constrained in paleoclimate datasets. More collection of these attributes could help constrain model simulations.

In the present climate, modeled dust distributions are evaluated primarily using satellite retrievals of aerosol optical depth in dusty regions, in situ measurements of dust size distributions, and ground-based measurements of dust concentrations (Huneeus et al., 2011; Albani et al., 2014; Kok et al., 2021; Leung et al., 2024). Outside the satellite era, model dust cycle constraints are based primarily on deposition records from ice cores, marine sediments, and terrestrial archives (Albani et al., 2014, Ohgaito et al., 2018). The fundamental differences between modern observational constraints and paleo proxy records, combined with uncertainties in model representations of particle properties and removal processes, motivate the need for systematic model–data integration and inversion approaches to reconstruct past dust variability.

Deleted: Important

Formatted: Default Paragraph Font, Font color: Black

Formatted: Normal, Centered, Border: Top: (No border), Bottom: (No border), Left: (No border), Right: (No border), Between : (No border), Tab stops: 3.25", Centered + 6.5", Right, Position: Horizontal: Left, Relative to: Column, Vertical: In line, Relative to: Margin, Wrap Around

Formatted: Font color: Black

3.1.1 Challenges in representing dust variability and radiative forcing across climate states

A primary application of dust models is to quantify dust impacts on climate during periods that are particularly informative for constraining climate sensitivity, most notably the PI-PD period and the LGM (Mahowald et al., 2006; Sherwood et al., 2020). During the PI–PD period, dust emissions have been altered by widespread human land-use changes and hydrological modifications, including agricultural expansion and the desiccation of lakes in arid and semi-arid regions (Goldewijk et al., 2011; Yao et al., 2023; Xi and Sokolik, 2016; Borda et al., 2022; Banks et al. 2022). Consistent with these drivers, numerous deposition records indicate long-term increases in dust flux over the historical period (McConnell et al., 2007b; Mulitza et al., 2010; Mahowald et al., 2010; Hooper and Marx, 2018). A recent proxy-constrained reconstruction estimated that global atmospheric dust loading increased by 55 ± 30% between the pre-industrial period (1841–1860) and 1981–2000 (Kok et al., 2023). However, this increase was not monotonic: dust loading peaked around the 1980s at approximately 75 ± 40% above pre-industrial levels. Dust subsequently declined, with a recent reconstruction of dust loading using satellite data and inverse modeling indicating a global decrease of 5 ± 4% per decade during 2003–2023 (Gupta et al., 2026).

In contrast, CMIP6 models simulate little to no change in atmospheric dustiness over the PI–PD period, both in fully coupled historical simulations and in AMIP simulations constrained by reconstructed sea surface temperatures (Kok et al., 2023; Leung et al., 2025). This discrepancy indicates that current emission schemes and land-surface datasets fail to capture key drivers of historical dust variability. As a result, reconstructed or prescribed historical dust emissions are often required for models to estimate dust radiative forcing and other Earth-system impacts (Mahowald et al., 2010; Leung et al., 2025).

On glacial–interglacial timescales (10^4-10^5 years), dust emissions respond strongly to large changes in climate, sea level, and the extent of ice sheets. In particular, continental ice sheets generate vast quantities of fine sediment through glacial erosion and grinding, providing an additional source of dust beyond low-latitude arid regions (Lambert et al., 2008; Gowan et al., 2021). Consequently, global dust deposition during the LGM is estimated to have been 3.1 ± 0.7 (1σ) times that during the mean pre-industrial Holocene (i.e., 11,700 years before present-1850 CE; Cosentino et al., 2024). This large contrast provides a key benchmark for evaluating dust–climate interactions in models (Mahowald et al., 2006; Kageyama et al., 2021), especially given the unrealistically weak PI-PD dust sensitivity simulated by CMIP6 models (Kok et al., 2023). In general, simulations that include additional LGM glaciogenic dust sources represent much better the large enhancement of dust in the LGM relative to the Holocene than simulations that do not (Albani et al., 2018; Lambert & Albani, 2021; Lambert et al., 2021).

The dust cycle also varied substantially during the Holocene, in response to orbital forcing and associated monsoon changes on precessional timescales (Otto-Bliesner et al., 2017). These changes are most evident during the African Humid Period, when dust emissions from the Sahara and Sahel were markedly reduced (deMenocal et al., 2000, Hopcroft and Valdes, 2019). Estimates based on model reconstructions using data assimilation report global dust loadings were approximately 10% less during the mid-Holocene (~6 ka BP) than during the late Holocene (1-3 ka BP) (Albani et al., 2015).

The quantitative comparability of recent reconstructions of PI–PD (Kok et al., 2023), Holocene (Albani et al., 2015), and LGM (Cosentino et al., 2024) dust variability is limited by differing definitions of the PI reference period, reliance on different proxy records, and distinct methodological approaches for estimating ratios relative to PI. These differences complicate cross-study syntheses of dust cycle changes.

Large uncertainties remain in representing LGM dust emissions and their spatial distribution. Dust source regions during the LGM likely differed substantially from today, with major contributions from glaciogenic sources at mid- and high latitudes in addition to expanded low-latitude deserts (Muhs et

Deleted: this

Deleted:), with

Deleted: reconstructions suggesting a 75 ± 40% increase in

Deleted: from the PI until the 1980s, followed

Deleted: a

Deleted: ± 20% decrease to the PD

Deleted: ;

Deleted: in review

Formatted: Default Paragraph Font, Font color: Black

Formatted: Normal, Centered, Border: Top: (No border), Bottom: (No border), Left: (No border), Right: (No border), Between : (No border), Tab stops: 3.25", Centered + 6.5", Right, Position: Horizontal: Left, Relative to: Column, Vertical: In line, Relative to: Margin, Wrap Around

Formatted: Font color: Black

al., 2014; Gowan et al., 2021) and exposed continental shelves. The glaciogenic sources are associated with distinct sediment properties, mineralogical compositions, bioavailability, and potentially finer particle size distributions that are not well represented by emission parameterisations developed for modern desert dust (Koffman et al., 2021; Panta et al., 2025, Shoenfelt et al., 2018). In addition, key boundary conditions controlling dust emission—such as insolation, greenhouse gas concentrations, vegetation cover, soil moisture, wind speeds and sea surface temperatures—differed markedly during the LGM and some of these remain uncertain themselves (Clark et al., 2009; Mahowald et al., 2024), compounding uncertainty in simulated dust fluxes.

Even when past dust loadings can be reconstructed, substantial uncertainty remains in translating changes in dust loading into radiative forcing and in comparing model simulations with proxy records. Among estimates of dust deposition from natural archives, only ice core data that directly measured dust using Coulter or laser particle counters necessarily provide co-located dust deposition flux and particle size distribution data. In many other cases—such as isotope and element proxies in marine sediments, peat, or loess records—dust fluxes and particle size distributions must be obtained from separate measurements. When size-resolved measurements are unavailable, assumptions are often made about the exact size range represented by the dust concentration measurements, for example by implicitly excluding coarse particles, despite their disproportionate contribution to dust mass, deposition and longwave radiative warming (Albani et al., 2014; Adebiyi et al., 2023; Kok et al., 2026). In addition, mineralogical and chemical differences between glaciogenic and desert dust may have caused differences in dust optical properties, ice-nucleating efficiency, and fertilization potential of downwind ecosystems. Radiative effects are very sensitive to surface albedo as well, which is not well known in past climates (Claquin et al., 2003; Potenza et al. 2016). Together, changes in optical properties and surface albedo imply that the dust radiative effect efficiency - the radiative effect of dust per unit mass or optical depth - differed from that in the present climate (Claquin et al., 2003; Potenza et al., 2016). Because many of the particle properties governing direct and indirect effects cannot be directly inferred from proxy archives and may vary across cloud regimes and ecosystems (Mahowald, 2011; Atkinson et al., 2013; David et al., 2019), improved reconstructions of past dust loading alone are insufficient to robustly constrain dust radiative forcing in past time periods.

Deleted: Together with changes in surface albedo, these factors…

3.1.2 How proxy data can help to constrain dust radiative forcing from models

Accurately constraining past dust radiative forcing requires that models and proxy observations be comparable in the quantities they represent and in the assumptions that link those quantities to dust loading and particle properties: this is discussed in more detail in section 2.3. Here we discuss specific issues with dust aerosols.

Geochemical fingerprinting—based on radiogenic or stable isotopes, REEs, major and trace elements, or mineral assemblages—provides an independent constraint on dust provenance by linking paleo dust records to potential source regions (Delmonte et al., 2008; Xie and Marcantonio, 2012; Beaudon et al., 2022; Torre et al., 2022; Újvári et al., 2022; Rousseau et al., 2025). In models, such information can be exploited by simulating dust from distinct source regions, enabling indirect comparison with provenance data and supporting data assimilation and inversion approaches that reconstruct past dust emissions and transport pathways (Mahowald et al., 2010; Albani et al., 2014; Kok et al., 2021, 2023).

Advances in model realism are required to translate reconstructed dust properties into estimates of radiative forcing. As discussed above, dust direct and indirect radiative effects depend sensitively on dust microphysical properties, namely its size distribution, mineralogical composition, shape, and mixing state (Perlwitz et al., 2015; Scanza et al., 2015; Huang et al., 2020; McGraw et al., 2020a; Gonçalves Ageitos et al., 2023). Although particle size distribution, mineralogy, and shape can in principle be obtained from proxy archives, the available data remain too sparse and geographically limited to

Formatted: Default Paragraph Font, Font color: Black

Formatted: Normal, Centered, Border: Top: (No border), Bottom: (No border), Left: (No border), Right: (No border), Between : (No border), Tab stops: 3.25", Centered + 6.5", Right, Position: Horizontal: Left, Relative to: Column, Vertical: In line, Relative to: Margin, Wrap Around

Formatted: Font color: Black

adequately constrain dust radiative effect efficiency. Consequently, bottom-up estimates of past dust radiative forcing from global models are likely to retain substantial uncertainty, even if reconstructions of past changes in dust loading improve.

Consequently, proxy datasets that jointly constrain dust amount, particle size distribution, provenance, and mineralogy are essential for constraining changes in both dust loading and dust radiative forcing efficiency across climate states. There is a particular need for such datasets spanning the sparsely-sampled (Figure 1) PI-to-PD period (Kok et al., 2023) and the LGM-to-PI transition (Cosentino et al., 2024), when changes in both dust loading and forcing efficiency are most relevant for constraining climate sensitivity (Sherwood et al., 2020; Mahowald et al., 2024). These limitations motivate the development of targeted observational strategies, physically constrained inversion frameworks, and community data standards, as discussed in Section 3.4.

3.2 Paleo dust proxies

3.2.1 Overview of paleoclimate archives and dust proxies

In section 2.2, details of different proxies were introduced. Here we discuss limitations and issues specific to dust proxies, in the view of the authors of this review. Mineral dust proxy records extracted from depositional archives such as marine sediment cores, corals, lake sediment cores, ice cores, loess deposits, and peat bogs are critical tools in paleoclimatology, enabling the reconstruction of past dust dynamics over timescales relevant to dust models (typically decadal to orbital) (Figure 1). All combined, these archives provide a quasi-global coverage of dust deposition fluxes, particle size, and particle composition, which are the most useful variables in the parametrization of direct and indirect effects of dust in models. However, the relationship between the measured proxy and environmental variables is often indirect, complex and specific to the paleo-dust archive from which it is derived.

Proxy records preserved across diverse geologic archives allow for the assessment of a common set of fundamental characteristics of dust: its abundance compared to other constituents, its rate of accumulation, its particle size distribution, its mineralogical and geochemical composition, and its provenance (Cosentino et al., 2024). Quantifying the proportion of aeolian material relative to other components in the archive (i.e., the aeolian dust fraction or AC) is crucial for isolating the atmospheric dust signal and calculating dust fluxes (see discussion in background). The mineralogical and geochemical composition captures the morphological and chemical nature of lithogenic material derived from the mechanical or chemical weathering of continental surfaces of potential source areas. The dust particle size distributions and provenance information can reveal transport energetics, distance from sources, and atmospheric circulation strength. Dust fluxes, along with their geochemical composition, allow for dust proxies to serve not only as “passive” recorders of landscape aridity and atmospheric circulation but also as proxies of the “active” role dust plays in biogeochemical cycling, with dust-borne nutrients (e.g., phosphorus, iron and trace metals) enhancing primary productivity and increasing carbon sequestration in the ocean at depth (Zan et al., 2025; Jickells et al., 2005; Martin, 1990).

Formatted: Default Paragraph Font, Font color: Black

Formatted: Normal, Centered, Border: Top: (No border), Bottom: (No border), Left: (No border), Right: (No border), Between : (No border), Tab stops: 3.25", Centered + 6.5", Right, Position: Horizontal: Left, Relative to: Column, Vertical: In line, Relative to: Margin, Wrap Around

Formatted: Font color: Black

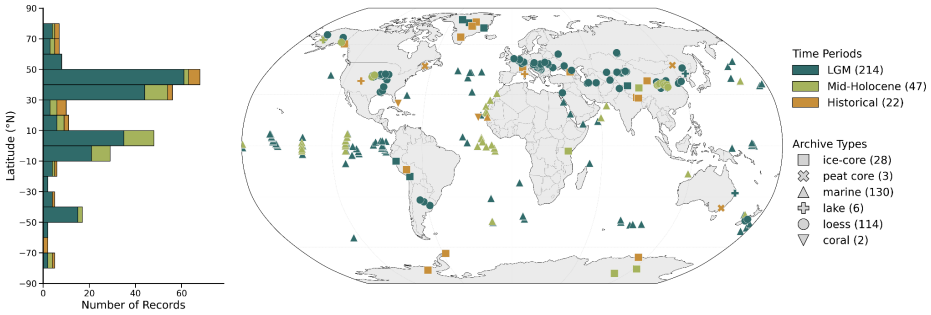

Figure 1. Spatial and temporal distribution of historical and paleodust records. *(Left) Latitudinal distribution of dust records binned by 10° intervals, color-coded by time period: Last Glacial Maximum / LGM (dark green, n=214), mid-Holocene (yellow-green, n=47), and historical (orange, n=22). (Right) Global map showing site locations of paleodust records, color-coded by time period and with symbols indicating archive type: ice cores (squares, n=28), peat cores (crosses, n=3), marine sediment cores (triangles, n=130), lake sediment cores (plus signs, n=6), loess (circles, n=114), and coral (inverted triangles, n=2). Data sources: LGM (Cosentino et al., 2024; Hansson, 1994; Schupbach et al., 2018; Thompson et al., 1995, 1998, 2018), mid-Holocene (Albani et al., 2015; Thompson et al., 2002, 2006), and historical (Kok et al., 2023; Kutuzov et al., 2019; Thompson et al., 2000, 2006b, 2013).*

3.2.2 Using a "reliable" dust record

For the purposes of this review, a dust record is considered reliable when 1) it captures past dust dynamics, 2) any influence from non-dust processes/feedback can be isolated, 3) there is minimal distortion from post-depositional processes, and 4) its signal can be interpreted across archives. The emission, transport and deposition of dust are influenced by multiple environmental variables (e.g., wind strength and position, landscape evolution, hydroclimate), making it a multivariable proxy with the potential to provide a holistic view of past climate and environment conditions and allowing integration with other organic and inorganic proxies (e.g., pollen, alkenones, microfossils, major and trace elements, trapped gasses, radiogenic isotopes) (Marx et al., 2018). A broad availability across many regions and archive types is another major strength of dust records. However, significant uncertainties remain. Comparability between dust records from different paleoarchives is often limited (e.g. marine vs ice cores), and measurement representativity can be affected by calibration issues, especially in size-distribution analyses (Albani et al., 2015). Many records report only dust concentrations and lack flux information, complicating interpretations of whether observed changes reflect atmospheric concentrations, deposition rates, or local site properties (Albani et al., 2015). Distinguishing the 'true' aeolian dust fraction is especially difficult at sites influenced by multiple dust (or detrital non-dust) sources, making particle size distribution measurements essential for interpreting 'close to source' / proximal sites (where we expect larger sizes), and for comparison with model simulations. Additional challenges common to all archives include dating uncertainties of the record, unclear site-dependent seasonality of dust deposition, limited information on atmospheric processes such as transport height, duration (atmospheric residence time), or chemical processing, and wet vs. dry deposition.

3.2.3. Limitations of individual archives for dust

Ice cores

Deleted: <*object*>¶

Deleted: A

Formatted: Default Paragraph Font, Font color: Black

Formatted: Normal, Centered, Border: Top: (No border), Bottom: (No border), Left: (No border), Right: (No border), Between : (No border), Tab stops: 3.25", Centered + 6.5", Right, Position: Horizontal: Left, Relative to: Column, Vertical: In line, Relative to: Margin, Wrap Around

Formatted: Font color: Black

Non-sea-salt calcium (nss-Ca) is a commonly used proxy in polar and alpine cores to estimate dust deposition, assuming carbonate dominated dust mineralogy and a Ca-to-dust ratio of 0.095 and 0.26 during cold and warm periods respectively, based on calibrations with particle counters (Rothlisberger et al., 2002, Albani et al., 2015). However, because the mass fraction of Ca in dust is sensitive to source composition, it may misrepresent actual dust fluxes (Zhang et al., 2015). Despite ice cores uniquely recording direct atmospheric deposition with high resolution, records providing direct particle concentrations and size information are sparse. Post depositional processes can also complicate the interpretation of ice core dust records, particularly in low-elevation sites where surface melt can percolate and mobilize soluble ions, or at extremely low accumulation sites where layers are thinned and compressed (Baccolo et al., 2026).

Provenance studies using Sr-Nd isotopes require careful particle size selection, particularly the <5 μm clay fraction, since isotopic signatures vary with particle size (e.g., Schettler et al., 2009; Biscaye et al., 1997). Similar geochemical fingerprints among potential source regions and marine influences on Sr-Nd compositions can obscure source attribution (Doebbert et al., 2014), with further complications, which are beyond the scope of this paper (e.g. Grousset and Biscaye, 2005).

Marine sediment cores

Early marine dust records from the 1960-1970s reconstructed aeolian input from bulk elemental proxies such as Fe, Al, and Ti (Arrhenius, 1963). This method is still commonly used but is sensitive to non-conservative behavior in seawater, including authigenic precipitation and biological cycling, as well as detrital inputs related to volcanism. Subsequent studies attempted to isolate the terrigenous fraction from the bulk using sequential chemical leaching of carbonate, biogenic silica, and authigenic minerals such as Fe-Mn oxides-hydroxides, but this still did not allow for successful separation of dust and non-dust terrigenous components such as volcanic ash (Rea & Janecek, 1981; Rea, 1994; Rea & Hovan, 1995). The climate signals inferred from these methods should thus be interpreted with caution and in tandem with the more conservative direct proxies of ^{232}Th and ^{4}He$_{terr}$ in bulk sediment, which predominantly reflect aeolian lithogenic material for open-ocean sites (~1000-2000 km from coasts) minimally influenced by riverine input or shelf erosion (Serno et al., 2014), and can prove useful for distinguishing dust from volcanic material (Patterson et al., 1999; McGee et al., 2016). Regional compilations evaluating marine sediment dust records derived from all of these proxies highlight similarities and discrepancies between dust proxies, and can be useful for characterizing the reliability of these proxies across space and time (e.g., Abell et al., 2026).

Additionally, many marine sediment-based paleodust records rely on age model-based accumulation rates to convert from dust concentration to dust fluxes, a method which is sensitive to the variable burial or preservation of non-dust components (e.g., carbonates or biogenic silica), changes in the lateral advection of sediment, age model uncertainty, and low-resolution age-depth tie-points. These issues imply that age model-derived fluxes reflect 'bulk' fluxes, and may not accurately represent the deposition rate of aeolian dust at the ocean surface (i.e., what we aim to reconstruct). To reduce these uncertainties and support comparability across marine sediment records, constant flux proxies (CFP) allow for the discernment of solely the vertical component of marine sediment (and in turn dust) fluxes.

^{230}Th-normalization, which relies on the observation that ^{230}Th is highly particle reactive and thus its flux to the sea floor equals its known production rate from ^{234}U decay in the water column, is the most widely used CFP approach, but is limited by its ~75 ka half-life (Cheng et al., 2013) to sediments deposited in the past ~500 ka (i.e., through the late Pleistocene). ^{3}He$_{ET}$, which refers to ^{3}He delivered to Earth in predominantly <25 µm interplanetary dust particles (Farley et al., 1997; Fenisse et al., 2025), is another CFP that can be applied in marine sediments across a much wider range of time. Key assumptions with this method include a relatively constant flux of ^{3}He$_{ET}$ to Earth and high retention in carrier minerals, both of which are supported by previous work (Schlosser & Winckler, 2002). Importantly, both constant flux proxies are sensitive to confounding influences, with sea-level fluctuations, boundary scavenging, sea ice, intense grain size sorting, and benthic nepheloid layers all potentially inducing uncertainty (Costa et al., 2020; McGee and Mukhopahdyday, 2013; Pavia et al., 2024; Tomchovska et al., 2025). Despite

Formatted: Default Paragraph Font, Font color: Black

Formatted: Normal, Centered, Border: Top: (No border), Bottom: (No border), Left: (No border), Right: (No border), Between : (No border), Tab stops: 3.25", Centered + 6.5", Right, Position: Horizontal: Left, Relative to: Column, Vertical: In line, Relative to: Margin, Wrap Around

Formatted: Font color: Black

these limitations, CFP-normalization is an essential tool for the accurate quantification of dust deposition rates in marine sediments, and broader adoption would promote more robust paleodust record intercomparison and paleoclimate inference.

Lake sediment cores

Separating the aeolian dust fraction from lake sediments is difficult because lakes commonly receive sediments from multiple sources (e.g., river inflow, surface runoff, shoreline erosion) (Mishra, 2023) requiring statistical unmixing with element concentrations or isotope systems used in provenance tracing. When the drainage basin contains abundant detrital material, the local lithogenic input can overwhelm the aeolian contribution unless aeolian dust fluxes are large (Langford, 1989). Mass accumulation rates may also fluctuate in response to changing lake levels, obscuring variations driven by atmospheric dust inputs (Bennett and Buck, 2016). Post-depositional processes, such as bioturbation, are able to disturb fine laminations (Sabatier et al., 2022), and diagenetic alteration may overprint trace element signatures, masking the aeolian geochemical fingerprint (Suhrhoff et al., 2024).

Loess and loess-paleosol sequences

Loess deposits represent direct continental aeolian sedimentation, making them excellent archives of terrestrial dust. Yet, their reliability requires careful consideration of depositional context, diagenetic alteration, and geochemical stability, since some loess deposits are sources of dust for other time periods. The main limitations surround the chronological uncertainties related to discontinuities in the loess accumulation. Hiatuses, erosional truncation, pedogenesis, and stratigraphic reworking obscure primary depositional signals and bias provenance and flux reconstructions (e.g., Kapp et al., 2025; Meijer and van der Meulen, 2023). Spatial variability in accumulation is also influenced by local geomorphology including surface roughness, vegetation density, and topographic trapping efficiency (Muhs et al., 2014; Peng et al., 2023). Post-depositional pedogenic modification and carbonate dissolution can alter the Sr isotopic signature and produce compositions that no longer reflect the original dust source (Shao et al., 2023), as well as modify the grain size distribution of dust at deposition (Kemp, 2001).

Peat bogs

Dust supply to peatlands/peatbogs is often low, restricting the amount of material available for isotopic or geochemical analyses, and occasionally making samples volume-limited. Similar to other remote paleoclimatic archives, peat bogs tend to trap mostly fine particles, since larger particles are lost during transport through gravitational settling. The predominantly organic matrix also contains only trace amounts of mineral material, and these low concentrations are sometimes below the detection limits for mineralogical characterization (Shotyk et al., 2023). Acidic peat porewaters alter clay minerals (in particular carbonates and easily weathered silicates), and mobilizes cations such as Ca, Mg, and Sr, thereby modifying the primary elemental signature of deposited dust (Veretennikova et al., 2021). Some metals may also be absorbed from porewaters rather than originating from atmospheric inputs, complicating provenance signals (Shotyk et al., 2023). Physical changes within the peat profile including humification, oxidation, erosion, and progressive compaction with depth, distort apparent accumulation rates and introduce uncertainty into reconstructions of dust flux, composition, and source (Tuukkanen et al., 2014).

Corals

Early work has shown that *Scleractinia* corals can hold both direct and indirect proxies of dust delivery to the surface ocean, capturing site-specific dust variability over centuries. Thus far, there is only one record of a direct dust proxy from modern *Porites* from Cape Verde using terrigenous ^{4}He in sediment extracted from the coral skeleton (Mukhopadhyay & Kreycik, 2008). ^{4}He in the Cape Verde coral provides annual-resolution records of North African dust emission from the mid-1950s to mid-1990s, with ^{4}He concentrations directly proportional to mineral dust content (Mukhopadhyay and

Formatted: Default Paragraph Font, Font color: Black

Formatted: Normal, Centered, Border: Top: (No border), Bottom: (No border), Left: (No border), Right: (No border), Between : (No border), Tab stops: 3.25", Centered + 6.5", Right, Position: Horizontal: Left, Relative to: Column, Vertical: In line, Relative to: Margin, Wrap Around

Formatted: Font color: Black

Kreycik, 2008). Given the proximity of this location to the Saharan dust source, it is as yet untested in the literature whether this proxy would extend across the Atlantic basin.

One other study has used trace element barium (Ba) as a proxy for wind-delivered dust in the Red Sea, where monsoon-driven winds funnel dust from the Tokar Gap in Sudan across the sea surface (Bryan et al., 2019). In this setting, aeolian dust releases labile Ba into seawater upon dissolution, which is then incorporated into the coral skeletal matrix in proportion to seawater concentrations (e.g., LaVigne et al., 2016). Ba/Ca ratios in Red Sea *Porites* corals therefore reflect summer South Asian monsoon circulation over 250 years at biweekly to annual resolution, and high-resolution measurements can resolve individual dust storm events. Two cores separated by 200 km show strong spatial coherence at decadal timescales, confirming that the Ba/Ca signal responds to large-scale monsoon circulation forcing rather than local effects (Bryan et al., 2019). However, this dust-Ba/Ca relationship is specific to an arid, river-limited setting where aeolian input dominates. In most other environments, Ba/Ca more commonly reflects river run-off, rainfall, or localized upwelling rather than dust, limiting its broader applicability as a wind proxy (e.g. Lea et al., 1989; Carriquiry and Horta-Puga, 2010; Horta-Puga and Carriquiry, 2012). Similarly, ^{4}He could in principle be delivered via riverine lithogenic material rather than atmospheric dust in river-influenced environments (Serno et al., 2013), meaning both proxies may record different or overlapping signals depending on the setting. Despite these limitations, both these approaches demonstrate the significant potential of using coral paleoclimate archives to investigate long-term dust variability across various marine settings and timescales, though they are likely very location dependent.

3.3 Paleo dust datasets

Compilations of dust fluxes derived from various natural archives (Section 3.2) are available for several key time periods and provide the primary observational constraints on past dust variability (Table 2). For the LGM, early dust datasets such as DIRTMAP (Mahowald et al., 1999; Kohfeld and Harrison, 2001) already included a relatively large number of sites , drawn predominantly from marine sediment records. Subsequent efforts included more continental and marine sites (Figure 1) and some of them added qualitative estimation of potential biases, quantitative uncertainty estimates, information on particle size ranges, dust provenance, and improved chronologies (Albani et al., 2014; Cosentino et al., 2024; Derbyshire, 2003; Kienast et al., 2016; Kohfeld et al., 2013; Maher et al., 2010; Mahowald et al., 2006). Those compilations also included average Holocene fluxes, often interpreted by modelling studies as “PI reference”, to be contrasted with average LGM fluxes. In Cosentino et al. (2024), top and bottom ages for individual sites allows a more targeted subsetting of time periods.

For the Holocene, the most recent dust dataset includes dust flux time series together with information on particle size distributions for the subset of sites with such information available, and both qualitative and quantitative uncertainty estimates (Albani et al., 2015). In contrast, datasets spanning the PI-to-PD period contain comparatively few deposition records (Figure 1) and lack co-located information on particle size distributions and mineralogy (Mahowald et al., 2010; Hooper and Marx, 2018; Kok et al., 2023).

Thus, deposition-based dust datasets provide important constraints on dust loading across different climate periods, but offer only limited constraints on dust radiative effect efficiency because they rarely include co-located information on particle size distributions, mineralogy, or optical properties.

3.3.1 Paleo dust data products

As the availability of observational records has expanded, recent efforts have sought to transform spatially sparse dust records into spatially continuous deposition fields. Such dust products are particularly valuable because current dust models still struggle to represent some of the key processes controlling emissions, transport, and deposition (Section 3.1), leading to large model-observation

Deleted:

Deleted:

Formatted: Default Paragraph Font, Font color: Black

Formatted: Normal, Centered, Border: Top: (No border), Bottom: (No border), Left: (No border), Right: (No border), Between : (No border), Tab stops: 3.25", Centered + 6.5", Right, Position: Horizontal: Left, Relative to: Column, Vertical: In line, Relative to: Margin, Wrap Around

Formatted: Font color: Black

discrepancies for both past and present climate states (Albani et al., 2018; Checa-Garcia et al., 2021; Leung et al., 2025).

Existing dust datasets (e.g., DIRTMAP) provide relatively broad, though uneven, spatial coverage for the Holocene and LGM. This enables geospatial interpolation approaches to derive continuous maps of dust deposition (Lambert et al., 2015; Cosentino et al., 2023), with physically motivated constraints introduced to reduce artifacts in data-sparse regions (e.g., Molina Catricheo et al., 2024). However, for the PI period, spatial coverage remains too limited to support robust direct interpolation, even in recent compilations (Hooper and Marx, 2018; Kok et al., 2023). Moreover, interpolation-based products only provide deposition fluxes. Although this makes them valuable for applications requiring surface dust fluxes as boundary conditions or inputs, such as ocean biogeochemical studies (e.g., Lambert et al., 2021), they do not directly constrain atmospheric dust loading, which is central to quantifying dust aerosol optical depth (DAOD) and radiative forcing.

Inferring dust emissions and atmospheric loading from deposition constraints therefore requires a physically based inversion framework that explicitly links emissions, transport, and deposition through model-simulated links between those variables. Such inversion approaches have been used to identify missing or underestimated dust sources (e.g., LGM glaciogenic dust; Mahowald et al., 2006) and to reduce biases in reconstructed dust levels and temporal trends over the historical period (Leung et al., 2025). When used as inputs or boundary conditions in ESMs, inversion-based dust products can reduce uncertainty in downstream estimates of dust loading, DAOD, DRE, and other related climate variables (e.g., Mahowald et al., 2010; Kageyama et al., 2017; Otto-Bliesner et al., 2017; Kok et al., 2026).

Given the sparsity and heterogeneity of paleo dust observations, the inverse problem is inherently under-constrained: multiple emission patterns can reproduce the same set of deposition records, and unconstrained optimization risks overfitting noise in observations rather than signal. Current inversion works address this challenge through structural constraints, including reducing the number of free parameters (e.g., solving for broad source regions rather than finer spatial scales), imposing prior assumptions on spatial emission patterns within the broad source regions, and assigning greater weight to more trustworthy observational records (e.g. Mahowald et al., 2006). Measurement and model uncertainties are also explicitly propagated to quantify uncertainty in the inferred emissions and atmospheric loading (Leung et al., 2025).

These constraints stabilize the inversion but do not eliminate key limitations. Inversion results remain sensitive to both prior assumptions, which may be incomplete or incorrect, and model biases in simulated transport or deposition, which can directly bias inferred dust emissions and loading. Using an ensemble of models (Kok et al., 2023) can partially quantify the model uncertainty, but shared structural biases among models (e.g., underestimating the lifetime of coarse dust, Adebiyi et al., 2023), will still lead to systematic bias rather than being captured as uncertainty. More observations, especially those providing information independent of existing constraints, are essential to test prior assumptions, identify model biases, and better constrain dust reconstructions, as discussed further in Section 3.4.

Table 2. State-of-the-art global paleodust datasets from individual observations* (currently recommended for model benchmarking and as the basis for developing derived products) and derived products **. Bulk refers to total mass, as opposed to a given size fraction. DMAR is the dust mass accumulation rate.

Reference	Features	Transient Historical	Transient Holocene	PI / MidHoloceene	PI / LGM
Kok et al., 2023 *	DMAR, dust concentration proxies (time series, bulk)	x			

Formatted Table

Formatted: Default Paragraph Font, Font color: Black

Formatted: Normal, Centered, Border: Top: (No border), Bottom: (No border), Left: (No border), Right: (No border), Between : (No border), Tab stops: 3.25", Centered + 6.5", Right, Position: Horizontal: Left, Relative to: Column, Vertical: In line, Relative to: Margin, Wrap Around

Formatted: Font color: Black

Albani et al., 2015 *	DMAR (time series, bulk), size distributions, quantitative uncertainties, label on confidence level		x	x	
Cosentino et al., 2024 *	DMAR (time slices, bulk), fraction < 10 µm diam., quantitative uncertainties				x
(Leung et al., 2025)**	Dust variables (time series, bulk) from model data assimilation: emission, deposition, loading, AOD, surface concentration	x			
PMIP4 (CESM) (Kageyama et al., 2017; Otto-Bliesner et al., 2017)**	Dust variables (time slices, model size distributions < 10 µm diam.) from model data assimilation: emission, deposition, load, 3D concentration, AOD, DRE			x	x
(Molina Catricheo et al., 2024)**	Dust deposition (time slices, bulk) from physics-informed neural networks data assimilation				x

3.4 Future research directions for constraining dust

Improved model performance demands stronger observational constraints on the global dust cycle. While expanding the geographical coverage of paleo dust records remains important—particularly in poorly sampled regions such as downwind of Southern Hemisphere source regions—there is an especially urgent need for additional dust deposition records that span the PI to PD period. Such records are currently scarce, with only 19 available in a recent compilation (Figure 1 and Kok et al., 2023), yet aerosol radiative effects during this interval play a critical role in constraining climate sensitivity (Sherwood et al., 2020). More generally, proxy records with sufficient temporal resolution to capture key climate transitions such as the last glacial termination (LGM to Holocene transition), millennial-scale variability, and abrupt events, are critically needed, as dust changes across these transition periods provide an important benchmark for transient climate simulations and constrain potential aerosol feedbacks. In addition to expanding coverage, much can be learned from the development of a limited number of well-characterized paleo dust "super-sites", such as EPICA Dome C (Delmonte et al., 2008; EPICA community members, 2004; Lambert et al., 2008, 2012; Lanci et al., 2008; Potenza et al., 2016, 2025). At such sites, multiple dust-related properties - including deposition rate, grain size, mineralogy, and geochemistry - can be quantified consistently on the same samples or at least at the same site, providing powerful multi-constraint datasets. Such records are critical for constraining changes in the radiative effect efficiency across climate states, for example due to changes in dust size distributions and optical properties.

Large uncertainties remain in paleo dust deposition rates inferred from proxy records (Albani et al., 2015; Cosentino et al., 2024). At the same time, complementary observational constraints, such as dust provenance information from geochemical and isotopic tracers have expanded rapidly (e.g., Delmonte et al., 2008; Xie and Marcantonio, 2012; Torre et al., 2022; Újvári et al., 2022; Rousseau et al., 2025). These observations provide independent information on dust source regions and transport pathways beyond the deposition constraints on which current reconstructions primarily rely, offering

Formatted: Default Paragraph Font, Font color: Black

Formatted: Normal, Centered, Border: Top: (No border), Bottom: (No border), Left: (No border), Right: (No border), Between : (No border), Tab stops: 3.25", Centered + 6.5", Right, Position: Horizontal: Left, Relative to: Column, Vertical: In line, Relative to: Margin, Wrap Around

Formatted: Font color: Black

opportunities to test prior assumptions and identify model biases. Inversion frameworks are well suited to integrate such information to penalize physically inconsistent solutions. This approach can produce more robust and physically interpretable paleo dust reconstructions with reduced uncertainty that can be propagated forward into model-based estimates of dust aerosol radiative forcing.

More broadly, inversion-based methods are not only a tool for reconstructing dust fields, but also provides a quantitative framework for evaluating how existing or potential observations constrain model reconstructions, which can help guide future sampling strategies. For candidate sites that are physically feasible for new measurements, one strategy is to examine the sink–source sensitivity patterns: optimal sites are those where sensitivity patterns are not well represented by combinations of patterns from existing sites, indicating that they add new, non-redundant information (Park and Kim, 2020). In addition, full inversions can be used to evaluate how including new sampling sites would influence posterior uncertainty in dust reconstructions. Sites that lead to meaningful reductions can therefore be considered valuable for improving reconstructions (Gloor et al., 2000). As a caveat, model-based decisions rely heavily on simulated transport and the resulting source-sink sensitivities, so comparison with multiple model results is recommended in practice to reduce biases and uncertainties associated with any single model.

To enable robust model benchmarking and inversion studies, paleo dust datasets must be published in forms that support recalculation and uncertainty propagation. This requires the availability of raw or minimally processed data, explicit uncertainty estimates (including flags for unquantifiable uncertainties), and assessments of spatial representativeness. Measurements of particle size distributions and mineralogical composition are particularly critical for constraining transport processes and the dust radiative forcing efficiency, and should therefore be prioritized.

4 Fires

Fire is a fundamental Earth system process that has shaped Earth's ecosystems for millennia (Bowman et al., 2009). While fire modulates the global carbon cycles through diverse land-atmosphere-ocean interactions, here we focus on fires' role in influencing the planet's energy balance and cloud formation processes through aerosol emissions (Lohmann et al., 2005; Andreae & Rosenfeld, 2008). Among these, black carbon (BC) and organic aerosols (OA) have received particular attention because biomass burning is a major atmospheric source of both components, especially prior to industrialization (Hamilton et al., 2018; Van der Werf et al., 2017). Fire aerosol REari is estimated to be slightly negative to slightly positive at the global scale under all-sky conditions (Ward et al., 2012; Rap et al. 2013), primarily due to absorption by BC and the light-absorbing fraction of OA (brown carbon, BrC) being relatively balanced by the light-scattering fraction of OA. Whereas REaci is typically estimated to be negative, largely driven by the influence of primary and secondary OA on cloud properties, although with substantial uncertainties (Jiang et al., 2020).

While uncertainties in fire aerosol radiative effects also depend on aerosol optical properties, mixing state, and cloud processes, in this section we primarily focus on uncertainties in fire emissions, which remain challenging for reconstructing past atmospheric states (Andreae & Rosenfeld, 2008; Van der Werf et al., 2013). Fire emission datasets used in (paleo)climate modeling studies have often assumed a relatively “unpolluted” PI world with lower or similar fire activity to today (van Marle et al., 2017), but a growing body of proxy evidence, including charcoal, ice-core chemistry, biomarkers, and tree-ring fire scars, suggests greater fire activity in many regions during the late 18th to 19th Century compared to the late 20th and early 21st Century (Hamilton et al., 2018, Liu et al., 2021; Marlon et al., 2009; Zennaro et al., 2014; Margolis et al. 2022; Parks et al. 2025), raising questions about estimates of fire-derived aerosol loading and associated radiative forcing. In addition, observational constraints become increasingly sparse for earlier periods extending back to the LGM, leaving fire emissions much more poorly constrained.This

Formatted: Default Paragraph Font, Font color: Black

Formatted: Normal, Centered, Border: Top: (No border), Bottom: (No border), Left: (No border), Right: (No border), Between : (No border), Tab stops: 3.25", Centered + 6.5", Right, Position: Horizontal: Left, Relative to: Column, Vertical: In line, Relative to: Margin, Wrap Around

Formatted: Font color: Black

section is organized into four parts: source of uncertainty in modeled fire emissions; evidence from fire proxies and their implications for PI fire activity; what recent reconstruction efforts have achieved; and remaining gaps and challenges. We then discuss future directions for model-data integration and consider how methodological advances, including machine learning may help improve reconstructions and reduce uncertainties.

4.1 Modeling of fire aerosols

4.1.1 The Pre-Industrial Fire Modeling Problem

Simulation of spatially and temporally continuous global fire regimes pre satellite-era (pre-1997, when the satellites acquired sufficient temporal and spatial coverage of appropriate variables) requires the use of fire models. However, fire models remain largely unconstrained for pre-industrial conditions because they have been formulated and evaluated primarily against satellite-era observations in a world with pronounced anthropogenic influence on fire (Hantson et al. 2020). The trajectory from preindustrial to present involves multiple interacting changes on the fire landscape; from changing pasture and agriculture-related deforestation and burning, to shifts associated with Indigenous burning practices (Mariani et al., 2022), from continuous landscapes to fragmented mosaics (Bowring et al., 2024), and from frequent low-intensity surface fires to infrequent high-intensity crown fires (Steel et al., 2015; Hessburg et al., 2005). All of these uncertainties propagate into simulations of fire occurrence, burned area, fire intensity, fuel consumption, and ultimately fire-derived aerosol emissions.

Implementing all of these processes in a unified modelling framework is a non-trivial task and here we identify some the key challenges to constrain and improve historical simulations of fire activity:

1) spatially inhomogeneous trends and sign reversals in human influence (Gammage, 2011; Gott, 2005; Mariani et al., 2022). While many Indigenous populations used fire for landscape management and these practices were often adopted by early settlers, these trends changed with time with permanent land use, high intensity grazing, and fire suppression policies leading to a decline in fire through the late 19th and 20th centuries (Kaplan et al., 2016, Taylor et al., 2016, Stambaugh et al., 2018).

2) fuel structure transformation: In many contexts, human impacts to fire regimes fundamentally altered forest, and wider landscape structure (Hessburg et al., 2005; van Wagtendonk & Lutz, 2007), leading to a change in fire regimes (Clements et al., 2018; Kreider et al., 2024), combustion efficiency , moisture content and black carbon emission percentages (Akagi et al., 2011; Urbanski 2013; Ottmar 2014);

3) fragmentation and fire size distributions: The modern fragmented landscape constrains individual fire sizes while altering ignition patterns and intensity (Bowring et al., 2024; Povak et al., 2018), compared with PIfires (Parks et al., 2025);

4) compound interactions: Fire suppression, fragmentation, and fuel accumulation interact synergistically through positive feedbacks and threshold effects (Kreider et al., 2024; Williams et al., 2019);

5) pathway dependence: The specific trajectory by which fire regimes transitioned from PIto PD(e.g. through cropland expansion or fire suppression) (Pfeiffer et al., 2013; Hantson et al., 2020). Fig. 3 illustrates the influence of land use on fire regimes in late Preindustrial North America with especially pronounced differences in central Mexico and the eastern United States where land use was most intensive already by 1850.

4.1.2 The LGM Fire Modeling Problem

Going further back toward the LGM presents a different set of issues, starting with CO_2 sensitivity. Under low CO_2 conditions, C_3 plants experience reduced photosynthetic efficiency and higher stomatal conductance to retain pre-ice age equivalent carbon assimilation (Ma et al., 2021; Knorr et al., 2016). Modern fire models typically link fuel moisture to climate inputs (e.g., vapor pressure deficit, precipitation, soil moisture) calibrated at ~400 ppm CO_2, where fertilization buffers plant water stress. At

Deleted: ¶

Deleted: regime

Formatted: Default Paragraph Font, Font color: Black

Formatted: Normal, Centered, Border: Top: (No border), Bottom: (No border), Left: (No border), Right: (No border), Between : (No border), Tab stops: 3.25", Centered + 6.5", Right, Position: Horizontal: Left, Relative to: Column, Vertical: In line, Relative to: Margin, Wrap Around

Formatted: Font color: Black

LGM levels, these relationships fail (Gerhart & Ward, 2010), although the magnitude of this difference is not clear (Swann et al., 2016; Mankin et al., 2017). In addition, the absence of megaherbivore grazing in modern models might mean fuel loads are overestimated for the LGM (Gill et al., 2009; Johnson, 2009; Malhi et al., 2016; Archibald & Bond, 2004; Staver et al., 2011).

The physics of fire spread in sub-zero, high-wind environments (i.e., katabatic winds from ice sheets) is also poorly represented in models developed for temperate/tropical biomes, and during the LGM one would expect more regions to be impacted by this bias (Parish & Waight, 1987; Parish & Bromwich, 2007), creating fire-spread environments with no modern analog. In addition, lightning ignition rates were likely different than today in colder LGM climates, depending on the mechanism assumed (Pérez-Invernón et al., 2023; Price and Rind, 1994; Price, 2009; Veraverbeke et al., 2017); human ignition rates are also unknown during the LGM. Large shifts in land area also affect biomass burning, as there was 8% more land exposed during the LGM due to lower sea level (Peltier & Fairbanks, 2006; Bird et al., 2005), while high latitudes had periglacial regions that could have fragmented landscapes and limited fire spread. Fig. 3 shows that fire may have been widespread in the unglaciated parts of North America with especially notable increases in fire relative to the Holocene in the desert southwest, which was significantly wetter at the LGM.

4.1.3 Agricultural Burning

A potentially large and often underrepresented source of uncertainty in fire emission reconstructions is agricultural burning, which releases high fractions of accumulation-mode aerosol and can contribute substantially to total fire emission budgets (Sahu et al., 2008). For purposes such as field clearing and residue management, agricultural biomass is commonly burned after harvest in many regions. In some cases, the mass of agricultural residue burned can exceed harvested crop yield mass, as has been estimated for present day regions such as India (Jethva et al., 2019). Disentangling human-driven agricultural burning from landscape fire contributions is particularly challenging because agricultural fires were present in both the PI and PD periods, but the spatial pattern of burning has likely changed significantly and heterogenously. As a result, paleofire data alone cannot easily distinguish between these two aerosol sources of aerosol.

Ambiguity of past emissions from agricultural burning is further compounded by large variability in changing crop types, agricultural practices, and legislation proscribing fire use in agriculture (Koopmans & Koppejan, 1997; Venkataraman et al., 2006). Temporal variability introduces uncertainty because fires can vary strongly by season or day (Kharol et al., 2012; Sahu et al., 2008). Over multidecadal scales, agricultural practices can significantly alter aerosol emissions, as demonstrated during India's Green Revolution (Liu et al., 2021).

Europe provides a useful illustration of the regional importance of agricultural burning and land clearing, contributing between 2.7% and 11.6% of European winter PM_{10} at present day (Cordell et al., 2016). Historically, extensive land clearing using fire occurred in Europe between 1000 and 1800 CE, during which 10–30% of forests were converted for agriculture and urbanization (Kaplan et al., 2009, 2017). In contrast to Europe, large-scale deforestation in North America occurred primarily after 1850 (Ryan et al., 2013). When agricultural burning is omitted or treated simplistically, models may misattribute BC signals recorded in ice cores or sediments to landscape fires alone, leading to potentially biased estimates of PI fire activity. Accurately representing agricultural burning therefore requires not only improved emission factors and combustion parameters, but also better constraints on historical land-use practices and their spatial evolution. Integrating agricultural burning more explicitly into fire emissions inventories is likely essential for reconciling discrepancies between proxy records and modeled fire emissions, particularly in regions with extensive human land-use change.

Formatted: Default Paragraph Font, Font color: Black

Formatted: Normal, Centered, Border: Top: (No border), Bottom: (No border), Left: (No border), Right: (No border), Between : (No border), Tab stops: 3.25", Centered + 6.5", Right, Position: Horizontal: Left, Relative to: Column, Vertical: In line, Relative to: Margin, Wrap Around

Formatted: Font color: Black

4.2 Paleoproxy reconstructions of fires

Motivated by growing evidence that commonly-used fire emissions inventories may underestimate past fire activity, several recent studies have sought to reconstruct fire emissions using combinations of paleoenvironmental archives and modeling approaches. While subject to many uncertainties, these studies tend to agree on several features of fire regime changes between the PI and PD. These include: (1) higher fire emissions in both the PI Northern and Southern Hemisphere (Hamilton et al., 2018; Liu et al., 2021; Zhang et al., 2024); (2) greater temporal variability in the Southern Hemisphere and boreal Asia than presently estimated (Eckhardt et al., 2023; Zhang et al., 2024); and (3) an overall global-scale decline in burned area throughout the 20th Century (Arora and Melton 2018), despite rapid population growth.

Most existing fire histories are inferred either directly from trends in paleo records (Grieman et al., 2018; Zennaro et a., 2014), from proxies that reflect aspects of fire activity rather than fire aerosol emissions or atmospheric loading themselves (Marlon et al., 2008; Marlon et al., 2016; Parks et al., 2025), or from tuning atmospheric concentrations in simplified box models to match relatively spatially homogeneous gas-phase records (Ferretti et al., 2005; Wang et al., 2010; Nicewonger et al., 2020a,b). Although these approaches provide a broad picture of past fire trends, they generally yield only qualitative or partially quantitative estimates of fire emissions at coarse spatial and temporal resolution.

Directly translating spatially sparse and heterogeneous paleofire records into Cartesian coordinate gridded fire emission datasets for model applications is challenging due to the diversity of fire proxies and their varied spatial sourcing (Marlon et al., 2016). Inverse modeling has helped bridge this gap by linking observational records of BC in ice cores to atmospheric aerosol loading and fire emissions through model-simulated source–sink sensitivities (Eckhardt et al., 2023; Zhang et al., 2024), producing emission reconstructions with improved agreement with observations and publicly available datasets (Zhang and Liu, 2024). These spatially and temporally resolved emission datasets can be directly incorporated into climate models to evaluate the implications of fire-emission uncertainties for aerosol loading and aerosol radiative forcing, particularly through changes in cloud-albedo forcing (Hamilton et al., 2018; Liu et al., 2021). Such changes may further affect the partitioning of historical climate forcing between greenhouse gases and aerosols, with implications for estimates of climate sensitivity (Smith et al., 2020a).

However, three main challenges remain in the ice-core BC based reconstructions. First, ice-core BC reflects mixed contributions from both biomass burning and fossil fuel sources, introducing uncertainty into reconstructed fire histories, particularly during the industrial era. Second, the spatial representativeness of currently available ice core BC records remains limited, partially because of the relatively short atmospheric lifetime of BC (4-7 days; Lund et al., 2018; Samset et al., 2014). Emissions from some major fire source regions (e.g., the Sahel and tropical West Africa, Central Asia, and Southeast Asia) are not effectively captured with currently available ice-core sites, leaving those regions largely unconstrained (Zhang et al., 2024). Third, because ice core records are measured at remote receptor sites, they provide limited information on fine-scale spatial patterns of emissions, and current reconstructions generally constrain emissions only at broad regional to continental scales. Finer-scale emission patterns within those regions remain strongly dependent on the prior inventory or model simulation. This limitation is particularly important because aerosol forcing efficiency is spatially heterogeneous (Wan et al., 2021), and emission reconstructions with similar agreement with those hemispheric-scale ice-core records may still produce different radiative forcing estimates, particularly when they differ in the representation of local emission hot spots (Wan et al. 2020; Zhang et al., 2024).

Additional information on past fire activity can be obtained from other proxy archives. Beyond rBC, ice-core archives preserve a variety of atmospheric tracers that have been used to infer past fire activity, including long-lived trace gases (e.g., CO, CH_4, and carbon isotopes; Wang et al., 2010; Ivo et

Deleted:

Formatted: Default Paragraph Font, Font color: Black

Formatted: Normal, Centered, Border: Top: (No border), Bottom: (No border), Left: (No border), Right: (No border), Between : (No border), Tab stops: 3.25", Centered + 6.5", Right, Position: Horizontal: Left, Relative to: Column, Vertical: In line, Relative to: Margin, Wrap Around

Formatted: Font color: Black

al., 2024), short-lived organic gases (e.g., ethane, acetylene; Nicewonger et al., 2018, 2020a,b), and organic species (e.g., levoglucosan, vanillic acid, para-hydroxybenzoic acid; McConnell et al., 2007a; Kawamura et al., 2012; Grieman et al., 2018; Zennaro et al., 2014). Compared with BC, some species may capture broader spatial signals due to a longer atmospheric lifetime. However, these records are currently more sparse in both space and time and often involve additional uncertainties associated with non-fire sources and atmospheric chemical processing. As a result, their interpretation is generally less direct than for BC. At present, these tracers are perhaps most useful as independent tests of BC-based fire reconstruction (McConnell et al., 2007a; Strawson et al., 2024) or where no BC ice core records exist (Liguori-Bills et al. 2026).

Beyond ice-core records, sedimentary charcoal and tree-ring fire-scar records provide information on past fire regime change across regions where ice-core archives are unavailable, thereby complementing the limited spatial coverage of ice-core records. However, their signals are strongly influenced by local environmental factors, fire characteristics, and archive-specific processes, often resulting in substantial variability among nearby records and requiring careful standardization and synthesis to derive robust regional trends. Moreover, these proxies generally reflect aspects of fire occurrence, frequency, or ecosystem disturbance more directly than atmospheric aerosol loading itself, and methodologies to more directly link to the atmospheric state variables needed for aerosol emissions reconstruction and model constraint needs continued development.

A single proxy provides only a partial view of past fire activity across space, time, and fire characteristics. To date, multiple proxies have rarely been integrated within a unified framework, despite their potential to provide a more complete picture of past fire regime change when used in combination. Such integration, however, introduces several additional challenges. First, they differ substantially in spatial representativeness, with tree-ring and charcoal records often reflecting relatively local source areas on the order of tens of kilometers (Margolis et al., 2022; McBride, 1983; Vachula 2021) whereas ice-core records typically integrate signals at regional to hemispheric scales (Legrand et al., 2016). Second, these proxies are linked to different aspects of fire, and their signals are shaped by different processes of production, transport, deposition, preservation, as well as by local environmental conditions, thus often requiring different interpretive frameworks (Marlon, 2020). Third, the underlying age models differ across archives, complicating direct comparison across records. Finally, publicly available datasets are still incomplete and often lack standardized metadata and uncertainty quantification.

Formatted: Default Paragraph Font, Font color: Black

Formatted: Normal, Centered, Border: Top: (No border), Bottom: (No border), Left: (No border), Right: (No border), Between : (No border), Tab stops: 3.25", Centered + 6.5", Right, Position: Horizontal: Left, Relative to: Column, Vertical: In line, Relative to: Margin, Wrap Around

Formatted: Font color: Black

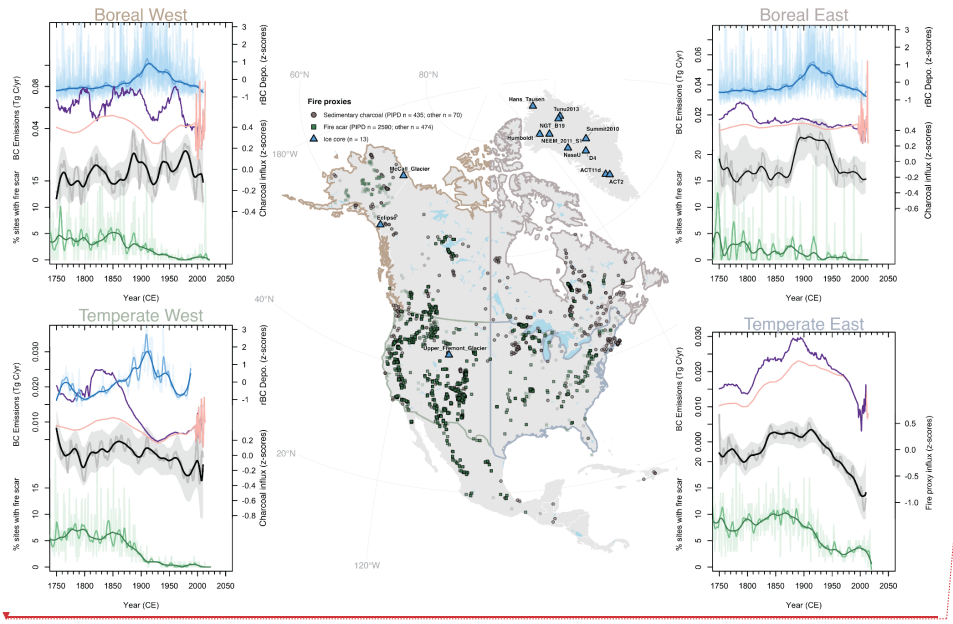

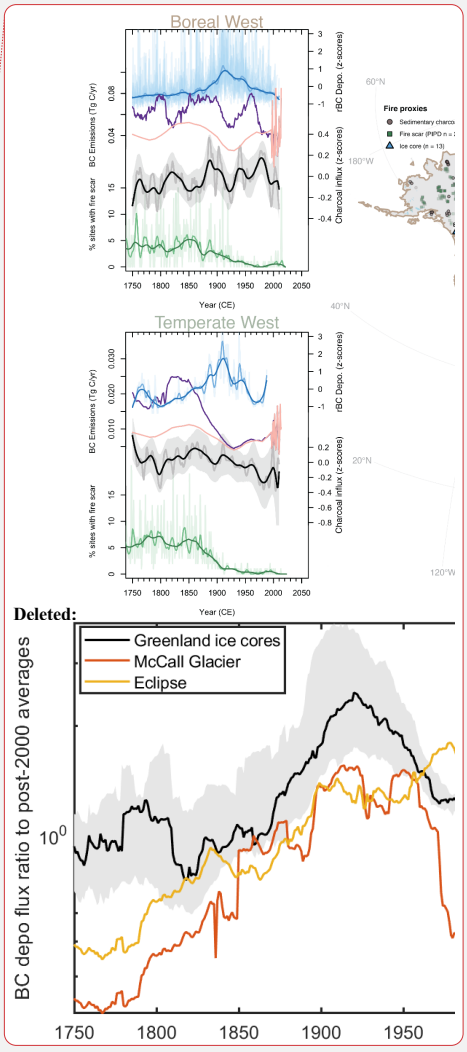

Figure 2. *Multiproxy paleofire history of North America. Map depicts the distribution of paleofire proxy sites: fire scars site in the North American Tree-Ring Fire-Scar Network (green squares) Margolis et al. 2022, influx of charcoal to lake sediments (black circles) from the Reading Paleofire Database (Harrison et al. 2022), and black carbon deposition rates in ice cores (blue triangles) (Zhang et al. 2024). Site markers with black outlines contain data within the pre- to post-industrial interval (1750 - 2010). Sites are categorized into four regions: boreal west, boreal east, temperate west, and temperate east in order to compare with model predictions of North American biomass burning emissions. Stacked time series plots for each region show black carbon deposition rates for individual ice cores (light blue) and smoothed curves in darker blue (Zhang et al. 2024), note Greenland ice cores are sensitive to fire emissions in both boreal regions and are therefore plotted in both; inverse-modeled regional biomass burning emissions rates based on ice core records (purple) and simulated regional biomass burning emissions (pink) (Zhang et al. 2024); lacustrine charcoal influx z-scores (black, dark grey) with 95% bootstrapped confidence intervals (light gray) from Harrison et al. (2022), regionally synthesized following methods described in Power et al. (2008); percentages of sites in the North American Tree-Ring Fire-Scar Network which contain a fire scar (light green, with smoothed curves in dark green) (Margolis et al., 2022) . All smoothed curves were calculated using a LOWESS smooth with 10-year (lighter color) and 30-year (darker color) windows.*

We illustrate the opportunity and challenge of using a mixed-proxy fire reconstruction using a North American example (Figure 2), where the histories of Greenland and Alpine ice core records overlap with extensive charcoal and tree-ring paleofire datasets. In addition to showing the spatial availability of different proxy types, we compare integrated trends from charcoal, tree-ring, and ice core records with both commonly used biomass burning emissions in CMIP6 and ice core based reconstructed fire emissions (Zhang et al., 2024). In temperate North America, where tree-ring and charcoal records are relatively dense and allow more robust characterization of regional trends, these proxies show broadly

Formatted: Default Paragraph Font, Font color: Black

Formatted: Normal, Centered, Border: Top: (No border), Bottom: (No border), Left: (No border), Right: (No border), Between : (No border), Tab stops: 3.25", Centered + 6.5", Right, Position: Horizontal: Left, Relative to: Column, Vertical: In line, Relative to: Margin, Wrap Around

Formatted: Font color: Black

similar behavior of relatively stable fire activity ca. 1750-1850, followed by a decline thereafter. Ice-core records from western U.S. glaciers show a similar early history but diverge during the late nineteenth and early twentieth centuries, resulting in a pronounced peak around the 1920s driven largely by anthropogenic emissions. After separating biomass burning and anthropogenic contributions from the mixed BC signal using a Bayesian inversion framework, the reconstructed biomass-burning emissions broadly track the trends inferred from the charcoal and tree-ring records (Zhang et al., 2024). In boreal North America, however, discrepancies across proxies are larger. Tree-ring records suggest a relatively stable or decreasing trend, whereas charcoal records show greater temporal variability. Greenland ice core records show a similar BC peak around 1920 to that seen in western U.S. glacier records, reflecting increased North American anthropogenic emissions. In contrast, ice-core records from North American glaciers show an additional post-1950 peak, with timing more consistent with increasing anthropogenic emissions from Asia. This pattern illustrates that ice core BC can reflect mixed contributions from multiple source regions and source categories. Reconstructed emissions based on ice core records also show greater temporal variability, but uncertainties are likely larger because attribution of the observed BC signal depends on assumptions regarding the relative contributions of biomass burning and anthropogenic sources, as well as contributions from different source regions. Together, this example illustrates both the value and the challenges of integrating multiple proxy archives. Broad agreement among several independent proxy records provide support in reconstructed regional fire histories and suggest that fire emissions in North America are likely to be underestimated in the fire inventories currently prescribed in models. At the same time, discrepancies among proxy types highlight regions and periods where uncertainties remain large.

4.3 Pre-Industrial to LGM and Mid-Holocene Fire Reconstruction

Simulations of fire in North America using LPJ-LMfire (Pfeiffer et al., 2013) forced with the PMIP4 multi-model mean climate indicate that fire was ubiquitous during the LGM despite reduced vegetation productivity under low CO2 concentrations (~180ppm), colder temperatures, and the expansion of ice sheets over formerly vegetated land. The spatial pattern of fire also shifts further back in time: more burned area is simulated towards coastal regions while reduced burned area is simulated within parts of the inner continent. Over North America (Figure 3), the Laurentide Ice Sheet covers most of the continent north of ~45°N, effectively eliminating fire in those regions except for Alaska/Yukon regions. Where ice-free land remains, burned area fractions generally fall within the range of 0-30%, concentrated below 35 degrees North in the southern United States, Mexico, and Central America. The northwestern United States, which had extensive paleolakes under the wetter LGM climate, shows minimal fire activity. Conversely, at the mid-Holocene fire burned area is reduced compared to the PI (with no land use) and with a more similar spatial distribution but with expansion toward Florida and the South East. The impact of PI human land use is examined through suppression of fire on managed landscapes (i.e., agricultural, pasture, rangeland, and urban areas). While the impact of human land use is a known driver of fire reduction over the Industrial era, these simulations highlight that a reduction in burned area could already have been imposed before PI, confounding the definition of what constitutes a PI baseline and further highlighting the need for cross-disciplinary initiatives to fully understand changes in natural aerosol regimes over centennial-to-millennia scales.

Formatted: Default Paragraph Font, Font color: Black

Formatted: Normal, Centered, Border: Top: (No border), Bottom: (No border), Left: (No border), Right: (No border), Between : (No border), Tab stops: 3.25", Centered + 6.5", Right, Position: Horizontal: Left, Relative to: Column, Vertical: In line, Relative to: Margin, Wrap Around

Formatted: Font color: Black

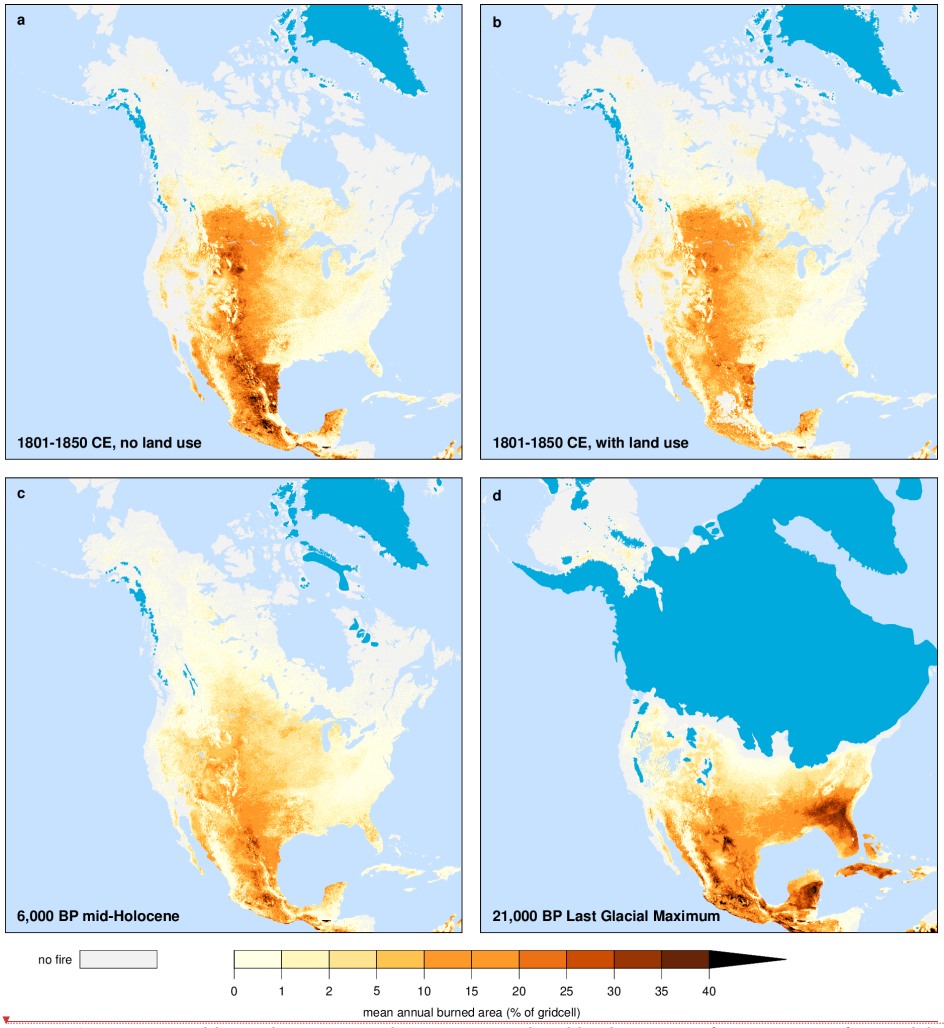

Figure 3 *Mean annual burned area in North America simulated by the LPJ-LMfire vegetation-fire model (Kaplan, 2026). Results are presented for the late preindustrial era (1801-1850 CE) (**a**) without land use, and (**b**) in a scenario where land use leads to fire suppression. Panel (**c**) shows mean annual burned area at the mid-Holocene (6 ka) using a paleoclimate simulation from GISS Model E2-R, and (**d**) burned area at the Last Glacial Maximum (21ka) using paleoclimate from the INM-CM4-8 model. For the 6 and 21 ka simulations burned area is averaged over a 180-year period.*

4.4 Future directions

Looking ahead, historical fire emission reconstructions could be improved along two complementary avenues of research.

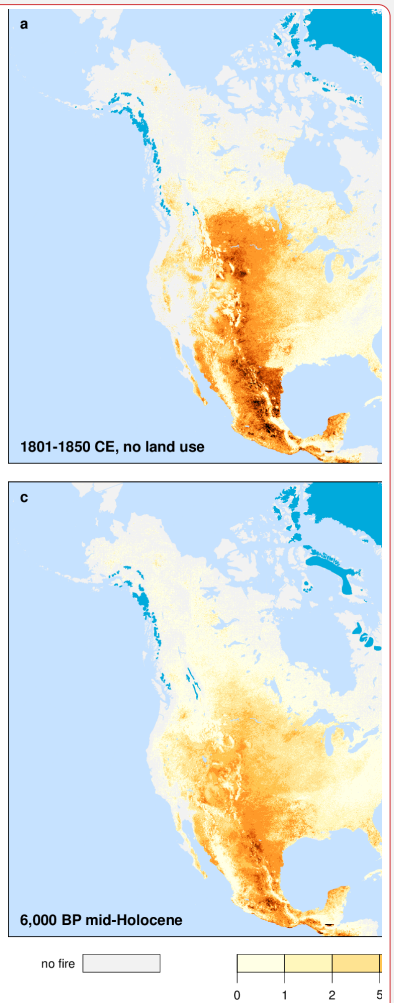

Deleted: me

Formatted: Default Paragraph Font, Font color: Black

Formatted: Normal, Centered, Border: Top: (No border), Bottom: (No border), Left: (No border), Right: (No border), Between : (No border), Tab stops: 3.25", Centered + 6.5", Right, Position: Horizontal: Left, Relative to: Column, Vertical: In line, Relative to: Margin, Wrap Around

Formatted: Font color: Black

Inverse-modeling-based constraints could be expanded by the incorporation of additional proxy information. For ice core records, additional sites in other locations, if available, would be especially valuable. For example, records from the Tibetan Plateau could help capture biomass-burning signals from central and southern Asia, which are not well constrained by the current ice-core network. Ice core records of other tracers, such as trace gas with longer atmospheric lifetimes, may improve the estimate of BB at broader, hemispheric scales.capture broader spatial source signals. Together, trace-gas records that constrain large-scale emissions and aerosol records that are more sensitive to nearby source regions could help reduce uncertainty in regions that remain weakly constrained by the current network. For charcoal and tree ring records, further efforts may focus on using these archives more systematically within Bayesian frameworks as indirect constraints on fire emissions. For example, they can inform the regional specification of prior uncertainty such that regions where multi-proxy evidence suggests larger disagreement with model-based fire histories are assigned higher prior uncertainty and greater flexibility in the inversion. In addition, in the underconstrained or ill-posed regions, proxy evidence can help narrowing solution space by ruling out solutions that are inconsistent with the broader multi-proxy records, even when these solutions provide similar good agreement with ice core BC records. Besides, because these archives are more directly related to fire activity than to anthropogenic emissions, they may help constrain broad fire trends and thereby improve separation of fire and anthropogenic signals, particularly during the industrial period when ice-core-BC-based reconstructions are most uncertain. In the near term, these approaches are likely to be most useful as complementary information that helps refine, regularize, and interpret rBC-based inversions, rather than as direct constraints on atmospheric aerosol emissions themselves.

More broadly, there is a clear need for integrated fire datasets that harmonize multiple proxy types to improve spatial and temporal coverage and reduce uncertainty. Future datasets should incorporate features discussed more broadly later in Section 7.4 while addressing fire-specific requirements, including explicit guidance on how individual proxies relate to different model variables. Clear documentation of proxy–model linkages would allow new measurements to be more effectively used to evaluate and improve model performance, helping to bridge observational and modeling communities. Integrated, multi-proxy fire datasets are therefore essential for reconciling discrepancies between proxy evidence and modeled emissions and for advancing our understanding of historical fire dynamics.

4.4.1 Emerging Machine Learning Techniques

Machine learning algorithms are useful tools for identifying anomalous patterns in complex datasets, a capability that can be applied for improved quality control in paleoenvironmental reconstructions. Unsupervised clustering techniques, for example, can segregate proxy records into distinct groups based on their multivariate characteristics, revealing hidden structures in the data that might represent different depositional environments, preservation conditions, or source region characteristics. Computer vision algorithms equipped with anomaly detection capabilities can identify and classify, for example, charcoal morphotypes, which may potentially indicate rare fuel types, extreme combustion conditions, or contamination from non-fire sources such as coal fragments in post-industrial sediments. These techniques have the potential to serve as quality control filters to flag suspicious proxy values that warrant further investigation, identify records that fall outside expected statistical distributions, or detect abrupt regime shifts in fire activity that might signal major climate transitions or ecosystem reorganizations.

Machine learning excels at constructing patterns from incomplete (proxy) data records. In data driven machine learning models, fire related climate factors, such as temperature, relative humidity, and vapor pressure deficit, could be simultaneously integrated with satellite observations and/or multiple proxy types, such as sedimentary charcoal, ice core black carbon, and tree-ring fire scars, to learn complex transfer functions and apply them to reconstructions. As a result, machine learning models have

Formatted: Default Paragraph Font, Font color: Black

Formatted: Normal, Centered, Border: Top: (No border), Bottom: (No border), Left: (No border), Right: (No border), Between : (No border), Tab stops: 3.25", Centered + 6.5", Right, Position: Horizontal: Left, Relative to: Column, Vertical: In line, Relative to: Margin, Wrap Around

Formatted: Font color: Black

shown promising performance in reproducing spatial distributions, seasonality, and interannual variability of fire patterns and emissions, outperforming traditional statistical and process-based models (Illarionova et al., 2025; Lampe et al., 2025; Wang et al., 2022).

Recent developments in explainable machine learning are improving our understanding of fire occurrence and emissions by identifying the dominant controlling factors across different scales and regions. In explainable machine learning, feature importance analysis through methods like SHAP (SHapley Additive exPlanations) values and permutation importance move beyond black-box predictions to provide mechanistic insights into fire dynamics (Breiman, 2001; Ribeiro et al., 2016). For example, feature importance analysis highlights the influence of urban proximity, wind patterns, and meteorological conditions related to fuel moisture on fire size prediction (Cilli et al., 2022; Malashin et al., 2025; Moghim and Mehrabi, 2024), with anthropogenic factors playing indirect roles compared to natural drivers in some regions.

4.5 Interactions between fire and dust aerosols

Fire and dust do not merely co-occur in the atmosphere; in some cases, they can affect the other. Dust emissions can be initiated by fires, which alter the meteorological conditions and land surface properties that facilitate dust uplift (Wagner et al. 2018; 2025; Wagenbrenner et al., 2025). The mass of the dust emitted to the atmosphere due to fire is currently highly uncertain, with potentially up to two orders of magnitude uncertainty (Hamilton et al. 2022). Fire enhances dust emissions through two pathways: (i) the intense lofting and entrainment processes that occur due to localized heating during an active burn, and (ii) the creation of newly erodible surfaces in post-fire landscapes (Meng et al., 2025).

During active burning, intense heating can generate pyro-convective updrafts that loft smoke away from the surface. The chemical composition of this smoke reflects both the combustion of fuels on the landscape and any dust entrained from the surrounding environment, whether lifted from the soil into the plume due to strong horizontal wind speeds or resuspended from prior deposition on vegetative surfaces (Hamilton et al. 2022). The intensity of the fire determines the strength of the updrafts, with exceptionally intense fires even being able to create aerosol transport pathways to the stratosphere via formation of pyrocumulonimbus clouds (Fromm et al. 2022).

After a severe fire, the removal of vegetation can expose bare soil, allowing dust emissions to continue until the ecosystem recovers. The magnitude and persistence of these post-fire dust emissions varies greatly with geographical setting, local meteorological conditions, and the length of the revegetation period (Whicker et al., 2006; Dukes et al.2018). As grasslands ignite easily, and their fine structured fuel are more readily consumed than forests, dust emitted from post-fire landscapes is majorly associated with savannah ecosystems (Yu and Ginoux 2022). However, sufficiently intense fires, such as the 2019–2020 Australian megafires (Weis et al. 2022), demonstrate that even forest biomes can produce substantial dust during and following fire. Fire therefore creates both an instantaneous and legacy impact on dust emissions that can last for days to months, or even potentially years, depending on the biome and severity of fire.

The broader impact of dust aerosol emitted within or after a fire on climate is not well understood. Aircraft measurements suggest the majority (approximately two-thirds) of the iron within fire plumes is likely to be of dust origin (Hamilton et al. 2022), affecting direct radiative forcing estimates and influencing the global carbon cycle through ocean fertilization when deposited in regions where iron is the limiting nutrient for phytoplankton growth (Hamilton et al. 2020; Rathod et al. 2022). The radiative implications of mixing dust and combustion products in hot smoke plumes are also poorly constrained. These internally-mixed particles (e.g., tarballs) might have radiative effects that differ significantly from the sum of each species, with indications that this is the case for ice nucleating ability (Burrows et al.

Formatted: Default Paragraph Font, Font color: Black

Formatted: Normal, Centered, Border: Top: (No border), Bottom: (No border), Left: (No border), Right: (No border), Between : (No border), Tab stops: 3.25", Centered + 6.5", Right, Position: Horizontal: Left, Relative to: Column, Vertical: In line, Relative to: Margin, Wrap Around

Formatted: Font color: Black

2022; Schill et al. 2020). Inclusion of mineral dust will generally facilitate ice nucleating ability, as will minerals formed during the combustion of plant material (Jahn et al. 2020), while organic coatings can disable ice nucleating active sites (Möhler et al., 2008). The interactions between chemical species in agglomerates are difficult to fully disentangle. Hence more observations are needed to understand these processes and also how they could have changed through time.

The impact of fire on dust may change during different time periods, as fire regimes shifted in the colder, drier world of the Last Glacial Maximum (Figure 3). Additionally, vegetation grows back slower in colder climates, potentially extending the period for post-fire dust. These instantaneous and legacy impacts of fire on dust emissions and thus climate can only be captured in models that couple fire and dust processes within a vegetation framework; a current gap for many Earth System models. Moreover, the coupling of these two Earth System cycles again highlights a need for interdisciplinary teams to collaborate to fully appreciate the impacts of changes to natural aerosol cycles over time and under human influence.

5 Volcanic sulfate aerosols and ash

Volcanic emissions, primarily SO_2, can increase the aerosol load in the stratosphere and shield the Earth from incoming shortwave radiation and exert a negative radiative forcing on the climate, resulting in a global net cooling at the surface (Marshall et al., 2022; Robock, 2000) that is often referred to as a "volcanic winter" (Rampino et al., 1988). SO_2 injected into the stratosphere by powerful eruptions is oxidized into sulfuric acid aerosols, that are distributed globally and can persist for months to years after the eruption, making volcanism the dominant external driver of global climate on seasonal-to-centennial timescales during the preindustrial (Schurer et al., 2014; Sigl et al., 2015; van Dijk, et al. 2024). Cold extremes have been associated with historical eruptions (Guillet et al., 2017; McCormick et al., 1995; Symons, 1888) including Pinatubo (Philippines, 1991), Krakatau (Indonesia, 1883), Tambora (Indonesia, 1815) and Samalas (Indonesia, 1257), which rank among the most powerful volcanic eruptions known in history (Newhall et al., 2018; Newhall and Self, 1982). However, knowledge about these eruptions becomes ever more uncertain with increasing age, as both geological traces and historical sources become scarcer (Deligne et al., 2010).

Ice cores from Greenland and Antarctica provide some of the most precise continuous timelines of past volcanism **(Figure 4)**. Sulfuric acid deposits in ice cores have been correlated to known historical eruptions and used to estimate past stratospheric sulfur load using established empirical relationships (Abbott and Davies, 2012; Hammer et al., 1980). Aggregating ice-core sulfate data from both polar ice sheets has allowed for improved approximation of eruption source latitudes by assuming that only eruptions in the tropics are able to produce contemporary sulfate peaks across both hemispheres **(Figure 4a-e)** and reduced uncertainties associated with glaciological noise by increasing the signal-to-noise ratio compared to relying on individual ice-core records (Cole-Dai, 2010; Gao et al., 2007; Gao et al., 2008; Gautier et al., 2016; Robock and Free, 1995). Methodology has been further refined to isolate the volcanic fraction of sulfur from the total concentrations of these species based on outlier detection algorithms (Cole-Dai et al., 2021).

The development of continuous flow ice-core analysis has improved the breadth, resolution, and accuracy of volcanic aerosols in ice (Sigl et al., 2014; Sigl et al., 2015) and paved the way to link numerous hitherto unattributed sulfate anomalies to their respective source eruptions (Abbott, et al., 2021; Dunbar et al., 2017; Gabriel et al., 2025; Gabriel et al., 2024; Hutchison et al., 2024; Hutchison et al., 2025; Jensen et al., 2014; McConnell et al., 2020; Pearson et al., 2022; Piva et al., 2023; Plunkett et al. 2023; Plunkett et al., 2022; Smith et al., 2020b; Sun et al., 2014). High-resolution analyses of sulfur **(Figure 4a)** and oxygen isotopes (i.e. ^{33}S, ^{34}S, ^{17}O) in volcanic sulfate deposited across the polar ice sheet are emerging as a powerful tool to disentangle the source latitudes of past volcanic eruptions, to constrain

Deleted: likely changes the further back in time is explored

Formatted: Default Paragraph Font, Font color: Black

Formatted: Normal, Centered, Border: Top: (No border), Bottom: (No border), Left: (No border), Right: (No border), Between : (No border), Tab stops: 3.25", Centered + 6.5", Right, Position: Horizontal: Left, Relative to: Column, Vertical: In line, Relative to: Margin, Wrap Around

Formatted: Font color: Black

the injection height of volcanic volatiles relative to the height of tropopause and to quantify the relative contributions of sulfate formed and transported in the stratosphere to the total mass of sulfate deposited at the ice-core sites (Baroni et al., 2008; Baroni et al., 2007; Burke et al., 2023; Burke et al., 2019; Crick et al., 2021; Gautier et al., 2019; Pearson et al., 2022; Savarino, et al., 2003).

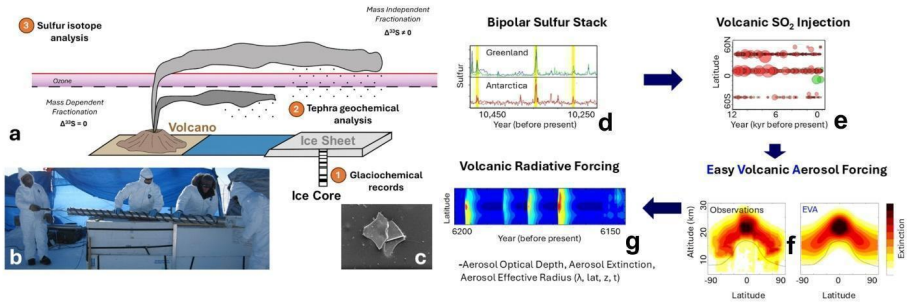

Deleted: <object>¶

Figure 4*: Schematic description of methods and workflow used to reconstruct changes in radiative forcing from ice-core records.* ***a:*** *Analytical methods used to reconstruct volcanic SO_2 emissions from polar ice cores include (1) glaciochemical records, (2) geochemical analyses of tephra, (3) sulfur isotope analyses;* ***b:*** *an ice core is extracted from Greenland;* ***c:*** *scanning electron image of tephra shards from an Alaskan eruption in an ice core from Greenland;* ***d:*** *synchronized and stacked ice-core sulfur records from Greenland and Antarctica during the early Holocene;* ***e:*** *estimated latitudes and stratospheric sulfur injections over the Holocene;* ***f:*** *observed aerosol extinction profiles for the eruption of Pinatubo against simulated profiles using the Easy Volcanic Aerosol (EVA) forcing generator;* ***g:*** *representative time series of optical properties (e.g. stratospheric aerosol optical depth: SAOD) inferred from EVA. Modified after Sigl et al., 2022; Toohey et al., 2016; (Credit: a: Will Hutchison / b,d,e Michael Sigl / c: Meredith Helmick / f,g: Matthew Toohey).*

5.1 Modeling Volcanic Aerosols

Model simulations of volcanism primarily focus on quantifying the **radiative forcing** from sulfate injected into the stratosphere and troposphere during an explosive eruption. Such simulations rely on ice-core derived estimates of stratospheric sulfur mass using one of two approaches. The first, interactive aerosol modeling, explicitly simulates the chemical and microphysical processes that convert SO_2 gas into sulfate particles with an evolving size distribution. The second, prescribed aerosol forcing, inputs aerosol optical properties directly into models based on simple scalings of eruption mass relative to a well-observed reference event – typically the 1991 Mt. Pinatubo eruption, as in the widely used Easy Volcanic Aerosol (EVA) generator (Toohey et al., 2016) **(Figure 4f,g)**. Moreover, long-lived effusive volcanism with generally lower emission heights introduces an additional, poorly constrained forcing pathway for delivering sulfate to the troposphere (Gettelman et al., 2015; Zoëga et al., 2025a; 2025b).

The size distribution of sulfate aerosols has a major impact on their radiative forcing and therefore is a key uncertainty for both modeling approaches, as proxy datasets do not preserve information on sulfate particle size to constrain models. For a given mass of sulfur, a larger number of smaller particles will scatter more solar radiation and consequently produce stronger cooling than an equivalent mass of larger ones (Pinto et al., 1989; Lacis et al., 1992). Additionally, larger particles more effectively absorb outgoing longwave radiation, and the inclusion of large ash particles in modeled eruptions have been shown to increase longwave absorption immediately after injection, contributing to

Formatted: Font: Not Bold

Formatted: Default Paragraph Font, Font color: Black

Formatted: Normal, Centered, Border: Top: (No border), Bottom: (No border), Left: (No border), Right: (No border), Between : (No border), Tab stops: 3.25", Centered + 6.5", Right, Position: Horizontal: Left, Relative to: Column, Vertical: In line, Relative to: Margin, Wrap Around

Formatted: Font color: Black

self-lofting of the plume and increased stratospheric lifetime and aerosol optical depth (AOD) (Stenchikov et al., 2021). Interactive aerosol models differ substantially in their predicted particle sizes, contributing to large spreads in inter-model volcanic forcing (Clyne et al., 2021; McGraw et al., 2024) and limiting confidence in how particle sizes should be specified in aerosol forcing generators.

Additional uncertainties, such as unknown eruption latitude, season, and injection altitude, complicate efforts to accurately constrain the radiative impact of past eruptions (Toohey et al., 2019; Marshall et al., 2020; Zhuo et al., 2024). Furthermore, studies have shown that downward longwave radiation from volcanic aerosol layers can alter cloud properties (Marshall et al., 2020; McGraw & Polvani, 2026), but the associated forcing remains uncertain and cloud-modulated forcings are notoriously difficult to constrain in global models.

In addition to sulfate, explosive volcanic eruptions emit **volcanic ash** (VA) into the atmosphere. While generally considered to be an insoluble particle when initially emitted with its physical properties determined by the type of eruptive magma, VA can become soluble as it reacts with plume chemicals with implications for bioavailability, ocean fertilization, and the global carbon cycle (Duggen et al., 2010; Langmann, 2013; Bisson et al., 2023). In the atmosphere, VA can impact aerosol radiative forcing directly by scattering or absorbing incoming solar radiation or indirectly by altering cloud properties (Langmann, 2013), as well as by affecting the stratospheric load and lifetime of volcanic sulfur (Stenchikov et al., 2021). Because the relatively short lifetime of VA results in a much smaller radiative forcing than that of sulfate (Langmann, 2014) and there is currently no long-term dataset of VA, it is currently neglected in global climate and Earth system models.

Also of potential radiative importance are the **gases** released by volcanic eruptions. This includes SO_2, which has a more modest - yet not negligible - cooling effect compared to the sulfate aerosols it forms (Osipov et al., 2020) and water vapor which can be substantial as observed for the climactic submarine eruption of Hunga Tonga–Hunga Ha'apai in the Southern Pacific Ocean in 2022 (APARC, 2025). Co-emitted stratospheric **halogens** also have been researched for their potential radiative effects, and it has been suggested that they could both enhance (Staunton-Sykes et al., 2021) or reduce (Brenna et al., 2020) sulfate-induced surface cooling However, it remains unclear whether sufficient amounts of halogens have reached the stratosphere following large historical eruptions (Wade et al., 2020; Textor et al., 2003).

5.2 Proxies for volcanic SO_2 emissions and other volcanic fallout

Volcanic eruptions release numerous gases into the atmosphere including CO_2, H_2O, SO_2, H_2S but also HBr, HCl either during passive degassing or in volcanic eruptions. SO_2 is the most important for understanding aerosol radiative forcing because of its wide geographical spread and long atmospheric lifetime of 1-3 years in the stratosphere as submicron sulfuric aerosol droplets. In addition to satellite observations of SO_2 during the past ~50 years and other ground based aerosol observations over the past ~150 years (see Datasets section), polar ice-core records of volcanic sulfate (or sulfur) and other volcanic tracers **(Figure 4a-d)** are the most direct proxy records of past atmospheric sulfate and currently extend from the present to >120 ka (Lin et al., 2022; Svensson et al., 2026; Wolff et al., 2023).

In ice cores, sulfate (determined with ion chromatography or photometry) or sulfur (determined with inductively coupled plasma mass spectrometry) concentrations can be measured in discrete samples or in online continuous-flow-analysis systems (Bigler et al., 2007; Severi et al., 2007; Sigl et al., 2013). Typical effective depth resolution for state-of-the-art analyses is between 1 and 5 cm, equivalent to a nominal age resolution between a month and a few years, depending on the accumulation rates and layer thinning at the ice-core sites (Figure 4). While there are continuous time series available from Greenland and Antarctica, there are biases towards eruptions of larger magnitudes (Volcanic Explosivity Index,

Deleted: 2024

Deleted: VOLCANIC EXPLOSIVITY INDEX

Formatted: Font: Gungsuh

Formatted: Default Paragraph Font, Font color: Black

Formatted: Normal, Centered, Border: Top: (No border), Bottom: (No border), Left: (No border), Right: (No border), Between : (No border), Tab stops: 3.25", Centered + 6.5", Right, Position: Horizontal: Left, Relative to: Column, Vertical: In line, Relative to: Margin, Wrap Around

Formatted: Font color: Black

(VEI) ≥5) and mid-to-higher latitudes. Volcanic sulfate contributions are also partly to largely masked during the 20th century in Greenland by the co-emissions of anthropogenic sulfur compounds and during the last glacial era by the co-emissions of dust with a high sulfate content (Lin et al., 2022; McConnell et al., 2007a).

Ice-core records of sulfate deposition can be further refined using sulfur isotopes (Baroni et al., 2008; Gautier et al., 2019). The $\delta^{34}S$ signature can be used to infer relative contribution from volcanic (explosive and quiescent), biogenic, and anthropogenic sulfur (Jongebloed et al., 2023) and the $\Delta^{33}S$ signature (Burke et al., 2019)—imparted by mass independent fractionation from UV photochemistry that occurs in the stratosphere—can be used to infer tropospheric versus stratospheric transport pathways and their relative contributions to the sulfate depositions at the ice-core sites (Pearson et al., 2022; Burke et al., 2023).

Ice-core records have been incorporated into reconstructions of volcanic forcing since the 1980s (Crowley and Unterman, 2013; Gao et al., 2008; Hammer et al., 1980; Robock and Free, 1995). Stratospheric sulfate injections are typically estimated from the cumulative sulfate mass deposition over the ice sheets following Toohey and Sigl (2017). Briefly, ice sheet average sulfate mass deposition for Antarctica f_A and Greenland f_G are related to injected sulfur mass M_S following:

$$M_S = \frac{1}{3}[L_G f_G + L_A f_A]$$

where L_G and L_A are transfer functions accounting for the spatial distribution of sulfate deposition over each hemisphere. Based on analysis of the spread and deposition of nuclides from nuclear bomb tests, sulfate from prior volcanic eruptions (i.e. Pinatubo 1991) and atmospheric model simulations (Gao et al., 2007), the transfer functions L_G and L_A are estimated to be 1 x 10^9 km^2 for tropical eruptions and 0.57 x 10^9 km^2 for extratropical eruptions. The method described above assumes that the ice-core sulfate deposition is directly proportional to the stratospheric sulfur injection. Some of the sulfate deposited may, however, originate from volcanic sulfur emissions into the troposphere, especially when volcanic eruptions are situated upwind (e.g., in Alaska) or near the Greenland ice sheet (e.g., in Iceland).

While sulfur is the most used volcanic tracer in ice, other chemical species can be used to identify certain eruptions. For example, some eruptions are known to be rich in halogens (e.g., F, Cl measured by IC or HR-ICP-MS) (Gabriel et al., 2024; McConnell et al., 2017) or trace metals (e.g., Bi, Tl measured by HR-ICP-MS) (McConnell et al., 2024; Hutchison et al., 2024; McConnell et al., 2017), though such species are less frequently measured in ice cores and so long-term records are rarer. High-resolution insoluble particle records in ice cores have led to precise identification of microscopic cryptotephra shards **(Figure 4c)** to geochemically fingerprint specific volcanic sources, allowing for more accurate modeling simulations of climate impacts by potentially constraining key emission source parameters such as exact location, timing, and sulfur injection height **(Figure 4a,e)** (McConnell et al., 2020; Hutchinson et al., 2024; Plunkett et al., 2023; Pearson et al., 2022; Cook et al., 2022).

5.3 Datasets

Several datasets quantify volcanic sulfur emissions and estimate changes in stratospheric aerosol properties **(Table 3)**. Satellite measurements available since 1978 have become a valuable source of information regarding modern volcanic sulfur emissions (e.g. MSVOLSO2L4, Carn et al., 2016), as well as the optical properties of aerosols **(Figure 4)**. During this time an average of 3 Tg of SO_2 per year stems from explosive and effusive eruptions and approximately 1 Tg of SO_2 per year is injected into the stratosphere. Around 23 Tg of SO_2 per year is released through passive (i.e. non-eruptive) degassing (Schmidt and Carn, 2022). Based on satellite-derived emissions, the Global Space-based Stratospheric

Formatted: Font: Cambria Math

Formatted: Default Paragraph Font, Font color: Black

Formatted: Normal, Centered, Border: Top: (No border), Bottom: (No border), Left: (No border), Right: (No border), Between : (No border), Tab stops: 3.25", Centered + 6.5", Right, Position: Horizontal: Left, Relative to: Column, Vertical: In line, Relative to: Margin, Wrap Around

Formatted: Font color: Black

Aerosol Climatology (GloSSAC (Kovilakam et al., 2020; Thomason et al., 2018)) provides global stratospheric aerosol properties focused on extinction coefficient measurements and is the recommended volcanic forcing dataset within CMIP6 and CMIP7 from 1979 to present (Aubry et al., 2025).

Before the satellite era, data on changes in stratospheric aerosols can be obtained from ground-based observations of the atmosphere using pyrheliometry that extend back to 1881 (Sato et al., 1993; Stothers, 1996). Such data, however, becomes increasingly scarce going back in time, and has large spatial and temporal biases skewed towards the Northern Hemisphere land and the summer season. These datasets are incorporated in previous reconstructions of volcanic aerosol forcing in CMIP5 and CMIP6 (Luo 2018). No SO_2 emission estimates exist based on pyrheliometry **(Figure 4)**.

Ice cores provide some of the most robust datasets of past atmospheric sulfate loadings **(Figure 4)**. The recommended volcanic forcing datasets for climate model simulations contributing to the PMIP4 (past 1000 years) and CMIP6 (historic since 1850) phase before 1900 CE are, therefore, primarily based on ice-core records (Jungclaus et al., 2017). The most recent ice core-based products are evolv2k (SO_2 emissions and aerosol properties such as stratospheric aerosol optical depth (SAOD) between 500 BCE and 1900 CE (Toohey and Sigl, 2017), HolVol (SO_2 emissions and aerosol properties) between 9500 BCE and 1900 CE (Sigl et al., 2022), and a reconstruction of bipolar sulfate deposition and estimated radiative forcing for extremely large eruptions between 60 and 9 ka BP (Lin et al., 2022). In addition to these sources there is also a reconstruction covering 130 ka to present based on the magnitude (M; Pyle, 2015) of volcanic eruptions from geologic eruption records (Brown et al., 2014) scaled against ice-core and satellite derived sulfur injection estimates (Schindlbeck-Belo et al., 2024) **(Figure 4)**.

Maximum dating uncertainties for ice-core sulfate records are estimated at ±2 years during the past 800 years, ±5 years during the past 2,500 years, ±10 years during the Holocene and increase to approximately ±300 years during the Last Glacial Maximum (Adolphi and Muscheler, 2016; Muscheler et al., 2020; Sigl et al., 2016; Toohey and Sigl, 2017; Sigl et al., 2022).

Table 3: Datasets of stratospheric volcanic SO_2 emissions and aerosol optical properties

Dataset (latest versions)	Input Data	Parameters	Time Period	Source
MSVOLSO2L4	Satellite retrieval from space-borne UV sensors	Volcano, eruption date, latitude, longitude, plume height, eruption style, mass of SO_2	1979-2025	Carn et al., (2016)
GloSSAC Version 2.23	MSVOLSO2L4	Climatology of stratospheric aerosol properties i.e. extinction coefficient at 525 & 1020 nm	1979-2024	Thomason et al., (2018)
Sato et al., 1993	Ground-based observations of solar irradiance, stellar and lunar extinction e.g. pyrheliometer	Climatology of stratospheric aerosol optical depths and effective radius of the aerosol particles	1850-1978	Sato et al., (1993)

Deleted: ¶ ... [1]

Formatted Table

Formatted: Default Paragraph Font, Font color: Black

Formatted: Normal, Centered, Border: Top: (No border), Bottom: (No border), Left: (No border), Right: (No border), Between : (No border), Tab stops: 3.25", Centered + 6.5", Right, Position: Horizontal: Left, Relative to: Column, Vertical: In line, Relative to: Margin, Wrap Around

Formatted: Font color: Black

VolcanEESM	Combination of global volcanic emissions of SO_2 (i.e. satellite & ice core)	Volcano, eruption date, latitude, longitude, injection height, VEI, mass of SO_2	1850-2015	Neely III & Schmidt (2016)
eVolv2k eVolv2k-ENS eVolv2k_version4	Ice-core records Greenland and Antarctica	Eruption year, estimated latitude, mass of stratospheric S; climatology of stratospheric aerosol optical depths	500 BCE - 1900	Toohey & Sigl (2017)
HolVol v.1.0	Ice-core records Greenland and Antarctica	Eruption year, estimated latitude, mass of stratospheric S; climatology of stratospheric aerosol optical depths	9500 BCE - 1900	Sigl et al., (2022)
Lin et al. 2022	Ice-core records Greenland and Antarctica	Eruption year, estimated latitude, stratospheric sulfate aerosol mass	60-9 ka BP	Lin et al., (2022)
PalVol v1	Estimated M from LAMEVE database; linear fit of M against SO2 injections from ice cores and satellites	Eruption year, latitude, stratospheric sulfur injection; ensemble of stratospheric aerosol optical depths	130-0 ka BP	Schindlbeck-Belo et al., (2024); Brown et al., (2014)

MSVOLSO2L4: https://disc.gsfc.nasa.gov/datasets/MSVOLSO2L4_4/summary

GloSSAC: https://doi.org/10.5067/GLOSSAC-L3-V2.23

Sato et al., 1993: https://data.giss.nasa.gov/modelforce/strataer/

VolcanEESM: http://catalogue.ceda.ac.uk/uuid/bfbd5ec825fa422f9a858b14ae7b2a0d

eVolv2k_v3: https://www.wdc-climate.de/ui/entry?acronym=eVolv2k_v3_ds

eVolv2k-ENS: https://www.wdc-climate.de/ui/entry?acronym=eVolv2k-ENS

eVolv2k_version4: https://doi.pangaea.de/10.1594/PANGAEA.971968

HolVol: https://doi.org/10.1594/PANGAEA.928646

Lin et al., 2022: https://doi.org/10.5194/cp-18-485-2022-supplement

PalVol: https://doi.org/10.26050/WDCC/PalVolv1

Formatted: Default Paragraph Font, Font color: Black

Formatted: Normal, Centered, Border: Top: (No border), Bottom: (No border), Left: (No border), Right: (No border), Between : (No border), Tab stops: 3.25", Centered + 6.5", Right, Position: Horizontal: Left, Relative to: Column, Vertical: In line, Relative to: Margin, Wrap Around

Formatted: Font color: Black

In addition to these larger data products reconstructions of volcanic aerosol emissions (or ice-core depositions) also have been made for specific time windows or eruptions **(Figure 5)** during the Common Era (Fang et al., 2023; Gabriel et al., 2025; Gabriel et al., 2024), Holocene (Pearson et al., 2022) and the last Glacial (Abbott et al., 2021; Innes et al., 2025; Lin et al., 2023).

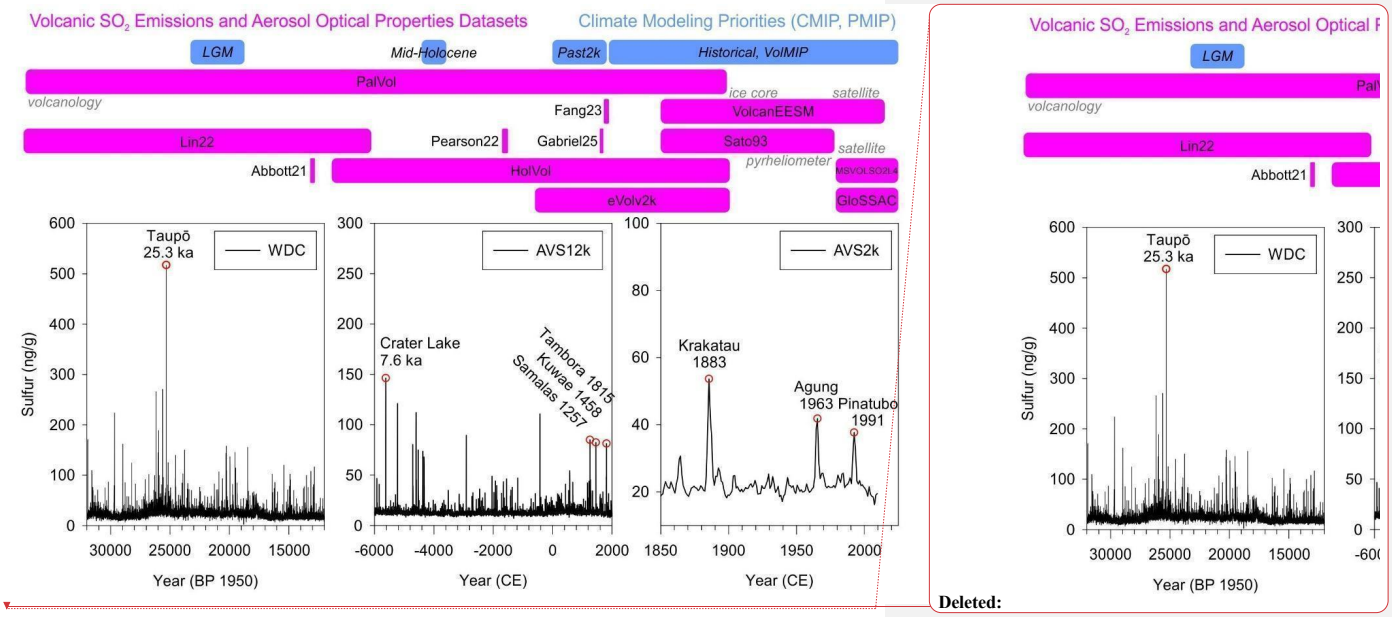

Figure 5: *Overview of available reconstructions of stratospheric volcanic SO_2 (or S) injections and changes in stratospheric aerosol optical properties using different data sources (satellites, pyrheliometer, volcanology, ice cores). All unspecified datasets are from ice cores; details are listed in Table 3. Panels below show representative sulfur concentrations records for Antarctica based on the West Antarctic Ice Sheet Divide ice core (WDC) or stacked ice-core composite records compiled over the Holocene (AVS12k) and the Common Era (AVS2k) synchronized on the WD2014 chronology (Sigl et al., 2016; Sigl et al., 2014; Sigl et al., 2022). Key eruptions during selected time windows are indicated (Davies et al., 2024; Dunbar et al., 2017; Lavigne et al., 2013; Ro et al., 2025). Blue squares mark priority periods identified within Paleoclimate Modeling Intercomparison Project (PMIP) and Coupled Model Intercomparison Project (CMIP) programs.*

5.4 Other indicators of volcanic aerosols and their climate impact

Historical documentary records are independent additional indicators of volcanic aerosols reporting observable atmospheric perturbations frequently accompanied by climatic anomalies and extreme weather. There is a wide range of valuable historical observations such as “dry fogs”, “dust veils”, “blue suns” describing a persistent, high-altitude haze, or the temporary dimming of celestial bodies (sun, moon, stars) (Deirmendjian, 1973; Lamb, 1970). These historical accounts allow for the reconstruction of volcanic forcing prior to modern instrumental monitoring and can complement the polar ice-core records (Sigl et al., 2015), as they often provide precise information on the spatio-temporal evolution of atmospheric aerosols with unmatched precision (down to a specific day or month). Before

Deleted:

Deleted: temporally

Formatted: Default Paragraph Font, Font color: Black

Formatted: Normal, Centered, Border: Top: (No border), Bottom: (No border), Left: (No border), Right: (No border), Between : (No border), Tab stops: 3.25", Centered + 6.5", Right, Position: Horizontal: Left, Relative to: Column, Vertical: In line, Relative to: Margin, Wrap Around

Formatted: Font color: Black

ice-core records were established Lamb (1970) developed a semi-quantitative "*Dust Veil Index*" to assess the impact of past volcanic eruptions on climate partly based on such documentary sources. Later Stothers and Rampino (1983) utilized ancient Greek, Roman, and medieval chronicles to identify "dry fogs" and link them to specific unidentified eruptions, such as the 536 CE "mystery cloud" (Stothers 1984) and expanded this inventory of reconstructed eruptions further back in time (Stothers, 2002) and into the instrumental period (Stothers, 1996). Documentary records are now widely used to independently evaluate reconstructions of volcanic aerosols in the atmosphere and to further constrain the dates of past volcanic eruptions during the pre-satellite era (Garrison et al., 2021; Guillet et al., 2023; Oppenheimer et al., 2017; Wullenweber et al., 2021; Yang and Ludlow, 2025).

Documentary records are also used to identify the climatic response to volcanic eruptions such as severe cooling or disruptions in monsoon circulation which were observed following historic eruptions such as Tambora in 1815 or Laki in 1783. Combined with the ice-core record and other climate proxies, in particular precisely dated tree-ring records of large-scale summer cooling extremes, these written archives have documented volcanic induced weather anomalies and climate perturbations during the Late Holocene (Büntgen et al., 2020; Büntgen et al., 2025; McCormick et al., 2007; Salzer and Hughes, 2007; Sigl et al., 2015).

Large-scale temperature reconstructions obtained primarily from tree-rings (Wilson et al., 2016) and global multiproxy compilations (e.g. PAGES2k Consortium (2017)) are essential for evaluating climate model simulations over the last 1000 years, particularly in assessing how the Earth system responds to sudden natural perturbations like volcanic eruptions (Lücke et al., 2023; Marshall et al., 2025). Detection and attribution studies (Schurer et al., 2014) employing these datasets have highlighted that volcanic eruptions are the primary driver of climate variability on decadal to centennial scales over the past millennium during the preindustrial (IPCC AR6). However, mismatches occur, in particular during the 1st millennium CE (Esper et al., 2024), and resolving these remains a priority task (Lücke et al., 2023; Marshall et al., 2025; Zhu et al., 2020).

5.5 Quantifying uncertainties

There remain large uncertainties in estimating stratospheric sulfur emissions from ice cores. Sources of errors can be random or systematic (Gao et al., 2008; Toohey and Sigl, 2017). A major source of uncertainty is the unconstrained emission source parameters related to the latitude, the seasonal timing, the injection height and, most critically, the mass of SO_2 injection, which collectively determines the lifetime and geographic spread of the stratospheric aerosol (Marshall et al., 2019; Marshall et al., 2021). Quantification of these uncertainties and potential biases in the reconstruction remain difficult to assess because there is limited overlap between common volcanic eruptions (across a range of emission source parameters) detectable in both the satellite products and the ice-core records from both hemispheres.

Ensemble reconstructions that account for uncertainty in volcanic emission source parameters offer significant potential for improving our understanding of volcanic climate forcing (Lücke et al., 2023; Verkerk et al., 2025). Using ensembles in a Monte Carlo approach allows for a comprehensive propagation of uncertainties associated with key emission source parameters, (e.g. the SO_2 mass injected into the stratosphere, eruption latitude, age uncertainty or emission height). Such studies demonstrate a significant spread in the reconstructed SAOD, effective radiative forcing (see **Figure 6**) and ultimately in the simulated temperature response that these uncertainties create, especially during periods of peak volcanic activity (Verkerk et al., 2025). By attempting to account for the full range of volcanic forcing uncertainties over the past millennium, ensemble members appear to better capture the variability from proxy records, helping to explain and resolve some of the discrepancies and providing empirical support for the climate impact of past volcanic eruptions (Lücke et al., 2023). However, large ensemble simulations have historically been computationally expensive and therefore often employ climate and

Formatted: Default Paragraph Font, Font color: Black

Formatted: Normal, Centered, Border: Top: (No border), Bottom: (No border), Left: (No border), Right: (No border), Between : (No border), Tab stops: 3.25", Centered + 6.5", Right, Position: Horizontal: Left, Relative to: Column, Vertical: In line, Relative to: Margin, Wrap Around

Formatted: Font color: Black

aerosol models of reduced complexity, or increasingly, machine-learned emulators. This limits the propagation of all known uncertainties, particularly those related to aerosol microphysics and atmospheric chemistry. There is potential to efficiently address uncertainty in model volcanic injection parameters, microphysics, and chemistry parameterizations (i.e., parametric uncertainty) simultaneously with the use of perturbed parameter ensemble (PPE) simulations (see Sect. 5.6 **Remaining Challenges and Future Avenues**).

Estimation of stratospheric sulfate injections from ice-core sulfate mass deposition is subject to large uncertainty (Fuglestvedt et al., 2024; Gao et al., 2007; Moore et al., 2012; Toohey and Sigl, 2017). Volcanic sulfate deposition as measured in ice cores is the locally accumulated sulfate mass density (in kg km^{-2}), but since volcanic sulfate deposition is not uniform across the Earth's surface, a transfer function is required to convert ice-sheet-wide deposition estimates into stratospheric sulfate loadings, to account for spatial inhomogeneity in deposition. These functions have been developed using climate-aerosol model simulations (e.g. the Goddard Institute for Space Studies ModelE, Gao et al., 2007), or by using the distribution of fission products in Greenland from thermonuclear testing as an analogue for stratospheric injection in the NHET (Clausen and Hammer, 1988). Currently, two separate functions are used: one for tropical eruptions and one for extratropical eruptions. Recent work using the Community Earth System Model (CESM) Whole Atmosphere Community Climate Model version 6 (WACCM6) suggests a lower transfer function with a larger uncertainty range for extratropical eruptions in the Northern Hemisphere (NHET) which produces stratospheric sulfate injections from NHET eruptions 20% smaller and uncertainties 50% larger when accounting for atmospheric variability and unknown eruption parameters (Fuglestvedt et al., 2024).

Distinguishing between volcanic and anthropogenic sources of sulfate is particularly difficult in Greenland ice cores for the 20th century. The co-emission of sulfate from anthropogenic sources peaking over the North Atlantic between 1960 and 2000 CE (Hoesly et al., 2018; McConnell et al., 2007a) makes it difficult to detect and quantify volcanic sulfate deposition in Greenland (e.g. following major eruptions of Agung 1963, El Chichon 1982 and Pinatubo 1991), and therefore makes it impossible to make a direct comparison with stratospheric sulfate observations using remote sensing in the Northern Hemisphere (Carn et al., 2016). This contributes to the large uncertainties in the transfer function.

A key assumption when using ice-core records is that all the deposited sulfate comes from the stratosphere. However, eruptions within the same hemisphere as the ice-core sites could also deliver sulfate to the polar ice sheets through tropospheric transport, which could bias the reconstruction of stratospheric sulfur injection (Gautier et al., 2019; Savarino et al., 2003). Recent work analyzing the sulfur isotopic composition (i.e. ^{33}S and ^{34}S) of volcanic sulfate in ice cores with a high temporal resolution for some key explosive eruptions demonstrated that the proportion of stratospheric sulfur within the total sulfur deposited varied from around 60% for eruptions in Alaska to 100% for eruptions in the tropics (Burke et al., 2023; Burke et al., 2019; Pearson et al., 2022). Correcting for the non-stratospheric component in ice-core records reduced estimates of sulfur injection for the respective eruptions (Burke et al., 2023). However, high-resolution sulfur isotope analyses of ice cores have thus far only been applied to a limited number of eruptions (Baroni et al., 2007; Burke et al., 2023; Burke et al., 2019; Hutchison et al., 2025; Pearson et al., 2022), and systematic analyses across both polar ice sheets remain to be conducted.

Formatted: Default Paragraph Font, Font color: Black

Formatted: Normal, Centered, Border: Top: (No border), Bottom: (No border), Left: (No border), Right: (No border), Between : (No border), Tab stops: 3.25", Centered + 6.5", Right, Position: Horizontal: Left, Relative to: Column, Vertical: In line, Relative to: Margin, Wrap Around

Formatted: Font color: Black

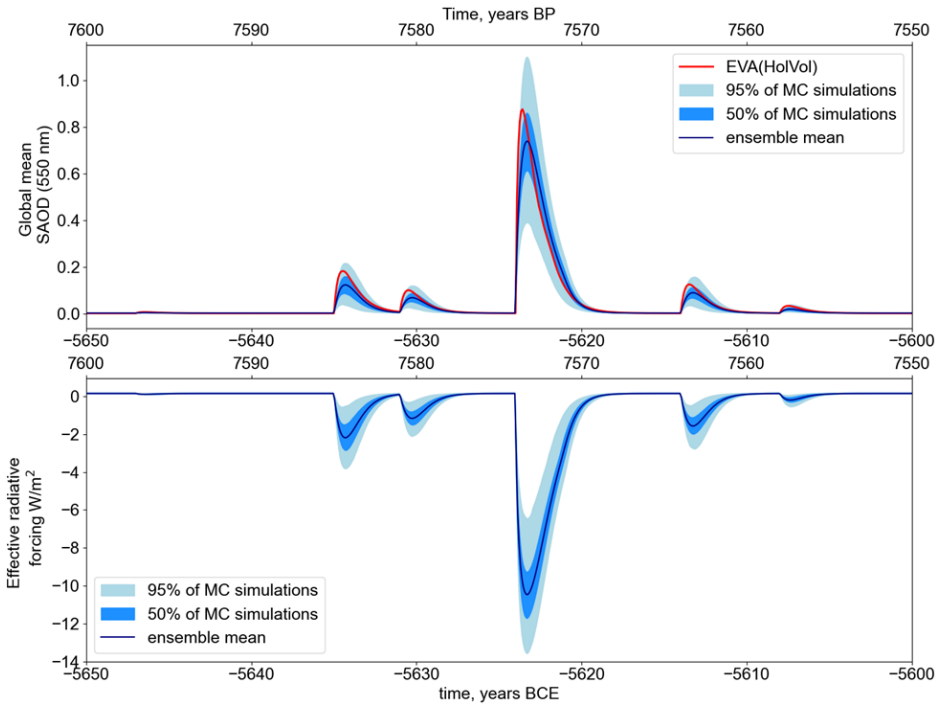

Figure 6: *(Upper panel) Global-mean stratospheric aerosol optical depth (SAOD) between 7600 and 7550 yr BP (lower panel) corresponding global-mean effective radiative forcing from an ensemble of 1000 simulations over this period, where injection and model parameters are resampled simultaneously using a Monte Carlo approach to propagate uncertainty on volcanic injection parameters (e.g. injection height, mass and latitude) and volcanic aerosol forcing modelling (e.g. aerosol lifetime, SAOD-ERF scaling); red line represents the central estimate of SAOD using the Easy Volcanic Aerosol (EVA; Toohey et al., 2016) forcing generator using the HolVol1.0 stratospheric sulfur injection inventory (Sigl et al., 2022) (Figure adapted from Verkerk et al., 2025).*

On longer (glacial) timescales, additional uncertainties arise from (1) reduced volcanic detection efficiencies in Greenland ice cores during stadials with increased atmospheric dust loading, (2) potential differences in the efficiency with which aerosols are scavenged during cold stadial versus warm interstadial periods and (3) sulfate peak broadening related to diffusion of sulfate and strong layer thinning with increasing depth (Lin et al., 2022; Rhodes et al., 2024; Svensson et al., 2026).

5.6 Remaining challenges and future avenues

Reconstruction of volcanic sulfur dioxide (SO_2) emissions from ice-core records remains challenging, due to the consistent **under-sampling of small to moderate eruptions** (typically defined as those with a Volcanic Explosivity Index of less than 5). A primary concern is the definition of the detection threshold, with the sulfate deposition from minor eruptions frequently falling within the range

Deleted: <*object*>¶

Formatted: Default Paragraph Font, Font color: Black

Formatted: Normal, Centered, Border: Top: (No border), Bottom: (No border), Left: (No border), Right: (No border), Between : (No border), Tab stops: 3.25", Centered + 6.5", Right, Position: Horizontal: Left, Relative to: Column, Vertical: In line, Relative to: Margin, Wrap Around

Formatted: Font color: Black

of natural background variability of sulfate, composed of tropospheric volcanic and marine biogenic emissions. Although these events are individually minor, collectively they contribute a significant proportion of the total SAOD. Recent research indicates that neglecting these smaller eruptions can result in an underestimation of volcanic forcing by up to 50% during volcanically less active decades (Chim et al., 2023). This under-sampling is further compounded by severe spatial biases, resulting in an underrepresentation of volcanic SO_2 emissions from small-to-moderate volcanic eruptions, especially in the tropics and in the Southern Hemisphere between 1750 and 1979 CE (Aubry et al., in review). Consequently, ice-core based reconstructions of radiative forcing of past volcanism are skewed towards massive, globally dispersive events, while the cumulative forcing from the more frequent, smaller eruptions remains poorly quantified. To mitigate these biases, recent efforts have been made to employ multi-core "stacking" techniques and high-resolution tephra and sulfur isotopic analyses (Gabriel et al., 2025; Gabriel et al., 2024; Hutchison et al., 2024) to better differentiate smaller volcanic sulfate spikes from non-volcanic backgrounds. However, the scarcity of suitable, high-accumulation ice cores (Fang et al., 2023) remains a limiting factor for global reconstructions.

The **transfer functions** used to translate ice core-based sulfate depositions into stratospheric aerosol loading remain a major source of uncertainty (Fuglestvedt et al., 2024). This issue is inextricably linked to **constraining the emission source parameters** (e.g. the location and season of the eruption) as these parameters may vary significantly between eruptions (Marshall et al., 2019) influencing aerosol lifetime and the depositions across both polar ice sheets. Further efforts are needed to better constrain the emission source parameters for past eruptions but also to increase observations of volcanic sulfate depositions across the polar ice sheets for more recent eruptions for which stratospheric aerosol spread and emission source parameters are well constrained by remote sensing.

On longer timescales, improved ice-core synchronization across both hemispheres and improved absolute dating of ice cores employing regional or global stratigraphic marker events (e.g. tephra, ^{10}Be, CH_4) will tighten the chronostratigraphic links to the geological record (providing key information on volcanic emission source parameters) as well as with the proxy records recording past climate (e.g. speleothems, marine and lake sediments, tree-rings).

Progress can be made on the modeling side by systematically integrating paleoclimate proxy evidence into the evaluation of volcanic aerosol simulations. This framework focuses on requiring simulated post-eruption climate responses to be consistent with proxy-derived signals of past eruption events. Several studies have demonstrated the value of restricting simulated volcanic forcing to scenarios consistent with tree-ring-based reconstructions of post-eruption cooling (e.g. Timmreck et al., 2009; McGraw et al., 2024). In this way, paleoproxy records act as an emergent constraint on volcanic forcing, helping to narrow the range of plausible radiative forcings and compatible aerosol properties.

While proxy-based constraints narrow the range of plausible responses, modeling efforts must also widen outcomes to sufficiently reflect uncertainties in the simulated physical and chemical processes controlling forcing results. An exciting avenue for addressing model parametric uncertainty in the simulation of volcanic eruptions is perturbed parameter ensembles (PPEs). A PPE varies tens of physical parameters pertaining to specific sub-gridscale processes randomly and simultaneously across hundreds of model simulations (Carslaw et al., 2025; Collins et al., 2011; Murphy et al., 2004). As for large ensemble simulations, storage and compute time are limitations to this approach. However, for a given computational cost, they can provide a greater depth of analysis across many different parameters. This large dataset allows for statistical analysis to determine key parameters affecting the key model outputs (Nugent et al., 2026; Eidhammer et al., 2024), and observational constraints can be applied to the PPE to isolate parameter combinations that give the best model-observational agreement (Regayre et al., 2018, Regayre et al., 2020; Johnson et al., 2020). A PPE framework for the Pinatubo volcanic eruption was proposed for the Interactive Stratospheric Aerosol Model Intercomparison Project (ISA-MIP) and referred

Formatted: Default Paragraph Font, Font color: Black

Formatted: Normal, Centered, Border: Top: (No border), Bottom: (No border), Left: (No border), Right: (No border), Between : (No border), Tab stops: 3.25", Centered + 6.5", Right, Position: Horizontal: Left, Relative to: Column, Vertical: In line, Relative to: Margin, Wrap Around

Formatted: Font color: Black

to as the Pinatubo Emulation in Multiple models (PoEMS) experiment (Timmreck et al., 2018). The PoEMS framework proposes a multiple model comparison of PinatuboPPEs that vary parameters pertaining to injection properties, sulfate budget, and aerosol microphysics. Analysis of this PPE will require constraint to multiple observational products (Quaglia et al., 2023; Visioni, 2026) in order to represent the micro and macro scale evolution of the plume, and caution must be taken in interpreting individual ensemble parametric combinations as agreement between the PPE and observational products may be dictated by different parameter combinations (Elsaesser et al., 2025). There is ongoing work to develop these PPEs which could help isolate the most important physical and chemical assumptions in explosive volcanic eruptions (see Section 5.1 **Modeling Volcanic Aerosols**).

6. Other aerosols

In addition to the three main aerosol classes discussed in the previous sections - mineral dust, aerosol from biomass burning, and volcanic aerosol - there is a broad range of natural and anthropogenic aerosols that can contribute to total aerosol concentrations, and whose emissions may be affected by different climates or because of human land use, as discussed above. Here in this section we discuss other natural aerosols, their potential feedbacks under climate change, as well as estimates for the proportion from anthropogenic changes where appropriate. The estimates for present day radiative effects, as well as the availability of paleodata to constrain the aerosols at sufficient spatial and temporal resolution from Sections 2-6 are available in Table 4 for present day, and Table 5 for paleo time periods.

6.1 Marine aerosols

6.1.1 Sea spray aerosols

In oceanic and coastal regions, sea spray aerosols (SSA) form when wind-driven sea water is mobilized into the lower atmosphere. An estimated 3-70 Pg of SSA are injected into the atmosphere annually, making it one of the largest sources of atmospheric aerosols along with dust (Grythe et al., 2014; Varlas et al., 2021). The primary radiative effect from SSA scattering ranges from -0.2 to -0.35 W m^{-2} (Thornhill et al., 2021), and because they can act as cloud condensation nuclei and ice-nucleating particles, SSA also have secondary forcing impacts (Fan et al., 2025; DeMott et al., 2016). The uncertainty on their radiative forcing is a result of the both strong dependence of SSA's refractive index on its chemical composition, which can vary by oceanic source region and time of year, and temporal and regional variations in climate, particularly wind speed (Fan et al., 2025).

In each global climate model, SSA production is typically estimated via a unique parameterization scheme that accounts for surface wind speed, sea-surface temperature, wave state, salinity, and whitecap coverage (Song et al. 2023). These different schemes, in combination with different atmospheric and oceanic models, yield widely different production rates of SSA and therefore large uncertainty in the RE of SSA in sensitivity experiments (ranging between -0.35 ± 0.04 W/m^2 and -2.28 ± 0.07 W/m^2; Thornhill et al., 2021). For example, within a single atmospheric model, varying the parameterization for the emission scheme alters both the amount and size distribution of SSA and consequently of RE, and can generate significant warming or cooling relative to a standard scheme (-2.66 W/m^2 to 2.69 W/m^2; Venugopal et al., 2025). Evaluating the realism of these schemes is a current goal of ongoing field campaigns and laboratory work. This suggests about -0.5 W/m^2 +/-1 is an appropriate range similar to some studies (Rapp et al, 2013).

Modern constraints on SSA can come from observational efforts (e.g. Marine Aerosol Network; Smirnov et al., 2011), satellite retrievals (Toth et al., 2013), and laboratory experiments (Prather et al. 2013; Sauer et al. 2022; Mehta et al. 2019; Bruch et al. 2021). At the time of writing, the best publicly available repository of field campaign data is maintained by the Pacific Marine Environmental Laboratory

Deleted: Rapp

Formatted: Default Paragraph Font, Font color: Black

Formatted: Normal, Centered, Border: Top: (No border), Bottom: (No border), Left: (No border), Right: (No border), Between : (No border), Tab stops: 3.25", Centered + 6.5", Right, Position: Horizontal: Left, Relative to: Column, Vertical: In line, Relative to: Margin, Wrap Around

Formatted: Font color: Black

(Quinn et al. 2023). These constraints are limited by the sparse coverage of field observations, particularly in the Southern Hemisphere where operational logistics are extremely challenging and extensive cloud cover obscures the surface from satellites. Extending this observational network would allow for better tests of model fidelity and therefore future promise of improved marine aerosol properties and their radiative effects. Sea spray aerosols are not emitted directly by human activity, but can respond to climate.

Reconstructions of past SSA can come from measurements of sea salts in polar ice cores (e.g. Na, Cl, other halogens), especially for coastal sites that are most sensitive to marine emissions (Maselli et al., 2017; Rhodes et al., 2017; Wolff et al., 2003). While SSA is relatively easily measured in these cores, its utility in understanding past oceanic and climatic conditions is limited because of a lack of spatial coverage over the oceans. Ongoing efforts to build this understanding include the study of chlorine aerosol production from blowing snow (Frey et al. 2020; Yang et al. 2019) or frost flowers when sea ice forms (Wolff et al., 2003), which may have been very important in past, colder climates. Generalizing SSA production from the present day to past continental configurations and biological activity remains a challenge. Several studies suggest the importance of sea surface temperatures for the generation of SSAs, which makes them sensitive to different climate regimes (Revell et al., 2021).

6.1.2 Dimethyl Sulfide

Ocean ecosystems produce dimethyl sulfide (DMS) after complicated chemical and biological processes in the upper ocean (Toole et al., 2008). This DMS reacts in the atmosphere to form sulfate, which forms cloud condensation nuclei. The interactions between DMS and climate have been one of the most studied, starting from the CLAW hypothesis (Charlson et al., 1987) (named from the authors of the study). This hypothesis argued that warmer conditions would promote more dimethyl sulfide production from the ocean, which would increase sulfate production in the atmosphere, reducing temperatures, thus providing an important negative feedback. Multiple studies have shown larger or smaller interactions with climate (e.g. Carslaw et al., 2010; Joge et al., 2025; Rap et al,. 2013). Uncertainties abound in both the oceanic source of DMS, since it is a residual term in complicated chemistry and biology, as well as the impact of additional sulfate on clouds over the ocean. Current estimates suggest an impact between -1 and -2.4 W m^{-2} from direct radiative effects plus aerosol cloud interactions (Joge et al., 2025; Rap et al., 2013). The DMS compound can be directly emitted from combustion processes, but here we focus on the natural emissions from oceans, which can be modified by climate changes.

There are no direct reconstructions of DMS from observations for past climates available, but ice core measurements of methanesulfonic acid (MSA), a product of atmospheric DMS oxidation, can be used as a proxy for past DMS changes in polar ice cores (e.g., Jongebloed et al., 2025; Legrand et al., 1991).

6.1.3 Marine organic aerosols

Recent studies have highlighted the generation of organics within marine ecosystems and their emissions into the atmosphere (e.g. Shaw et al., 2010). Similar to land based emissions (6.2.2), emissions of compounds such as isoprene and other compounds can lead to the production of organic aerosols either due to chemical reactions, or physical processes such as cooling or a combination of effects (Ayers et al., 1997; Cui et al., 2019; Lewis et al., 2001; Rocco et al., 2025; Shaw et al., 2010). Quantities of emitted marine organic compounds that are aerosol precursors can be of the same magnitude as DMS (Rocco et a., 2025), although much less studied. Organic aerosol species can also be emitted as part of sea spray, and maybe included in some studies as sea spray aerosols (e.g. Burrows et a., 2014; Wang et al., 2015). Organic aerosol precursors can be emitted directly by humans as well, but here we focus on the marine emissions, which can be modified by climate.

Deleted: humans

Formatted: Default Paragraph Font, Font color: Black

Formatted: Normal, Centered, Border: Top: (No border), Bottom: (No border), Left: (No border), Right: (No border), Between : (No border), Tab stops: 3.25", Centered + 6.5", Right, Position: Horizontal: Left, Relative to: Column, Vertical: In line, Relative to: Margin, Wrap Around

Formatted: Font color: Black

While some Earth system models include marine organic aerosols (Rasch et al., 2019), this is not very common (e.g. Danabasoglu et al., 2020). Estimates of the radiative effect of marine organic aerosols are not available. Paleo-proxy estimates of organic compounds are available in ice cores, but not in other media, limiting the ability to make estimates of changes in marine organic aerosols in historical or paleotime periods.

6.2 Land based aerosols

6.2.1 Nitrate and ammonium

Nitrate and ammonium aerosols have implications for radiative forcing, as they can impact the aerosol refractive index and cloud formation, and are important for tropospheric atmospheric chemistry and photochemistry (Feng & Penner, 2007; Xu & Penner, 2012). Both can be emitted from anthropogenic and natural sources at present day, with nitrate primarily sourced from fossil fuel combustion, soil emissions, lightning, and biomass burning (Delmas et al., 1997) and ammonium primarily sourced from agriculture with lesser contributions from biomass burning, fossil fuels, and other sources (Van Damme et al., 2014). Nitrate and ammonium aerosols interact with sulfate in the atmosphere in a complex set of reactions that impacts aerosol optical depth depending on the relative amount of each species (Martin et al., 2004; Paulot et al., 2016). Over recent decades emissions inventories (Crippa et al., 2023), EDGAR dataset (https://edgar.jrc.ec.europa.eu/index.php/dataset_ap81)) and satellite-based measurements (Clarisse et al., 2009; Liu et al., 2020) provide detailed constraints on the emissions and atmospheric budget for these two species. In global climate models, nitrate and ammonium are not always included in radiative forcing estimates since the nitrate component requires tropospheric photochemistry and a chemical equilibrium with the gas phase (e.g. Nenes et al., 2011). The sum of direct radiative effects and aerosol cloud interactions of nitrate aerosols is estimated to be about -1W m^{-2} (Lu et al., 2021), which includes anthropogenic emissions of these constituents, which likely dominates current emissions (Naik et al., 2021). Long-term reconstructions of both species are primarily derived from polar and alpine ice cores (Fischer et al., 2015; Hastings et al., 2009; Kaufmann et al., 2010; Preunkert et al., 2003; Wendl et al., 2015), which provide accurate information only in the vicinity of these cores, leaving most of the mid-latitudes and tropics unresolved.

6.2.2 Natural primary and secondary organics

There are many natural sources of primary and secondary organic aerosols, including direct emission of organic compounds in aerosol phase, such as from trees, bacteria or fungi, or the emission of biogenic volatile organic compounds (BVOC) (Tsigaridis et al., 2014; Mahowald et al., 2011). Because of the multiple of types of organic compounds, and the difficulty in measuring both total organic matter and the different organic compositions there is substantial uncertainty in the distribution and types of aerosols (Moschos et al., 2022; Mahowald et al., 2025; Sun et al., 2025). In many regions and times of the year, anthropogenic organic aerosols or aerosols from fires dominate (e.g. Moschos et al., 2022), which are discussed elsewhere. In terms of their impact on climate, the most explored natural organic aerosols not from fires are the BVOCs (Tsigaridis and Kanakidou, 2018; Weber et al., 2022; Lin et al. 2014, Spore et al, 2019). They are released naturally from vegetation, and are converted in the atmosphere to particles. Because of their secondary formation in the atmosphere, they can contribute substantially to the number of aerosols and thus to the number of cloud condensation nuclei (Weber et al., 2022; JLin et al. 2014, Sporre et al, 2019). Estimates suggest substantial forcing from these natural aerosols, such as feedback under warming of -0.3W m^{-2} (Sporre et al., 2019), but similar to other aerosols, the forcing is uncertain (we assign here +/-0.3). While human activity can directly emit primary and secondary organics, here we focus on naturally emitted compounds, which can be modified by humans through land use or management as well as due to climate changes.

Deleted: ..

Deleted: and

Deleted: humans

Formatted: Default Paragraph Font, Font color: Black

Formatted: Normal, Centered, Border: Top: (No border), Bottom: (No border), Left: (No border), Right: (No border), Between : (No border), Tab stops: 3.25", Centered + 6.5", Right, Position: Horizontal: Left, Relative to: Column, Vertical: In line, Relative to: Margin, Wrap Around

Formatted: Font color: Black

Observational and proxy records to constrain past BVOCs are extremely limited, with only a few sparse records from alpine (e.g., Burgay et al., 2025; Legrand et al, 2025, 2013) and polar ice (e.g. Zangrando et al., 2020) cores providing data over limited geographic regions and timeframes.

6.3 Fossil fuel and biofuel aerosols

While anthropogenic activities have an impact on nearly all aforementioned aerosol classes, the magnitude of such emissions can be relatively well-constrained compared to emissions from natural sources. Records of fossil fuel consumption combined with emissions factors for specific chemical species can be used to develop gridded emissions datasets to constrain the magnitude of the anthropogenic component for many aerosol classes (e.g. Hoesly et al., 2018, EDGAR) over recent decades. Anthropogenic activities can also result in emissions of other aerosols with detrimental environmental and health impacts, such as metals (Mahowald et al., 2018; McConnell & Edwards, 2008) and organics (Nault et al., 2021), that do not have strong direct radiative forcing. While these emissions are relatively well characterized, small uncertainties in anthropogenic and biomass burning emissions can muddle estimates of the sensitivity of clouds to aerosol changes and the resulting climate impacts (Hamilton et al., 2018; Brown et al., 2026). Aerosol and cloud microphysics within Earth system models (ESMs) are tuned with these sensitivities in mind, and their uncertainties have implications for future climate projections with these models.

7. Cross-cutting synthesis of natural aerosol uncertainty and paleo proxy constraints

7.1 Current estimates and uncertainties in natural aerosols

Through the review of existing estimates of dust, biomass burning, volcanic and other aerosols (Sections 3-6), we have compiled estimates of effective radiative effects in the present day, separating aerosol-radiation (ari) and aerosol-cloud (aci) interactions (Table 4). For earlier periods like the PI or LGM, we have paleo proxies to constrain variability of dust and volcanic aerosols, which inform estimates of their radiative effects for different time periods. However, we have limited information for aerosols from open fires and other types of biomass burning (e.g. residential wood burning in the PI) (Table 5), which is problematic because variability in fire aerosol represents radiative effects that can reach up to 2 W/m^2 (Figure 7). In addition, there are several other natural aerosols (Section 6) that have likely changed due to climate effects (DMS, sea spray) or due to climate and land use changes (BVOC) for which we only have ice core data, which means we cannot estimate the changes far from the ice cores. These aerosols also have the potential for significant changes and impacts (Figure 7). One important issue is that paleo-aerosol modelers should calculate the effective radiative forcing, not just the instantaneous radiative forcing, since effective radiative forcing is needed for climate sensitivity calculations.

For aerosol types with sparse or absent paleo constraints, a key challenge is how to estimate uncertainty in aerosol radiative forcing between time periods. Dust provides a useful cautionary example. Early model estimates of Last Glacial Maximum dust changes were incomplete until proxy compilations and model–data comparisons showed the importance of source changes due to vegetation shifts and additional glaciogenic dust sources (e.g. Mahowald et al., 1999). The resulting inferred change in dust loading from PD to LGM was a factor of ~2.5. This raises the question of whether other natural aerosols have also changed substantially between paleoclimate periods. However, applying the change in dust as a generic uncertainty estimate for other aerosol types would not be justified because the processes controlling emissions of DMS, sea spray, BVOCs, and biomass burning aerosols differ from those controlling dust, so that their sensitivities to climate, land use and ecosystem change are unlikely to scale in similar ways.

Deleted:

Deleted: paleoaerosol

Deleted: .

Formatted: Default Paragraph Font, Font color: Black

Formatted: Normal, Centered, Border: Top: (No border), Bottom: (No border), Left: (No border), Right: (No border), Between : (No border), Tab stops: 3.25", Centered + 6.5", Right, Position: Horizontal: Left, Relative to: Column, Vertical: In line, Relative to: Margin, Wrap Around

Formatted: Font color: Black

Our goal for this paper is to identify a path forward to improve these estimates and uncertainties and we describe a pathway in the next few sections. Notice that for many aerosols there is not sufficient information in the Tables to be complete (Table 4 and 5). More studies of natural aerosols in the current climate (Table 4) and combined with paleo-data proxies are needed (Table 5). In addition, for several time periods that are being used for climate sensitivity studies (e.g. Sherwood et al., 2021) there are no aerosol syntheses, meaning they are subject to large uncertainties in their aerosol forcings (e.g. 6kbp, Last Millennial, Pliocene).

Table 4: Natural aerosol present day (PD) effective radiative effect (ERE) from Sections 3-6.

ERE ari= Effective Radiative Forcing, aerosol radiation interaction; ERE aci= aerosol cloud interaction. DMS=dimethyl sulfide, BVOC=biogenic volatile organic compounds. The ERE ari and ERE aci may be derived from separate studies as the ERE (and thus not add up) or may not be available for all species. If the paper does not include an uncertainty for the ERE value, we indicate with †.

Process	PD ERE ari (W/m^2)	PD EREaci (W/m^2)	PD ERE (W/m^2)	Paleodata availability	Citation
Dust	-0.15 +/- 0.35	-0.03 +/- 0.28	-0.20 +/- 0.50	Medium	Kok et al., 2023
Open Fires	-0.9+/-0.3		-0.9 +/- 1.1	Low-medium	Wan et al., 2020; Penner et al., 1992; Jiang et al., 2021
Volcanic	-0.2 +/- 0.2	-0.6 +/- 0.6	-0.4+/-0.2	Medium	Aubry et al., 2026; Rap et al., 2013
Sea spray aerosol	-0.4 †	-0.04 †	-0.5 +/- 1	Low	Rap et al., 2013; Thornhill et al., 2021; Venugopal et al., 2025
DMS	-0.2 †	-0.8 †	-1.0+/-0.5	Low	Rap et al., 2013
BVOC			-0.3 +/- 0.3	Low	Rap et al., 2013

Deleted: 2
Deleted: ERF
Deleted: ERF
Formatted Table
Deleted: ERF
Deleted: ERFaci
Deleted: ERF
Formatted Table
Deleted: 7 to +
Deleted: 2.
Deleted: 23 to -
Deleted: 44
Deleted: ,
Deleted: 23
Deleted: 76
Deleted: +.-

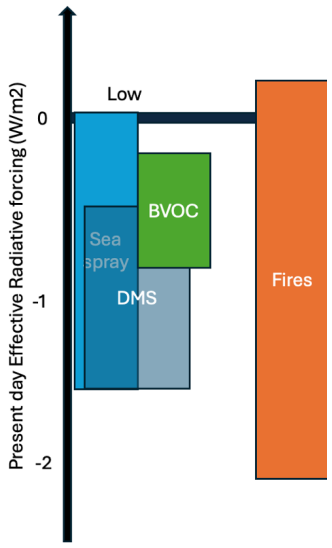

Deleted:

Formatted: Default Paragraph Font, Font color: Black
Formatted: Normal, Centered, Border: Top: (No border), Bottom: (No border), Left: (No border), Right: (No border), Between : (No border), Tab stops: 3.25", Centered + 6.5", Right, Position: Horizontal: Left, Relative to: Column, Vertical: In line, Relative to: Margin, Wrap Around
Formatted: Font color: Black

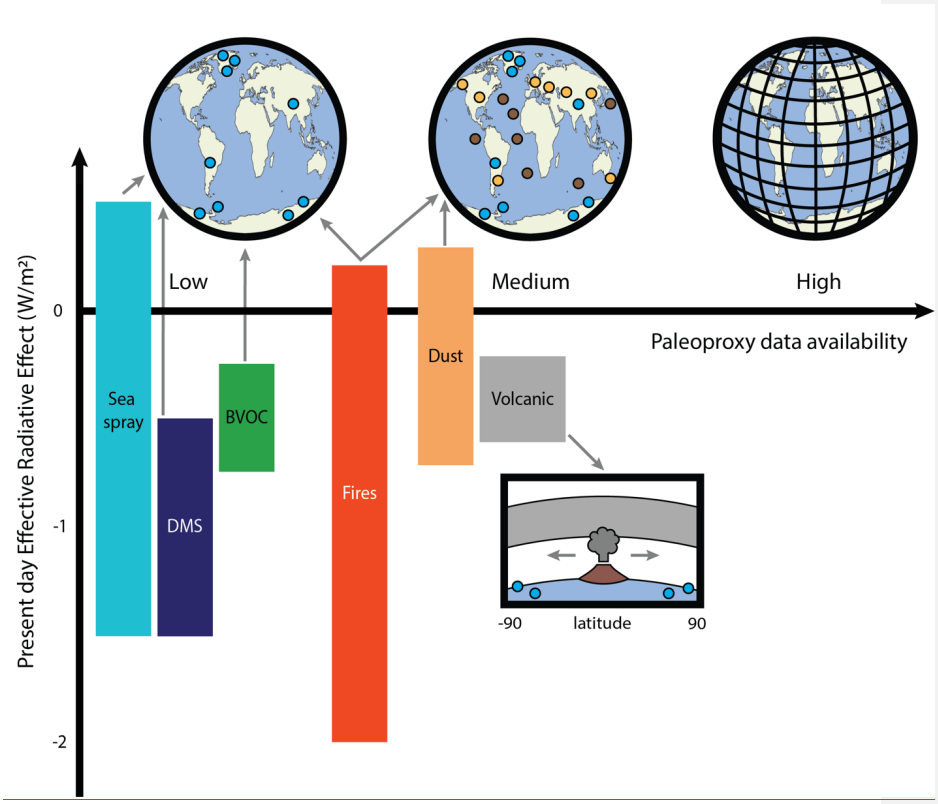

Figure 7*: Bar graphs: Estimates of the aerosol effective radiative effect of each 'natural' aerosol type for present day conditions, and the paleo-data proxy availability, as discussed in the above sections, and in Table 4 (citations in Table 4). "Fire" means direct and precursor emissions from fire sources, while volcanic is emissions of precursors from volcanoes. Above the bar graphs, the globes show the spatial distribution of cores available for the different particle types. Most particle types are available in the ice cores (blue dots), which are only available in a few locations, mostly high latitudes. Fires and dust have not only ice cores but the possibility of marine, terrestrial and lake sediment records (medium). Quantitative records of volcanic aerosols are only available in ice cores, but they are well mixed since in the stratosphere (inset image). To have high paleoproxy availability, proxies would need to be available across regular grids across the globe (high).*

Formatted: Font: Not Bold

Formatted: Default Paragraph Font, Font color: Black

Formatted: Normal, Centered, Border: Top: (No border), Bottom: (No border), Left: (No border), Right: (No border), Between : (No border), Tab stops: 3.25", Centered + 6.5", Right, Position: Horizontal: Left, Relative to: Column, Vertical: In line, Relative to: Margin, Wrap Around

Formatted: Font color: Black

Table 5: Estimates of aerosol radiative forcing for different time periods. PD=present day, PI=preindustrial, ERF=effective radiative forcing, LGM=last glacial maximum, 6kbp=6000 years ago, Last Millenium: last 1000 years. For aerosols not included in this table, there is no estimate available. For papers which did not include uncertainty estimates, we indicate with †. *Represents the difference in instantaneous ERE.

Process	PD-PI ERF (W/m^2)	LGM-PI ERF (W/m^2)	6kbp-PI ERF (W/m^2)	Last millenium-PI (W/m^2)	Citation
Dust	-0.07±0.18				Kok et al., 2023
		-1 +/- 1			Albani et al., 2018
			+0.04*†		Albani and Mahowald, 2019
Open Fires	-0.4 †				Unger et al., 2012
	±1.6	±2.4			Mahowald et al., 2024
	-1.2+/-0.6				Hamilton et al. 2018
	-0.6+/- 0.8				Wan et al., 2020
Volcanic	0.2 +/-0.1		-0.1†	-0.1†	Aubry et al., 2026

7.2 A roadmap for proxy-model integration

We propose a conceptual "Proxy Integration Ladder" describing the progressive translation of paleoenvironmental archive data into reconstructions of aerosol emissions for calculating radiative forcing. The ladder spans five stages representing increasing levels of synthesis and environmental interpretation (Figure 8): (1) proxy observations, (2) harmonized proxy metrics, (3) proxy synthesis, (4) environmental process interpretation linking proxy variability to aerosol emissions and atmospheric loading, and (5) integrated multi-proxy aerosol emission and radiative forcing reconstructions.

Advancing along this ladder requires coordinated methodological development, increasing integration of proxy archives, improved representation of proxy-environment relationships, along with systematic and propagating uncertainty quantification. The following tiered framework outlines pathways through which the proxy community can progressively move toward these integration goals. To illustrate,

Deleted: Millenial

Deleted: RF

Deleted: 6bp

Formatted Table

Deleted: RF

Deleted: RF

Deleted: 2.0 to +0.

Deleted: *

Deleted: *

Deleted: -0.7 to

Deleted: 8

Deleted: +

Deleted: 2 to -1.4

Deleted: .

Deleted: -

Deleted: to -0.33

Deleted: *Represents the difference in instantaneous rRE.¶

Deleted: ,.

Deleted: :

Formatted: Default Paragraph Font, Font color: Black

Formatted: Normal, Centered, Border: Top: (No border), Bottom: (No border), Left: (No border), Right: (No border), Between : (No border), Tab stops: 3.25", Centered + 6.5", Right, Position: Horizontal: Left, Relative to: Column, Vertical: In line, Relative to: Margin, Wrap Around

Formatted: Font color: Black

we use the example of the Last Glacial Maximum dust cycle, which evolved over many years before the first synthesis of paleo-data generated aerosol radiative effects.

Tier 1: Development of standardized, publicly accessible global proxy datasets

The first step involves compiling globally distributed proxy datasets with standardized formats and rich metadata, including age models, chronological uncertainties, analytical methods, site characteristics, and proxy measurement protocols. Major progress has been made within several proxy communities (see Sections 3, 4 and 5). For the LGM dust cycle, different papers synthesized different proxies, for example Rea (1994) compiled marine sediment records, while Kohfeld and Harrison (2003) synthesized terrestrial sediment records.

It is also recommended to report not only the total uncertainty associated with individual records, but also uncertainties arising from different sources, including measurement and calibration processes, assumptions made to address missing information, and spatial representativeness (e.g., Cosentino et al., 2024). For example, two records using the same measurement techniques may share systematic uncertainties and therefore should not automatically be treated as having independent errors (e.g., Dolman et al., 2021). Identifying these sources would help avoid overconfidence in conclusions drawn from multiple records, whether in proxy synthesis or in data–model integration (e.g., Wahl et al., 2022; Okazaki et al., 2025).

Tier 2: Harmonization of proxy measurements into standardized metrics

The second step involves transforming raw proxy measurements into standardized metrics that improve comparability both within and across proxy types (see examples, Section 3, 4 and 5). This transformation requires accounting for site-specific depositional processes, sampling resolution, and methodological differences that may bias temporal trends. Efforts to harmonize different measurements across different sizes and types can continue for years: for example for the LGM dust example, there are still papers trying to understand how best to treat different sources and sizes (Maher et al. 2010; Cosentino et al., 2024).

Harmonization should also assess the consistency of records that provide comparable environmental information across different datasets. For example, newly incorporated observations should be compared with nearby records, where available (Albani et al., 2015). Substantial discrepancies, whether in magnitude or in the inferred direction of change (e.g., increasing versus decreasing), should be documented and investigated to identify possible causes. Unresolved discrepancies should be clearly reported, and any exclusion of conflicting records should be justified, so that subsequent proxy synthesis and data-model integration efforts can evaluate the reliability of conflicting observations and determine how to account for them.

Tier 3: Proxy synthesis of spatial and temporal variability

The third step involves integrating multiple proxy records of different types to reconstruct regional to global spatiotemporal aerosol deposition variability. Because individual proxy records differ in spatial representativeness, temporal resolution, and sensitivity to environmental processes, synthesis should consider whether changes observed at individual sites reflect broader environmental patterns or local and regional variability. As an example, DIRTMAP created a new publicly available compilation of paleodust including more tracers of dust, including terrestrial, marine, and ice cores (Kohfeld and Harrison, 2001). Previous studies had looked only at the ice cores, which showed much larger changes than closer to the main source areas (e.g. Andersen and Genthon, 1996). These differences illustrate why records from a single region may not be representative of global changes, highlighting the importance of integrating observations across different regions to capture spatial heterogeneity. Such spatial patterns provide valuable observational constraints for model-based reconstructions of aerosol emissions.

Deleted: footprint, temporal resolution, and sensitivity to environmental processes, direct quantitative comparisons are often challenging

Formatted: Default Paragraph Font, Font color: Black

Formatted: Normal, Centered, Border: Top: (No border), Bottom: (No border), Left: (No border), Right: (No border), Between : (No border), Tab stops: 3.25", Centered + 6.5", Right, Position: Horizontal: Left, Relative to: Column, Vertical: In line, Relative to: Margin, Wrap Around

Formatted: Font color: Black

Tier 4: Translation of proxy signals into aerosol emission data

The fourth step involves translating proxy measurements into physically meaningful aerosol metrics such as emission fluxes or atmospheric concentrations through physical model and data-model integration (e.g. see examples in Sections 3, 4 and 6). This is challenging because aerosol deposition reflects not only emissions but also atmospheric transport and removal processes. Care should therefore be taken not to attribute all model-observation discrepancies to emission errors, as adjustments to emissions may compensate for biases in modeled transport or deposition. Comparing model performance across multiple observations can help identify discrepancies that cannot be explained by emission changes alone. Furthermore, using multiple models can help assess model uncertainty, although systematic biases shared across models may remain undetected (e.g., Kok et al., 2021).

For the LGM example, early modeling studies estimated dust emissions and evaluated simulated deposition against paleo-observations (e.g. Mahowald et al., 1999), while subsequent studies used inverse modeling to quantitatively constrain regional dust emissions from compiled deposition records (e.g., Albani et al., 2014). More studies using data assimilation after proxy calibration would provide guidance on the best practices for regularizing inversion approaches and assessing the robustness of reconstructed emissions.

Tier 5: Integrated multi-proxy reconstructions of aerosol emissions and radiative forcing

The ultimate objective is the development of global multi-proxy aerosol emission and radiative forcing reconstructions that optimally integrate the spatial representativeness and strengths of each proxy archive. Fully integrated global reconstructions remain rare, but recent studies have begun linking proxy-constrained emission reconstructions to estimates of aerosol radiative forcing.

Early studies estimated LGM dust radiative forcing using modeled dust distributions (e.g., Claquin et al., 2003). Subsequent work incorporated multiple observational constraints, including dust deposition, particle size distributions, and provenance information, to improve dust simulations and their estimates of radiative forcing (e.g., Albani et al., 2014). More recently, proxy-constrained historical dust emission reconstructions have been used in eight Earth system models to quantify dust direct radiative forcing since the pre-industrial era (Leung et al., 2025; Haugvaldstad et al., 2026). However, systematically propagating uncertainties from proxy observations through emission reconstructions and atmospheric processes to radiative forcing remains a major challenge that requires further investigation.

Deleted: (e.g. see examples in Sections 3, 4 and 6). Progress has been made within individual proxy communities.

Deleted:

Deleted: although ongoing methodological advances in

Deleted: calibration, data assimilation, and Earth system modeling provide promising pathways.

Formatted: Pattern: Clear

Formatted: Default Paragraph Font, Font color: Black

Formatted: Normal, Centered, Border: Top: (No border), Bottom: (No border), Left: (No border), Right: (No border), Between : (No border), Tab stops: 3.25", Centered + 6.5", Right, Position: Horizontal: Left, Relative to: Column, Vertical: In line, Relative to: Margin, Wrap Around

Formatted: Font color: Black

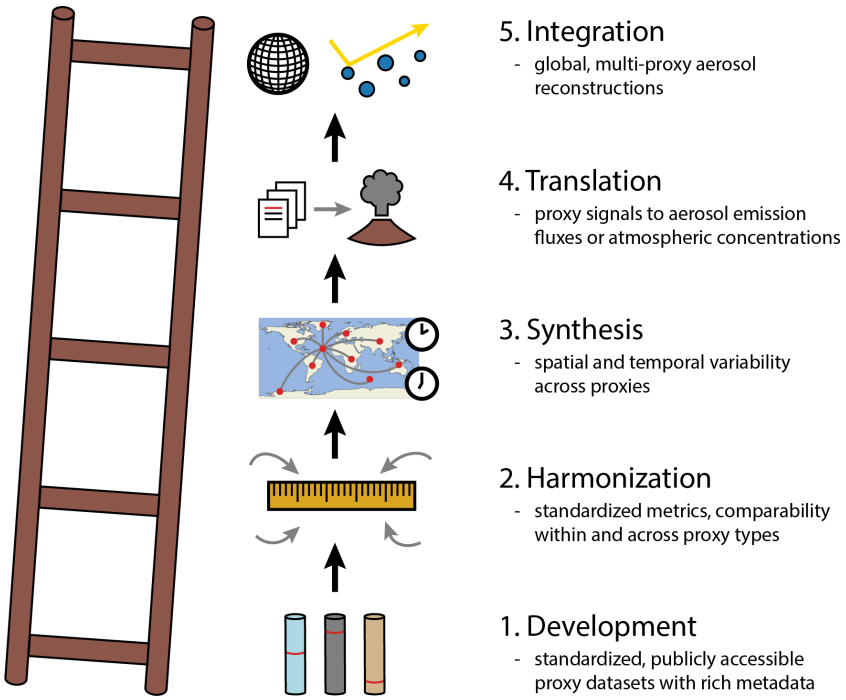

Figure 8. Illustration of the conceptual "Proxy Integration Ladder" framework. This takes a bottom-up approach, starting from Tier 1: Development and moving to Tier 2: Harmonization, Tier 3: Synthesis, Tier 4: Translation, and Tier 5: Integration.

Effective collaboration starts with a community commitment to learning each other's fundamental knowledge, challenges and the language used in different fields of study. This paper represents an effort to integrate and discuss issues between aerosol modelers, paleo-proxy observationalists, paleo-modelers and other scientists.

Structural changes could help bridge the gap between aerosol proxy development and emission modeling. Funding programs that support scholar exchange and joint mentorship, such as cross-disciplinary graduate training or collaborative postdocs, can foster long-term integration between proxy and modeling communities. Co-designed experiments are especially promising: forward models that simulate proxy signals (e.g., dust, charcoal, SO2 fluxes, etc.) from climate and emissions scenarios can help proxy experts explore signal formation processes, while modeling frameworks can be used to test how measurement uncertainties propagate through atmospheric transport and deposition. Focused workshops aimed at specific inconsistencies, such as mismatches between reconstructions and model output, can accelerate progress through iterative hypothesis testing. Establishing transparent norms around early-stage collaboration and co-authorship will further promote trust and shared ownership. Together, these efforts could shift aerosol emission reconstruction from a set of parallel efforts into a more integrated community science enterprise—capable of constraining past climate forcing and improving future projections.

Formatted: Default Paragraph Font, Font color: Black

Formatted: Normal, Centered, Border: Top: (No border), Bottom: (No border), Left: (No border), Right: (No border), Between : (No border), Tab stops: 3.25", Centered + 6.5", Right, Position: Horizontal: Left, Relative to: Column, Vertical: In line, Relative to: Margin, Wrap Around

Formatted: Font color: Black

7.3 Propagating uncertainties

Assessing the aerosol radiative effect requires accounting for several distinct sources of uncertainty. A key, and often under-constrained, source is the emission strength itself. Constraining past emissions using improved paleodata is therefore central to reducing overall uncertainty and represents a main goal of this paper.

A second source of uncertainty lies in aerosol properties and the physicochemical processes related to aerosol-radiation and aerosol-cloud interactions. Optical properties, particle morphology and aerosol size distributions, which vary with composition and aging, directly influence the aerosol direct radiative effect. Chemical composition and particle morphology further affect cloud formation and lifetime by determining how aerosols act as cloud condensation nuclei (CCN) and ice nucleating particles (INPs) (Hamilton et al., 2018; Mahrt et al., 2018, 2020; Schill et al., 2020), thereby influencing cloud albedo and lifetime (Carslaw et al., 2013; McGraw et al., 2020a-b).

A third source of uncertainty arises from the choice of baseline time period. In standard IPCC terminology, the PI reference period is typically defined as ca. 1850, yet radiative forcing changes are sometimes calculated relative to 1750 (Szopa et al, 2021). For some aerosol sources, such as fires, there is evidence that emissions in 1750 differed substantially from those in 1850, introducing additional ambiguity in the aerosol burden assigned to PI conditions (Marlon et al., 2016).

Critically, these sources of uncertainty do not affect radiative forcing independently. Instead, they propagate through a chain of linked steps: (i) proxy measurement and interpretation, (ii) translation of proxy signals into aerosol emission estimates, (iii) simulation of atmospheric aerosol loading and properties from those emissions, and (iv) quantification of the resulting radiative forcing. Uncertainties at each stage compound, and the chain is further complicated by nonlinearities, particularly in aerosol–cloud interactions, where small differences in baseline aerosol concentrations can alter the magnitude or even reverse the sign of regional forcing estimates (Carslaw et al., 2013).

Once uncertainties have been quantified for individual aerosol species, combining them into a total uncertainty estimate requires knowledge of the correlations of these uncertainties between species. In practice, these correlations are poorly known, and uncertainties are therefore typically combined in quadrature – that is, by taking the square root of the sum or squared individual uncertainties – under the assumption that errors are uncorrelated. As improved paleodata and multi-species proxy records become available, it should become possible to better characterize these inter-species correlations and thereby refine total uncertainty estimates. More studies need to address the best approach for addressing different uncertainties and adding them together.

7.4 Important properties of datasets

Global aerosol datasets, i.e. coherently organized compilations of past aerosol records from natural archives (typically deposition fluxes, in some cases AC) (Albani et al., 2014; Harrison et al., 2022; Kohfeld and Harrison, 2001; Legrand et al., 2016; Liu et al., 2021; Marlon et al., 2016; Sigl et al., 2015) have been the backbone for model benchmarking and validation over the last decades (Hamilton et al., 2018; Hopcroft et al., 2015; Mahowald et al., 2010; Takemura et al., 2009; Werner et al., 2002). Paleo-aerosol datasets also constitute the basis for *derived products, i.e., global gridded fields resulting from data assimilation procedures, using ESMs* (Albani et al., 2016; Leung et al., 2025; Mahowald et al., 2006), chemical transport models (Eckhardt et al., 2023; Zhang et al., 2024), *or statistical techniques* (Lambert et al., 2015; Cosentino et al., 2023; Molina Catricheo et al., 2024). Derived products can be useful to estimate global aerosol loads and radiative effects (Albani et al., 2015; Mahowald et al., 2006), and constitute input fields for ESMs that don't have the capability to prognostically simulate aerosol variability across climate states (Kageyama et al., 2018), or for standalone models such as those simulating ocean biogeochemistry (Heinemann et al., 2019; Lambert et al., 2021; Opazo et al., 2025).

Formatted: Default Paragraph Font, Font color: Black

Formatted: Normal, Centered, Border: Top: (No border), Bottom: (No border), Left: (No border), Right: (No border), Between : (No border), Tab stops: 3.25", Centered + 6.5", Right, Position: Horizontal: Left, Relative to: Column, Vertical: In line, Relative to: Margin, Wrap Around

Formatted: Font color: Black

A key challenge in constructing these datasets is the short atmospheric lifetimes of aerosols (hours to days), which leads to strong spatial and temporal variability in both atmospheric load and deposition. The implication is that a relatively dense spatial coverage (~200km) of synchronized records is needed in order to constrain past aerosol spatial extent and variability. This, in turn, necessitates leveraging multiple natural archives that sample locations proximal to their sources as well as at intermediate and remote deposition sites (Cosentino et al., 2024; Marlon et al., 2016; McConnell et al., 2021; Sigl et al., 2015).

In addition to aerosol deposition fluxes, additional constraints on aerosol size distribution and provenance (typically inferred from the geochemical composition) are key elements to fully constrain the magnitude and spatial variability of their global cycles (emission, atmospheric load during transport, and deposition). Particle size distributions and distance from the source are tightly linked to surface fluxes, and become particularly important when comparing paleo-aerosol data from natural archives with ESMs, whose simulated aerosol size distributions are restricted and also need to be validated with paleo data (Mahowald et al., 2014).

To maximize the impact of paleodust datasets for model benchmarking and use as a tool for data assimilation and derived products, paleo-aerosol datasets should follow the FAIR (Findable, Accessible, Interoperable, and Reusable) principles (Wilkinson et al., 2016), be amenable to revision subject to new chronologies or assumptions, and emerge from a community effort involving both data users and data producers. In practice, this means that paleo-aerosol datasets should be indexed and publicly available through open repositories, accompanied by a peer-reviewed publication including data producers as co-authors – which would give some authoritative value to the shared results of the harmonization procedures that are necessary to coherently review and organize the multiplicity of individual records arising from different natural archives and proxies.

An inherent difficulty is that different natural archives and dating possibilities do not offer, with very few exceptions, the opportunity of having records spanning both the historical period and older paleoclimate states. Consequently, global paleo-aerosol datasets are intrinsically inconsistent, being linked to a specific climate period, resulting in heterogeneous temporal coverage and resolution (Table 2), which must be accounted for in their interpretation and application.

7.5 The Value of Multi-proxy Studies and Simulations

Individual aerosol species and their proxies each receive the attention of large communities of specialists, but ESMs offer an opportunity for multi-proxy evaluation that integrates this expertise. Multiple observation types provide independent constraints upon ESMs and climate hypotheses. The contrasting sensitivity of different proxies to different aspects of the climate allow ESMs to investigate a broader set of climate mechanisms and their interaction, allowing more comprehensive hypotheses to be tested. For example, Legrande et al. (2006) simulate the response of dust, water isotopes, ^{10}Be and wetland methane emissions to freshwater inflow into the Labrador Sea, a hypothesis for the temporary cooling of the North Atlantic at 8.2 ka. We recommend that model intercomparisons of past climates encourage multi-species and multi-proxy forward modeling. Many PMIP4 simulations of the LGM used PI dust, missing an opportunity for deeper analysis of the processes maintaining the LGM climate and its eventual transition into an interglacial.

7.6 Are Changes in Natural Aerosols Feedbacks or Forcings?

Direct and indirect radiative effect estimates for natural aerosols are used for many purposes in climate science, from a general quest to understand the importance of aerosols (Shao et al., 2011) to constraining the climate sensitivity that is an indicator of warming over the next century (Sherwood et al., 2020). Climate sensitivity (S) is classically defined as the change in global surface air temperature (ΔT_s)

Deleted: paleoaerosol

Deleted:

Formatted: Default Paragraph Font, Font color: Black

Formatted: Normal, Centered, Border: Top: (No border), Bottom: (No border), Left: (No border), Right: (No border), Between : (No border), Tab stops: 3.25", Centered + 6.5", Right, Position: Horizontal: Left, Relative to: Column, Vertical: In line, Relative to: Margin, Wrap Around

Formatted: Font color: Black

arising from a change in effective radiative forcing (ΔF), usually from a doubling of CO_2, (ΔF_{2xCO2}) (Stocker et al., 2015):

$$S = \Delta F_{2xCO2} / \lambda,$$

where λ is the feedback parameter in the budget for planetary energy (E),

$$dE/dt = \Delta F - \lambda \Delta T_s ,$$

. The term $\lambda \Delta T_s$ represents the radiative adjustment at the top of atmosphere that increasingly offsets the forcing ΔF with time as the climate returns to equilibrium. The climate sensitivity is the surface temperature evaluated after full adjustment to the forcing, so that the left side of the equation is zero.

If we want to attribute the observed temperature change to forcing over the historical period, then we need to distinguish radiative perturbations that are independent of the warming, and are thus a forcing, from radiative changes in response to the warming (and thus should be included within λ as a feedback). For example, the change in the ERF resulting from expanded dust sources following human land degradation (like the North American Dust Bowl) is a forcing, while changes in the dust ERF that results from changing source extent in response to climate-induced vegetation shifts would be a feedback. This distinction between forcing and feedback is not absolute, because processes like vegetation demographics that are approximately unchanging on decadal time scales will eventually respond to a changing climate over multiple decades and centuries (for example, through the replacement of high-latitude tundra with a boreal forest that reduces the visible albedo) In practice, climate scientists distinguish between the 'fast' Charney climate sensitivity that anticipates climate trends over the coming decades, when the extent of vegetation and continental ice sheets are approximately fixed (Charney et al., 1979), and the Earth System Sensitivity that characterizes the temperature change accounting for feedbacks that are slower to respond to the changing climate (over centuries or millennia for the continental ice sheets) (Lunt et al., 2010; Schmidt, 2012).

When estimating climate sensitivity from palaeo records, the temporal resolution of the record can be used to distinguish whether a process is a forcing or a feedback (PALAEOSENS, 2012). For example, if changes in temperature and radiative forcing can be inferred from a proxy archive with temporal resolution less than a century, processes that vary more slowly (like the variation of surface albedo with vegetation or ice sheet extent) can be treated as a forcing, even though these processes are a feedback that influences the temperature adjustment over a longer time interval.

In paleoclimate contexts, it is common to consider natural aerosols as 'fast' feedbacks within the system (e.g. Hansen and Sato, 2012; Sherwood et al., 2020; Szopa et al., 2021). For example, the higher LGM dust load is attributed to increasing surface winds (McGee et al., 2010) and expanded dust source areas related to a contraction of vegetation caused by a reduction of CO_2 fertilization compared to the PI (Mahowald et al., 1999).

PALAEOSENS (2012) recommend notation that explicitly denotes the degree of interactivity of the system. They propose subscripting the climate sensitivity S as such: $S_{[x]}$ where *[x]* denotes the factors that are assumed fixed and independent of the changing climate, and are thus regarded as forcings. Thus $S_{[GHG,LI,AE,VEG]}$ is the Charney sensitivity (with no greenhouse gas, land ice, vegetation or aerosol feedbacks), $S_{[CO2,LI,VEG]}$ would be the sensitivity of a system with interactive atmospheric composition, and $S_{[CO2]}$ would be the Earth System Sensitivity where all natural feedbacks can operate. For each $S_{[x]}$ there is a corresponding distinction between ΔF and λ.

The usefulness of estimating Earth system feedbacks from palaeoclimate to evaluate models used for future projections is related to the range of feedbacks represented within the model simulation. Early climate models had fixed atmospheric composition and no interactive emissions of short-lived climate forcings, and thus their (Charney) sensitivity is functionally different from modern ESMs that do include (some) of these feedbacks. Whether characterized as a forcing or feedback, for many natural aerosols, there are no pre-industrial or palaeoclimatic observations available (e.g. DMS, seasalt, etc.), and those for

Formatted: Default Paragraph Font, Font color: Black

Formatted: Normal, Centered, Border: Top: (No border), Bottom: (No border), Left: (No border), Right: (No border), Between : (No border), Tab stops: 3.25", Centered + 6.5", Right, Position: Horizontal: Left, Relative to: Column, Vertical: In line, Relative to: Margin, Wrap Around

Formatted: Font color: Black

which we do have data, dust for example, require heavy tuning of the models to match the observations for past climates (e.g. Albani et al., 2014; Albani et al., 2016). Model estimates of the changes in dust deposition over the historical period are one or two orders of magnitude too small compared to the limited model-data based estimates (Table 6), suggesting that our models may not yet be able to effectively simulate these feedbacks (for example, due to warming-induced changes in vegetation and dust source extent) or else that models are missing anthropogenic dust sources. This makes the distinction between forcing and feedback for aerosols uncertain in practice.

Table 6: Feedback estimates from models and obs-model compared. Dust feedbacks for LGM are calculated here as the effective radiative forcing change LGM to PI (Table 5: -1+/-1 W/m^2) over the temperature change for LGM-PI (-6.2 ± 1.7ºC) (Gulev et al., 2021).

	Model based estimate	Obs-model based estimate	
	(W/m^2)/ºC	(W/m^2)/ºC	
Process	Feedback	Feedback	Citation
Dust		-0.04 to +0.02	Kok et al., 2018
		+0.16 ± 0.26	Here: LGM to PI
	-0.004 ± 0.007		Thornhill et al., 2021
Sea spray aerosol	-0.049 ± 0.050		Thornhill et al., 2021
DMS	0.005 ± 0.006		Thornhill et al., 2021
BVOC	-0.09 ± 0.10		Thornhill et al., 2021

Using the nomenclature "natural" for land-based aerosols like dust, biomass burning, or BVOC is especially ambiguous in the Anthropocene, when 30% of the land surface is intensely managed by humans, while another 30% is moderately managed (Arneth et al., 2019). These aerosol emissions have been heavily modified by humans and are no longer solely controlled by natural processes (e.g. Kok et al.,. 2023; Fowler et al., 2013; van der Werf et al., 2006). This component of these aerosol species should be included in estimates of anthropogenic radiative forcing, because they are externally driven by anthropogenic activity and are not part of the response to the warming climate. However, these aerosols have not been treated consistently in the IPCC: for example dust was included as an external forcer in AR5 (fig 8.17) but as a feedback in AR6 (Szopa et al., 2021; Stocker et al., 2015). Some fraction of dust and biomass burning aerosol variations may be a feedback if they result from the response to forced climate trends: for example, wind shifts, drying, or changing natural vegetation under warming.

Deleted:

Deleted: 6: -2 to 0.

Formatted Table

Formatted: Default Paragraph Font, Font color: Black

Formatted: Normal, Centered, Border: Top: (No border), Bottom: (No border), Left: (No border), Right: (No border), Between : (No border), Tab stops: 3.25", Centered + 6.5", Right, Position: Horizontal: Left, Relative to: Column, Vertical: In line, Relative to: Margin, Wrap Around

Formatted: Font color: Black

Distinguishing aerosol changes that are forcings from feedbacks requires models (which are imperfect) and is a remaining uncertainty that is important to estimates of climate sensitivity. The current dust aerosol feedback inferred since the pre-industrial deduced from combined observational-model analysis (Kok et al., 2018) is quite different in magnitude than that seen in the LGM to PI changes (Table 6). This may reflect uncertainty in the attribution between forcing and feedback, or a dependence of this distinction upon the particular climates whose contrast is used for attribution.

For aerosol-cloud interactions in the Anthropocene, it may also be an error to refer to any aerosol impact as natural, since only 14% of the current atmosphere is actually in preindustrial conditions following anthropogenic emissions (Hamilton et al., 2014), and the aerosol-cloud interactions are thought to be strongly dependent upon the base climate (Carslaw et al., 2013). Aerosols emitted in a pristine climate are estimated to cause much greater impacts on clouds than in a polluted climate (Carslaw et al, 2013). Thus, the ERF_aci has a possibly large dependence on the base climate state, depending, for example, on what year (or years) is chosen to represent the "PI". One implication is that the Earth system sensitivity derived from paleoclimates potentially including 'natural' aerosol feedbacks on clouds can provide only limited understanding for how future climate change will evolve in a polluted environment.

The radiative effect of any change in atmospheric constituents (whether from anthropogenic forcing or natural feedbacks, or usually a combination), should usually be included in the estimate of the forcing for calculating the Charney climate sensitivity($S_{[GHG,LI,AE,VEG]}$). Thus 'natural' aerosol changes between preindustrial and present day should be included in these estimates, similar to solar or volcanic forcing. In many cases (e.g. DMS or BVOC) we do not have the observations to constrain how large the change in natural aerosols that results is. In that case we should include the uncertainty in these calculations, so that we explicitly identify what we know (and do not know) about the corresponding radiative forcing of the climate system. Recently, the availability of large ensembles has enabled the attribution of different climate forcings for different warming or precipitation trends (e.g. Kay et al., 2015). Unfortunately, the results of these studies depend on the time series for aerosol emissions in the CMIP database which, as discussed above, have larger uncertainties than acknowledged. Any time period before 1980 has very little data to describe the state of aerosols (e.g. see compilation of Mahowald et al., (2025) and the lack of data before this time period), and thus should include the uncertainties estimated in Section 7.2 for those aerosols for which we do not have high quality data.

Since models and emission estimates for past time periods for 'natural' aerosols such as dust and biomass burning are not able to match available observations, basing estimates of 'natural' aerosols on model estimates seems unlikely to provide accurate projections of climate until more paleodata is available. Careful consideration of the uncertainty of natural aerosols in the past and future is thus important for improving our estimates of climate sensitivity and future climate trends.

8. Conclusions

Aerosols dominate the uncertainty in IPCC estimates of radiative forcing (Szopa et al., 2021), and thus are very important for attribution of different climate impacts as well as for calculating climate sensitivity (Sherwood et al., 2020). Unfortunately, many previous estimates of aerosol uncertainty for periods prior to the satellite era did not include the uncertainties associated with changes in aerosol emissions (Mahowald et al., 2024). Whether 'natural' aerosols are considered as a feedback or forcing depends on the context, and should be carefully considered. It is important to recognize that Earth system responses in the Anthropocene may be quite different than during earlier paleo periods, especially because of land use changes and the dependence of the sensitivity of clouds to the aerosol perturbation upon the original, unperturbed aerosol composition and load (e.g., Carslaw et al., 2013). Dust illustrates this problem: the limited inferred sensitivities of dust to climate based on observations differ substantially between current climate changes and LGM to PI changes (Kok et al, 2018; Table 6). This review

Deleted: ..

Deleted:

Formatted: Default Paragraph Font, Font color: Black

Formatted: Normal, Centered, Border: Top: (No border), Bottom: (No border), Left: (No border), Right: (No border), Between : (No border), Tab stops: 3.25", Centered + 6.5", Right, Position: Horizontal: Left, Relative to: Column, Vertical: In line, Relative to: Margin, Wrap Around

Formatted: Font color: Black

describes the state of the modeling and paleo-proxy development that can help in constraining the emissions of aerosols using existing paleo-proxy observations, and describes both their strengths and their weaknesses. The review also summarizes existing datasets that can be put together to improve estimates of model radiative effects, as well as future research priorities (e.g. Figure 8).

In this review we present an assessment of the current state of uncertainty in aerosols, and how well observed they are (Table 5). This is highly uneven across aerosol types. For dust and volcanic aerosols, estimates of the radiative forcing due to aerosol loading changes are available based on model-data combinations for several time periods (e.g. preindustrial, LGM) (Table 6). There is some data and some estimates for biomass burning (e.g. preindustrial, Table 5). However, for many other important natural aerosols (DMS, sea spray, BVOC) proxy data are not available at sufficient spatial resolution to deduce possible global changes in past climates, much less their effective radiative forcing. In addition, for time periods besides preindustrial LGM, there are no available data-model syntheses, and thus we must assume large uncertainties in aerosol forcings until such estimates are available (Table 6). Moreover, the modeled sensitivity of dust aerosols to climate change during the historical period is one to two orders of magnitude too small compared to model-observational estimates, and thus we should be skeptical that changes in other natural aerosols are accurately simulated by models. Paleo-aerosol modelers are encouraged to calculate effective radiative forcing, not just instantaneous forcing to be more consistent and useful for climate studies. Treating these poorly constrained changes in aerosols and their radiative forcing as negligible risks underestimating uncertainty in the attribution of climate changes to aerosols and in climate-sensitivity constraints. Quantifying and reducing uncertainty in natural aerosol radiative forcing is therefore essential for attributing past climate changes to aerosols and for using paleoclimate records to constrain climate sensitivity. A central goal of paleoclimate aerosol research is therefore to better constrain aerosol radiative forcings across key paleoclimate periods and the pre-industrial to present-day transition. Achieving this goal requires not only improved reconstructions of past natural aerosol loading, but also reduced uncertainty in radiative effect efficiency - the radiative effect per unit aerosol loading - which varies with aerosol type, particle size, composition, morphology, vertical distribution, and climate state. We propose a "Proxy Integration Ladder" (Figure 8), where progress therefore requires (i) improved physical realism in models to enable more sophisticated and consistent model–observation comparisons, including alignment in represented particle properties and size ranges, (ii) expanded and better-targeted observational constraints, (iii) systematic inversion frameworks that integrate proxy data with models while explicitly propagating uncertainty, and (iv) community standards for paleo-aerosol datasets that enable robust uncertainty quantification. Together, these advances are required to constrain not only the variation over time of atmospheric loading of natural aerosols between climate states, but also changes in each aerosol's radiative effect efficiency.

Our review adds to a growing body of literature finding that changes in natural aerosols contribute a critical uncertainty in reconstructing past radiative forcing (Hamilton et al., 2018, Kok et al., 2023; Mahowald et al., 2024). Quantifying and reducing this uncertainty will require coordinated proxy development, model improvement, and an uncertainty-aware synthesis between models and observations. These advances would enable climate model simulations of both paleoclimate periods and the pre-industrial to present-day period to account for previously neglected changes in natural aerosols, thereby avoiding overconfidence in past radiative forcing estimates and in the climate inferences drawn from them.

Data availability: Figure 3 data is available at Kaplan, 2026. Otherwise only publicly available datasets, with appropriate links and citations, were used in this article.

Author Contribution

Deleted: Paleoaerosol

Deleted:

Formatted: Default Paragraph Font, Font color: Black

Formatted: Normal, Centered, Border: Top: (No border), Bottom: (No border), Left: (No border), Right: (No border), Between : (No border), Tab stops: 3.25", Centered + 6.5", Right, Position: Horizontal: Left, Relative to: Column, Vertical: In line, Relative to: Margin, Wrap Around

Formatted: Font color: Black

N.M., H.L., J.M. K.T., G.W. along with all the participants designed the outline. All authors contributed to writing and editing the text.

Competing interests: At least one of the (co-)authors is a member of the editorial board of Atmospheric Chemistry and Physics.

Acknowledgement: This work was made possible thanks to AIMES, IGAC, Schmidt Sciences, and PAGES (Past Global Changes), which received support from the Swiss Academy of Sciences and the Chinese Academy of Sciences.

Financial Support

J. F. K. was supported by National Science Foundation (NSF) grants 2151093 and 2336111. J. R. M. was supported by NSF grant 2536518. N. J. C. was supported by Agence Nationale de la Recherche (ANR) grant ANR-25-CE01-5199. GAS, RM, KM, SB, and KT are supported by the NASA Earth Science Division through the Integrated Model Virtual Institute (IMVI).

Glossary

AC: aerosol concentration

ACI: aerosol cloud interaction

AOD: aerosol optical depth

AMIP: Atmospheric Model Intercomparison Project

ARE: Aerosol Radiative Effect

BB: biomass burning

BC: black carbon

BCE: Before the Common Era

BVOC: biogenic volatile organic compounds

CCN: cloud condensation nuclei

CE: Common Era

CFP: constant flux proxies

CMIP: Coupled Model Intercomparison Project

DAOD: dust aerosol optical depth

DMAR: dust mass accumulation rates

DMS: dimethyl sulfide

DRE: direct radiative effect

Deleted: ;

Formatted: Default Paragraph Font, Font color: Black

Formatted: Normal, Centered, Border: Top: (No border), Bottom: (No border), Left: (No border), Right: (No border), Between : (No border), Tab stops: 3.25", Centered + 6.5", Right, Position: Horizontal: Left, Relative to: Column, Vertical: In line, Relative to: Margin, Wrap Around

Formatted: Font color: Black

ERF: effective radiative forcing

ESM: Earth System Model

IPCC: Intergovernmental Panel on Climate Change

LOP: lignin oxidation products

LGM: Last Glacial Maximum

MA: monosaccharide anhydrides

MAR: mass accumulation rate

MH: mid-Holocene

MSA: methanesulfonic acid

OC: organic carbon

PAH: polycyclic aromatic hydrocarbons

PD: present day

PI: preindustrial

PMIP: Paleoclimate Modeling Intercomparison Project

PPE: perturbed parameter ensembles

PSD: particle size distribution

PSM: proxy system models

REE: rare Earth elements

RF: radiative forcing

RE: radiative effects

SAOD: stratospheric aerosol optical depth

SSA: sea spray aerosols

VA: volcanic ash

Bibliography

Abbott, P. M., and Davies, S. M.: Volcanism and the Greenland ice-cores: the tephra record, Earth-Sci. Rev., 115, 173-191, https://doi.org/10.1016/j.earscirev.2012.09.001, 2012.

Abbott, P. M., Niemeier, U., Timmreck, C., Riede, F., McConnell, J. R., Severi, M., Fischer, H., Svensson, A., Toohey, M., Reinig, F., and Sigl, M.: Volcanic climate forcing preceding the inception of the Younger Dryas: Implications for tracing the Laacher See eruption, Quaternary Sci. Rev., 274, https://doi.org/10.1016/j.quascirev.2021.107260, 2021.

Formatted: Default Paragraph Font, Font color: Black

Formatted: Normal, Centered, Border: Top: (No border), Bottom: (No border), Left: (No border), Right: (No border), Between : (No border), Tab stops: 3.25", Centered + 6.5", Right, Position: Horizontal: Left, Relative to: Column, Vertical: In line, Relative to: Margin, Wrap Around

Formatted: Font color: Black

Abell, J. T., Winckler, G., Anderson, R. F., and Herbert, T. D.: Poleward and weakened westerlies during Pliocene warmth, Nature, 589, 70–75, https://doi.org/10.1038/s41586-020-03062-1, 2021.
Abell, J. T., Winckler, G., Bridges, J. D., Anderson, R. F., Herbert, T. D., Molnar, P., and Garzione, C.:. Iron fertilization of the North Pacific did not drive long-term Pliocene to Quaternary cooling, AGU Advances, 7(3), e2025AV002043, https://doi.org/10.1029/2025AV002043, 2026.
Adebiyi, A.A., and Kok, J. F.: Climate models miss most of the coarse dust in the atmosphere, Science Advances, 6, eaaz9507, https://doi.org/10.1126/sciadv.aaz9507, 2020.
Adebiyi, A., Kok, J. F., Murray, B. J., Ryder, C. L., Stuut, J.-B. W., Kahn, R. A., Knippertz, P., Formenti, P., Mahowald, N. M., Pérez García-Pando, C., Klose, M., Ansmann, A., Samset, B. H., Ito, A., Balkanski, Y., Di Biagio, C., Romanias, M. N., Huang, Y., and Meng, J.: A review of coarse mineral dust in the Earth system, Aeolian Res., 60, 100849, https://doi.org/10.1016/j.aeolia.2022.100849, 2023.
Adolphi, F., and Muscheler, R.: Synchronizing the Greenland ice core and radiocarbon timescales over the Holocene - Bayesian wiggle-matching of cosmogenic radionuclide records, Clim. Past, 12, 15-30, https://doi.org/10.5194/cp-12-15-2016, 2016.
Akagi, S. K., Yokelson, R. J., Wiedinmyer, C., Alvarado, M. J., Reid, J. S., Karl, T., Crounse, J. D., and Wennberg, P. O.: Emission factors for open and domestic biomass burning for use in atmospheric models. Atmos. Chem. Phys., 11, 4039–4072, https://doi.org/10.5194/acp-11-4039-2011, 2011.
Albani, S., Mahowald, N. M., Perry, A. T., Scanza, R. A., Zender, C. S., Heavens, N. G., Maggi, V., Kok, J. F., and Otto-Bliesner, B. L.: Improved dust representation in the Community Atmosphere Model, J. Adv. Model. Earth Sy., 6, 541–570, https://doi.org/10.1002/2013MS000279, 2014.
Albani, S., Mahowald, N. M., Winckler, G., Anderson, R. F., Bradtmiller, L. I., Delmonte, B., Francois, R., Goman, M., Heavens, N. G., Hesse, P. P., Hovan, S. A., Kang, S. G., Kohfeld, K. E., Lu, H., Maggi, V., Mason, J. A., Mayeswki, P., McGee, D., Miao, X., Otto-Bliesner, B. L., Perry, A. T. A., Pourmand, A., Roberts, H. M., Rosenbloom, N., Stevens, T., Sun, J., François, R., Goman, M., Heavens, N. G., Hesse, P. P., Hovan, S. A., Kang, S. G., Kohfeld, K. E., Lu, H., Maggi, V., Mason, J. A., Mayewski, P. A., McGee, D., Miao, X., Otto-Bliesner, B. L., Perry, A. T. A., Pourmand, A., Roberts, H. M., Rosenbloom, N., Stevens, T., and Sun, J.: Twelve thousand years of dust: the Holocene global dust cycle constrained by natural archives, Clim. Past, 11, 869–2015, https://doi.org/10.5194/cp-11-869-2015, 2015.
Albani, S., Mahowald, N. M., Murphy, L. N., Raiswell, R., Moore, J. K., Anderson, R. F., McGee, D., Bradtmiller, L. I., Delmonte, B., Hesse, P. P., and Mayewski, P. A.: Paleodust variability since the Last Glacial Maximum and implications for iron inputs to the ocean, Geophys. Res. Lett., 43, 3944–3954, https://doi.org/10.1002/2016GL067911, 2016.
Albani, S., Balkanski, Y., Mahowald, N., Winckler, G., Maggi, V., and Delmonte, B.: Aerosol-Climate Interactions During the Last Glacial Maximum, Current Climate Change Reports, 4, 99–114, https://doi.org/10.1007/s40641-018-0100-7, 2018.
Albani, S., and Mahowald, N. M.: Paleodust Insights into Dust Impacts on Climate, J. Climate, 32, 7897–7913, https://doi.org/10.1175/JCLI-D-18-0742.1, 2019.
Allen, C. D., Anderson, R. S., Jass, R. B., Toney, J. L., and Baisan, C. H.: Paired charcoal and tree-ring records of high-frequency Holocene fire from two New Mexico bog sites, Int. J. Wildland Fire, 17, 115–130, https://doi.org/10.1071/WF07165, 2008.
Andersen, K. K., & Genthon, C. (1996). Modeling the present and last glacial maximum transportation of dust to the arctic with an extended source scheme. In S. Guerzoni & R. Chester (Eds.), The Impact of Desert Dust Across the Mediterranean (pp. 123–132). Kluwer Academic Publishers.
Andreae, M. O, and Rosenfeld, D.: Aerosol-cloud-precipitation interactions. Part 1. The nature and sources of cloud-active aerosols, Earth-Sci. Rev., 89, 13–41,https://doi.org/10.1016/j.earscirev.2008.03.001, 2008.
APARC: The Hunga Volcanic Eruption Atmospheric Impacts Report. Yunqian Zhu, Graham Mann, Paul A. Newman, William Randel (Eds.), APARC Report No., 11 WCRP Report No. 10/2025,

Formatted: Indent: Left: 0", First line: 0"

Formatted: Default Paragraph Font, Font color: Black

Formatted: Normal, Centered, Border: Top: (No border), Bottom: (No border), Left: (No border), Right: (No border), Between : (No border), Tab stops: 3.25", Centered + 6.5", Right, Position: Horizontal: Left, Relative to: Column, Vertical: In line, Relative to: Margin, Wrap Around

Formatted: Font color: Black

https://doi.org/10.34734/FZJ-2025 05237, available at https://aparc-climate.org/publications/aparc-report-no-11/, 2025.
Archibald, S., and Bond, W. J.: Grazer movements: spatial and temporal responses to burning in a tall-grass African savanna, Int. J. Wildland Fire, 13, 377-385, https://doi.org/10.1071/WF03070, 2004.
Arneth, A., Barbosa, H., Benton, T., Calvin, K., Calvo, E., Connors, S., Cowie, A., Davin, E. L., and IPCC, A.: Climate Change and Land: Summary for Policy Makers, in: Climate Change and Land, Cambridge University Press, Cambridge, UK and New York, NY, USA and the International Institute for Applied Systems Analysis (IIASA), Laxenburg, Austria, 2019.
Arrhenius, G. 1963. Pelagic sediments. In The sea, M.N. Hill (ed.), Vol., 3 655–727. New.
Aubry, T. J., Toohey, M., Khanal, S., Chim, M. M., Verkerk, M., Johnson, B., Schmidt, A., Kovilakam, M., Sigl, M., Nicholls, Z., Thomason, L., Naik, V., Rieger, L., Stiller, D., Ziegler, E., Durack, P., and Smith, I. H.: Stratospheric aerosol forcing for CMIP7 – Part 1: optical properties for pre-industrial, historical, and scenario simulations, Geosci. Model Dev., 19, 3725–3756, https://doi.org/10.5194/gmd-19-3725-2026, 2026.
Ayers, G. P., Gillett, R. W., Granek, H., de Serves, C., and Cox, R. A.: Formaldehyde production in clean marine air. Geophy. Res. Lett., 24(4), 401–404, https://doi.org/10.1029/97GL00123, 1997.
Bacon, M. P., and Anderson, R. F.: Distribution of thorium isotopes between dissolved and particulate forms in the deep sea, J. Geophys. Res.-Oceans, 87, 2045–2056, https://doi.org/10.1029/JC087iC03p02045, 1982.
Baisan, C. H., and Swetnam, T. W.: Fire history on a desert mountain range: Rincon Mountain Wilderness, Arizona, USA, Can. J. Forest Res., 20, 1559–1569, https://doi.org/10.1139/x90-208, 1990.
Baker, A., Mariethoz, G., Comas-Bru, L., Hartmann, A., Frisia, S., Borsato, A., Treble, P. C., and Asrat, A.: The properties of annually laminated Stalagmites-A global synthesis, Rev. Geophys., 59, e2020RG000722, https://doi.org/10.1029/2020RG000722, 2021.
Baroni, M., Savarino, J., Cole-Dai, J. H., Rai, V. K., and Thiemens, M. H.: Anomalous sulfur isotope compositions of volcanic sulfate over the last millennium in Antarctic ice cores, J. Geophys. Res.-Atmos., 113, https://doi.org/10.1029/2008JD010185, 2008.
Baroni, M., Thiemens, M. H., Delmas, R. J., and Savarino, J.: Mass-independent sulfur isotopic compositions in stratospheric volcanic eruptions, Science, 315, 84-87, https://doi.org/10.1126/science.1131754, 2007.
Beaudon, E., Sheets, J. M., Martin, E., Sierra-Hernández, M. R., Mosley-Thompson, E., and Thompson, L. G.: Aeolian dust preserved in the Guliya Ice Cap (Northwestern Tibet): A promising paleo-environmental messenger, Geosciences, 12, 366, https://doi.org/10.3390/geosciences12100366, 2022.
Bellouin, N., Quaas, J., Gryspeerdt, E., Kinne, S., Stier, P., Watson-Parris, D., Boucher, O., Carslaw, K. S., Christensen, M., Daniau, A. L., Dufresne, J. L., Feingold, G., Fiedler, S., Forster, P., Gettelman, A., Haywood, J. M., Lohmann, U., Malavelle, F., Mauritsen, T., McCoy, D. T., Myhre, G., Mülmenstädt, J., Neubauer, D., Possner, A., Rugenstein, M., Sato, Y., Schulz, M., Schwartz, S. E., Sourdeval, O., Storelvmo, T., Toll, V., Winker, D., and Stevens, B.: Bounding Global Aerosol Radiative Forcing of Climate Change, Rev. Geophys., 58, https://doi.org/10.1029/2019RG000660, 2020.
Bennett, K, and Buck, C. E: Interpretation of lake sediment accumulation rates, Holocene, 26, 1092-1102, https://doi.org/10.1177/0959683616632880, 2016.
Bigler, M., Svensson, A., Steffensen, J. P., & Kaufmann, P.: A new continuous high-resolution detection system for sulphate in ice cores, Ann. Glaciol., 45, 178–182, https://doi.org/10.3189/172756407782282471, 2007.
Bigler, M., Wagenbach, D., Fischer, H., Kipfstuhl, J., Millar, H., Sommer, S., and Stauffer, B.: Sulphate record from a northeast Greenland ice core over the last, 1200 years based on continuous flow analysis, Ann. Glaciol., 35, 250-256, https://doi.org/10.3189/172756402781817158, 2002.

Formatted: Default Paragraph Font, Font color: Black

Formatted: Normal, Centered, Border: Top: (No border), Bottom: (No border), Left: (No border), Right: (No border), Between : (No border), Tab stops: 3.25", Centered + 6.5", Right, Position: Horizontal: Left, Relative to: Column, Vertical: In line, Relative to: Margin, Wrap Around

Formatted: Font color: Black

Bird, M. I., Taylor, D., and Hunt, C.: Palaeoenvironments of insular Southeast Asia during the Last Glacial Period: a savanna corridor in Sundaland?, Quaternary Sci. Rev., 24, 2228-2242, https://doi.org/10.1016/j.quascirev.2005.04.004, 2005.

Biscaye, P. E., Grousset, F. E., Revel, M., Van der Gaast, S., Zielinski, G. A., Vaars, A. and Kukla, G.: Asian provenance of glacial dust (stage 2) in the Greenland Ice Sheet Project, 2 ice core, Summit, Greenland, J. Geophys. Res.-Oceans, 102, 26765-26781, https://doi.org/10.1029/97JC01249, 1997.

Bisson, K. M., Gassó, S., Mahowald, N., Wagner, S., Koffman, B., Carn, S. A., Deutsch, S., Gazel, E., Kramer, S., Krotkov, N., Mitchell, C., Pritchard, M. E., Stamieszkin, K., and Wilson, C.: Observing ocean ecosystem responses to volcanic ash, Remote Sens. Environ., 296, 113749, https://doi.org/10.1016/j.rse.2023.113749, 2023.

Blard, P.-H., Protin, M., Tison, J.-L., Fripiat, F., Dahl-Jensen, D., Steffensen, J. P., Mahaney, W. C., Bierman, P. R., Christ, A. J., Corbett, L. B., Debaille, V., Rigaudier, T., Claeys, P., and ASTER team: Basal debris of the NEEM ice core, Greenland: a window into sub-ice-sheet geology, basal ice processes and ice-sheet oscillations, J. Glaciol., 69, 1011–1029, https://doi.org/10.1017/jog.2022.122, 2023.

Borda, L. G., Cosentino, N. J., Iturri, L. A., García, M. G., and Gaiero, D. M.: Is dust derived from shrinking saline lakes a risk to soil sodification in southern South America? J. Geophys. Res-Earth., 127, e2021JF006585, https://doi.org/10.1029/2021JF006585, 2022.

Bowman, D. M. J. S., Balch, J. K., Artaxo, P., Bond, W. J., Carlson, J. M., Cochrane, M. A., D'Antonio, C. M., DeFries, R. S., Doyle, J. C., Harrison, S. P., Johnston, F. H., Keeley, J. E., Krawchuk, M. A., Kull, C. A., Marston, J. B., Moritz, M. A., Prentice, I. C., Roos, C. I., Scott, A. C., and Pyne, S. J.: Fire in the earth system, Science, 324, 481–484, https://doi.org/10.1126/science.1163886, 2009.

Bowman, D. M. J. S., Balch, J., Artaxo, P., Bond, W. J., Cochrane, M. A., D'Antonio, C. M., DeFries, R., Johnston, F. H., Keeley, J. E., Krawchuk, M. A., Kull, C. A., Mack, M., Moritz, M. A., Pyne, S., Roos, C. I., Scott, A. C., Sodhi, N. S., and Swetnam, T. W.: The human dimension of fire regimes on Earth, J. Biogeogr., 38, 2223-2236, https://doi.org/10.1111/j.1365-2699.2011.02595.x, 2011.

Bowring, S. P. K., Li, W., Mouillot, F., Rosan, T. M., and Ciais, P.: Road fragment edges enhance wildfire incidence and intensity, while suppressing global burned area, Nat. Commun., 15, 9176, https://doi.org/10.1038/s41467-024-53460-6, 2024.

Braconnot, P., Zhu, D., Marti, O., and Servonnat, J.: Strengths and challenges for transient Mid- to Late Holocene simulations with dynamical vegetation, Clim. Past, 15, 997–1024, https://doi.org/10.5194/cp-15-997-2019, 2019.

Brenna, H., Kutterolf, S., Mills, M. J., and Kruger, K.: The potential impacts of a sulfur- and halogen-rich supereruption such as Los Chocoyos on the atmosphere and climate, Atmos. Chem. Phys., 20, 6521-6539, https://doi.org/10.5194/acp-20-6521-2020, 2020.

Brown, S. K., Crosweller, H. S., Sparks, R. S. J., Cottrell, E., Deligne, N. I., Guerrero, N. O., Hobbs, L., Kiyosugi, K., Loughlin, S. C., Siebert, L., and Takarada, S.: Characterisation of the Quaternary eruption record: analysis of the Large Magnitude Explosive Volcanic Eruptions (LaMEVE) database, Journal of Applied Volcanology, 3, 5, https://doi.org/10.1186/2191-5040-3-5, 2014.

Brown, H. Y., McCoy, D. T., Nugent, J. M., Wang, H., Wu, M., Zhang, K., and Burrows, S. M.: Sensitivity of anthropogenic cloud droplet number change to preindustrial emission inventories and physics parameterizations, Geophys. Res. Lett., 53, e2025GL121443, https://doi.org/10.22541/essoar.176860194.44608635/v1, 2026.

Bruch, W., Piazzola, J., Branger, H., van Eijk, A. M. J., Luneau, C., Bourras, D., and Tedeschi, G.: Sea-Spray-Generation Dependence on Wind and Wave Combinations: A Laboratory Study, Bound.-Lay. Meteorol., 180, 477–505, https://doi.org/10.1007/s10546-021-00636-y, 2021.

Burgay, F., Salionov, D., Singer, T., Eichler, A., Brütsch, S., Jenk, T. M., Vogel, A. L., Papina, T., Bjelić, S., and Schwikowski, M.: Nontarget screening of a Siberian ice core reveals changes in the pre-

Formatted: Default Paragraph Font, Font color: Black

Formatted: Normal, Centered, Border: Top: (No border), Bottom: (No border), Left: (No border), Right: (No border), Between : (No border), Tab stops: 3.25", Centered + 6.5", Right, Position: Horizontal: Left, Relative to: Column, Vertical: In line, Relative to: Margin, Wrap Around

Formatted: Font color: Black

industrial to industrial organic aerosol composition, Science Advances, 11, https://doi.org/10.1126/sciadv.adr1923, 2025.
Burke, A., Moore, K. A., Sigl, M., Nita, D. C., McConnell, J. R., and Adkins, J. F.: Stratospheric eruptions from tropical and extra-tropical volcanoes constrained using high-resolution sulfur isotopes in ice cores, Earth Planet. Sc. Lett., 521, 113-119, https://doi.org/10.1016/j.epsl.2019.06.006, 2019.
Burke, A., Innes, H. M., Crick, L., Anchukaitis, K. J., Byrne, M. P., Hutchison, W., McConnell, J. R., Moore, K. A., Rae, J. W. B., Sigl, M., and Wilson, R.: High sensitivity of summer temperatures to stratospheric sulfur loading from volcanoes in the Northern Hemisphere, P. Natl. Acad. Sci. USA, 120, e2221810120, https://doi.org/10.1073/pnas.2221810120, 2023.
Büntgen, U., Arseneault, D., Boucher, É., Churakova, O. V., Gennaretti, F., Crivellaro, A., Hughes, M. K., Kirdyanov, A. V., Klippel, L., Krusic, P. J., Linderholm, H. W., Ljungqvist, F. C., Ludescher, J., McCormick, M., Myglan, V. S., Nicolussi, K., Piermattei, A., Oppenheimer, C., Reinig, F., Sigl, M., Vaganov, E. A., and Esper, J.: Prominent role of volcanism in Common Era climate variability and human history, Dendrochronologia, 64, 125757, https://doi.org/10.1016/j.dendro.2020.125757, 2020.
Büntgen, U., Cosmo, N. D., Esper, J., Frachetti, M., Khalidi, L., Mauelshagen, F., Rohland, E., and Oppenheimer, C.: Volcanoes, Climate, and Society, Annu. Rev. Earth. Pl. Sc., 54, https://doi.org/10.1146/annurev-earth-032524-013254, 2025.
Cakmur, R. V., Miller, R. L., Perlwitz, J., Geogdzhayev, I. V., Ginoux, P., Koch, D., Kohfeld, K. E., Tegen, I., and Zender, C. S.: Constraining the magnitude of the global dust cycle by minimizing the difference between a model and observations, J. Geophys. Res.-Atmos, 111, D06207, https://doi.org/10.1029/2005JD005791, 2006.
Campbell, M., McDonough, L., Treble, P. C., Baker, A., Kosarac, N., Coleborn, K., Wynn, P. M., and Schmitt, A. K.: A Review of Speleothems as Archives for Paleofire Proxies, With Australian Case Studies. Rev. Geophys., 61, e2022RG000790, https://doi.org/10.1029/2022RG000790, 2023
Carn, S. A., Clarisse, L., and Prata, A. J.: Multi-decadal satellite measurements of global volcanic degassing, J. Volcanol. Geoth. Res, 311, 99-134, https://doi.org/10.1016/j.jvolgeores.2016.01.002, 2016.
Carslaw, K. S., Boucher, O., Spracklen, D., Mann, G., Rae, J. G., Woodward, S., and Kumala, M.: A review of natural aerosol interactions and feedbacks within the Earth System, Atmos. Chem. Phys., 10, 1701–1737, https://doi.org/10.5194/acp-10-1701-2010, 2010.
Carslaw, K. S., Gordon, H., Hamilton, D. S., Johnson, J. S., Regayre, L. A., Yoshioka, M., and Pringle, K. J.: Aerosols in the Pre-industrial Atmosphere, Current Climate Change Reports, 3, 1-15, https://doi.org/10.1007/s40641-017-0061-2, 2017.
Carslaw, K. S., Lee, L. A., Reddington, C. L., Pringle, K. J., Rap, A., Forster, P. M., Mann, G. W., Spracklen, D. V., Woodhouse, M. T., Regayre, L. A., and Pierce, J. R.: Large contribution of natural aerosols to uncertainty in indirect forcing, Nature, 503, 67-71, https://doi.org/10.1038/nature12674, 2013.
Carslaw, K. S., Lee, L. A., Regayre, L. A., and Johnson, J. S.: Climate models are uncertain, but we can do something about it, Eos, 99, https://doi.org/10.1029/2018EO093757. Published on, 26 February 2018.
Carslaw, K. S., Regayre, L. A., Proske, U., Gettelman, A., Sexton, D. M. H., Qian, Y., Marshall, L., Wild, O., Van Lier-Walqui, M., Oertel, A., Peatier, S., Yang, B., Johnson, J. S., Li, S., McCoy, D. T., Sanderson, B. M., Williamson, C. J., Elsaesser, G. S., Yamazaki, K., and Booth, B. B. B.: Opinion: The importance and future development of perturbed parameter ensembles in climate and atmospheric science, Atmos. Chem. Phys., 26, 4651-4667, https://doi.org/10.5194/acp-26-4651-2026, 2026.
Chambers, F. M., Barber, K. E., Maddy, D., and Brew, J.: A 5500-year proxy-climate and vegetation record from blanket mire at Talla Moss, Borders, Scotland, Holocene, 7, 391–399, https://doi.org/10.1177/095968369700700402, 1997.

Formatted: Default Paragraph Font, Font color: Black

Formatted: Normal, Centered, Border: Top: (No border), Bottom: (No border), Left: (No border), Right: (No border), Between : (No border), Tab stops: 3.25", Centered + 6.5", Right, Position: Horizontal: Left, Relative to: Column, Vertical: In line, Relative to: Margin, Wrap Around

Formatted: Font color: Black

Charlson, R. J., Lovelock, J. E., Andrae, M., Warren, S. G., Andreae, M., and Warren, S. G.: Oceanic phytoplankton, atmospheric sulfur, cloud albedo and climate, Nature, 326, 655–661, https://doi.org/10.1038/326655a, 1987.

Checa-Garcia, R., Balkanski, Y., Albani, S., Bergman, T., Carslaw, K., Cozic, A., Dearden, C., Marticorena, B., Michou, M., van Noije, T., Nabat, P., O'Connor, F. M., Olivié, D., Prospero, J. M., Le Sager, P., Schulz, M., and Scott, C.: Evaluation of natural aerosols in CRESCENDO Earth system models (ESMs): mineral dust, Atmos. Chem. Phys., 21, 10295–10335, https://doi.org/10.5194/acp-21-10295-2021, 2021.

Cheng, H., Lawrence Edwards, R., Shen, C.-C., Polyak, V. J., Asmerom, Y., Woodhead, J., Hellstrom, J., Wang, Y., Kong, X., Spötl, C., Wang, X., and Calvin Alexander, E.: Improvements in ^{230}Th dating, ^{230}Th and ^{234}U half-life values, and U–Th isotopic measurements by multi-collector inductively coupled plasma mass spectrometry, Earth Planet. Sc. Lett., 371–372, 82–91. https://doi.org/10.1016/j.epsl.2013.04.006, 2013.

Chim, M. M., Aubry, T. J., Abraham, N. L., Marshall, L., Mulcahy, J., Walton, J., and Schmidt, A.: Climate Projections Very Likely Underestimate Future Volcanic Forcing and Its Climatic Effects, Geophys. Res. Lett., 50, e2023GL103743, https://doi.org/10.1029/2023GL103743, 2023.

Claquin, T., Roelandt, C., Kohfeld, K., Harrison, S., Tegen, I., Prentice, I., Balkanski, Y., Bergametti, G., Hansson, M., Mahowald, N., Rodhe, H., and Schulz, M.: Radiative forcing of climate by ice-age atmospheric dust, Clim. Dynam., 20, 193–202, https://doi.org/10.1007/s00382-002-0269-1, 2003.

Clarisse, L., Clerbaux, C., Dentener, F., Hurtmans, D., and Coheur, P.-F.: Global ammonia distribution derived from infrared satellite observations, Nat. Geosci., 2, 479–483, https://doi.org/10.1038/ngeo551, 2009.

Clark, P. U., Dyke, A. S., Shakun, J. D., Carlson, A. E., Clark, J., Wohlfarth, B., Mitrovica, J. X., Hostetler, S. W., and McCabe, A. M.: The Last Glacial Maximum, Science, 325, 710–714, https://doi.org/10.1126/science.1172873, 2009.

Clausen, H. B., and Hammer, C. U.: The Laki and Tambora Eruptions as Revealed in Greenland Ice Cores from 11 Locations, Ann. Glaciol., 10, 16-22, https://doi.org/10.3189/S0260305500004092, 1988.

Clyne, M., Lamarque, J. F., Mills, M. J., Khodri, M., Ball, W., Bekki, S., Dhomse, S. S., Lebas, N., Mann, G., Marshall, L., Niemeier, U., Poulain, V., Robock, A., Rozanov, E., Schmidt, A., Stenke, A., Sukhodolov, T., Timmreck, C., Toohey, M., Tummon, F., Zanchettin, D., Zhu, Y., and Toon, O. B.: Model physics and chemistry causing intermodel disagreement within the VolMIP-Tambora Interactive Stratospheric Aerosol ensemble, Atmos. Chem. Phys., 21, 3317-3343, https://doi.org/10.5194/acp-21-3317-2021, 2021.

Cohen, A. S.: Paleolimnology: the history and evolution of lake systems, Oxford University Press, New York, 1 pp., https://doi.org/10.1093/oso/9780195133530.001.0001, 2020.

Cole-Dai, J.: Volcanoes and climate, Wires Clim Change, 1, 824-839, 2010.

Cole-Dai, J., Ferris, D. G., Kennedy, J. A., Sigl, M., McConnell, J. R., Fudge, T. J., Geng, L., Maselli, O. J., Taylor, K. C., & Souney, J. M.: Comprehensive Record of Volcanic Eruptions in the Holocene (11,000 years) From the WAIS Divide, Antarctica Ice Core, J. Geophys. Res.-Atmos., 126(7), https://doi.org/10.1029/2020JD032855, 2021.

Collins, M., Booth, B. B. B., Bhaskaran, B., Harris, G. R., Murphy, J. M., Sexton, D. M. H., and Webb, M. J.: Climate model errors, feedbacks and forcings: a comparison of perturbed physics and multi-model ensembles, Clim. Dynam., 36, 1737–1766, https://doi.org/10.1007/s00382-010-0808-0, 2011.

Comola, F., Giometto, M. G., Salesky, S. T., Parlange, M. B., and Lehning, M.: Preferential Deposition of Snow and Dust Over Hills: Governing Processes and Relevant Scales, J. Geophys. Res.-Atmos., 124, 7951–7974, https://doi.org/10.1029/2018JD029614, 2019.

Cook, E., Abbott, P. M., Pearce, N. J. G., Mojtabavi, S., Svensson, A., Bourne, A. J., Rasmussen, S. O., Seierstad, I. K., Vinther, B. M., Harrison, J., Street, E., Steffensen, J. P., Wilhelms, F., and Davies, S. M.: Volcanism and the Greenland ice cores: A new tephrochronological framework for

Formatted: Default Paragraph Font, Font color: Black

Formatted: Normal, Centered, Border: Top: (No border), Bottom: (No border), Left: (No border), Right: (No border), Between : (No border), Tab stops: 3.25", Centered + 6.5", Right, Position: Horizontal: Left, Relative to: Column, Vertical: In line, Relative to: Margin, Wrap Around

Formatted: Font color: Black

the last glacial-interglacial transition (LGIT) based on cryptotephra deposits in three ice cores, Quaternary Sci. Rev., 292, https://doi.org/10.1016/j.quascirev.2022.107596, 2022.
Cosentino, N. J., Opazo, N. E., Lambert, F., Osses, A., and van 't Wout, E.: Global-Krigger: A global interpolation toolbox with paleoclimatology examples, Geochem. Geophys. Geosyst., 24, e2022GC010821, https://doi.org/10.1029/2022GC010821, 2023.
Cosentino, N. J., Torre, G., Lambert, F., Albani, S., De Vleeschouwer, F., and Bory, A. J.-M.: Paleo-Dust: quantifying uncertainty in paleo-dust deposition across archive types, Earth Syst. Sci. Data, 16, 941–959, https://doi.org/10.5194/essd-16-941-2024, 2024.
Costa, K. M., Hayes, C. T., Anderson, R. F., Pavia, F. J., Bausch, A., Deng, F., Dutay, J.-C., Geibert, W., Heinze, C., Henderson, G., Hillaire-Marcel, C., Hoffmann, S., Jaccard, S. L., Jacobel, A. W., Kienast, S. S., Kipp, L., Lerner, P., Lippold, J., Lund, D., Marcantonio, F., McGee, D., McManus, J. F., Mekik, F., Middleton, J. L., Missiaen, L., Not, C., Pichat, S., Robinson, L. F., Rowland, G. H., Roy-Barman, M., Tagliabue, A., Torfstein, A., Winckler, G. and Zhou, Y.: ^{230}Th Normalization: New Insights on an Essential Tool for Quantifying Sedimentary Fluxes in the Modern and Quaternary Ocean, Paleoceanography, 35, e2019PA003820, https://doi.org/10.1029/2019PA003820, 2020.
Crick, L., Burke, A., Hutchison, W., Kohno, M., Moore, K. A., Savarino, J., Doyle, E. A., Mahony, S., Kipfstuhl, S., Rae, J. W. B., Steele, R. C. J., Sparks, R. S. J., and Wolff, E. W.: New insights into the ~ 74 ka Toba eruption from sulfur isotopes of polar ice cores, Clim. Past, 17, 2119-2137, https://doi.org/10.5194/cp-17-2119-2021, 2021.
Crippa, M., Guizzardi, D., Butler, T., Keating, T., Wu, R., Kaminski, J., Kuenen, J., Kurokawa, J., Chatani, S., Morikawa, T., Pouliot, G., Racine, J., Moran, M. D., Klimont, Z, Manseau, P. M., Mashayekhi, R., Henderson, B. H., Smith, S. J., Suchyta, H., Foley, K.: The HTAPv3 emission mosaic: merging regional and global monthly emissions (2000–2018) to support air quality modelling and policies, Earth Syst. Sci. Data, 15, 2667–2694, https://doi.org/10.5194/essd-15-2667-2023, 2023.
Crowley, T. J., and Unterman, M. B.: Technical details concerning development of a 1200 yr proxy index of global volcanism, Earth Syst. Sci. Data, 5, 187-197, https://doi.org/10.5194/essd-5-187-2013, 2013, 2013.
Cruz, J. A., McDermott, F., Turrero, M. J., Edwards, R. L., and Martín-Chivelet, J.: Strong links between Saharan dust fluxes, monsoon strength, and North Atlantic climate during the last 5000 years, Science Advances, 7, eabe6102, https://doi.org/10.1126/sciadv.abe6102, 2021.
Cui, T., Green, H. S., Selleck, P. W., Zhang, Z., O'Brien, R. E., Gold, A., Keywood, M., Kroll, J. H., and Surratt, J. D.: Chemical Characterization of Isoprene- and Monoterpene-Derived Secondary Organic Aerosol Tracers in Remote Marine Aerosols over a Quarter Century, ACS Earth and Space Chemistry, 3(6), 935–946. https://doi.org/10.1021/acsearthspacechem.9b00061, 2019.
Dana, M. T., and Hales, J. M.: Statistical aspects of the washout of polydisperse aerosols, Atmos. Environ., 10, 44-50, https://doi.org/10.1016/0004-6981(76)90258-4, 1976.
Danabasoglu, G., Lamarque, J. F., Bacmeister, J., Bailey, D. A., DuVivier, A. K., Edwards, J., Emmons, L. K., Fasullo, J., Garcia, R., Gettelman, A., Hannay, C., Holland, M. M., Large, W. G., Lauritzen, P. H., Lawrence, D. M., Lenaerts, J. T. M., Lindsay, K., Lipscomb, W. H., Mills, M. J., Neale, R., Oleson, K. W., Otto-Bliesner, B., Phillips, A. S., Sacks, W., Tilmes, S., van Kampenhout, L., Vertenstein, M., Bertini, A., Dennis, J., Deser, C., Fischer, C., Fox-Kemper, B., Kay, J. E., Kinnison, D., Kushner, P. J., Larson, V. E., Long, M. C., Mickelson, S., Moore, J. K., Nienhouse, E., Polvani, L., Rasch, P. J., and Strand, W. G.: The Community Earth System Model Version 2 (CESM2), J. Adv. Model. Earth Sy., 12(2), 1–35, https://doi.org/10.1029/2019MS001916, 2020.
Davies, S. M., Albert, P. G., Bourne, A. J., Owen, S., Svensson, A., Bolton, M. S. M., Cook, E., Jensen, B. J. L., Jones, G., Ponomareva, V. V., and Suzuki, T.: Exploiting the Greenland volcanic ash repository to date caldera-forming eruptions and widespread isochrons during the Holocene, Quaternary Sci. Rev., 334, 108707, https://doi.org/10.1016/j.quascirev.2024.108707, 2024.

Formatted: Default Paragraph Font, Font color: Black

Formatted: Normal, Centered, Border: Top: (No border), Bottom: (No border), Left: (No border), Right: (No border), Between : (No border), Tab stops: 3.25", Centered + 6.5", Right, Position: Horizontal: Left, Relative to: Column, Vertical: In line, Relative to: Margin, Wrap Around

Formatted: Font color: Black

Dee, S., Emile-Geay, J., Evans, M. N., Allam, A., Steig, E. J., and Thompson, D. M.: PRYSM: An open-source framework for PRoxY System Modeling, with applications to oxygen-isotope systems. J. Adv. Model. Earth Sy., 7, 1220-1247, https://doi.org/10.1002/2015MS000447, 2015.

De Vleeschouwer, F., Pazdur, A., Luthers, C., Streel, M., Mauquoy, D., Wastiaux, C., Le Roux, G., Moschen, R., Blaauw, M., Pawlyta, J., Sikorski, J., and Piotrowska, N.: A millennial record of environmental change in peat deposits from the Misten bog (East Belgium), Quatern. Int., 268, 44–57, https://doi.org/10.1016/j.quaint.2011.12.010, 2012.

Deirmendjian, D.: On volcanic and other particulate turbidity anomalies, Adv. Geophys., 16, 267-296, https://doi.org/10.1016/S0065-2687(08)60353-2, 1973.

Deligne, N. I., Coles, S. G., and Sparks, R. S. J.: Recurrence rates of large explosive volcanic eruptions, J. Geophys. Res.-Sol. Ea., 115, https://doi.org/10.1029/2009JB006554, 2010.

Delmas, R., Serça, D., and Jambert, C.: Global inventory of NOx sources. Nutrient Cycling in Agroecosystems, 48, 51–60, https://doi.org/10.1023/A:1009793806086, 1997.

Delmonte, B., Andersson, P. S., Hansson, M., Schöberg, H., Petit, J. R., Basile-Doelsch, I., and Maggi, V.: Aeolian dust in East Antarctica (EPICA-Dome C and Vostok): Provenance during glacial ages over the last, 800 kyr, Geophys. Res. Lett., 35, 2008GL033382, https://doi.org/10.1029/2008GL033382, 2008.

deMenocal, P., Ortiz, J., Guilderson, T., and Sarnthein, M.: Coherent High- and Low-Latitude Climate Variability During the Holocene Warm Period, Science, 288, 2198-2202, doi:10.1126/science.288.5474.2198, 2000.

DeMott, P. J, Hill, T. C. J, McCluskey, C. S, Prather, K. A, Collins, D. B, Sullivan, R. C, Ruppel, M. J, Mason, R. H, Irish, V. E, Lee, T, Hwang, C. Y, Rhee, T. S, Snider, J. R, McMeeking, G. R, Dhaniyala, S, Lewis, E. R, Wentzell, J. J. B, Abbatt, J, Lee, C.. Franc, G. D: Sea spray aerosol as a unique source of ice nucleating particles, Proc. Natl. Acad. Sci. U.S.A., 113(21), 5797–5803. https://doi.org/10.1073/pnas.1514034112, 2016.

Derbyshire, E.: Loess, and the Dust Indicators and Records of Terrestrial and Marine Palaeoenvironments (DIRTMAP) database, Quaternary Sci. Rev., 22, 1813–1819, https://doi.org/10.1016/S0277-3791(03)00209-9, 2003.

Dieterich, J. H., and Swetnam, T. W.: Dendrochronology of a fire scarred ponderosa pine, Forest Sci., 30, 238–247, https://doi.org/10.1093/forestscience/30.1.238, 1984.

Doebbert, A. C., Johnson, C. M., Carroll, A. R., Beard, B. L., Pietras, J. T., Carson, M. R., Norsted, B., and Throckmorton, L. A.: Controls on Sr isotopic evolution in lacustrine systems: Eocene green river formation, Wyoming, Chem. Geol., 380, 172–189, https://doi.org/10.1016/j.chemgeo.2014.04.008, 2014.

Dolman, A. M., Kunz, T., Groeneveld, J., and Laepple, T.: A spectral approach to estimating the timescale-dependent uncertainty of paleoclimate records – Part 2: Application and interpretation, Clim. Past, 17, 825–841, https://doi.org/10.5194/cp-17-825-2021, 2021.

Domínguez, E., and Vega, D.: Funciones y servicios ecosistémicos de las turberas en Magallanes. Punta Arenas, Chile, 2015.

Drakaki, E., Amiridis, V., Tsekeri, A., Gkikas, A., Proestakis, E., Mallios, S., Solomos, S., Spyrou, C., Marinou, E., Ryder, C. L., Bouris, D., and Katsafados, P.: Modeling coarse and giant desert dust particles, Atmos. Chem. Phys., 22, 12727–12748, https://doi.org/10.5194/acp-22-12727-2022, 2022.

Duggen, S., Olgun, N., Croot, P., Hoffmann, L., Dietze, H., Delmelle, P., and Teschner, C.: The role of airborne volcanic ash for the surface ocean biogeochemical iron-cycle: A review, Biogeosciences, 7, 827–844, https://doi.org/10.5194/bg-7-827-2010, 2010.

Dunbar, N. W., Iverson, N. A., Van Eaton, A. R., Sigl, M., Alloway, B. V., Kurbatov, A. V., Mastin, L. G., McConnell, J. R., and Wilson, C. J. N.: New Zealand supereruption provides time marker for the Last Glacial Maximum in Antarctica, Sci. Rep.-UK, 7, 12238, https://doi.org/10.1038/s41598-017-11758-0, 2017.

Formatted: Default Paragraph Font, Font color: Black

Formatted: Normal, Centered, Border: Top: (No border), Bottom: (No border), Left: (No border), Right: (No border), Between : (No border), Tab stops: 3.25", Centered + 6.5", Right, Position: Horizontal: Left, Relative to: Column, Vertical: In line, Relative to: Margin, Wrap Around

Formatted: Font color: Black

Eakin, M. C., and Grottoli, A. G.: Coral reef records of past climatic change, in: Coastal and Estuarine Studies, vol., 61 edited by: Phinney, J. T., Hoegh-Guldberg, O., Kleypas, J., Skirving, W., and Strong, A., American Geophysical Union, Washington, D. C., 33–54, https://doi.org/10.1029/61CE04, 2006.

Eckhardt, S., Pisso, I., Evangeliou, N., Zwaaftink, C. G., Plach, A., McConnell, J. R., Sigl, M., Ruppel, M., Zdanowicz, C., Lim, S., Chellman, N., Opel, T., Meyer, H., Steffensen, J. P., Schwikowski, M., and Stohl, A.: Revised historical Northern Hemisphere black carbon emissions based on inverse modeling of ice core records, Nat. Commun., 14, 271, https://doi.org/10.1038/s41467-022-35660-0, 2023.

Eidhammer, T., Gettelman, A., Thayer-Calder, K., Watson-Parris, D., Elsaesser, G., Morrison, H., Van Lier-Walqui, M., Song, C., and McCoy, D.: An extensible perturbed parameter ensemble for the Community Atmosphere Model version 6, Geosci. Model Dev., 17, 7835–7853, https://doi.org/10.5194/gmd-17-7835-2024, 2024.

Elsaesser, G. S., Van Lier-Walqui, M., Yang, Q., Kelley, M., Ackerman, A. S., Fridlind, A. M., Cesana, G. V., Schmidt, G. A., Wu, J., Behrangi, A., Camargo, S. J., De, B., Inoue, K., Leitmann-Niimi, N. M., and Strong, J. D. O.: Using Machine Learning to Generate a GISS ModelE Calibrated Physics Ensemble (CPE), J. Adv. Model. Earth Sy., 17, e2024MS004713, https://doi.org/10.1029/2024MS004713, 2025.

EPICA community members: Eight glacial cycles from an Antarctic ice core, Nature, 429, 623–628, https://doi.org/10.1038/nature02599, 2004.

Erhardt, T., Bigler, M., Federer, U., Gfeller, G., Leuenberger, D., Stowasser, O., Röthlisberger, R., Schüpbach, S., Ruth, U., Twarloh, B., Wegner, A., Goto-Azuma, K., Kuramoto, T., Kjær, H. A., Vallelonga, P. T., Siggaard-Andersen, M.-L., Hansson, M. E., Benton, A. K., Fleet, L. G., Mulvaney, R., Thomas, E. R., Abram, N., Stocker, T. F., and Fischer, H.: High-resolution aerosol concentration data from the Greenland NorthGRIP and NEEM deep ice cores, Earth Syst. Sci. Data, 14, 1215–1231, https://doi.org/10.5194/essd-14-1215-2022, 2022.

Esper, J., Smerdon, J. E., Anchukaitis, K. J., Allen, K., Cook, E. R., D'Arrigo, R., Guillet, S., Ljungqvist, F. C., Reinig, F., Schneider, L., Sigl, M., Stoffel, M., Trnka, M., Wilson, R., and Büntgen, U.: The IPCC's reductive Common Era temperature history, Communications Earth & Environment, 5, 222, https://doi.org/10.1038/s43247-024-01371-1, 2024.

Evans, M. N., Tolwinski-Ward, S. E, Thompson, D. M., and Anchukaitis, K. J.: Applications of proxy system modeling in high resolution paleoclimatology, Quaternary Sci. Rev., 76, 16–28. https://doi.org/10.1016/j.quascirev.2013.05.024, 2013.

Eyring, V., Bony, S., Meehl, G. A., Senior, C. A., Stevens, B., Stouffer, R. J., and Taylor, K. E.: Overview of the Coupled Model Intercomparison Project Phase, 6 (CMIP6) experimental design and organization, Geosci. Model Dev., 9, 1937–1958, https://doi.org/10.5194/gmd-9-1937-2016, 2016.

Fairchild, I. J., Smith, C. L., Baker, A., Fuller, L., Spötl, C., Mattey, D., McDermott, F., and E.I.M.F.: Modification and preservation of environmental signals in speleothems, Earth-Sci. Rev., 75, 105–153, https://doi.org/10.1016/j.earscirev.2005.08.003, 2006.

Falk, D. A., Heyerdahl, E. K., Brown, P. M., Farris, C., Fulé, P. Z., McKenzie, D., Swetnam, T. W., Taylor, A. H., and Van Horne, M. L.: Multi-scale controls of historical forest-fire regimes: new insights from fire-scar networks, Front. Ecol. Environ., 9, 446–454, https://doi.org/10.1890/100052, 2011.

Fan, C., He, B., Guo, S., Qiu, J., and Zhao, C.: Insights into the real part of natural sea spray aerosol refractive index in the Pacific Ocean, Atmos. Chem. Phys., 25, 5761–5771, https://doi.org/10.5194/acp-25-5761-2025, 2025.

Fang, S.-W., Sigl, M., Toohey, M., Jungclaus, J., Zanchettin, D., and Timmreck, C.: The role of small to moderate volcanic eruptions in the early 19th century climate, Geophys. Res. Lett., 50, e2023GL105307, https://doi.org/10.1029/2023GL105307: 2023, 2023.

Formatted: Default Paragraph Font, Font color: Black

Formatted: Normal, Centered, Border: Top: (No border), Bottom: (No border), Left: (No border), Right: (No border), Between : (No border), Tab stops: 3.25", Centered + 6.5", Right, Position: Horizontal: Left, Relative to: Column, Vertical: In line, Relative to: Margin, Wrap Around

Formatted: Font color: Black

Farley, K. A., Love, S. G., and Patterson, D. B.: Atmospheric entry heating and helium retentivity of interplanetary dust particles, Geochim. Cosmochim. Ac., 61(11), 2309-2316, https://doi.or/10.1016/S0016-7037(97)00068-9, 1997.

Farris, C. A., Margolis, E. Q., Iniguez, J. M., Falk, D. A., Gerow, K. G., Baisan, C. H., Allen, C. D., and Swetnam, T. W.: New methods provide a 300-year perspective on modern area burned in two wilderness areas of the southwest United States, Ecosphere, 17, e70471, https://doi.org/10.1002/ecs2.70471, 2026.

Feng, Y., and Penner, J. E.: Global modeling of nitrate and ammonium: Interaction of aerosols and tropospheric chemistry, J. Geophys. Res.-Atmos., 112, https://doi.org/10.1029/2005JD006404, 2007.

Fénisse, G., Bekaert, D. V., Blard, P. H., Duprat, J., Mattia, I., Genge, M., Suttle, M. D., Barres, O., Engrand, C., and Marrocchi, Y.: The extraterrestrial dust accretion rate on Earth at Dome C, Antarctica: a fresh look with 3He, Earth Planet. Sc. Lett., 663, 119396, https://doi.org/10.1016/j.gca.2025.12.016, 2025.

Ferretti, D. F., Miller, J. B., White, J. W. C., Etheridge, D. M., Lassey, K. R., Lowe, D. C., Meure, C. M. M., Dreier, M. F., Trudinger, C. M., van Ommen, T. D., and Langenfelds, R. L.: Unexpected Changes to the Global Methane Budget over the Past 2000 Years, Science, 309, 1714-1717, https://doi.org/10.1126/science.1115193, 2005.

Fischer, H., Schüpbach, S., Gfeller, G., Bigler, M., Röthlisberger, R., Erhardt, T., Stocker, T. F., Mulvaney, R., and Wolff, E. W.: Millennial changes in North American wildfire and soil activity over the last glacial cycle, Nat. Geosci., 8, 723–727. https://doi.org/10.1038/ngeo2495, 2015.

Forster, P., Alterskjaer, K., Smith, C., Colman, R., Damon Matthews, H., Ramaswamy, V., Storelvmo, T., Armour, K., Collins, W., Dufresne, J., Frame, D., Lunt, D., Mauritsen, T., Watanabe, M., Wild, M., Zhang, H., Pirani, A., Connors, S., Péan, C., Berger, S., Caud, N., Chen, Y., Goldfarb, L., Gomis, M., Huang, M., Leitzell, K., Lonnoy, E., Matthews, J., Maycock, T., Waterfield, T., Yelekçi, O., Yu, R., and Zhou, B.: Chapter 7: The Earth's Energy Budget, Climate Feedbacks and Climate Sensitivity, in: Climate Change 2021: The Physical Science Basis. Contribution of Working Group I to the Sixth Assessment Report of the Intergovernmental Panel on Climate Change, edited by: Masson-Delmotte, V. , P. Zhai, A. Pirani, S.L. Connors, C. Péan, S. Berger, N. Caud, Y. Chen, L. Goldfarb, M.I. Gomis, M. Huang, K. Leitzell, E. Lonnoy, J.B.R. Matthews, T.K. Maycock, T. Waterfield, O. Yelekçi, R. Yu, and Zhou, B., Cambridge University Press, Cambridge, United Kingdom and New York, NY, USA, 923–1054, https://doi.org/10.1017/9781009157896.009, 2021.

Forster, P., Storelvmo, T., Armour, K., Collins, W., Dufresne, J.-L., Frame, D., Lunt, D. J., Mauritsen, T., Palmer, M. D., Watanabe, M., Wild, M., and Zhang, H.: The Earth's Energy Budget, Climate Feedbacks, and Climate Sensitivity. In Climate Change 2021: The Physical Science Basis. Contribution of Working Group I to the Sixth Assessment Report of the Intergovernmental Panel on Climate Change [Masson-Delmotte, V., P. Zhai, A. Pirani, S.L. Connors, C. Péan, S. Berger, N. Caud, Y. Chen, L. Goldfarb, M.I. Gomis, M. Huang, K. Leitzell, E. Lonnoy, J.B.R. Matthews, T.K. Maycock, T. Waterfield, O. Yelekçi, R. Yu, and B. Zhou (eds.)]. Cambridge University Press, Cambridge, United Kingdom and New York, NY, USA, pp. 923–1054, https://doi.org/10.1017/9781009157896.009, 2021.

Fowler, D., Coyle, M., Skiba, U., Sutton, M. A., Cape, J. N., Reis, S., Sheppard, L. J., Jenkins, A., Grizzetti, B., Galloway, J. N., Vitousek, P., Leach, A., Bouwman, A. F., Butterbach-Bahl, K., Dentener, F., Stevenson, D., Amann, M., and Voss, M.: The global nitrogen cycle in the twenty-first century, Philos. T. Roy. Soc. B, 368, 20130164, https://doi.org/10.1098/rstb.2013.0164, 2013.

Francois, R., Frank, M., Rutgers Van Der Loeff, M. M., and Bacon, M. P.:, ^{230}Th normalization: An essential tool for interpreting sedimentary fluxes during the late Quaternary, Paleoceanography, 19, 2003PA000939, https://doi.org/10.1029/2003PA000939, 2004.

Formatted: Default Paragraph Font, Font color: Black

Formatted: Normal, Centered, Border: Top: (No border), Bottom: (No border), Left: (No border), Right: (No border), Between : (No border), Tab stops: 3.25", Centered + 6.5", Right, Position: Horizontal: Left, Relative to: Column, Vertical: In line, Relative to: Margin, Wrap Around

Formatted: Font color: Black

Freundt, A., Schindlbeck-Belo, J. C., Kutterolf, S., and Hopkins, J. L.: Tephra layers in the marine environment: a review of properties and emplacement processes, Geological Society of London Special Publications, 520, 595–637, https://doi.org/10.1144/SP520-2021-50, 2023.

Frey, M. M., Norris, S. J., Brooks, I. M., Anderson, P. S., Nishimura, K., Yang, X., Jones, A. E., Nerentorp Mastromonaco, M. G., Jones, D. H., and Wolff, E. W.: First direct observation of sea salt aerosol production from blowing snow above sea ice, Atmos. Chem. Phys., 20, 2549–2578, https://doi.org/10.5194/acp-20-2549-2020, 2020.

Froyd, K. D., Yu, P., Schill, G. P., Brock, C. A., Kupc, A., Williamson, C. J., Jensen, E. J., Ray, E., Rosenlof, K. H., Bian, H., Darmenov, A. S., Colarco, P. R., Diskin, G. S., Bui, T., and Murphy, D. M.: Dominant role of mineral dust in cirrus cloud formation revealed by global-scale measurements. Nat. Geosci., 15, 177–183, https://doi.org/10.1038/s41561-022-00901-w, 2022.

Frumkin, A., & Stein, M. (2004). The Sahara–East Mediterranean dust and climate connection revealed by strontium and uranium isotopes in a Jerusalem speleothem. *Earth and Planetary Science Letters*, *217*(3–4), 451–464. https://doi.org/10.1016/S0012-821X(03)00589-2

Fuglestvedt, H. F., Zhuo, Z., Toohey, M., and Krüger, K.: Volcanic forcing of high-latitude Northern Hemisphere eruptions, npj Climate and Atmospheric Science, 7, 10, https://doi.org/10.1038/s41612-023-00539-4, 2024.

Fécan, F., Marticorena, B., and Bergametti, G.: Parametrization of the increase of the aeolian erosion threshold wind friction velocity due to soil moisture for arid and semi-arid areas, Ann. Geophys., 17, 149–157, https://doi.org/10.1007/s00585-999-0149-7, 1999.

Gabriel, I., Innes, H. M., Abbott, P. M., Franke, J., Behrens, M., Chellman, N. J., Hörhold, M., Hutchison, W., McConnell, J. R., Twarloh, B., and Sigl, M.: Constraining the timing and climate forcing of the Long Island (Papua New Guinea) and Tarumae (Japan) eruptions and other 17th century volcanic eruptions, J. Volcanol. Geoth. Res., 464, 108346, https://doi.org/10.1016/j.jvolgeores.2025.108346, 2025.

Gabriel, I., Plunkett, G., Abbott, P. M., Behrens, M., Burke, A., Chellman, N., Cook, E., Fleitmann, D., Hörhold, M., Hutchison, W., McConnell, J. R., Óladóttir, B. A., Preiser-Kapeller, J., Sliwinski, J. T., Sugden, P., Twarloh, B., and Sigl, M.: Decadal-to-centennial increases of volcanic aerosols from Iceland challenge the concept of a Medieval Quiet Period, Communications Earth & Environment, 5, 194, https://doi.org/10.1038/s43247-024-01350-6, 2024.

Gao, C. C., Oman, L., Robock, A., and Stenchikov, G. L.: Atmospheric volcanic loading derived from bipolar ice cores: Accounting for the spatial distribution of volcanic deposition, J. Geophys. Res.-Atmos., 112, https://doi.org/10.1029/2006JD007461, 2007.

Gao, C. C., Robock, A., and Ammann, C.: Volcanic forcing of climate over the past 1500 years: An improved ice core-based index for climate models, J. Geophys. Res.-Atmos., 113, https://doi.org/10.1029/2008JD010239, 2008.

Garrison, C., Kilburn, C., Smart, D., and Edwards, S.: The blue suns of 1831: was the eruption of Ferdinandea, near Sicily, one of the largest volcanic climate forcing events of the nineteenth century?, Clim. Past, 17, 2607-2632, https://doi.org/10.5194/cp-17-2607-2021, 2021.

Gautier, E., Savarino, J., Hoek, J., Erbland, J., Caillon, N., Hattori, S., Yoshida, N., Albalat, E., Albarede, F., and Farquhar, J.: 2600-years of stratospheric volcanism through sulfate isotopes, Nat. Commun., 10, https://doi.org/10.1038/s41467-019-08357-0, 2019.

Gautier, E., Savarino, J., Erbland, J., Lanciki, A., and Possenti, P.: Variability of sulfate signal in ice core records based on five replicate cores, Clim. Past, 12, 103-113, https://doi.org/10.5194/cp-12-103-2016, 2016.

Gerhart, L. M. and Ward, J. K.: Plant responses to low [CO2] of the past, New Phytol., 188, 674-695, https://doi.org/10.1111/j.1469-8137.2010.03441.x, 2010.

Gettelman, A., Schmidt, A., and Kristjansson, J. E.: Icelandic volcanic emissions and climate, Nat. Geosci., 8, https://doi.org/10.1038/ngeo2376, 2015.

Formatted: Default Paragraph Font, Font color: Black

Formatted: Normal, Centered, Border: Top: (No border), Bottom: (No border), Left: (No border), Right: (No border), Between : (No border), Tab stops: 3.25", Centered + 6.5", Right, Position: Horizontal: Left, Relative to: Column, Vertical: In line, Relative to: Margin, Wrap Around

Formatted: Font color: Black

Gilgen, A., Adolf, C., Brugger, S. O., Ickes, L., Schwikowski, M., Van Leeuwen, J. F. N., Tinner, W., and Lohmann, U.: Implementing microscopic charcoal particles into a global aerosol–climate model, Atmos. Chem. Phys., 18, 11813-11829, https://doi.org/10.5194/acp-18-11813-2018, 2018.

Gill, J. L., Williams, J. W., Jackson, S. T., Lininger, K. B., and Robinson, G. S.: Pleistocene Megafaunal Collapse, Novel Plant Communities, and Enhanced Fire Regimes in North America, Science, 326, 1100-1103, https://doi.org/10.1126/science.1179504, 2009.

Ginoux, P.: Effects of nonsphericity on mineral dust modeling, J. Geophys. Res.-Atmos., 108, https://doi.org/10.1029/2002JD002516, 2003.

Ginoux, P., Prospero, J., Gill, T. E., Hsu, N. C., & Zhao, M. (2012). Global scale attribution of anthropogenic and natural dust sources and their emission rates based on MODIS deep blue aerosol products. *Reviews of Geophysics*, *50,*(RG3005,), RG3005. https://doi.org/DOI:10.1029/2012RG000388

Gkinis, V., Vinther, B. M., Popp, T. J., Quistgaard, T., Faber, A.-K., Holme, C. T., Jensen, C.-M., Lanzky, M., Lütt, A.-M., Mandrakis, V., Ørum, N.-O., Pedersen, A.-S., Vaxevani, N., Weng, Y., Capron, E., Dahl-Jensen, D., Hörhold, M., Jones, T. R., Jouzel, J., … White, J. W. C. (2021). A 120,000-year long climate record from a NW-Greenland deep ice core at ultra-high resolution. *Scientific Data*, *8*(1), 141. https://doi.org/10.1038/s41597-021-00916-9

Gloor, M., Fan, S.-M., Pacala, S., and Sarmiento, J.: Optimal sampling of the atmosphere for purpose of inverse modeling: A model study, Global Biogeochem. Cy., 14, 407-428, https://doi.org/10.1029/1999GB900052, 2000.

Goldewijk, K.K., Beusen, A., van Drecht, G., de Vos, M.: The HYDE 3.1 spatially explicit database of human-induced global land-use change over the past 12,000 years, Global Ecol. Biogeogr., 20 73-86, https://doi.org/10.1111/j.1466-8238.2010.00587.x, 2011.

González-Romero, A., González-Flórez, C., Panta, A., Yus-Díez, J., Córdoba, P., Alastuey, A., Moreno, N., Kandler, K., Klose, M., Clark, R. N., Ehlmann, B. L., Greenberger, R. N., Keebler, A. M., Brodrick, P., Green, R. O., Querol, X., and Pérez García-Pando, C.: Probing Iceland's dust-emitting sediments: particle size distribution, mineralogy, cohesion, Fe mode of occurrence, and reflectance spectra signatures, Atmos. Chem. Phys., 24, 6883–6910, https://doi.org/10.5194/acp-24-6883-2024, 2024.

Gonçalves Ageitos, M., Obiso, V., Miller, R. L., Jorba, O., Klose, M., Dawson, M., Balkanski, Y., Perlwitz, J., Basart, S., Di Tomaso, E., Escribano, J., Macchia, F., Montané, G., Mahowald, N. M., Green, R. O., Thompson, D. R., and Pérez García-Pando, C.: Modeling dust mineralogical composition: sensitivity to soil mineralogy atlases and their expected climate impacts, Atmos. Chem. Phys., 23, 8623–8657, https://doi.org/10.5194/acp-23-8623-2023, 2023.

Gott, B.: Aboriginal fire management in south-eastern Australia: aims and frequency, J. Biogeogr., 32, 1203-1208, https://doi.org/10.1111/j.1365-2699.2004.01233.x, 2005.

Gowan, E. J., Zhang, X., Khosravi, S. et al. A new global ice sheet reconstruction for the past 80 000 years. Nat. Commun., 12, 1199, https://doi.org/10.1038/s41467-021-21469-w, 2021.

Grieman, M. M., Aydin, M., Isaksson, E., Schwikowski, M., and Saltzman, E. S.: Aromatic acids in an Arctic ice core from Svalbard: a proxy record of biomass burning, Clim. Past, 14, 637-651, https://doi.org/10.5194/cp-14-637-2018, 2018.

Grythe, H., Ström, J., Krejci, R., Quinn, P., and Stohl, A.: A review of sea-spray aerosol source functions using a large global set of sea salt aerosol concentration measurements, Atmos. Chem. Phys., 14, 1277–1297, https://doi.org/10.5194/acp-14-1277-2014, 2014.

Guillet, S., Corona, C., Stoffel, M., Khodri, M., Lavigne, F., Ortega, P., Eckert, N., Sielenou, P. D., Daux, V., Churakova (Sidorova), O. V., Davi, N., Edouard, J.-L., Zhang, Y., Luckman, B. H., Myglan, V. S., Guiot, J., Beniston, M., Masson-Delmotte, V., and Oppenheimer, C.: Climate response to the Samalas volcanic eruption in 1257 revealed by proxy records, Nat. Geosci., 10, 123-128, https://doi.org/10.1038/ngeo2875, 2017.

Formatted: Default Paragraph Font, Font color: Black

Formatted: Normal, Centered, Border: Top: (No border), Bottom: (No border), Left: (No border), Right: (No border), Between : (No border), Tab stops: 3.25", Centered + 6.5", Right, Position: Horizontal: Left, Relative to: Column, Vertical: In line, Relative to: Margin, Wrap Around

Formatted: Font color: Black

Guillet, S., Corona, C., Oppenheimer, C., Lavigne, F., Khodri, M., Ludlow, F., Sigl, M., Toohey, M., Atkins, P. S., Yang, Z., Muranaka, T., Horikawa, N., and Stoffel, M.: Lunar eclipses illuminate timing and climate impact of medieval volcanism, Nature, 616, 90-95, https://doi.org/10.1038/s41586-023-05751-z, 2023.

Gulev, S. K., Thorne, P. W., Ahn, J., Dentener, F. J., Domingues, C. M., Gerland, S., Gong, D., Kaufman, D. S., Nnamchi, H. C., Quaas, J., Rivera, J. A., Sathyendranath, S., Smith, S. L., Trewin, B., von Schuckmann, K., & Vose, R. ,S. (2021). Chapter 2: Changing State of the Climate System. In V. , Masson-Delmotte, P. Zhai, A. Pirani, S. L. Connors, C. Péan, S. Berger, N. Caud, Y. Chen, L. Goldfarb, M. I. Gomis, M. Huang, K. Leitzell, E. Lonnoy, J. B. R. Matthews, T. K. Maycock, T. Waterfield, O. Yelekçi, R. Yu, & B. Zhou (Eds.), *Climate Change 2021: The Physical Science Basis. Contribution of Working Group I to the Sixth Assessment Report of the Intergovernmental Panel on Climate Change* (pp. 287–422). Cambridge University Press, Cambridge, United Kingdom and New York, NY, USA. https://doi.org/10.1017/9781009157896.004

Gupta, A. K., J. F. Kok, V. Amiridis, A. Gkikas, R. Konstantinos, E. Proestakis, S. Logothetis, E. Marinou, and C, Pérez García-Pando (2026), A global decline in atmospheric dust during the 21st century, Science Advances, 12, eaef5691, https://10.1126/sciadv.aef5691

Gutsell, S. L. and Johnson, E. A.: How fire scars are formed: coupling a disturbance process to its ecological effect, Can. J. Forest Res., 26, 166–174, https://doi.org/10.1139/x26-020, 1996.

Hall, S. A.: Vegetation and wildfire history of Ocate Mesa, Northern New Mexico, USA, Rev. Palaeobot. Palyno., 283, 104327, https://doi.org/10.1016/j.revpalbo.2020.104327, 2020.

Hamilton, D. S., Hantson, S., Scott, C. E., Kaplan, J. O., Pringle, K. J., Nieradzik, L. P., Rap, A., Folberth, G. A., Spracklen, D. V., and Carslaw, K. S.: Reassessment of pre-industrial fire emissions strongly affects anthropogenic aerosol forcing, Nat. Commun., 9, 3182, https://doi.org/10.1038/s41467-018-05592-9, 2018.

Hamilton, D. S., Lee, L. A., Pringle, K. J., Reddington, C. L., Spracklen, D. V., and Carslaw, K. S.: Occurrence of pristine aerosol environments on a polluted planet, P. Natl. Acad. Sci. USA, 111, 18466-18471, https://doi.org/10.1073/pnas.1415440111, 2014.

Hamilton, D. S., Perron, M. M. G., Bond, T. C., Bowie, A. R., Buchholz, R. R., Guieu, C., Ito, A., Maenhaut, W., Myriokefalitakis, S., Olgun, N., Rathod, S. D., Schepanski, K., Tagliabue, A., Wagner, R., and Mahowald, N. M.: Earth, Wind, Fire, and Pollution: Aerosol Nutrient Sources and Impacts on Ocean Biogeochemistry, Annual Review of Marine Science, 14, 303-330, https://doi.org/10.1146/annurev-marine-031921-013612, 2022.

Hammer, C. U., Clausen, H. B., and Dansgaard, W.: Greenland Ice-Sheet Evidence of Post-Glacial Volcanism and Its Climatic Impact, Nature, 288, 230-235, https://doi.org/10.1038/288230a0, 1980.

Hansen JE, Sato M. 2012 Paleoclimate implications for human-made climate change. In Climate change: inferences from paleoclimate and regional aspects (eds A Berger, F Mesinger, DŠijaèki), pp. 21–48. Vienna, Austria: Springer.

Hansson, M. E.: The Renland ice core. A Northern Hemisphere record of aerosol composition over 120,000 years, Tellus B, 46, 390-418, https://doi.org/10.3402/tellusb.v46i5.15813, 1994.

Hantson, S., Arneth, A., Harrison, S. P., Kelley, D. I., Prentice, I. C., Rabin, S. S., Archibald, S., Mouillot, F., Arnold, S. R., Artaxo, P., Bachelet, D., Ciais, P., Forrest, M., Friedlingstein, P., Hickler, T., Kaplan, J. O., Kloster, S., Knorr, W., Lasslop, G., Li, F., Mangeon, S., Melton, J. R., Meyn, A., Sitch, S., Spessa, A., van der Werf, G. R., Voulgarakis, A., and Yue, C.: The status and challenge of global fire modelling, Biogeosciences, 13, 3359-3375, https://doi.org/10.5194/bg-13-3359-2016, 2016.

Hantson, S., Kelley, D. I., Arneth, A., Harrison, S. P., Archibald, S., Bachelet, D., Forrest, M., Hickler, T., Lasslop, G., Li, F., Mangeon, S., Melton, J. R., Nieradzik, L., Rabin, S. S., Prentice, I. C., Sheehan, T., Sitch, S., Teckentrup, L., Voulgarakis, A., and Yue, C.: Quantitative assessment of fire and vegetation properties in simulations with fire-enabled vegetation models from the Fire

Formatted: Default Paragraph Font, Font color: Black

Formatted: Normal, Centered, Border: Top: (No border), Bottom: (No border), Left: (No border), Right: (No border), Between : (No border), Tab stops: 3.25", Centered + 6.5", Right, Position: Horizontal: Left, Relative to: Column, Vertical: In line, Relative to: Margin, Wrap Around

Formatted: Font color: Black

Model Intercomparison Project, Geosci. Model Dev., 13, 3299-3318, https://doi.org/10.5194/gmd-13-3299-2020, 2020.

Harrison, S. P., Villegas-Diaz, R., Cruz-Silva, E., Gallagher, D., Kesner, D., Lincoln, P., Shen, Y., Sweeney, L., Colombaroli, D., Ali, A., Barhoumi, C., Bergeron, Y., Blyakharchuk, T., Bobek, P., Bradshaw, R., Clear, J. L., Czerwiński, S., Daniau, A.-L., Dodson, J., Edwards, K. J., Edwards, M. E., Feurdean, A., Foster, D., Gajewski, K., Gałka, M., Garneau, M., Giesecke, T., Gil Romera, G., Girardin, M. P., Hoefer, D., Huang, K., Inoue, J., Jamrichová, E., Jasiunas, N., Jiang, W., Jiménez-Moreno, G., Karpińska-Kołaczek, M., Kołaczek, P., Kuosmanen, N., Lamentowicz, M., Lavoie, M., Li, F., Li, J., Lisitsyna, O., López-Sáez, J. A., Luelmo-Lautenschlaeger, R., Magnan, G., Magyari, E. K., Maksims, A., Marcisz, K., Marinova, E., Marlon, J., Mensing, S., Miroslaw-Grabowska, J., Oswald, W., Pérez-Díaz, S., Pérez-Obiol, R., Piilo, S., Poska, A., Qin, X., Remy, C. C., Richard, P. J. H., Salonen, S., Sasaki, N., Schneider, H., Shotyk, W., Stancikaite, M., Šteinberga, D., Stivrins, N., Takahara, H., Tan, Z., Trasune, L., Umbanhowar, C. E., Väliranta, M., Vassiljev, J., Xiao, X., Xu, Q., Xu, X., Zawisza, E., Zhao, Y., Zhou, Z., and Paillard, J.: The Reading Palaeofire Database: an expanded global resource to document changes in fire regimes from sedimentary charcoal records, Earth Syst. Sci. Data, 14, 1109–1124, https://doi.org/10.5194/essd-14-1109-2022, 2022.

Hastings, M. G., Jarvis, J. C., and Steig, E. J.: Anthropogenic Impacts on Nitrogen Isotopes of Ice-Core Nitrate, Science, 324, 1288–1288, https://doi.org/10.1126/science.1170510, 2009.

Haugvaldstad, O. W., Schulz, M., Storelvmo, T., Leung, D. M., Gupta, A., Jones, A. C., Regayre, L. A., Kawai, K., Matsui, H., Gonçalves Ageitos, M., Pérez García-Pando, C., van Noije, T., Karydis, V. A., Tsimpidi, A. P., Klingmueller, K., Balkanski, Y., Checa-Garcia, R., Tsigaridis, K., Miller, R. L., and Kok, J. F.: Multi-Model Assessment of Dust Direct Radiative Forcing from Reconstructed Dust Increases Since the Pre-Industrial Era, ESS Open Archive [preprint], https://doi.org/10.22541/essoar.15012137/v1, 2026.

Hawkins, E., Ortega, P., Suckling, E., Schurer, A., Hegerl, G., Jones, P., Joshi, M., Osborn, T. J., Masson-Delmotte, V., Mignot, J., Thorne, P., and van Oldenborgh, G. J.: Estimating changes in global temperature since the pre-industrial period, B. Am. Meteorol. Soc., 98, 1841–1856, https://doi.org/10.1175/BAMS-D-16-0007.1, 2017

Hayes, C. T.: Timekeepers for trace elements in the global ocean: The thorium stopwatches, Oceanography 37, 156–161, https://doi.org/10.5670/oceanog.2024.412, 2024

He, C., Liu, Z., Otto-Bliesner, B. L., Brady, E. C., Zhu, C., Tomas, R., Clark, P. U., Zhu, J., Jahn, A., Gu, S., Zhang, J., Nusbaumer, J., Noone, D., Cheng, H., Wang, Y., Yan, M., and Bao, Y.: Hydroclimate footprint of pan-Asian monsoon water isotope during the last deglaciation, Science Advances, 7, eabe2611, https://doi.org/10.1126/sciadv.abe2611, 2021.

Heinemann, M., Segschneider, J., and Schneider, B.: CO_2 drawdown due to particle ballasting by glacial aeolian dust: an estimate based on the ocean carbon cycle model MPIOM/HAMOCC version 1.6.2p3, Geosci. Model Dev., 12, 1869–1883, https://doi.org/10.5194/gmd-12-1869-2019, 2019.

Héon, J., Arseneault, D., and Parisien, M.-A.: Resistance of the boreal forest to high burn rates, P. Natl. Acad. Sci. USA., 111, 13888–13893, https://doi.org/10.1073/pnas.1409316111, 2014.

Hess, K., Fu, R. R., Piascik, S., Stríkis, N. M., Trindade, R. I. F., Kukla, T., Brenner, A. R., Jaqueto, P., Petaev, M. I., Cruz, F. W., Buarque, P. F. S. M., Pérez-Mejías, C., and Cheng, H.: Investigating speleothem magnetism as a proxy for dust mobilization and rainfall. Quaternary Sci. Rev., 330, 108598. https://doi.org/10.1016/j.quascirev.2024.108598, 2024

Hessburg, P. F., Agee, J. K., and Franklin, J. F.: Dry forests and wildland fires of the inland Northwest USA: Contrasting the landscape ecology of the pre-settlement and modern eras, Forest Ecol. Manag., 211, 117-139, https://doi.org/10.1016/j.foreco.2005.02.016, 2005.

Hessilt, T. D., Abatzoglou, J. T., Chen, Y., Randerson, J. T., Scholten, R. C., van der Werf, G., and Veraverbeke, S.: Future increases in lightning ignition efficiency and wildfire occurrence expected from drier fuels in boreal forest ecosystems of western North America, Environ. Res. Lett., 17, 054008, https://doi.org/10.1088/1748-9326/ac6311, 2022.

Formatted: Default Paragraph Font, Font color: Black

Formatted: Normal, Centered, Border: Top: (No border), Bottom: (No border), Left: (No border), Right: (No border), Between : (No border), Tab stops: 3.25", Centered + 6.5", Right, Position: Horizontal: Left, Relative to: Column, Vertical: In line, Relative to: Margin, Wrap Around

Formatted: Font color: Black

Higuera, P. E., Shuman, B. N., and Wolf, K. D.: Rocky Mountain subalpine forests now burning more than any time in recent millennia, P. Natl. Acad. Sci. USA., 118, e2103135118, https://doi.org/10.1073/pnas.2103135118, 2021.
Higuera, P. E., Whitlock, C., and Gage, J. A.: Linking tree-ring and sediment-charcoal records to reconstruct fire occurrence and area burned in subalpine forests of Yellowstone National Park, USA, Holocene, 21, 327-341, https://doi.org/10.1177/0959683610374882, 2011.
Hoesly, R. M., Smith, S. J., Feng, L., Klimont, Z., Janssens-Maenhout, G., Pitkanen, T., Seibert, J. J., Vu, L., Andres, R. J., Bolt, R. M., Bond, T. C., Dawidowski, L., Kholod, N., Kurokawa, J. I., Li, M., Liu, L., Lu, Z., Moura, M. C. P., O'Rourke, P. R., and Zhang, Q.: Historical (1750–2014) anthropogenic emissions of reactive gases and aerosols from the Community Emissions Data System (CEDS), Geosci. Model Dev., 11, 369–408. https://doi.org/10.5194/gmd-11-369-2018, 2018.
Hooper, J., and Marx, S.: A global doubling of dust emissions during the Anthropocene?, Global Planet. Change, 169, 70–91, https://doi.org/10.1016/j.gloplacha.2018.07.003, 2018.
Hooper, J. N., and May, J. H.: Palaeo-dust records: a window to understanding past environments, Global. Planet. Change, 165, 13-43, https://doi.org/10.1016/j.gloplacha.2018.03.001, 2018.
Hopcroft, P. O., Valdes, P. J., Woodward, S., and Joshi, M. M.: Last glacial maximum radiative forcing from mineral dust aerosols in an Earth system model, J. Geophys. Res.-Atmos, 120, 8186–8205, https://doi.org/10.1002/2015JD023742, 2015.
Hopcroft, P. O., and Valdes, P. J.: On the Role of Dust-Climate Feedbacks During the Mid-Holocene, Geophys. Res. Lett., 46, 1612–1621, https://doi.org/10.1029/2018GL080483, 2019.
Hopcroft, P. O., and Valdes, P. J.: Green Sahara tipping points in transient climate model simulations of the Holocene, Environ. Res. Lett., 17, 085001, https://doi.org/10.1088/1748-9326/ac7c2b, 2022.
Horowitz, Koch, D., Krol, M. C., Landing, W., Liu, X., Mahowald, N., Miller, R. L., Morcrette, J.-J., Myhre, G., Penner, J. E., Perlwitz, J. P., Stier, P., Takemura, T., and Zender, C.: Global dust model intercomparison in AeroCom phase I, Atmos. Chem. Phys., 11, 7781-7816, https://doi.org/10.5194/acp-11-7781-2011, 2011.
Hovan, S. A., and Rea, D. K.: The Cenozoic Record of Continental Mineral Deposition on Broken and Ninetyeast Ridges, Indian Ocean: Southern African Aridity and Sediment Delivery from the Himalayas, Paleoceanography, 7, 833–860, https://doi.org/10.1029/92PA02176, 1992.
Hua, Q., McDonald, J., Redwood, D., Drysdale, R., Lee, S., Fallon, S., and Hellstrom, J.: Robust chronological reconstruction for young speleothems using radiocarbon, Quat. Geochronol., 14, 67-80, https://doi.org/10.1016/j.quageo.2012.04.017, 2012.
Huang, Y., Kok, J. F., Kandler, K., Lindqvist, H., Nousiainen, T., Sakai, T., Adebiyi, A., and Jokinen, O.: Climate Models and Remote Sensing Retrievals Neglect Substantial Desert Dust Asphericity, Geophys. Res. Lett., 47, https://doi.org/10.1029/2019GL086592, 2020.
Huneeus, N., Schulz, M., Balkanski, Y., Griesfeller, J., Kinne, S., Prospero, J., Bauer, S., Boucher, O., Chin, M., Dentener, F., Diehl, T., Easter, R., Fillmore, D., Ghan, S., Ginoux, P., Grini, A., Horowitz, L., Koch, D., Krol, M. C., Landing, W., Liu, X., Mahowald, N., Miller, R. L., Morcrette, J.-J., Myhre, G., Penner, J. E., Perlwitz, J., Stier, P., Takemura, T., and Zender, C. S.: Global dust model intercomparison in AeroCom phase I, Atmos. Chem. Phys., 11, 7781–7816, https://doi.org/10.5194/acp-11-7781-2011, 2011.
Hutchison, W., Gabriel, I., Plunkett, G., Burke, A., Sugden, P., Innes, H., Davies, S., Moreland, W. M., Krüger, K., Wilson, R., Vinther, B. M., Dahl-Jensen, D., Freitag, J., Oppenheimer, C., Chellman, N. J., Sigl, M., and McConnell, J. R.: High-Resolution Ice-Core Analyses Identify the Eldgjá Eruption and a Cluster of Icelandic and Trans-Continental Tephras Between 936 and 943 CE, J. Geophys. Res.-Atmos., 129, e2023JD040142, https://doi.org/10.1029/2023JD040142, 2024.
Hutchison, W., Sugden, P., Burke, A., Abbott, P., Ponomareva, V. V., Dirksen, O., Portnyagin, M. V., MacInnes, B., Bourgeois, J., Fitzhugh, B., Verkerk, M., Aubry, T. J., Engwell, S. L., Svensson, A., Chellman, N. J., McConnell, J. R., Davies, S., Sigl, M., and Plunkett, G.: The 1831 CE

Formatted: Default Paragraph Font, Font color: Black

Formatted: Normal, Centered, Border: Top: (No border), Bottom: (No border), Left: (No border), Right: (No border), Between : (No border), Tab stops: 3.25", Centered + 6.5", Right, Position: Horizontal: Left, Relative to: Column, Vertical: In line, Relative to: Margin, Wrap Around

Formatted: Font color: Black

mystery eruption identified as Zavaritskii caldera, Simushir Island (Kurils), P. Natl. Acad. Sci. USA, 122, e2416699122, https://doi.org/10.1073/pnas.2416699122, 2025.
Innes, H. M., Hutchison, W., Sigl, M., Crick, L., Abbott, P. M., Bigler, M., Chellman, N. J., Davies, S. M., Kutterolf, S., McConnell, J. R., Severi, M., Sparks, R. S. J., Svensson, A., Wolff, E. W., Rae, J. W. B., and Burke, A.: Ice core evidence for the Los Chocoyos supereruption disputes millennial-scale climate impact, Communications Earth & Environment, 6, 137, https://doi.org/10.1038/s43247-025-02095-6, 2025.
IPCC: Climate Change 2023: Synthesis Report. Contribution of Working Groups I, II and III to the Sixth Assessment Report of the Intergovernmental Panel on Climate Change [Core Writing Team, H. Lee and J. Romero (eds.)]. IPCC, Geneva, Switzerland, pp. 35-115, https://doi.org/10.59327/IPCC/AR6-9789291691647, 2023.
Ivanovic, R. F., Gregoire, L. J., Kageyama, M., Roche, D. M., Valdes, P. J., Burke, A., Drummond, R., Peltier, W. R., and Tarasov, L.: Transient climate simulations of the deglaciation 21–9 thousand years before present (version 1) – PMIP4 Core experiment design and boundary conditions, Geosci. Model Dev., 9, 2563–2587, https://doi.org/10.5194/gmd-9-2563-2016, 2016.
Jensen, B. J. L., Pyne-O'Donnell, S., Plunkett, G., Froese, D. G., Hughes, P. D. M., Sigl, M., McConnell, J. R., Amesbury, M. J., Blackwell, P. G., van den Bogaard, C., Buck, C. E., Charman, D. J., Clague, J. J., Hall, V. A., Koch, J., Mackay, H., Mallon, G., McColl, L., and Pilcher, J. R.: Transatlantic distribution of the Alaskan White River Ash, Geology, 42, 875-878, https://doi.org/10.1130/G35945.1, 2014.
Jiang, Y., Yang, X.-Q., Liu, X., Qian, Y., Zhang, K., Wang, M., Li, F., Wang, Y., and Lu, Z.: Impacts of Wildfire Aerosols on Global Energy Budget and Climate: The Role of Climate Feedbacks, Journal of Climate, 33, 3351-3366, https://doi.org/10.1175/JCLI-D-19-0572.1, 2020.
Jickells, T. D., An, Z. S., Andersen, K. K., Baker, A. R., Bergametti, G., Brooks, N., Cao, J. J., Boyd, P. W., Duce, R. A., Hunter, K. A., Kawahata, H., Kubilay, N., laRoche, J., Liss, P. S., Mahowald, N., Prospero, J. M., Ridgwell, A. J., Tegen, I., and Torres, R.: Global Iron Connections Between Desert Dust, Ocean Biogeochemistry, and Climate, Science, 308, 67-71, https://doi.org/10.1126/science.1105959, 2015.
Joge, S. D., Mansour, K., Simó, R., Galí, M., Steiner, N., Saiz-Lopez, A., and Mahajan, A. S.: Climate warming increases global oceanic dimethyl sulfide emissions, P. Natl. Acad. Sci. USA, 122, https://doi.org/10.1073/pnas.2502077122, 2025.
Johnson, C. N.: Ecological consequences of Late Quaternary extinctions of megafauna, P. Roy. Soc. B-Biol. Sci., 276, 2509-2519, https://doi.org/10.1098/rspb.2008.1921, 2009.
Johnson, J. S., Regayre, L. A., Yoshioka, M., Pringle, K. J., Turnock, S. T., Browse, J., Sexton, D. M. H., Rostron, J. W., Schutgens, N. A. J., Partridge, D. G., Liu, D., Allan, J. D., Coe, H., Ding, A., Cohen, D. D., Atanacio, A., Vakkari, V., Asmi, E., and Carslaw, K. S.: Robust observational constraint of uncertain aerosol processes and emissions in a climate model and the effect on aerosol radiative forcing, Atmos. Chem. Phys., 20, 9491–9524, https://doi.org/10.5194/acp-20-9491-2020, 2020.
Jongebloed, U. A., Chalif, J. I., Tashmim, L., Porter, W. C., Bates, K. H., Chen, Q., Osterberg, E. C., Koffman, B. G., Cole-Dai, J., Winski, D. A., Ferris, D. G., Kreutz, K. J., Wake, C. P., and Alexander, B.: Dimethyl sulfide chemistry over the industrial era: comparison of key oxidation mechanisms and long-term observations, Atmos. Chem. Phys., 25, 4083–4106, https://doi.org/10.5194/acp-25-4083-2025, 2025.
Jongebloed, U. A., Schauer, A. J., Hattori, S., Cole-Dai, J., Larrick, C. G., Salimi, S., Edouard, S. R., Geng, L., and Alexander, B.: Sulfur isotopes quantify the impact of anthropogenic activities on industrial-era Arctic sulfate in a Greenland ice core, Environ. Res. Lett., 18, https://doi.org/10.1088/1748-9326/acdc3d, 2023.
Jungclaus, J. H., Bard, E., Baroni, M., Braconnot, P., Cao, J., Chini, L. P., Egorova, T., Evans, M., González-Rouco, J. F., Goosse, H., Hurtt, G. C., Joos, F., Kaplan, J. O., Khodri, M., Klein Goldewijk, K., Krivova, N., LeGrande, A. N., Lorenz, S. J., Luterbacher, J., Man, W., Maycock,

Formatted: Default Paragraph Font, Font color: Black

Formatted: Normal, Centered, Border: Top: (No border), Bottom: (No border), Left: (No border), Right: (No border), Between : (No border), Tab stops: 3.25", Centered + 6.5", Right, Position: Horizontal: Left, Relative to: Column, Vertical: In line, Relative to: Margin, Wrap Around

Formatted: Font color: Black

A. C., Meinshausen, M., Moberg, A., Muscheler, R., Nehrbass-Ahles, C., Otto-Bliesner, B. I., Phipps, S. J., Pongratz, J., Rozanov, E., Schmidt, G. A., Schmidt, H., Schmutz, W., Schurer, A., Shapiro, A. I., Sigl, M., Smerdon, J. E., Solanki, S. K., Timmreck, C., Toohey, M., Usoskin, I. G., Wagner, S., Wu, C. J., Yeo, K. L., Zanchettin, D., Zhang, Q., and Zorita, E.: The PMIP4 contribution to CMIP6 – Part 3: The last millennium, scientific objective, and experimental design for the PMIP4 past1000 simulations, Geosci. Model Dev., 10, 4005-4033, https://doi.org/10.5194/gmd-10-4005-2017, 2017.

Kageyama, M., Albani, S., Braconnot, P., Harrison, S. P., Hopcroft, P. O., Ivanovic, R. F., Lambert, F., Marti, O., Peltier, W. R., Peterschmitt, J.-Y., Roche, D. M., Tarasov, L., Zhang, X., Brady, E. C., Haywood, A. M., LeGrande, A. N., Lunt, D. J., Mahowald, N. M., Mikolajewicz, U., Nisancioglu, K. H., Otto-Bliesner, B. L., Renssen, H., Tomas, R. A., Zhang, Q., Abe-Ouchi, A., Bartlein, P. J., Cao, J., Li, Q., Lohmann, G., Ohgaito, R., Shi, X., Volodin, E., Yoshida, K., Zhang, X., and Zheng, W.: The PMIP4 contribution to CMIP6 – Part 4: Scientific objectives and experimental design of the PMIP4-CMIP6 Last Glacial Maximum experiments and PMIP4 sensitivity experiments, Geosci. Model Dev., 10, 4035–4055, https://doi.org/10.5194/gmd-10-4035-2017, 2017.

Kageyama, M., Braconnot, P., Harrison, S. P., Haywood, A. M., Jungclaus, J. H., Otto-Bliesner, B. L., Peterschmitt, J.-Y., Abe-Ouchi, A., Albani, S., Bartlein, P. J., Brierley, C., Crucifix, M., Dolan, A., Fernandez-Donado, L., Fischer, H., Hopcroft, P. O., Ivanovic, R. F., Lambert, F., Lunt, D. J., Mahowald, N. M., Peltier, W. R., Phipps, S. J., Roche, D. M., Schmidt, G. A., Tarasov, L., Valdes, P. J., Zhang, Q., and Zhou, T.: The PMIP4 contribution to CMIP6 – Part 1: Overview and over-arching analysis plan, Geosci. Model Dev., 11, 1033–1057, https://doi.org/10.5194/gmd-11-1033-2018, 2018.

Kageyama, M., Harrison, S. P., Kapsch, M.-L., Lofverstrom, M., Lora, J. M., Mikolajewicz, U., Sherriff-Tadano, S., Vadsaria, T., Abe-Ouchi, A., Bouttes, N., Chandan, D., Gregoire, L. J., Ivanovic, R. F., Izumi, K., LeGrande, A. N., Lhardy, F., Lohmann, G., Morozova, P. A., Ohgaito, R., Paul, A., Peltier, W. R., Poulsen, C. J., Quiquet, A., Roche, D. M., Shi, X., Tierney, J. E., Valdes, P. J., Volodin, E., and Zhu, J.: The PMIP4 Last Glacial Maximum experiments: preliminary results and comparison with the PMIP3 simulations, Clim. Past, 17, 1065–1089, https://doi.org/10.5194/cp-17-1065-2021, 2021.

Kaplan, J. O., Krumhardt, K. M., and Zimmermann, N.: The prehistoric and preindustrial deforestation of Europe, Quat. Sci. Rev., 28, 3016–3034, https://doi.org/10.1016/j.quascirev.2009.09.028, 2009.

Kaplan, J. O., Pfeiffer, M., Kolen, J. C. A., and Davis, B. A. S.: Large Scale Anthropogenic Reduction of Forest Cover in Last Glacial Maximum Europe, Plos One, 11, e0166726, https://doi.org/10.1371/journal.pone.0166726, 2016.

Kaplan, J. O., Krumhardt, K. M., Gaillard, M., Sugita, S., Trondman, A., Fyfe, R., Marquer, L., Mazier, F., and Nielsen, A. B.: Constraining the Deforestation History of Europe : Evaluation of Historical Land Use Scenarios with Pollen-based Land Cover Reconstructions, land, 6, 1–20, https://doi.org/10.3390/land6040091, 2017.

Kaplan, J. O. (2026). Vegetation cover and wildfire in the late Preindustrial, mid-Holocene, and Last Glacial Maximum (Version v1.0.0) [Dataset]. Zenodo. https://doi.org/10.5281/zenodo.20821425

Kapp, P., Pullen, A., Abell, J. T., and Zhang, L.: Wind erosion in northern China: Insights from the western Qaidam fold belt, Loess Plateau, and Hami Basin, Earth-Sci. Rev., 261, 105037, https://doi.org/10.1016/j.earscirev.2024.105037, 2025.

Kawamura, K., Izawa, Y., Mochida, M., and Shiraiwa, T.: Ice core records of biomass burning tracers (levoglucosan and dehydroabietic, vanillic and p-hydroxybenzoic acids) and total organic carbon for past 300years in the Kamchatka Peninsula, Northeast Asia, Geochim. Cosmochim. Ac., 99, 317-329, https://doi.org/10.1016/j.gca.2012.08.006, 2012.

Kaufmann, P., Fundel, F., Fischer, H., Bigler, M., Ruth, U., Udisti, R., Hansson, M., de Angelis, M., Barbante, C., Wolff, E. W., Hutterli, M., and Wagenbach, D.: Ammonium and non-sea salt

Formatted: Default Paragraph Font, Font color: Black

Formatted: Normal, Centered, Border: Top: (No border), Bottom: (No border), Left: (No border), Right: (No border), Between : (No border), Tab stops: 3.25", Centered + 6.5", Right, Position: Horizontal: Left, Relative to: Column, Vertical: In line, Relative to: Margin, Wrap Around

Formatted: Font color: Black

sulfate in the EPICA ice cores as indicator of biological activity in the Southern Ocean, Quaternary Sci. Rev., 29(1–2), 313–323, https://doi.org/10.1016/j.quascirev.2009.11.009, 2010.

Kay, J. E., Deser, C., Phillips, A., Mai, A., Hannay, C., Strand, G., Arblaster, J. M., Bates, S. C., Danabasoglu, G., and Edwards, J.: The Community Earth System Model (CESM) large ensemble project: A community resource for studying climate change in the presence of internal climate variability, B. Am. Meteorol. Soc., 96, 1333–1349, https://doi.org/10.1175/BAMS-D-13-00255.1, 2015.

Kemp, R. A.: Pedogenic modification of loess: significance for paleoclimatic reconstructions, Earth-Sci. Rev., 54, 145-156, https://doi.org/10.1016/S0012-8252(01)00045-9, 2001.

Kienast, S. S., Winckler, G., Lippold, J., Albani, S., and Mahowald, N. M.: Tracing dust input to the global ocean using thorium isotopes in marine sediments: ThoroMap, Global Biogeochem. Cy., 30, 1526–1541, https://doi.org/10.1002/2016GB005408, 2016.

Knorr, W., Jiang, L., and Arneth, A.: Climate, CO_2 and human population impacts on global wildfire emissions, Biogeosciences, 13, 267-282, https://doi.org/10.5194/bg-13-267-2016, 2016.

Koffman, B. G., Yoder, M. F., Methven, T., Hanschka, L., Sears, H. B., Saylor, P. L., and Wallace, K. L.: Glacial dust surpasses both volcanic ash and desert dust in its iron fertilization potential, Global Biogeochem. Cy., 35, e2020GB006821, https://doi.org/10.1029/2020GB006821, 2021.

Kohfeld, K. E., and Harrison, S. P.: DIRTMAP: the geological record of dust, Earth-Sci. Rev., 54, 81–114, https://doi.org/10.1016/S0012-8252(01)00042-3, 2001.

Kohfeld, K., & Harrison, S. (2003). Glacial-interglacial changes in dust deposition on the Chinese Loess Plateau. Quarternary Science Reviews, 22, 1859–1878.

Kohfeld, K. E., Graham, R. M., de Boer, A. M., Sime, L. C., Wolff, E. W., Le Quéré, C., and Bopp, L.: Southern Hemisphere westerly wind changes during the Last Glacial Maximum: paleo-data synthesis, Quaternary Sci. Rev., 68, 76–95, https://doi.org/10.1016/j.quascirev.2013.01.017, 2013.

Kok, J. F.: A scaling theory for the size distribution of emitted dust aerosols suggests climate models underestimate the size of the global dust cycle, P. Natl. Acad. Sci. USA, 108, 1016-1021, https://doi.org/10.1073/pnas.1014798108, 2011.

Kok, J. F.: Does the size distribution of mineral dust aerosols depend on the wind speed at emission?, Atmos. Chem. Phys., 11, 10149-10156, https://doi.org/10.5194/acp-11-10149-2011, 2011.

Kok, J. F., Parteli, E. J. R., Michaels, T. I., and Karam, D. B: The physics of wind-blown sand and dust, 75, 106901, https://doi.org/10.1088/0034-4885/75/10/106901, 2012.

Kok, J. F., Mahowald, N. M., Fratini, G., Gillies, J. A., Ishizuka, M., Leys, J. F., Mikami, M., Park, M.-S., Park, S.-U., Van Pelt, R. S., and Zobeck, T. M.: An improved dust emission model – Part 1: Model description and comparison against measurements, Atmos. Chem. Phys., 14, 13023–13041, https://doi.org/10.5194/acp-14-13023-2014, 2014.

Kok, J. F., Ridley, D. A., Zhou, Q., Miller, R. L., Zhao, C., Heald, C. L., Ward, D. S., Albani, S., and Haustein, K.: Smaller desert dust cooling effect estimated from analysis of dust size and abundance, Nat. Geosci., 10, 274-8, https://doi.org/10.1038/ngeo2912, 2017.

Kok, J. F., Adebiyi, A. A., Albani, S., Balkanski, Y., Checa-Garcia, R., Chin, M., Colarco, P. R., Hamilton, D. S., Huang, Y., Ito, A., Klose, M., Leung, D. M., Li, L., Mahowald, N. M., Miller, R. L., Obiso, V., Pérez García-Pando, C., Rocha-Lima, A., Wan, J. S., and Whicker, C. A.: Improved representation of the global dust cycle using observational constraints on dust properties and abundance, Atmos. Chem. Phys., 21, 8127-8167, https://doi.org/10.5194/acp-21-8127-2021, 2021.

Kok, J. F., Adebiyi, A. A., Albani, S., Balkanski, Y., Checa-Garcia, R., Chin, M., Colarco, P. R., Hamilton, D. S., Huang, Y., Ito, A., Klose, M., Li, L., Mahowald, N. M., Miller, R. L., Obiso, V., Pérez García-Pando, C., Rocha-Lima, A., and Wan, J. S.: Contribution of the world's main dust source regions to the global cycle of desert dust, Atmos. Chem. Phys., 21, 8169–8193, https://doi.org/10.5194/acp-21-8169-2021, 2021.

Formatted: Default Paragraph Font, Font color: Black

Formatted: Normal, Centered, Border: Top: (No border), Bottom: (No border), Left: (No border), Right: (No border), Between : (No border), Tab stops: 3.25", Centered + 6.5", Right, Position: Horizontal: Left, Relative to: Column, Vertical: In line, Relative to: Margin, Wrap Around

Formatted: Font color: Black

Kok, J. F., Storelvmo, T., Karydis, V. A., Adebiyi, A. A., Mahowald, N. M., Evan, A. T., He, C., and Leung, D. M.: Mineral dust aerosol impacts on global climate and climate change, Nature Reviews Earth and Environment, 4, 71–86. https://doi.org/10.1038/s43017-022-00379-5, 2023.

Kok, J. F., Gupta, A. K., Evan, A. T., Adebiyi, A. A., Li, L., Albani, S., Balkanski, Y., Checa-Garcia, R., Colarco, P. R., Hamilton, D. S., Huang, Y., Ito, A., Klose, M., Mahowald, N. M., Miller, R. L., Obiso, V., Pérez García-Pando, C., Rocha-Lima, A., and Wan, J. S.: Desert dust exerts twice the longwave radiative heating estimated by climate models, Nat. Commun., 17, 3191, https://doi.org/10.1038/s41467-026-70952-9, 2026.

Kok, J. F., D. S. Ward, N. M. Mahowald, and A. T. Evan (2018), Global and regional importance of the direct dust-climate feedback, *Nature Comm.*, 9, 241.

Kovilakam, M., Thomason, L. W., Ernest, N., Rieger, L., Bourassa, A., and Millán, L.: The Global Space-based Stratospheric Aerosol Climatology (version 2.0): 1979-2018, Earth Syst. Sci. Data, 12, 2607-2634, https://doi.org/10.5194/essd-12-2607-2020, 2020.

Kreider, M. R., Higuera, P. E., Parks, S. A., Rice, W. L., White, N., and Larson, A. J.: Fire suppression makes wildfires more severe and accentuates impacts of climate change and fuel accumulation, Nat. Commun., 15, 2412, https://doi.org/10.1038/s41467-024-46702-0, 2024.

Kutuzov, S., Legrand, M., Preunkert, S., Ginot, P., Mikhalenko, V., Shukurov, K., Poliukhov, A. and Toropov, P.: The Elbrus (Caucasus, Russia) ice core record–Part 2: history of desert dust deposition, Atmos. Chem. Phys., 19, 14133-14148, https://doi.org/10.5194/acp-19-14133-2019, 2019.

Lacis, A., Hansen, J., and Sato, M.: Climate forcing by stratospheric aerosols, Geophys. Res. Lett., 19, 1607–1610, https://doi.org/10.1029/92GL01620, 1992.

Lamb, H. H.: Volcanic Dust in the Atmosphere; with a Chronology and Assessment of Its Meteorological Significance, Philos. T. R. Soc. S.-A, 266, 425-533, https://doi.org/10.1098/rsta.1970.0010, 1970.

Lambert, F. (2025). Dust archives within polar ice cores. In *Encyclopedia of Quaternary Science* (pp. 571–578). Elsevier. https://doi.org/10.1016/B978-0-323-99931-1.00183-5

Lambert, F., Delmonte, B., Petit, J. R., Bigler, M., Kaufmann, P. R., Hutterli, M. A., Stocker, T. F., Ruth, U., Steffensen, J. P., and Maggi, V.: Dust-climate couplings over the past, 800000 years from the EPICA Dome C ice core, Nature, 452, 616–619, https://doi.org/10.1038/nature06763, 2008.

Lambert, F., Tagliabue, A., Shaffer, G., Lamy, F., Winckler, G., Farias, L., Gallardo, L., and De Pol-Holz, R.: Dust fluxes and iron fertilization in Holocene and Last Glacial Maximum climates, Geophys. Res. Lett., 42, 6014–6023, https://doi.org/10.1002/2015GL064250, 2015.

Lambert, F., Opazo, N., Ridgwell, A., Winckler, G., Lamy, F., Shaffer, G., Kohfeld, K., Ohgaito, R., Albani, S., and Abe-Ouchi, A.: Regional patterns and temporal evolution of ocean iron fertilization and CO_2 drawdown during the last glacial termination, Earth Planet. Sc. Lett., 554, 116675, https://doi.org/10.1016/j.epsl.2020.116675, 2021.

Lambert, F., and Albani, S.: Mineral dust in PMIP simulations: A short review, Past Global Changes Magasize, 29, 86–87, https://doi.org/10.22498/pages.29.2.86, 2021.

Lanci, L., Delmonte, B., Maggi, V., Petit, J. R., and Kent, D. V.: Ice magnetization in the EPICA-Dome C ice core: Implication for dust sources during glacial and interglacial periods, J. Geophys. Res.-Atmos., 113, https://doi.org/10.1029/2007JD009678, 2008.

Langford, R. P.: Fluvial-aeolian interactions: Part I, modern systems, Sedimentology, 36, 1023-1035, https://doi.org/10.1111/j.1365-3091.1989.tb01540.x, 1989.

Langmann, B.: Volcanic Ash versus Mineral Dust: Atmospheric Processing and Environmental and Climate Impacts, International Scholarly Research Notices, 245076, https://doi.org/10.1155/2013/245076, 2013.

Langmann, B.: On the Role of Climate Forcing by Volcanic Sulphate and Volcanic Ash, Adv. Meteorol., 2014, 340123, https://doi.org/10.1155/2014/340123, 2014.

Lavigne, F., Degeai, J. P., Komorowski, J. C., Guillet, S., Robert, V., Lahitte, P., Oppenheimer, C., Stoffel, M., Vidal, C. M., Surono, Pratomo, I., Wassmer, P., Hajdas, I., Hadmoko, D. S., and De

Formatted: Default Paragraph Font, Font color: Black

Formatted: Normal, Centered, Border: Top: (No border), Bottom: (No border), Left: (No border), Right: (No border), Between : (No border), Tab stops: 3.25", Centered + 6.5", Right, Position: Horizontal: Left, Relative to: Column, Vertical: In line, Relative to: Margin, Wrap Around

Formatted: Font color: Black

Belizal, E.: Source of the great A.D. 1257 mystery eruption unveiled, Samalas volcano, Rinjani Volcanic Complex, Indonesia, P. Natl. Acad. Sci. USA, 110, 16742-16747, https://doi.org/10.1073/pnas.1307520110, 2013.

LaVigne, M., Grottoli, A. G., Palardy, J. E., and Sherrell, R. M.: Multi-colony calibrations of coral Ba/Ca with a contemporaneous in situ seawater barium record, Geochim. Cosmochim. Ac., 179, 203-216, https://doi.org/10.1016/j.gca.2015.12.038, 2016.

Legrand, M., Feniet-Saigne, C., Sattzman, E. S., Germain, C., Barkov, N. I., and Petrov, V. N.: Ice-core record of oceanic emissions of dimethylsulphide during the last climate cycle, Nature, 350, 144–146, https://doi.org/10.1038/350144a0, 1991.

Legrand, M., Preunkert, S., May, B., Guilhermet, J., Hoffman, H., and Wagenbach, D.: Major 20th century changes of the content and chemical speciation of organic carbon archived in Alpine ice cores: Implications for the long-term change of organic aerosol over Europe, J. Geophys. Res.-Atmos., 118, 3879–3890, https://doi.org/10.1002/jgrd.50202, 2013.

Legrand, M., McConnell, J. R., Preunkert, S., Wachs, D., Chellman, N. J., Rehfeld, K., Bergametti, G., Wensman, S. M., Aeschbach, W., Oberthaler, M. K., and Friedrich, R.: Alpine ice core record of large changes in dust, sea-salt, and biogenic aerosol over Europe during deglaciation, PNAS Nexus, 4, pgaf186, https://doi.org/10.1093/pnasnexus/pgaf186, 2025.

Legrand, M., McConnell, J., Fischer, H., Wolff, E. W., Preunkert, S., Arienzo, M., Chellman, N., Leuenberger, D., Maselli, O., Place, P., Sigl, M., Schüpbach, S., and Flannigan, M.: Boreal fire records in Northern Hemisphere ice cores: a review, Clim. Past, 12, 2033-2059, https://doi.org/10.5194/cp-12-2033-2016, 2016.

LeGrande, A. N., Schmidt, G. A., Shindell, D. T., Field, C. V., Miller, R. L., Koch, D. M., Faluvegi, G., and Hoffmann, G.: Consistent simulations of multiple proxy responses to an abrupt climate change event. P. Natl. Acad. Sci. USA, 103, 837-842, https://doi.org/10.1073/pnas.0510095103, 2006.

Leung, D. M., Kok, J. F., Li, L., Okin, G. S., Prigent, C., Klose, M., Pérez García-Pando, C., Menut, L., Mahowald, N. M., Lawrence, D. M., and Chamecki, M.: A new process-based and scale-respecting desert dust emission scheme for global climate models – Part I: description and evaluation against inverse modeling emissions, Atmos. Chem. Phys., 23, 6487–6523, https://doi.org/10.5194/acp-23-6487-2023, 2023.

Leung, D. M., Kok, J. F., Li, L., Lawrence, D. M., Mahowald, N. M., Tilmes, S., and Kluzek, E.: A global dust emission dataset for estimating dust radiative forcings in climate models, Atmos. Chem. Phys., 25, 2311–2331, https://doi.org/10.5194/acp-25-2311-2025, 2025.

Lewis, A. C., Carpenter, L. J., and Pilling, M. J.: Nonmethane hydrocarbons in Southern Ocean boundary layer air, J. Geophy. Res.-Atmos., 106(D5), 4987–4994, https://doi.org/10.1029/2000JD900634, 2001.

Li, Y., Shi, W., Aydin, A., Beroya-Eitner, M. A., and Gao, G.: Loess genesis and worldwide distribution, Earth-Sci. Rev., 201, 102947, https://doi.org/10.1016/j.earscirev.2019.102947, 2020.

Li, J., Carlson, B. E., Yung, Y. L., Lv, D., Hansen, J., Penner, J. E., Liao, H., Ramaswamy, V., Kahn, R. A., Zhang, P., Dubovik, O., Ding, A., Lacis, A. A., Zhang, L., and Dong, Y.: Scattering and absorbing aerosols in the climate system, Nature Reviews Earth and Environment, 3, 363–379, https://doi.org/10.1038/s43017-022-00296-7, 2022.

Li, L. L., Mahowald, N. M., Kok, J. F., Liu, X. H., Wu, M. X., Leung, D. M., Hamilton, D. S., Emmons, L..K., Huang, Y., Sexton, N., Meng, J., Wan, J. S. C.: Importance of different parameterization changes for the updated dust cycle modeling in the Community Atmosphere Model (version 6.1), Geosci. Model Dev., 15, 8181-8219, https://doi.org/10.5194/gmd-15-8181-2022, 2022.

Li, F., Song, X., Harrison, S. P., Marlon, J. R., Lin, Z., Leung, L. R., Schwinger, J., Marécal, V., Wang, S., Ward, D. S., and Dong, X.: Evaluation of global fire simulations in CMIP6 Earth system models, Geosci. Model Dev., 17, 8751–8771, https://doi.org/10.5194/gmd-17-8751-2024, 2024.

Li, F., Lawrence, D. M., Rogers, B. M., Burton, C., Huang, H., Jiang, Y., Kaiser, J. W., Kasoar, M., Lee, H., Leung, R., Nieradzik, L., Wang, A., Ward, D. S., Ce, L., Li, Y., Lin, Z., Voulgarakis, A., and

Formatted: Default Paragraph Font, Font color: Black

Formatted: Normal, Centered, Border: Top: (No border), Bottom: (No border), Left: (No border), Right: (No border), Between : (No border), Tab stops: 3.25", Centered + 6.5", Right, Position: Horizontal: Left, Relative to: Column, Vertical: In line, Relative to: Margin, Wrap Around

Formatted: Font color: Black

Xue, Y.: The Fire Modeling Intercomparison Project (FireMIP) for CMIP7, Geosci. Model Dev., 19, 3989–4007, https://doi.org/10.5194/gmd-19-3989-2026, 2026.
Lin, G., Penner, J. E., Flanner, M. G., Sillman, S., Xu, L., and Zhou, C.: Radiative forcing of organic aerosol in the atmosphere and on snow: Effects of SOA and brown carbon, J. Geophys. Res.-Atmos., 119, 7453–7476. https://doi.org/10.1002/2013JD021186, 2014.
Lin, J., Svensson, A., Hvidberg, C. S., Lohmann, J., Kristiansen, S., Dahl-Jensen, D., Steffensen, J. P., Rasmussen, S. O., Cook, E., Kjær, H. A., Vinther, B. M., Fischer, H., Stocker, T., Sigl, M., Bigler, M., Severi, M., Traversi, R., and Mulvaney, R.: Magnitude, frequency and climate forcing of global volcanism during the last glacial period as seen in Greenland and Antarctic ice cores (60–9 ka), Clim. Past, 18, 485-506, https://doi.org/10.5194/cp-18-485-2022, 2022.
Lin, J., Abbott, P. M., Sigl, M., Steffensen, J. P., Mulvaney, R., Severi, M., and Svensson, A.: Bipolar ice-core records constrain possible dates and global radiative forcing following the ~74 ka Toba eruption, Quaternary Sci. Rev., 312, 108162, https://doi.org/10.1016/j.quascirev.2023.108162, 2023.
Liu, L., Zhang, X., Xu, W., Liu, X., Lu, X., Wei, J., Li, Y., Yang, Y., Wang, Z., and Wong, A. Y. H.: Reviewing global estimates of surface reactive nitrogen concentration and deposition using satellite retrievals, Atmos. Chem. Phys., 20, 8641–8658, https://doi.org/10.5194/acp-20-8641-2020, 2020.
Liu, P., Kaplan, J. O., Mickley, L. J., Li, Y., Chellman, N. J., Arienzo, M. M., Kodros, J. K., Pierce, J. R., Sigl, M., Freitag, J., Mulvaney, R., Curran, M. A. J., and McConnell, J. R.: Improved estimates of preindustrial biomass burning reduce the magnitude of aerosol climate forcing in the Southern Hemisphere, Science Advances, 7, eabc1379, https://doi.org/10.1126/sciadv.abc1379, 2021.
Lohmann, U, and Feichter, J.: Global indirect aerosol effects: a review, 5, 715–737, https://doi.org/10.5194/acp-5-715-2005, 2005.
Lorius, C., Jouzel, J., Raynaud, D., Hansen, J., and Treut, H. L.: The ice-core record: climate sensitivity and future greenhouse warming, Nature, 347, 139–145, https://doi.org/10.1038/347139a0, 1990.
Lu, Z., Liu, X., Zaveri, R. A., Easter, R. C., Tilmes, S., Emmons, L. K., Vitt, F., Singh, B., Wang, H., Zhang, R., and Rasch, P. J.: Radiative Forcing of Nitrate Aerosols From 1975 to 2010 as Simulated by MOSAIC Module in CESM2-MAM4, J. Geophys. Res.-Atmos., 126, https://doi.org/10.1029/2021JD034809, 2021.
Lund, M. T., Samset, B. H., Skeie, R. B., Watson-Parris, D., Katich, J. M., Schwarz, J. P., and Weinzierl, B.: Short Black Carbon lifetime inferred from a global set of aircraft observations, npj Climate and Atmospheric Science, 1, 31, https://doi.org/10.1038/s41612-018-0040-x, 2018.
Lunt, D. J., Haywood, A. M., Schmidt, G. A., Salzmann, U., Valdes, P. J., and Dowsett, H. J.: Earth system sensitivity inferred from Pliocene modelling and data, Nat. Geosci., 3, 60–64, https://doi.org/10.1038/ngeo706, 2010.
Luo, B.: Stratospheric aerosol data for use in CMIP6 models – data description. ftp://iacftp.ethz.ch/pubread/luo/CMIP6/ReadmeDataDescription.pdf (last accessed Feb, 17 2023), 2018.
Lücke, L. J., Schurer, A. P., Toohey, M., Marshall, L. R., and Hegerl, G. C.: The effect of uncertainties in natural forcing records on simulated temperature during the last millennium, Clim. Past, 19, 959-978, https://doi.org/10.5194/cp-19-959-2023, 2023.
Ma, W., Zhai, L., Pivovaroff, A., Shuman, J., Buotte, P., Ding, J., Christoffersen, B., Knox, R., Moritz, M., Fisher, R. A., Koven, C. D., Kueppers, L., and Xu, C.: Assessing climate change impacts on live fuel moisture and wildfire risk using a hydrodynamic vegetation model, Biogeosciences, 18, 4005–4020, https://doi.org/10.5194/bg-18-4005-2021, 2021.
Maher, B. A., Prospero, J. M., Mackie, D., Gaiero, D., Hesse, P. P., and Balkanski, Y.: Global connections between aeolian dust, climate and ocean biogeochemistry at the present day and at the last glacial maximum, Earth-Sci. Rev., 99, 61–97, https://doi.org/10.1016/j.earscirev.2009.12.001, 2010.

Formatted: Default Paragraph Font, Font color: Black

Formatted: Normal, Centered, Border: Top: (No border), Bottom: (No border), Left: (No border), Right: (No border), Between : (No border), Tab stops: 3.25", Centered + 6.5", Right, Position: Horizontal: Left, Relative to: Column, Vertical: In line, Relative to: Margin, Wrap Around

Formatted: Font color: Black

Mahowald, N. M., Kohfeld, K., Hansson, M., Balkanski, Y., Harrison, S. P., Prentice, I. C., Schulz, M., and Rodhe, H.: Dust sources and deposition during the last glacial maximum and current climate: A comparison of model results with paleodata from ice cores and marine sediments, J. Geophys. Res.-Atmos., 104, 15895–15916, https://doi.org/10.1029/1999JD900084, 1999.

Mahowald, N. M., Muhs, D. R., Levis, S., Rasch, P. J., Yoshioka, M., Zender, C. S., and Luo, C.: Change in atmospheric mineral aerosols in response to climate: Last glacial period, preindustrial, modern, and doubled carbon dioxide climates, J. Geophys. Res., 111, D10202, https://doi.org/10.1029/2005JD006653, https://doi.org/10.1029/2005JD006653, 2006.

Mahowald, N.: Aerosol indirect effect on biogeochemical cycles and climate, Science, 334, 794-796, https://doi.org/10.1126/science.1207374, 2011.

Mahowald, N. M., Albani, S., Engelstaedter, S., Winckler, G., and Goman, M.: Model insight into glacial–interglacial paleodust records, Quaternary Sci. Rev., 30, 832–854, https://doi.org/10.1016/j.quascirev.2010.09.007, 2011.

Mahowald, N. M., Kloster, S. Engelstaedter, S., Moore, J. K., Mukhopadhyay, S., McConnell, J. R., Albani, S., Doney, S. C., Bhattacharya, A., Curran, M. A. J., Flanner, M. G., Hoffman, F. M., Lawrence, D. M., Lindsay, K., Mayewski, P. A., Neff, J., Rothenberg, D., Thomas, E., Thornton, P. E., Zender, C. S.: Observed 20th century desert dust variability: impact on climate and biogeochemistry, Atmos. Chem. Phys., 10, 10875-10893, https://doi.org/10.5194/acp-10-10875-2010, 2010.

Mahowald, N., Ward, D. S., Kloster, S., Flanner, M. G., Heald, C. L., Heavens, N. G., Hess, P. G., Lamarque, J.-F., and Chuang, P. Y.: Aerosol impacts on climate and biogeochemistry, Annu. Rev. Env. Resour., 36, https://doi.org/10.1146/annurev-environ-042009-094507, 2011.

Mahowald, N. M., Albani, S., Kok, J. F., Engelstaeder, S., Scanza, R., Ward, D. S., and Flanner, M. G.: The size distribution of desert dust aerosols and its impact on the Earth system, Aeolian Res., 15, 53–71, https://doi.org/10.1016/j.aeolia.2013.09.002, 2014.

Mahowald, N. M., Scanza, R., Brahney, J., Goodale, C. L., Hess, P. G., Moore, J. K., and Neff, J.: Aerosol Deposition Impacts on Land and Ocean Carbon Cycles, Curr. Clim. Change Rep., 3, 16–31, https://doi.org/10.1007/s40641-017-0056-z, 2017.

Mahowald, N. M., Hamilton, D. S., Mackey, K. R. M., Moore, J. K., Baker, A. R., Scanza, R. A., and Zhang, Y.: Aerosol trace metal leaching and impacts on marine microorganisms, Nat. Commun., 9, 2614, https://doi.org/10.1038/s41467-018-04970-7, 2018.

Mahowald, N. M., Li, L., Albani, S., Hamilton, D. S., and Kok, J. F.: Opinion: The importance of historical and paleoclimate aerosol radiative effects, Atmos. Chem. Phys., 24, 533–551, https://doi.org/10.5194/acp-24-533-2024, 2024.

Mahowald, N. M., Li, L., Vira, J., Prank, M., Hamilton, D. S., Matsui, H., Miller, R. L., Lu, P. L., Akyuz, E., Meidan, D., Hess, P., Lihavainen, H., Wiedinmyer, C., Hand, J., Alaimo, M. G., Alves, C., Alastuey, A., Artaxo, P., Barreto, A., Barraza, F., Becagli, S., Calzolai, G., Chellam, S., Chen, Y., Chuang, P., Cohen, D. D., Colombi, C., Diapouli, E., Dongarra, G., Eleftheriadis, K., Engelbrecht, J., Galy-Lacaux, C., Gaston, C., Gomez, D., González Ramos, Y., Harrison, R. M., Heyes, C., Herut, B., Hopke, P., Hüglin, C., Kanakidou, M., Kertesz, Z., Klimont, Z., Kyllönen, K., Lambert, F., Liu, X., Losno, R., Lucarelli, F., Maenhaut, W., Marticorena, B., Martin, R. V., Mihalopoulos, N., Morera-Gómez, Y., Paytan, A., Prospero, J., Rodríguez, S., Smichowski, P., Varrica, D., Walsh, B., Weagle, C. L., and Zhao, X.: AERO-MAP: a data compilation and modeling approach to understand spatial variability in fine- and coarse-mode aerosol composition, Atmos. Chem. Phys., 25, 4665–4702, https://doi.org/10.5194/acp-25-4665-2025, 2025.

Mahrt, F., Marcolli, C., David, R. O., Grönquist, P., Barthazy Meier, E. J., Lohmann, U., and Kanji, Z. A.: Ice nucleation abilities of soot particles determined with the Horizontal Ice Nucleation Chamber, Atmos. Chem. Phys., 18, 13363-13392, https://doi.org/10.5194/acp-18-13363-2018, 2018.

Formatted: Default Paragraph Font, Font color: Black

Formatted: Normal, Centered, Border: Top: (No border), Bottom: (No border), Left: (No border), Right: (No border), Between : (No border), Tab stops: 3.25", Centered + 6.5", Right, Position: Horizontal: Left, Relative to: Column, Vertical: In line, Relative to: Margin, Wrap Around

Formatted: Font color: Black

Mahrt, F., Kilchhofer, K., Marcolli, C., Grönquist, P., David, R. O., Rösch, M., Lohmann, U., and Kanji, Z. A.: The Impact of Cloud Processing on the Ice Nucleation Abilities of Soot Particles at Cirrus Temperatures, J. Geophys. Res.-Atmos., 125, e2019JD030922, https://doi.org/10.1029/2019JD030922, 2020.

Malhi, Y., Doughty, C. E., Galetti, M., Smith, F. A., Svenning, J.-C., and Terborgh, J. W.: Megafauna and ecosystem function from the Pleistocene to the Anthropocene, P. Natl. Acad. Sci. USA, 113, 838-846, https://doi.org/10.1073/pnas.1502540113, 2016.

Mankin, J. S., Seager, R., Smerdon, J. E., Cook, B. I., & Williams, A. P. (2019). Mid-latitude freshwater availability reduced by projected vegetation responses to climate change. *Nature Geoscience*, *12*(12), 983–988. https://doi.org/10.1038/s41561-019-0480-x

Margolis, E. Q., Guiterman, C. H., Chavardès, R. D., Coop, J. D., Copes-Gerbitz, K., Dawe, D. A., Falk, D. A., Johnston, J. D., Larson, E., Li, H., Marschall, J. M., Naficy, C. E., Naito, A. T., Parisien, M.-A., Parks, S. A., Portier, J., Poulos, H. M., Robertson, K. M., Speer, J. H., Stambaugh, M., Swetnam, T. W., Tepley, A. J., Thapa, I., Allen, C. D., Bergeron, Y., Daniels, L. D., Fulé, P. Z., Gervais, D., Girardin, M. P., Harley, G. L., Harvey, J. E., Hoffman, K. M., Huffman, J. M., Hurteau, M. D., Johnson, L. B., Lafon, C. W., Lopez, M. K., Maxwell, R. S., Meunier, J., North, M., Rother, M. T., Schmidt, M. R., Sherriff, R. L., Stachowiak, L. A., Taylor, A., Taylor, E. J., Trouet, V., Villarreal, M. L., Yocom, L. L., Arabas, K. B., Arizpe, A. H., Arseneault, D., Tarancón, A. A., Baisan, C., Bigio, E., Biondi, F., Cahalan, G. D., Caprio, A., Cerano-Paredes, J., Collins, B. M., Dey, D. C., Drobyshev, I., Farris, C., Fenwick, M. A., Flatley, W., Floyd, M. L., Gedalof, Z. e., Holz, A., Howard, L. F., Huffman, D. W., Iniguez, J., Kipfmueller, K. F., Kitchen, S. G., Lombardo, K., McKenzie, D., Merschel, A. G., Metlen, K. L., Minor, J., O'Connor, C. D., Platt, L., Platt, W. J., Saladyga, T., Stan, A. B., Stephens, S., Sutheimer, C., Touchan, R., and Weisberg, P. J.: The North American tree-ring fire-scar network, Ecosphere, 13, e4159, https://doi.org/10.1002/ecs2.4159, 2022.

Margolis, E. Q., Wion, A., Abatzoglou, J., Daniels, L., Falk, D., Guiterman, C., Johnston, J., Kipfmueller, K., Lafon, C., Loehman, R., Lonergan, M., Naficy, C., Parisien, M., Parks, S., Portier, J., Stambaugh, M., Whitman, E., Williams, A. P., and Yocom, L.: Spatiotemporal Synchrony of Climate and Fire Occurrence Across North American Forests (1750–1880), Global Ecol. Biogeogr., 34, e13937, https://doi.org/10.1111/geb.13937, 2025.

Mariani, M., Connor, S. E., Theuerkauf, M., Herbert, A., Kuneš, P., Bowman, D., Fletcher, M.-S., Head, L., Kershaw, A. P., Haberle, S. G., Stevenson, J., Adeleye, M., Cadd, H., Hopf, F., and Briles, C.: Disruption of cultural burning promotes shrub encroachment and unprecedented wildfires, Front. Ecol. Environ., 20, 292-300, https://doi.org/10.1002/fee.2395, 2022.

Marlon, J. R., Bartlein, P. J., Carcaillet, C., Gavin, D. G., Harrison, S. P., Higuera, P. E., Joos, F., Power, M. J., and Prentice, I. C.: Climate and human influences on global biomass burning over the past two millennia, Nat. Geosci., 1, 697-702, https://doi.org/10.1038/ngeo313, 2008.

Marlon, J. R., Bartlein, P. J., Walsh, M. K., Harrison, S. P., Brown, K. J., Edwards, M. E., Higuera, P. E., Power, M. J., Anderson, R. S., Briles, C., and Brunelle, A.: Wildfire responses to abrupt climate change in North America, P. Natl. Acad. Sci. USA, 106, 2519-2524, https://doi.org/10.1073/pnas.0808212106, 2009.

Marlon, J. R., Kelly, R., Daniau, A. L., Vannière, B., Power, M. J., Bartlein, P., Higuera, P., Blarquez, O., Brewer, S., Brücher, T., Feurdean, A., Romera, G. G., Iglesias, V., Maezumi, S. Y., Magi, B., Courtney Mustaphi, C. J., and Zhihai, T.: Reconstructions of biomass burning from sediment-charcoal records to improve data–model comparisons, Biogeosciences, 13, 3225-3244, https://doi.org/10.5194/bg-13-3225-2016, 2016.

Marlon, J. R.: What the past can say about the present and future of fire, Quaternary Res., 96, 66–87, https://doi.org/10.1017/qua.2020.48, 2020.

Marshall, L., Johnson, J. S., Mann, G. W., Lee, L., Dhomse, S. S., Regayre, L., Yoshioka, M., Carslaw, K. S., and Schmidt, A.: Exploring How Eruption Source Parameters Affect Volcanic Radiative

Formatted: Default Paragraph Font, Font color: Black

Formatted: Normal, Centered, Border: Top: (No border), Bottom: (No border), Left: (No border), Right: (No border), Between : (No border), Tab stops: 3.25", Centered + 6.5", Right, Position: Horizontal: Left, Relative to: Column, Vertical: In line, Relative to: Margin, Wrap Around

Formatted: Font color: Black

Forcing Using Statistical Emulation, J. Geophys. Res.-Atmos., 124, 964-985, https://doi.org/10.1029/2018JD028675, 2019.
Marshall, L. R., Maters, E. C., Schmidt, A., Timmreck, C., Robock, A., and Toohey, M.: Volcanic effects on climate: recent advances and future avenues, B. Volcanol., 84, 54, https://doi.org/10.1007/s00445-022-01559-3, 2022.
Marshall, L. R., Smith, C. J., Forster, P. M., Aubry, T. J., Andrews, T., and Schmidt, A.: Large Variations in Volcanic Aerosol Forcing Efficiency Due to Eruption Source Parameters and Rapid Adjustments, Geophys. Res. Lett., 47, e2020GL090241, https://doi.org/10.1029/2020GL090241, 2020.
Marshall, L. R., Schmidt, A., Johnson, J. S., Mann, G. W., Lee, L. A., Rigby, R., and Carslaw, K. S.: Unknown Eruption Source Parameters Cause Large Uncertainty in Historical Volcanic Radiative Forcing Reconstructions, J. Geophys. Res.-Atmos., 126, e2020JD033578, https://doi.org/10.1029/2020JD033578, 2021.
Marshall, L. R., Schmidt, A., Schurer, A. P., Abraham, N. L., Lücke, L. J., Wilson, R., Anchukaitis, K. J., Hegerl, G. C., Johnson, B., Otto-Bliesner, B. L., Brady, E. C., Khodri, M., and Yoshida, K.: Last-millennium volcanic forcing and climate response using SO_2 emissions, Clim. Past, 21, 161-184, https://doi.org/10.5194/cp-21-161-2025, 2025.
Marticorena, B., and Bergametti, G.: Modeling the atmospheric dust cycle: 1. Design of a soil-derived dust emission scheme, J. Geophys. Res.-Atmos., 100, 16415–16430, https://doi.org/10.1029/95JD00690, 1995.
Martin, J. H.: Glacial-interglacial CO_2 change: The iron hypothesis, Paleoceanography, 5, 1-13, https://doi.org/10.1029/PA005i001p00001, 1990.
Martin, S. T., Hung, H. M., Park, R. J., Jacob, D. J., Spurr, R. J. D., Chance, K. V., and Chin, M.: Effects of the physical state of tropospheric ammonium-sulfate-nitrate particles on global aerosol direct radiative forcing, Atmos. Chem. Phys., 4, 183–214, https://doi.org/10.5194/acp-4-183-2004, 2004.
Maselli, O. J., Chellman, N. J., Grieman, M., Layman, L., McConnell, J. R., Pasteris, D., Rhodes, R. H., Saltzman, E., and Sigl, M.: Sea ice and pollution-modulated changes in Greenland ice core methanesulfonate and bromine, Clim. Past, 13, 39–59, https://doi.org/10.5194/cp-13-39-2017, 2017.
Mason, A. J., Vaks, A., Breitenbach, S. F. M., Hooker, J. N., and Henderson, G. M.: A simplified isotope dilution approach for the U–Pb dating of speleogenic and other low-^{232}Th carbonates by multi-collector ICP-MS, Geochronology, 4, 33–54. https://doi.org/10.5194/gchron-4-33-2022, 2022.
Matsui, H., Hamilton, D. S., and Mahowald, N. M.: Black carbon radiative effects highly sensitive to emitted particle size when resolving mixing-state diversity, Nat. Commun., 9, 3446, https://doi.org/10.1038/s41467-018-05635-1, 2018.
McBride, J. R. (1983). Analysis of tree rings and fire scars to establish fire history.
McConnell, J. R., Edwards, R., Kok, G. L., Flanner, M. G., Zender, C. S., Saltzman, E. S., Banta, J. R., Pasteris, D. R., Carter, M. M., and Kahl, J. D. W.: 20th-Century Industrial Black Carbon Emissions Altered Arctic Climate Forcing, Science, 317, 1381-1384, https://doi.org/10.1126/science.1144856, 2007a.
McConnell, J. R, Aristarain, A. J., Banta, J. R., Edwards, P. R., and Simoes, J. C.: 20th-Century doubling in dust archived in an Antarctic Peninsula ice core parallels climate change and desertification in South America, P. Natl. Acad. Sci. USA, 104, 5743-5748, https://doi.org/10.1073/pnas.0607657104, 2007b.
McConnell, J. R., Burke, A., Dunbar, N. W., Kohler, P., Thomas, J. L., Arienzo, M. M., Chellman, N. J., Maselli, O. J., Sigl, M., Adkins, J. F., Baggenstos, D., Burkhart, J. F., Brook, E. J., Buizert, C., Cole-Dai, J., Fudge, T. J., Knorr, G., Graf, H. F., Grieman, M. M., Iverson, N., McGwire, K. C., Mulvaney, R., Paris, G., Rhodes, R. H., Saltzman, E. S., Severinghaus, J. P., Steffensen, J. P., Taylor, K. C., and Winckler, G.: Synchronous volcanic eruptions and abrupt climate change

Formatted: Default Paragraph Font, Font color: Black

Formatted: Normal, Centered, Border: Top: (No border), Bottom: (No border), Left: (No border), Right: (No border), Between : (No border), Tab stops: 3.25", Centered + 6.5", Right, Position: Horizontal: Left, Relative to: Column, Vertical: In line, Relative to: Margin, Wrap Around

Formatted: Font color: Black

similar to 17.7 ka plausibly linked by stratospheric ozone depletion, P. Natl. Acad. Sci. USA, 114, 10035-10040, https://doi.org/10.1073/pnas.1705595114, 2017.
McConnell, J. R., Sigl, M., Plunkett, G., Burke, A., Kim, W. M., Raible, C. C., Wilson, A. I., Manning, J. G., Ludlow, F., Chellman, N. J., Innes, H. M., Yang, Z., Larsen, J. F., Schaefer, J. R., Kipfstuhl, S., Mojtabavi, S., Wilhelms, F., Opel, T., Meyer, H., and Steffensen, J. P.: Extreme climate after massive eruption of Alaska's Okmok volcano in 43 BCE and effects on the late Roman Republic and Ptolemaic Kingdom, P. Natl. Acad. Sci. USA, 117, 15443-15449, https://doi.org/10.1073/pnas.2002722117, 2020.
McConnell, J. R., Chellman, N. J., Mulvaney, R., Eckhardt, S., Stohl, A., Plunkett, G., Kipfstuhl, S., Freitag, J., Isaksson, E., Gleason, K. E., Brugger, S. O., McWethy, D. B., Abram, N. J., Liu, P., and Aristarain, A. J.: Hemispheric black carbon increase after the 13th-century Māori arrival in New Zealand, Nature, 598, 82–85, https://doi.org/10.1038/s41586-021-03858-9, 2021.
McConnell, J. R., Chellman, N. J., Wensman, S. M., Plach, A., Stanish, C., Santibáñez, P. A., Brugger, S. O., Eckhardt, S., Freitag, J., Kipfstuhl, S., and Stohl, A.: Hemispheric-scale heavy metal pollution from South American and Australian mining and metallurgy during the Common Era, Sci. Total Environ., 912, https://doi.org/10.1016/j.scitotenv.2023.169431, 2024.
McCormick, M. P., Thomason, L. W., and Trepte, C. R.: Atmospheric effects of the Mt Pinatubo eruption, Nature, 373, 399-404, https://doi.org/10.1038/373399a0, 1995.
McCormick, M., Dutton, P. E., and Mayewski, P. A.: Volcanoes and the climate forcing of Carolingian Europe, A.D. 750-950 (Harvard University), Speculum, 82, 865-895, 2007.
McDonough, L. K., Treble, P. C., Baker, A., Borsato, A., Frisia, S., Nagra, G., Coleborn, K., Gagan, M. K., Zhao, J., and Paterson, D.: Past fires and post-fire impacts reconstructed from a southwest Australian stalagmite, Geochim. Cosmochim. Ac., 325, 258–277, https://doi.org/10.1016/j.gca.2022.03.020, 2022.
McGee, D., Broecker, W. S., and Winckler, G.: Gustiness: the driver of glacial dustiness?, Quaternary Sci. Rev., 29, 2340-2350, https://doi.org/10.1016/j.quascirev.2010.06.009, 2010.
McGee, D., and Mukhopadhyay, S.: Extraterrestrial He in sediments: From recorder of asteroid collisions to timekeeper of global environmental changes, In The noble gases as geochemical tracers (pp. 155-176). Berlin, Heidelberg: Springer Berlin Heidelberg, 2013.
McGee, D., Winckler, G., Borunda, A., Serno, S., Anderson, R. F., Recasens, C., Bory, A., Gaiero, D., Jaccard, S. L., Kaplan, M., McManus, J. F., Revel, M., and Sun, Y.: Tracking eolian dust with helium and thorium: Impacts of grain size and provenance, Geochim. Cosmochim. Ac., 175, 47–67, https://doi.org/10.1016/j.gca.2015.11.023, 2016.
McGraw, Z., Storelvmo, T., David, R. O., and Sagoo, N.: Global radiative impacts of mineral dust perturbations through stratiform clouds, J. Geophys. Res.-Atmos., 125, e2019JD031807, https://doi.org/10.1029/2019JD031807, 2020.
McGraw, Z., Storelvmo, T., Samset, B. H., and Stjern, C. W.: Global Radiative Impacts of Black Carbon Acting as Ice Nucleating Particles, Geophys. Res. Lett., 47, e2020GL089056, https://doi.org/10.1029/2020GL089056, 2020.
McGraw, Z., Dallasanta, K., Polvani, L. M., Tsigaridis, K., Orbe, C., and Bauer, S. E.: Severe Global Cooling After Volcanic Super-Eruptions? The Answer Hinges on Unknown Aerosol Size, J. Climate, 37, 1449-1464, https://doi.org/10.1175/JCLI-D-23-0116.1, 2024.
McGraw, Z., and Polvani, L. M.: Direct radiative impacts of stratospheric aerosols on the tropical troposphere: clouds, precipitation, and circulation in convection-resolving and global simulations. J. Climate, e250688, https://doi.org/10.1175/JCLI-D-25-0688.1, 2026.
Mehta, S., Ortiz-Suslow, D. G., Smith, A. W., and Haus, B. K.: A Laboratory Investigation of Spume Generation in High Winds for Fresh and Seawater, J. Geophys. Res.-Atmos., 124, 11297–11312, https://doi.org/10.1029/2019JD030928, 2019.
Meijer, N., and van der Meulen, B.: Loss of loess in the geological record due to poor preservation, Terra Nova, 35, 185-192, https://doi.org/10.1111/ter.12642, 2023.

Moved (insertion) [1]
Deleted: and
Deleted: .: How
Deleted: Aerosols Globally Inhibit Precipitation, Geophys. Res. Lett., 51, e2023GL107930
Deleted: 1029/2023GL107930
Moved up [1]: Dallasanta, K.,
Deleted: ., Tsigaridis, K., Orbe, C., and Bauer, S. E.: Severe Global Cooling After Volcanic Super-Eruptions? The Answer Hinges
Deleted: Unknown Aerosol Size,
Formatted: Indent: First line: 0"
Deleted: 37, 1449-1464
Deleted: 23-0116
Deleted: 2024
Formatted: Default Paragraph Font, Font color: Black
Formatted: Normal, Centered, Border: Top: (No border), Bottom: (No border), Left: (No border), Right: (No border), Between : (No border), Tab stops: 3.25", Centered + 6.5", Right, Position: Horizontal: Left, Relative to: Column, Vertical: In line, Relative to: Margin, Wrap Around
Formatted: Font color: Black

Meng, J., Huang, Y., Leung, D. M., Li, L., Adebiyi, A. A., Ryder, C. L., Mahowald, N. M., and Kok, J. F.: Improved parameterization for the size distribution of emitted dust aerosols reduces model underestimation of super coarse dust, Geophys. Res. Lett., 49, e2021GL097287, https://doi.org/10.1029/2021GL097287, 2022.

Meng, X., Yu, Y., and Ginoux, P.: Rise in dust emissions from burned landscapes primarily driven by small fires. Nat. Geosci., 18(7), 586–592, https://doi.org/10.1038/s41561-025-01730-3, 2025.

Miller, R. L., Cakmur, R. V., Perlwitz, J. P., Geogdzhayev, I. V., Ginoux, P., Kohfeld, K. E., Koch, D., Prigent, C., Ruedy, R., Schmidt, G. A., and Tegen, I.: Mineral dust aerosols in the NASA Goddard Institute for Space Sciences ModelE atmospheric general circulation model, J. Geophys. Res.-Atmos., 111, D06208, doi:10.1029/2005JD005796, 2006.

Miller, R. L., Knippertz, P., Pérez García-Pando, C., Perlwitz, J. P., and Tegen, I.: Impact of Dust Radiative Forcing upon Climate, In: Knippertz, P, Stuut, JB. (eds) Mineral Dust. Springer, Dordrecht. https://doi.org/10.1007/978-94-017-8978-313, 2014.

Mishra, P. K.: Lake Sediments and Climate Studies, In: The Application of Lake Sediments for Climate Studies. SpringerBriefs in Environmental Science, 2023.

Molina Catricheo, C. A., Lambert, F., Salomon, J., and Van 'T Wout, E.: Modeling global surface dust deposition using physics-informed neural networks, Commun. Earth Environ., 5, 778, https://doi.org/10.1038/s43247-024-01942-2, 2024.

Moore, J. C., Beaudon, E., Kang, S., Divine, D., Isaksson, E., Pohjola, V. A., and van de Wal, R. S.: Statistical extraction of volcanic sulphate from nonpolar ice cores, J. Geophys. Res.-Atmos., 117, D03306, ttps://doi.org/10.1029/2011JD016592, 2012

Moschos, V., Dzepina, K., Bhattu, D., Lamkaddam, H., Casotto, R., Daellenbach, K. R., Canonaco, F., Rai, P., Aas, W., Becagli, S., Calzolai, G., Eleftheriadis, K., Moffett, C. E., Schnelle-Kreis, J., Severi, M., Sharma, S., Skov, H., Vestenius, M., Zhang, W., Hakola, H., Hellén, H., Huang, L., Jaffrezo, J. L., Massling, A., Nøjgaard, J. K., Petäjä, T., Popovicheva, O., Sheesley, R. J., Traversi, R., Yttri, K. E., Schmale, J., Prévôt, A. S. H., Baltensperger, U., and El Haddad, I.: Equal abundance of summertime natural and wintertime anthropogenic Arctic organic aerosols, Nat. Geosci., 15, 196–202, https://doi.org/10.1038/s41561-021-00891-1, 2022.

Muhs, D. R., Ager, T. A., Been, J., Bradbury, J. P., and Dean, W. E.: A late Quaternary record of eolian silt deposition in a maar lake, St. Michael Island, western Alaska, Quaternary Res., 60, 110–122, https://doi.org/10.1016/S0033-5894(03)00062-0, 2003.

Muhs, D. R., Cattle, S. R., Crouvi, O., Rousseau, D. D., Sun, J., Zárate, M. A.: Loess Records, In: Knippertz, P, Stuut, JB. (eds) Mineral Dust. Springer, Dordrecht. https://doi.org/10.1007/978-94-017-8978-316, 2014.

Mukhopadhyay, S., and Kreycik, P.: Dust generation and drought patterns in Africa from helium-4 in a modern Cape Verde coral, Geophys. Res. Lett., 35, https://doi.org/10.1029/2008GL035722, 2008.

Mulitza, S., Heslop, D., Pittauerova, D., Fischer, H. W., Meyer, I., Stuut, J. B., Zabel, M., Mollenhauer, G., Collins, J. A., Kuhnert, H., Schulz, M.: Increase in African dust flux at the onset of commercial agriculture in the Sahel region, Nature, 466, 226-228, https://doi.org/10.1038/nature09213, 2010.

Murphy, J. M., Sexton, D. M. H., Barnett, D. N., Jones, G. S., Webb, M. J., Collins, M., and Stainforth, D. A.: Quantification of modelling uncertainties in a large ensemble of climate change simulations, Nature, 430, 768–772, https://doi.org/10.1038/nature02771, 2004.

Muscheler, R., Adolphi, F., Heaton, T. J., Bronk Ramsey, C., Svensson, A., van der Plicht, J., and Reimer, P. J.: Testing and Improving the IntCal20 Calibration Curve with Independent Records, Radiocarbon, 62, 1079-1094, https://doi.org/10.1017/RDC.2020.54, 2020.

Nault, B. A., Jo, D. S., McDonald, B. C., Campuzano-Jost, P., Day, D. A., Hu, W., Schroder, J. C., Allan, J., Blake, D. R., Canagaratna, M. R., Coe, H., Coggon, M. M., DeCarlo, P. F., Diskin, G. S., Dunmore, R., Flocke, F., Fried, A., Gilman, J. B., Gkatzelis, G., and Jimenez, J. L.: Secondary organic aerosols from anthropogenic volatile organic compounds contribute substantially to air

Formatted: Default Paragraph Font, Font color: Black

Formatted: Normal, Centered, Border: Top: (No border), Bottom: (No border), Left: (No border), Right: (No border), Between : (No border), Tab stops: 3.25", Centered + 6.5", Right, Position: Horizontal: Left, Relative to: Column, Vertical: In line, Relative to: Margin, Wrap Around

Formatted: Font color: Black

pollution mortality, Atmos. Chem. Phys., 21, 11201–11224, https://doi.org/10.5194/acp-21-11201-2021, 2021.
Nenes, A., Murray, B., and Bougiatioti, A.: Mineral Dust and its Microphysical Interactions with Clouds, In: Knippertz, P, Stuut, JB. (eds) Mineral Dust. Springer, Dordrecht. https://doi.org/10.1007/978-94-017-8978-312, 2014.
Nenes, A., Krom, M., Mihalopoulos, N., VanCapellen, P., Shi, Z., Bougiatioti, A., Zarmpas, P., & Herut, B. (2011). Atmospheric acidification of mineral aerosols: a source of bioavailable phosphorus to the oceans. *Atmospheric Chemistry and Physics*, *11*, 2011–6265. https://doi.org/https://doi.org/10.5194/acp-11-6265-2011
Newhall, C. G., and Self, S.: The volcanic explosivity index (VEI) an estimate of explosive magnitude for historical volcanism, J. Geophys. Res.-Oceans, 87, 1231-1238, https://doi.org/10.1029/JC087iC02p01231, 1982.
Newhall, C., Self, S., and Robock, A.: Anticipating future Volcanic Explosivity Index (VEI) 7 eruptions and their chilling impacts, Geosphere, 14, 572-603, https://doi.org/10.1130/GES01513.1, 2018.
Nicewonger, M. R., Aydin, M., Prather, M. J., and Saltzman, E. S.: Extracting a History of Global Fire Emissions for the Past Millennium From Ice Core Records of Acetylene, Ethane, and Methane, J. Geophys. Res.-Atmos., 125, e2020JD032932, https://doi.org/10.1029/2020JD032932, 2020a.
Nicewonger, M. R., Aydin, M., Prather, M. J., and Saltzman, E. S.: Reconstruction of Paleofire Emissions Over the Past Millennium From Measurements of Ice Core Acetylene, Geophys. Res. Lett., 47, e2019GL085101, https://doi.org/10.1029/2019GL085101, 2020b.
Nicewonger, M. R., Aydin, M., Prather, M. J., and Saltzman, E. S.: Large changes in biomass burning over the last millennium inferred from paleoatmospheric ethane in polar ice cores, P. Natl. Acad. Sci. USA, 115, 12413-12418, https://doi.org/10.1073/pnas.1807172115, 2018.
Niklasson, M., and Granström, A.: Numbers and sizes of fires: Long-term spatially explicit fire history in a Swedish boreal landscape, Ecology, 81, 1484–1499, https://doi.org/10.1890/0012-9658(2000)081%255B1484:NASOFL%255D2.0.CO;2, 2000.
North Greenland Ice Core project members: High-resolution record of Northern Hemisphere climate extending into the last interglacial period, Nature, 431(7005), 147–151, https://doi.org/10.1038/nature02805, 2004.
Nugent, J. M., Brown, H., Kirby, A., McCoy, D. T., Allen, G., Aerenson, T., Burrows, S. M., Caulton, D., Fan, J., Feng, Y., Gettelman, A., Griswold, J., Jones, D. B., Leung, L. R., Mahfouz, N., Mikkelsen, A., Mülmenstädt, J., Qian, Y., Shan, Y., Shpund, J., Silber, I., Song, C., Song, X., Wang, H., Wu, M., Xie, S., Zelinka, M. D., Zhang, D., Zhang, G. J., and Zhang, K.: Overview of the Nephele Perturbed Parameter Ensemble for Aerosol-Cloud Interactions in E3SMv3, J. Adv. Model. Earth Sy., 18, e2025MS004989, https://doi.org/10.1029/2025MS004989, 2026.
Obiso, V., Gonçalves Ageitos, M., Pérez García-Pando, C., Schuster, G. L., Bauer, S. E., Di Biagio, C., Formenti, P., Perlwitz, J. P., Tsigaridis, K., and Miller, R. L.: Observationally constrained regional variations of shortwave absorption by iron oxides emphasize the cooling effect of dust, Atmos. Chem. Phys., 24, 5337-5367, https://doi.org/10.5194/acp-24-5337-2024, 2024.
Obiso, V., Huang, Y., Gonçalves Ageitos, M., Pérez García-Pando, C., Perlwitz, J. P., and Miller, R. L.: Do we really know by how much ellipsoidal shapes enhance the extinction of solar radiation by dust?, J. Geophys. Res.-Atmos., 131, e2025JD044032, https://doi.org/10.1029/2025JD044032, 2026.
Ohgaito, R., Abe-Ouchi, A., O'ishi, R., Takemura, T., Ito, A., Hajima, T., Watanabe, S., and Kawamiya, M.: Effect of high dust amount on surface temperature during the Last Glacial Maximum: a modelling study using MIROC-ESM, Clim. Past, 14, 1565–1581, https://doi.org/10.5194/cp-14-1565-2018, 2018.
Okazaki, A., Carrió, D. S., Dalaiden, Q., Harrison-Lofthouse, J., Kotsuki, S., and Yoshimura, K.: Observation error estimation in climate proxies with data assimilation and innovation statistics, Clim. Past, 21, 1801–1819, https://doi.org/10.5194/cp-21-1801-2025, 2025.

Formatted: Default Paragraph Font, Font color: Black

Formatted: Normal, Centered, Border: Top: (No border), Bottom: (No border), Left: (No border), Right: (No border), Between : (No border), Tab stops: 3.25", Centered + 6.5", Right, Position: Horizontal: Left, Relative to: Column, Vertical: In line, Relative to: Margin, Wrap Around

Formatted: Font color: Black

Okin, G. S.: Where and How Often Does Rain Prevent Dust Emission?, Geophys. Res. Lett., 49, e2021GL095501, https://doi.org/10.1029/2021GL095501, 2022.
Opazo, N., Cosentino, N. J., Ridgwell, A., and Lambert, F.: Sensitivity of Atmospheric Carbon Dioxide to Dust Iron Solubility During the Last Glacial-Interglacial Cycle, Paleoceanography, 40, e2025PA005132, https://doi.org/10.1029/2025PA005132, 2025.
Oppenheimer, C., Wacker, L., Xu, J., Galvan, J. D., Stoffel, M., Guillet, S., Corona, C., Sigl, M., Di Cosmo, N., Hajdas, I., Pan, B., Breuker, R., Schneider, L., Esper, J., Fei, J., Hammond, J. O. S., and Büntgen, U.: Multi-proxy dating the 'Millennium Eruption' of Changbaishan to late 946 CE, Quaternary Sci. Rev., 158, 164-171, https://doi.org/10.1016/j.quascirev.2016.12.024, 2017.
Osipov, S., Stenchikov, G., Tsigaridis, K., LeGrande, A. N., and Bauer, S. E.: The Role of the SO Radiative Effect in Sustaining the Volcanic Winter and Soothing the Toba Impact on Climate, J. Geophys. Res.-Atmos., 125, e2019JD031726, https://doi.org/10.1029/2019JD031726, 2020.
Ottmar, R.D., 2014. Wildland fire emissions, carbon, and climate: Modeling fuel consumption. Forest Ecology and Management, 317, pp.41-50.
Otto-Bliesner, B. L., Braconnot, P., Harrison, S. P., Lunt, D. J., Abe-Ouchi, A., Albani, S., Bartlein, P. J., Capron, E., Carlson, A. E., Dutton, A., Fischer, H., Goelzer, H., Govin, A., Haywood, A., Joos, F., LeGrande, A. N., Lipscomb, W. H., Lohmann, G., Mahowald, N., Nehrbass-Ahles, C., Pausata, F. S. R., Peterschmitt, J.-Y., Phipps, S. J., Renssen, H., and Zhang, Q.: The PMIP4 contribution to CMIP6 – Part 2: Two interglacials, scientific objective and experimental design for Holocene and Last Interglacial simulations, Geosci. Model Dev., 10, 3979–4003, https://doi.org/10.5194/gmd-10-3979-2017, 2017.
PAGES 2k Consortium: A global multiproxy database for temperature reconstructions of the Common Era, Scientific Data, 4, https://doi.org/10.1038/sdata.2017.88, 2017.
PALAEOSENS Project Members: Making sense of palaeoclimate sensitivity, Nature, 491, 683–691, https://doi.org/10.1038/nature11574, 2012.
Panta, A., Kandler, K., Schepanski, K., Alastuey, A., Dagsson Waldhauserova, P., Dupont, S., Eknayan, M., González-Flórez, C., González-Romero, A., Klose, M., Montag, M., Querol, X., Yus-Díez, J., and Pérez García-Pando, C.: Unveiling single-particle composition, size, shape, and mixing state of freshly emitted Icelandic dust via electron microscopy analysis, Atmos. Chem. Phys., 25, 10457–10478, https://doi.org/10.5194/acp-25-10457-2025, 2025.
Parish, T. R., and Bromwich, D. H.: Reexamination of the Near-Surface Airflow over the Antarctic Continent and Implications on Atmospheric Circulations at High Southern Latitudes, Mon. Weather Rev., 135, 1961-1973, https://doi.org/10.1175/MWR3374.1, 2007.
Parish, T. R., and Waight, K. T.: The Forcing of Antarctic Katabatic Winds, Mon. Weather Rev., 115, 2214-2226, https://doi.org/10.1175/1520-0493(1987)1152.0.CO;2, 1987.
Park, J., and Kim, H. M.: Design and evaluation of CO_2 observation network to optimize surface CO_2 fluxes in Asia using observation system simulation experiments, Atmos. Chem. Phys., 20, 5175-5195, https://doi.org/10.5194/acp-20-5175-2020, 2020.
Parks, S. A., Guiterman, C. H., Margolis, E. Q., Lonergan, M., Whitman, E., Abatzoglou, J. T., Falk, D. A., Johnston, J. D., Daniels, L. D., Lafon, C. W., Loehman, R. A., Kipfmueller, K. F., Naficy, C. E., Parisien, M.-A., Portier, J., Stambaugh, M. C., Williams, A. P., Wion, A. P., and Yocom, L. L.: A fire deficit persists across diverse North American forests despite recent increases in area burned, Nat. Commun., 16, 1493, https://doi.org/10.1038/s41467-025-56333-8, 2025.
Patterson, D. B, Farley, K. A, and Norman, M. D: ^{4}He as a tracer of continental dust: A 1.9 million year record of aeolian flux to the west equatorial Pacific Ocean, Geochim. Cosmochim. Ac., 63, 615-625, https://doi.org/10.1016/S0016-7037(99)00077-0, 1999.
Pavia, F. J., Abell, J. T., Middleton, J. L., Leal, A., Vivancos, S. M., Fleisher, M. Q., and Anderson, R. F.: Discrepant mass accumulation rates of sediments in the South Pacific Ocean from ^{230}Th and ^{3}He measurements, Geochim. Cosmochim. Ac., 365, 215-228, https://doi.org/10.1016/j.gca.2023.11.019, 2024.

Formatted: Default Paragraph Font, Font color: Black

Formatted: Normal, Centered, Border: Top: (No border), Bottom: (No border), Left: (No border), Right: (No border), Between : (No border), Tab stops: 3.25", Centered + 6.5", Right, Position: Horizontal: Left, Relative to: Column, Vertical: In line, Relative to: Margin, Wrap Around

Formatted: Font color: Black

Pearson, C., Sigl, M., Burke, A., Davies, S., Kurbatov, A., Severi, M., Cole-Dai, J., Innes, H., Albert, P. G., and Helmick, M.: Geochemical ice-core constraints on the timing and climatic impact of Aniakchak II (1628 BCE) and Thera (Minoan) volcanic eruptions, PNAS Nexus, https://doi.org/10.1093/pnasnexus/pgac048, 2022.
Peltier, W. R., and Fairbanks, R. G.: Global glacial ice volume and Last Glacial Maximum duration from an extended Barbados sea level record, Quaternary Sci. Rev., 25, 3322-3337, https://doi.org/10.1016/j.quascirev.2006.04.010, 2006.
Peng, W., Zhang, H., Pullen, A., Li, M., Pan, B., Xiao, W., and Nie, J.: Stepwise increased spatial provenance contrast on the Chinese Loess Plateau over late Miocene–Pleistocene, Commun. Earth Environ., 4, 1–12, https://doi.org/10.1038/s43247-023-00721-9, 2023.
Perlwitz, J. P., Pérez García-Pando, C., and Miller, R. L.: Predicting the mineral composition of dust aerosols–Part 1: Representing key processes, Atmos. Chem. Phys., 15, 11593–11627, https://doi.org/10.5194/acp-15-11593-2015, 2015.
Pfeiffer, M., Spessa, A., and Kaplan, J. O.: A model for global biomass burning in preindustrial time: LPJ-LMfire (v1.0), Geosci. Model Dev., 6, 643-685, https://doi.org/10.5194/gmd-6-643-2013, 2013.
Pinto, J. P., Turco, R. P., and Toon, O. B.: Self-Limiting Physical and Chemical Effects in Volcanic-Eruption Clouds, J. Geophys. Res.-Atmos., 94, 11165-11174, https://doi.org/10.1029/JD094iD08p11165, 1989.
Piva, S. B., Barker, S. J., Iverson, N. A., Winton, V. H. L., Bertler, N. A. N., Sigl, M., Wilson, C. J. N., Dunbar, N. W., Kurbatov, A. V., Carter, L., Charlier, B. L. A., and Newnham, R. M.: Volcanic glass from the 1.8 ka Taupo eruption (New Zealand) detected in Antarctic ice at ~ 230 CE, Sci. Rep.-UK, 13, 16720, https://doi.org/10.1038/s41598-023-42602-3, 2023.
Plunkett, G., Sigl, M., Schwaiger, H. F., Tomlinson, E. L., Toohey, M., McConnell, J. R., Pilcher, J. R., Hasegawa, T., and Siebe, C.: No evidence for tephra in Greenland from the historic eruption of Vesuvius in 79 CE: implications for geochronology and paleoclimatology, Clim. Past, 18, 45-65, https://doi.org/10.5194/cp-18-45-2022, 2022.
Plunkett, G., Sigl, M., McConnell, J. R., Pilcher, J. R., and Chellman, N. J.: The significance of volcanic ash in Greenland ice cores during the Common Era, Quaternary Sci. Rev., 301, 107936, https://doi.org/10.1016/j.quascirev.2022.107936, 2023.
Potenza, M. A. C., Albani, S., Delmonte, B., Villa, S., Sanvito, T., Paroli, B., Pullia, A., Baccolo, G., Mahowald, N., and Maggi, V.: Shape and size constraints on dust optical properties from the Dome C ice core, Antarctica, Sci. Rep.-UK, 6, https://doi.org/10.1038/srep28162, 2016.
Potenza, M. A. C., Cremonesi, L., Becagli, S., Delmonte, B., Del Guasta, M., Ciardini, V., Scarchilli, C., Paroli, B., Passerini, A., Pullia, A., Traversi, R., and Maggi, V.: Monitoring optical properties of atmospheric aerosols at dome C, East Antarctic Plateau, provides insights into radiative transfer estimates, Sci. Rep.-UK, 15, 39793, https://doi.org/10.1038/s41598-025-23538-2, 2025.
Povak, N. A., Hessburg, P. F., and Salter, R. B.: Evidence for scale-dependent topographic controls on wildfire spread, Ecosphere, 9, e02443, https://doi.org/10.1002/ecs2.2443, 2018.
Power, M. J., Marlon, J., Ortiz, N., Bartlein, P. J., Harrison, S. P., Mayle, F. E., Ballouche, A., Bradshaw, R. H. W., Carcaillet, C., Cordova, C., Mooney, S., Moreno, P. I., Prentice, I. C., Thonicke, K., Tinner, W., Whitlock, C., Zhang, Y., Zhao, Y., Ali, A. A., Anderson, R. S., Beer, R., Behling, H., Briles, C., Brown, K. J., Brunelle, A., Bush, M., Camill, P., Chu, G. Q., Clark, J., Colombaroli, D., Connor, S., Daniau, A.-L., Daniels, M., Dodson, J., Doughty, E., Edwards, M. E., Finsinger, W., Foster, D., Frechette, J., Gaillard, M.-J., Gavin, D. G., Gobet, E., Haberle, S., Hallett, D. J., Higuera, P., Hope, G., Horn, S., Inoue, J., Kaltenrieder, P., Kennedy, L., Kong, Z. C., Larsen, C., Long, C. J., Lynch, J., Lynch, E. A., McGlone, M., Meeks, S., Mensing, S., Meyer, G., Minckley, T., Mohr, J., Nelson, D. M., New, J., Newnham, R., Noti, R., Oswald, W., Pierce, J., Richard, P. J. H., Rowe, C., Sanchez Goñi, M. F., Shuman, B. N., Takahara, H., Toney, J., Turney, C., Urrego-Sanchez, D. H., Umbanhowar, C., Vandergoes, M., Vanniere, B., Vescovi, E., Walsh, M., Wang, X., Williams, N., Wilmshurst, J., and Zhang, J. H.: Changes in fire regimes since the Last

Formatted: Default Paragraph Font, Font color: Black

Formatted: Normal, Centered, Border: Top: (No border), Bottom: (No border), Left: (No border), Right: (No border), Between : (No border), Tab stops: 3.25", Centered + 6.5", Right, Position: Horizontal: Left, Relative to: Column, Vertical: In line, Relative to: Margin, Wrap Around

Formatted: Font color: Black

Glacial Maximum: an assessment based on a global synthesis and analysis of charcoal data, Clim. Dynam., 30, 887–907, https://doi.org/10.1007/s00382-007-0334-x, 2008.
Prather, K. A., Bertram, T. H., Grassian, V. H., Deane, G. B., Stokes, M. D., DeMott, P. J., Aluwihare, L. I., Palenik, B. P., Azam, F., Seinfeld, J. H., Moffet, R. C., Molina, M. J., Cappa, C. D., Geiger, F. M., Roberts, G. C., Russell, L. M., Ault, A. P., Baltrusaitis, J., Collins, D. B., and Zhao, D.: Bringing the ocean into the laboratory to probe the chemical complexity of sea spray aerosol, P. Natl. Acad. Sci. USA, 110, 7550–7555, https://doi.org/10.1073/pnas.1300262110, 2013.
Preunkert, S., Wagenbach, D., and Legrand, M.: A seasonally resolved alpine ice core record of nitrate: Comparison with anthropogenic inventories and estimation of preindustrial emissions of NO in Europe, J. Geophys. Res.-Atmos., 108, https://doi.org/10.1029/2003jd003475, 2003.
Price, C., and Rind, D.: Possible implications of global climate change on global lightning distributions and frequencies, J. Geophys. Res.-Atmos., 99, 10823-10831, https://doi.org/10.1029/94JD00019, 1994.
Price, C.: Thunderstorms, Lightning and Climate Change, in: Lightning: Principles, Instruments and Applications: Review of Modern Lightning Research, edited by: Betz, H. D., Schumann, U., and Laroche, P., Springer Netherlands, Dordrecht, 521-535, https://doi.org/10.1007/978-1-4020-9079-024, 2009.
Prospero, J. M., Ginoux, P., Torres, O., Nicholson, S. E., and Gill, T. E.: Environmental characterization of global sources of atmospheric soil dust identified with the nimbus 7 total ozone mapping spectrometer (TOMS) absorbing aerosol product, Rev. Geophys., 40, 1002, https://doi.org/10.1029/2000RG000095, 2002.
Pyle, D. M.: Chapter, 13 - Sizes of Volcanic Eruptions. In: The Encyclopedia of Volcanoes (Second Edition), Sigurdsson, H. (Ed.), Academic Press, Amsterdam, 2015.
Pérez-Invernón, F. J., Gordillo-Vázquez, F. J., Huntrieser, H., and Jöckel, P.: Variation of lightning-ignited wildfire patterns under climate change, Nat. Commun., 14, 739, https://doi.org/10.1038/s41467-023-36500-5, 2023.
Quaas, J., Arola, A., Cairns, B., Christensen, M., Deneke, H., Ekman, A. M. L., Feingold, G., Fridlind, A., Gryspeerdt, E., Hasekamp, O., Li, Z., Lipponen, A., Mülmenstädt, J., Nenes, A., Penner, J. E., Rosenfeld, D., Schrödner, R., Sinclair, K., Sourdeval, O., Stier, P., Tesche, M., van Diedenhoven, B., and Wendisch, M.: Constraining the Twomey effect from satellite observations: Issues and perspectives, Atmos. Chem. Phys., 20(23), 15079–15099, https://doi.org/10.5194/acp-20-15079-2020, 2020.
Quaglia, I., Timmreck, C., Niemeier, U., Visioni, D., Pitari, G., Brodowsky, C., Brühl, C., Dhomse, S. S., Franke, H., Laakso, A., Mann, G. W., Rozanov, E., and Sukhodolov, T.: Interactive stratospheric aerosol models' response to different amounts and altitudes of SO_2 injection during the 1991 Pinatubo eruption, Atmos. Chem. Phys., 23, 921–948, https://doi.org/10.5194/acp-23-921-2023, 2023.
Quinn, P. K., Bates, T. S., Coffman, D. J., Johnson, J. E., and Upchurch, L. M.: Climate Roles of Non-Sea Salt Sulfate and Sea Spray Aerosol in the Atmospheric Marine Boundary Layer: Highlights of 40 Years of PMEL Research, Oceanography, 36, 168-174, , 2023.
Rampino, M. R., Self, S., and Stothers, R. B.: Volcanic Winters, Annu. Rev. Earth. Pl. Sc., 16, 73-99, 1988.
Rap, A., Scott, C. E., Spracklen, D. V., Bellouin, N., Forster, P. M., Carslaw, K. S., Schmidt, A., and Mann, G.: Natural aerosol direct and indirect radiative effects, Geophys. Res. Lett., 40, 3297–3301, https://doi.org/10.1002/grl.50441, 2013.
Rasch, P. J., Xie, S., Ma, P. L., Lin, W., Wang, H., Tang, Q., Burrows, S. M., Caldwell, P., Zhang, K., Easter, R. C., Cameron-Smith, P., Singh, B., Wan, H., Golaz, J. C., Harrop, B. E., Roesler, E., Bacmeister, J., Larson, V. E., Evans, K. J., Qian, Y., Taylor, M., Leung, L. R., Zhang, Y., Brent, L., Branstetter, M., Hannay, C., Mahajan, S., Mametjanov, A., Neale, R., Richter, J. H., Yoon, J.-H., Zender, C. S., Bader, D., Flanner, M., Foucar, J. G., Jacob, R., Keen, N., Klein, S. A., Liu, X., Salinger, A. G., Shrivastava, M., and Yang, Y.: An Overview of the Atmospheric Component of

Formatted: Default Paragraph Font, Font color: Black

Formatted: Normal, Centered, Border: Top: (No border), Bottom: (No border), Left: (No border), Right: (No border), Between : (No border), Tab stops: 3.25", Centered + 6.5", Right, Position: Horizontal: Left, Relative to: Column, Vertical: In line, Relative to: Margin, Wrap Around

Formatted: Font color: Black

the Energy Exascale Earth System Model. J. Adv. Model. Earth Sy., 11(8), 2377–2411, https://doi.org/10.1029/2019MS001629, 2019.
Rea, D. K., and Janecek, T. R.: Late cretaceous history of eolian deposition in the mid-pacific mountains, central North Pacific Ocean, Palaeogeogr. Palaeoclimatol. Palaeoecol., 36, 55–67, https://doi.org/10.1016/0031-0182(81)90048-1, 1981.
Rea, D. K.: The paleoclimatic record provided by eolian deposition in the deep sea: The geologic history of wind. *Reviews of Geophysics*, *32*(2), 159-195, https://doi.org/10.1029/93RG03257, 1994.
Rea, D. K., and Hovan, S. A.: Grain size distribution and depositional processes of the mineral component of abyssal sediments: Lessons from the North Pacific, Paleoceanography, 10(2), 251-258, https://doi.org/10.1029/94PA03355, 1995.
Regayre, L. A., Johnson, J. S., Yoshioka, M., Pringle, K. J., Sexton, D. M. H., Booth, B. B. B., Lee, L. A., Bellouin, N., and Carslaw, K. S.: Aerosol and physical atmosphere model parameters are both important sources of uncertainty in aerosol ERF, Atmos. Chem. Phys., 18, 9975–10006, https://doi.org/10.5194/acp-18-9975-2018, 2018.
Regayre, L. A., Schmale, J., Johnson, J. S., Tatzelt, C., Baccarini, A., Henning, S., Yoshioka, M., Stratmann, F., Gysel-Beer, M., Grosvenor, D. P., and Carslaw, K. S.: The value of remote marine aerosol measurements for constraining radiative forcing uncertainty, Atmos. Chem. Phys., 20, 10063–10072, https://doi.org/10.5194/acp-20-10063-2020, 2020.
Rhodes, R. H., Yang, X., Wolff, E. W., McConnell, J. R., and Frey, M. M.: Sea ice as a source of sea salt aerosol to Greenland ice cores: a model-based study, Atmos. Chem. Phys., 17, 9417–9433, https://doi.org/10.5194/acp-17-9417-2017, 2017.
Rhodes, R. H., Bollet-Quivogne, Y., Barnes, P., Severi, M., and Wolff, E. W.: New estimates of sulfate diffusion rates in the EPICA Dome C ice core, Clim. Past, 20, 2031-2043, https://doi.org/10.5194/cp-20-2031-2024, 2024.
Ro, S., Hur, S. D., Ekaykin, A., Han, Y., Ro, C.-U., Hong, S.-B., Lee, M. J., Chang, C., Lee, S., Moon, J., Jung, H., Veres, A., Lee, A., and Hong, S.: Origin of the 1458/59 CE volcanic eruption revealed through analysis of glass shards in the firn core from Antarctic Vostok station, Commun. Earth Environ., 6, 828, https://doi.org/10.1038/s43247-025-02797-x, 2025.
Robock, A., and Free, M. P.: Ice Cores as an Index of Global Volcanism from 1850 to the Present, J. Geophys. Res.-Atmos., 100, 11549-11567, https://doi.org/10.1029/95JD00825, 1995.
Robock, A.: Volcanic eruptions and climate, Rev. Geophys., 38, 191-219, https://doi.org/10.1029/1998RG000054, 2000.
Rocco, M., Dunne, E., Peltola, M., Barthelmeß, T., Salignat, R., Chamba, G., Saint-Macary, A., Barr, N., Safi, K., Marriner, A., Deppeler, S., Harnwell, J., Engel, A., Colomb, A., Saiz-Lopez, A., Law, C. S., and Sellegri, K.: Fluxes of Biogenic and Oxygenated VOCs From In Situ Mesocosm Studies of Seawaters From the South-West Pacific Ocean. J. Geophy. Res.-Atmos., 130(15), https://doi.org/10.1029/2024JD043056, 2025.
Rodakoviski, R., Kok, J., and Chamecki, M.: Dust settling from turbulent layers in the free troposphere: Implications for the Saharan Air Layer, J. Geophys. Res.-Atmos., 128, e2022JD037724, https://doi.org/10.1029/2022JD037724, 2023.
Rojo-Garibaldi, B., Aguilar-Hernández, A. I., & Martínez–Mekler, G. (2024). Nonlinear comparative analysis of Greenland and Antarctica ice cores data. *Chaos: An Interdisciplinary Journal of Nonlinear Science*, *34*(8). https://doi.org/10.1063/5.0206846
Rousseau, D.-D., Chauvel, C., Hopcroft, P. O., Gutiérrez, P., Saulnier-Copard, S., Antoine, P., Fuchs, M., and Ustrzycka, A.: A remote input of African dust to Last Glacial Europe, Commun. Earth Environ., 6, 847, https://doi.org/10.1038/s43247-025-02888-9, 2025.
Sabatier, P., Moernaut, J., Bertrand, S., Van Daele, M., Kremer, K., Chaumillon, E., and Arnaud, F.: A Review of Event Deposits in Lake Sediments, Quaternary, 5, 34, https://doi.org/10.3390/quat5030034, 2022.
Salzer, M. W., and Hughes, M. K.: Bristlecone pine tree rings and volcanic eruptions over the last 5000 yr, Quaternary Res., 67, 57-68, https://doi.org/10.1016/j.yqres.2006.07.004, 2007.

Formatted: Default Paragraph Font, Font color: Black

Formatted: Normal, Centered, Border: Top: (No border), Bottom: (No border), Left: (No border), Right: (No border), Between : (No border), Tab stops: 3.25", Centered + 6.5", Right, Position: Horizontal: Left, Relative to: Column, Vertical: In line, Relative to: Margin, Wrap Around

Formatted: Font color: Black

Samset, B. H., Myhre, G., Herber, A., Kondo, Y., Li, S. M., Moteki, N., Koike, M., Oshima, N., Schwarz, J. P., Balkanski, Y., Bauer, S. E., Bellouin, N., Berntsen, T. K., Bian, H., Chin, M., Diehl, T., Easter, R. C., Ghan, S. J., Iversen, T., Kirkevåg, A., Lamarque, J. F., Lin, G., Liu, X., Penner, J. E., Schulz, M., Seland, Ø., Skeie, R. B., Stier, P., Takemura, T., Tsigaridis, K., and Zhang, K.: Modelled black carbon radiative forcing and atmospheric lifetime in AeroCom Phase II constrained by aircraft observations, Atmos. Chem. Phys., 14, 12465-12477, https://doi.org/10.5194/acp-14-12465-2014, 2014.

Sato, M., Hansen, J. E., McCormick, M. P., and Pollack, J. B.: Stratospheric aerosol optical depths, 1850-1990, J. Geophys. Res.-Atmos., 98, 22987-22994, https://doi.org/10.1029/93JD02553, 1993.

Sauer, J. S., Mayer, K. J., Lee, C., Alves, M. R., Amiri, S., Bahaveolos, C. J., Franklin, E. B., Crocker, D. R., Dang, D., Dinasquet, J., Garofalo, L. A., Kaluarachchi, C. P., Kilgour, D. B., Mael, L. E., Mitts, B. A., Moon, D. R., Moore, A. N., Morris, C. K., Mullenmeister, C. A., Prather, K. A.: The Sea Spray Chemistry and Particle Evolution study (SeaSCAPE): Overview and experimental methods, Environmental Science: Processes and Impacts, 24, 290–315, https://doi.org/10.1039/D1EM00260K, 2022.

Savarino, J., Bekki, S., Cole-Dai, J. H., and Thiemens, M. H.: Evidence from sulfate mass independent oxygen isotopic compositions of dramatic changes in atmospheric oxidation following massive volcanic eruptions, J. Geophys. Res.-Atmos., 108, https://doi.org/10.1029/2003JD003737, 2003.

Scanza, R. A., Mahowald, N., Ghan, S., Zender, C. S., Kok, J. F., Liu, X., Zhang, Y., and Albani, S.: Modeling dust as component minerals in the Community Atmosphere Model: development of framework and impact on radiative forcing, Atmos. Chem. Phys., 15, 537–561, https://doi.org/10.5194/acp-15-537-2015, 2015.

Schill, G. P., DeMott, P. J., Emerson, E. W., Rauker, A. M. C., Kodros, J. K., Suski, K. J., Hill, T. C. J., Levin, E. J. T., Pierce, J. R., Farmer, D. K., and Kreidenweis, S. M.: The contribution of black carbon to global ice nucleating particle concentrations relevant to mixed-phase clouds, P. Natl. Acad. Sci. USA., 117, 22705-22711, https://doi.org/10.1073/pnas.2001674117, 2020.

Schindlbeck-Belo, J. C., Toohey, M., Jegen, M., Kutterolf, S., and Rehfeld, K.: PalVol v1: a proxy-based semi-stochastic ensemble reconstruction of volcanic stratospheric sulfur injection for the last glacial cycle (140 000–50 BP), Earth Syst. Sci. Data, 16, 1063-1081, https://doi.org/10.5194/essd-16-1063-2024, 2024.

Schmidt, A., and Carn, S.: Chapter 17 - Volcanic emissions, aerosol processes, and climatic effects. In: Aerosols and Climate, Carslaw, K. S. (Ed.), Elsevier, 2022.

Schmidt, G. A.: Climate sensitivity--How sensitive is Earth's climate to CO2?, PAGES Newsletter, 20, 10–11, 2012.

Schurer, A. P., Tett, S. F. B., and Hegerl, G. C.: Small influence of solar variability on climate over the past millennium, Nat. Geosci., 7, 104-108, https://doi.org/10.1038/ngeo2040, 2014.

Schüpbach, S., Fischer, H., Bigler, M., Erhardt, T., Gfeller, G., Leuenberger, D., Mini, O., Mulvaney, R., Abram, N. J., Fleet, L. and Frey, M. M.: Greenland records of aerosol source and atmospheric lifetime changes from the Eemian to the Holocene, Nat. Commun., 9, 1476, https://doi.org/10.1038/s41467-018-03924-3, 2018.

Seelos, K., Sirocko, F., and Dietrich, S.: A continuous high-resolution dust record for the reconstruction of wind systems in central Europe (Eifel, Western Germany) over the past 133 ka, Geophys. Res. Lett., 36, 2009GL039716, https://doi.org/10.1029/2009GL039716, 2009.

Serno, S., Winckler, G., Anderson, R. F., Hayes, C. T., McGee, D., Machalett, B., Ren, H., Straub, S. M., Gersonde, R., and Haug, G. H.: Eolian dust input to the Subarctic North Pacific, Earth Planet. Sc. Lett., 387, 252-263, https://doi.org/10.1016/j.epsl.2013.11.008, 2014.

Severi, M., Becagli, S., Castellano, E., Morganti, A., Traversi, R., Udisti, R., Ruth, U., Fischer, H., Huybrechts, P., Wolff, E., Parrenin, F., Kaufmann, P., Lambert, F., and Steffensen, J. P.: Synchronisation of the EDML and EDC ice cores for the last 52 kyr by volcanic signature matching, Clim. Past, 3, 367-374, https://doi.org/10.5194/cp-3-367-2007, 2007.

Formatted: Default Paragraph Font, Font color: Black

Formatted: Normal, Centered, Border: Top: (No border), Bottom: (No border), Left: (No border), Right: (No border), Between : (No border), Tab stops: 3.25", Centered + 6.5", Right, Position: Horizontal: Left, Relative to: Column, Vertical: In line, Relative to: Margin, Wrap Around

Formatted: Font color: Black

Shao, M., Adnan, M., Zhang, L., Liu, P., Cao, J., and Qin, X.: Carbonate mineral dissolution and its carbon sink effect in Chinese loess, Land, 12, 133, https://doi.org/10.3390/land12010133, 2023.
Shaw, S. L., Gantt, B., and Meskhidze, N.: Production and Emissions of Marine Isoprene and Monoterpenes: A Review, Adv. Meteorol., 2010, https://doi.org/10.1155/2010/408696, 2010.
Sherwood, S. C., Bony, S., Boucher, O., Bretherton, C., Forster, P. M., Gregory, J. M., and Stevens, B.: Adjustments in the Forcing-Feedback Framework for Understanding Climate Change, B. Am. Meteorol. Soc., 96, 217–228, https://doi.org/10.1175/BAMS-D-13-00167.1, 2015.
Sherwood, S. C., Webb, M. J., Annan, J. D., Armour, K. C., Forster, P. M., Hargreaves, J. C., Hegerl, G., Klein, S. A., Marvel, K. D., Rohling, E. J., Watanabe, M., Andrews, T., Braconnot, P., Bretherton, C. S., Foster, G. L., Hausfather, Z., von der Heydt, A. S., Knutti, R., Mauritsen, T., Norris, J. R., Proistosescu, C., Rugenstein, M., Schmidt, G. A., Tokarska, K. B., and Zelinka, M. D.: An Assessment of Earth's Climate Sensitivity Using Multiple Lines of Evidence, Rev. Geophys., 58, 1–92, https://doi.org/10.1029/2019RG000678, 2020.
Shao, Y., Wyrwoll, K.-H., Chappel, A., Huang, J., Lin, Z., McTainsh, G., Mikami, M., Tanaka, T., Wang, X., and Yoon, S.: Dust cycle: an emerging core theme in Earth system science, Aeolian Res., 2, 181–204, https://doi.org/10.1016/j.aeolia.2011.02.001, 2011.
Shoenfelt, E. M., Winckler, G., Lamy, F., Anderson, R. F., and Bostick, B. C.: Highly bioavailable dust-borne iron delivered to the Southern Ocean during glacial periods, P. Natl. Acad. Sci. USA, 115, 11180-11185, https://doi.org/10.1073/pnas.1809755115, 2018.
Shotyk, W., Weiss, D., Kramers, J. D., Frei, R., Cheburkin, A. K., Gloor, M., and Reese, S.: Geochemistry of the peat bog at Etang de la Gruère, Jura Mountains, Switzerland, and its record of atmospheric Pb and lithogenic trace metals (Sc, Ti, Y, Zr, and REE) since 12370 14 C yr BP, Geochim. Cosmochim. Ac., 65, 2337–2360, https://doi.org/10.1016/S0016-7037(01)00586-5, 2001.
Shotyk, W., Barraza, F., Butt, S., Chen, N., Cuss, C. W., Devito, K., Frost, L., Grant-Weaver, I., Javed, M. B., Noernberg, T., and Oleksandrenko, A.: Trace elements in peat bog porewaters: indicators of dissolution of atmospheric dusts and aerosols from anthropogenic and natural sources, Environ. Sci.-Wat. Res., 9, 2401-2416, https://doi.org/10.1039/D3EW00241A, 2023.
Sigl, M., McConnell, J. R., Layman, L., Maselli, O., McGwire, K., Pasteris, D., Dahl-Jensen, D., Steffensen, J. P., Vinther, B., Edwards, R., Mulvaney, R., and Kipfstuhl, S.: A new bipolar ice core record of volcanism from WAIS Divide and NEEM and implications for climate forcing of the last 2000 years, J. Geophys. Res.-Atmos., 118, 1151-1169, https://doi.org/10.1029/2012JD018603, 2013.
Sigl, M., McConnell, J. R., Toohey, M., Curran, M., Das, S. B., Edwards, R., Isaksson, E., Kawamura, K., Kipfstuhl, S., Kruger, K., Layman, L., Maselli, O. J., Motizuki, Y., Motoyama, H., Pasteris, D. R., and Severi, M.: Insights from Antarctica on volcanic forcing during the Common Era, Nat. Clim. Change, 4, 693-697, https://doi.org/10.1038/nclimate2293, 2014.
Sigl, M., Winstrup, M., McConnell, J. R., Welten, K. C., Plunkett, G., Ludlow, F., Büntgen, U., Caffee, M., Chellman, N., Dahl-Jensen, D., Fischer, H., Kipfstuhl, S., Kostick, C., Maselli, O. J., Mekhaldi, F., Mulvaney, R., Muscheler, R., Pasteris, D. R., Pilcher, J. R., Salzer, M., Schüpbach, S., Steffensen, J. P., Vinther, B. M., and Woodruff, T. E.: Timing and climate forcing of volcanic eruptions for the past 2500 years, Nature, 523, 543–549, https://doi.org/10.1038/nature14565, 2015.
Sigl, M., Fudge, T. J., Winstrup, M., Cole-Dai, J., Ferris, D., McConnell, J. R., Taylor, K. C., Welten, K. C., Woodruff, T. E., Adolphi, F., Bisiaux, M., Brook, E. J., Buizert, C., Caffee, M. W., Dunbar, N. W., Edwards, R., Geng, L., Iverson, N., Koffman, B., Layman, L., Maselli, O. J., McGwire, K., Muscheler, R., Nishiizumi, K., Pasteris, D. R., Rhodes, R. H., and Sowers, T. A.: The WAIS Divide deep ice core WD2014 chronology - Part 2: Annual-layer counting (0-31 ka BP), Clim. Past, 12, 769-786, 2016.
Sigl, M., Toohey, M., McConnell, J. R., Cole-Dai, J., and Severi, M.: Volcanic stratospheric sulfur injections and aerosol optical depth during the Holocene (past 11 500 years) from a bipolar ice-

Formatted: Default Paragraph Font, Font color: Black

Formatted: Normal, Centered, Border: Top: (No border), Bottom: (No border), Left: (No border), Right: (No border), Between : (No border), Tab stops: 3.25", Centered + 6.5", Right, Position: Horizontal: Left, Relative to: Column, Vertical: In line, Relative to: Margin, Wrap Around

Formatted: Font color: Black

core array, Earth Syst. Sci. Data, 14, 3167-3196, https://doi.org/10.5194/essd-14-3167-2022, 2022.
Smalley, I., Marković, S. B., and Svirčev, Z.: Loess is [almost totally formed by] the accumulation of dust, Quatern. Int., 240, 4–11, https://doi.org/10.1016/j.quaint.2010.07.011, 2011.
Smirnov, A., Holben, B. N., Giles, D. M., Slutsker, I., O'Neill, N. T., Eck, T. F., Macke, A., Croot, P., Courcoux, Y., Sakerin, S. M., Smyth, T. J., Zielinski, T., Zibordi, G., Goes, J. I., Harvey, M. J., Quinn, P. K., Nelson, N. B., Radionov, V. F., Duarte, C. M., and Diehl, T. L.: Maritime aerosol network as a component of AERONET – first results and comparison with global aerosol models and satellite retrievals, Atmos. Meas. Tech., 4, 583–597, https://doi.org/10.5194/amt-4-583-2011, 2011.
Smith, C. J., Kramer, R. J., Myhre, G., Alterskjær, K., Collins, W., Sima, A., Boucher, O., Dufresne, J., Nabat, P., Michou, M., Yukimoto, S., and Cole, J.: Effective radiative forcing and adjustments in CMIP6 models, Atmos. Chem. Phys., 20, 9591–9618, https://doi.org/10.5194/acp-20-9591-2020, 2020a.
Smith, V. C., Costa, A., Aguirre-Diaz, G., Pedrazzi, D., Scifo, A., Plunkett, G., Poret, M., Tournigand, P. Y., Miles, D., Dee, M. W., McConnell, J. R., Sunye-Puchol, I., Harris, P. D., Sigl, M., Pilcher, J. R., Chellman, N., and Gutierrez, E.: The magnitude and impact of the 431 CE Tierra Blanca Joven eruption of Ilopango, El Salvador, P. Natl. Acad. Sci. USA, 117, 26061-26068, https://doi.org/10.1073/pnas.2003008117, 2020b.
Smith, C. J., Harris, G. R., Palmer, M. D., Bellouin, N., Collins, W., Myhre, G., Schulz, M., Golaz, J. C., Ringer, M., Storelvmo, T., and Forster, P. M.: Energy Budget Constraints on the Time History of Aerosol Forcing and Climate Sensitivity, J. Geophys. Res.-Atmos., 126, https://doi.org/10.1029/2020JD033622, 2021.
Song, A., Li, J., Tsona, N. T., and Du, L.: Parameterizations for sea spray aerosol production flux, Appl. Geochem., 157, 105776, https://doi.org/10.1016/j.apgeochem.2023.105776, 2023.
Song Q., Zhang, Z., Yu, H., Kok, J. F., Di Biagio, C., Albani, S., Zheng, J., and Ding, J.: Size-Resolved Dust Direct Radiative Effect Efficiency Derived from Satellite Observations, Atmos. Chem. Phys., 22, 13115–13135, https://doi.org/10.5194/acp-22-13115-2022, 2022.
Stambaugh, M. C., Marschall, J. M., Abadir, E. R., Jones, B. C., Brose, P. H., Dey, D. C., and Guyette, R. P.: Wave of fire: an anthropogenic signal in historical fire regimes across central Pennsylvania, USA, Ecosphere, 9, e02222, https://doi.org/10.1002/ecs2.2222, 2018.
Staunton-Sykes, J., Aubry, T. J., Shin, Y. M., Weber, J., Marshall, L. R., Luke Abraham, N., Archibald, A., and Schmidt, A.: Co-emission of volcanic sulfur and halogens amplifies volcanic effective radiative forcing, Atmos. Chem. Phys., 21, 9009-9029, https://doi.org/10.5194/acp-21-9009-2021, 2021.
Staver, A.C., Archibald, S. and Levin, S., 2011. Tree cover in sub-Saharan Africa: rainfall and fire constrain forest and savanna as alternative stable states. Ecology, 92(5), pp.1063-1072.
Steel, Z. L., Safford, H. D., and Viers, J. H.: The fire frequency-severity relationship and the legacy of fire suppression in California forests, Ecosphere, 6, 8, https://doi.org/10.1890/ES14-00224.1, 2015.
Stenchikov, G., Ukhov, A., Osipov, S., Ahmadov, R., Grell, G., Cady-Pereira, K., Mlawer, E., and Iacono, M.: How Does a Pinatubo-Size Volcanic Cloud Reach the Middle Stratosphere?, J. Geophys. Res.-Atmos., 126, e2020JD033829, https://doi.org/10.1029/2020JD033829, 2021.
Stocker and T.F., D. Qin, G.-K. Plattner, M. Tignor, S.K. Allen, J. Boschung, A. Nauels, Y. Xia, V. B. and P. M. M. (eds.): Summary for Policymakers. In: Climate Change 2013: The Physical Science Basis. Contribution of Working Group I to the Fifth Assessment Report of the Intergovernmental Panel on Climate Change, CEUR Workshop Proc., 1542, 33–36, https://doi.org/10.1017/CBO9781107415324.004, 2015.
Stothers, R. B.: Major optical depth perturbations to the stratosphere from volcanic eruptions: Pyrheliometric period, 1881-1960, J. Geophys. Res.-Atmos., 101, 3901-3920, https://doi.org/10.1029/95JD03237, 1996.

Formatted: Default Paragraph Font, Font color: Black

Formatted: Normal, Centered, Border: Top: (No border), Bottom: (No border), Left: (No border), Right: (No border), Between : (No border), Tab stops: 3.25", Centered + 6.5", Right, Position: Horizontal: Left, Relative to: Column, Vertical: In line, Relative to: Margin, Wrap Around

Formatted: Font color: Black

Stothers, R. B., and Rampino, M. R.: Volcanic eruptions in the Mediterranean before AD 630 from written and archaeological sources, J. Geophys. Res.-Sol. Ea., 88, 6357-6371, https://doi.org/10.1029/JB088iB08p06357, 1983.

Stothers, R. B.: Mystery Cloud of Ad-536, Nature, 307, 344-345, https://doi.org/10.1038/307344a0, 1984.

Stothers, R. B.: Cloudy and clear stratospheres before AD 1000 inferred from written sources, J. Geophys. Res.-Atmos., 107, AAC 17-1-AAC 17-10, https://doi.org/10.1029/2002JD002105, 2002.

Strawson, I., Faïn, X., Bauska, T. K., Muschitiello, F., Vladimirova, D. O., Tetzner, D. R., Humby, J., Thomas, E. R., Liu, P., Zhang, B., Grilli, R., and Rhodes, R. H.: Historical Southern Hemisphere biomass burning variability inferred from ice core carbon monoxide records, P. Natl. Acad. Sci. USA, 121, e2402868121, https://doi.org/10.1073/pnas.2402868121, 2024.

Ström, J., Svensson, J., Beaudon, E., Marja-Aho, I., and Ruppel, M. M.: Using non-combustible residual particles as a proxy for mineral dust deposition to estimate its contribution to light absorption in the 300-year Holtedahlfonna ice core, Aeolian Res., 75, 101025, https://doi.org/10.1016/j.aeolia.2025.101025, 2026.

Sudarchikova, N., Mikolajewicz, U., Timmreck, C., O'Donnell, D., Schurgers, G., Sein, D., and Zhang, K.: Modelling of mineral dust for interglacial and glacial climate conditions with a focus on Antarctica, Clim. Past, 11, 765–779. https://doi.org/10.5194/cp-11-765-2015, 2015.

Suhrhoff, T. J., Rickli, J., Christl, M., Vologina, E. G., Prokopenko, A., and Vance, D.: Extracting paleo-weathering signals from authigenic phases in lake sediments: A case-study of Lake Baikal, Chem. Geol., 654, 122054, https://doi.org/10.1016/j.chemgeo.2024.122054, 2024.

Sun, C. Q., Plunkett, G., Liu, J. Q., Zhao, H. L., Sigl, M., McConnell, J. R., Pilcher, J. R., Vinther, B., Steffensen, J. P., and Hall, V.: Ash from Changbaishan Millennium eruption recorded in Greenland ice: Implications for determining the eruption's timing and impact, Geophys. Res. Lett., 41, 694-701, https://doi.org/10.1002/2013GL058642, 2014.

Sun, Y., Luo, H., Li, Y., Zhou, W., Xu, W., Fu, P., and Zhao, D.: Atmospheric organic aerosols: online molecular characterization and environmental impacts, npj Climate and Atmospheric Science, 8, 305, https://doi.org/10.1038/s41612-025-01199-2, 2025.

Svensson, A., Vettoretti, G., Lin, J.-m., Sinnl, G., Dahl-Jensen, D., Steffensen, J. P., Rasmussen, S. O., Vinther, B., Hvidberg, C., Kjær, H. A., Gkinis, V., Cook, E., Lohmann, J., Melcher, J. O., Halkjær, S., Kipfstuhl, S., Wilhelms, F., Adolphi, F., Fischer, H., Bigler, M., Sigl, M., Landais, A., Bouchet, M., Klüssendorf, A., Parrenin, F., Mulvaney, R., Wolff, E., Burke, A., Innes, H., Severi, M., Buizert, C., McConnell, J. R., Chellman, N., Wensman, S., Beer, J., Oyabu, I., and Muscheler, R.: Bipolar volcanic ice-core synchronization of the entire last glacial period, Quaternary Sci. Rev., 375, 109755, https://doi.org/10.1016/j.quascirev.2025.109755, 2026.

Swann, A. L. S., Hoffman, F. M., Koven, C. D., and Randerson, J. T.: Plant responses to increasing CO_2 reduce estimates of climate impacts on drought severity, P. Natl. Acad. Sci. USA, 113, 10019-10024, https://doi.org/10.1073/pnas.1604581113, 2016.

Swetnam, T. W.: Fire history and climate change in giant sequoia groves, Science, 262, 885–889, https://doi.org/10.1126/science.262.5135.885, 1993.

Swetnam, T. W., Baisan, C. H., Caprio, A. C., Brown, P. M., Touchan, R., Anderson, R. S., and Hallett, D. J.: Multi-millennial fire history of the giant forest, Sequoia National Park, California, USA, Fire Ecol., 5, 120–150, https://doi.org/10.4996/fireecology.0503120, 2009.

Symons, G. J.: The Eruption of Krakatoa and Subsequent Phenomena, Q J Roy Meteor Soc, 14, 301-307, 1888.

Szopa, S., Naik, V., Adhikary, B., Artaxo, P., Berntsen, T., Collins, W. D., Aas, W., Akritidis, D., Allen, R. J., Kanaya, Y., Prather, M. J., Kuo, C., Zhai, P., Pirani, A., Connors, S., Péan, C., Berger, S., Caud, N., Chen, Y., Goldfarb, L., Gomis, M., Huang, M., Leitzell, K., Lonnoy, E., Matthews, J., Maycock, T., Waterfield, T., Yelekçi, O., Yu, R., and Zhou, B.: Chapter 6: Short-lived Climate Forcers, in: Climate Change 2021: The Physical Science Basis. Contribution of Working Group I to the Sixth Assessment Report of the Intergovernmental Panel on Climate Change, edited by:

Formatted: Default Paragraph Font, Font color: Black

Formatted: Normal, Centered, Border: Top: (No border), Bottom: (No border), Left: (No border), Right: (No border), Between : (No border), Tab stops: 3.25", Centered + 6.5", Right, Position: Horizontal: Left, Relative to: Column, Vertical: In line, Relative to: Margin, Wrap Around

Formatted: Font color: Black

Masson-Delmotte, V., Zhai, P., A. Pirani, A., Connors, S. L., Péan, C. S., Berger, S., Caud, N., Chen, Y., Goldfarb, L., Gomis, M. I., Huang, M., Leitzell, K., Lonnoy, E., Matthews, J. B. R., Maycock, T. K., Waterfield, T., Yelekçi, O., Yu, R., and Zhou, B., Cambridge University Press, Cambridge, United Kingdom and New York, NY, USA, 816–921, https://doi.org/10.1017/9781009157896.008, 2021.

Takemura, T., Egashira, M., Matsuzawa, K., Ichijo, H., O'ishi, R., and Abe-Ouchi, A.: A simulation of the global distribution and radiative forcing of soil dust aerosols at the Last Glacial Maximum, Atmos. Chem. Phys., 9, 3061–3073, https://doi.org/10.5194/acp-9-3061-2009, 2009.

Tan, Z., Han, Y., Cao, J., Chang Huang, C., and An, Z.: Holocene wildfire history and human activity from high-resolution charcoal and elemental black carbon records in the Guanzhong Basin of the Loess Plateau, China, Quaternary Sci. Rev., 109, 76–87, https://doi.org/10.1016/j.quascirev.2014.11.013, 2015.

Taylor, A. H., Trouet, V., Skinner, C. N., and Stephens, S.: Socioecological transitions trigger fire regime shifts and modulate fire–climate interactions in the Sierra Nevada, USA, 1600–2015 CE, Proceedings of the National Academy of Sciences, 113, 13684–13689, https://doi.org/10.1073/pnas.1609775113, 2016.

Tegen, I., and Fung, I.: Modeling of mineral dust in the atmosphere: Sources, transport, and optical thickness, J. Geophys. Res.-Atmos., 99, 22897-22914, https://doi.org/10.1029/94JD01928, 1994.

Tegen, I., and Lacis, A. A.: Modeling of particle size distribution and its influence on the radiative properties of mineral dust aerosol, J. Geophys. Res.-Atmos., 101, 19237-19244, https://doi.org/10.1029/95JD03610, 1996.

Tepley, A. J., and Veblen, T. T.: Spatiotemporal fire dynamics in mixed-conifer and aspen forests in the San Juan Mountains of southwestern Colorado, USA, Ecol. Monogr., 85, 583–603, https://doi.org/10.1890/14-1496.1, 2015.

Thomason, L. W., Ernest, N., Millán, L., Rieger, L., Bourassa, A., Vernier, J. P., Manney, G., Luo, B., Arfeuille, F., and Peter, T.: A global space-based stratospheric aerosol climatology: 1979–2016, Earth Syst. Sci. Data, 10, 469-492, https://doi.org/10.5194/essd-10-469-2018, 2018.

Thompson, L. G., Mosley-Thompson, E., Davis, M. E., Zagorodnov, V. S., Howat, I. M., Mikhalenko, V. N., and Lin, P. N.: Annually resolved ice core records of tropical climate variability over the past ~1800 years, Science, 340, 945-950. https://doi.org/10.1126/science.1234210, 2013.

Thompson, L. G., Davis, M. E., Mosley-Thompson, E., Sowers, T. A., Henderson, K. A., Zagorodnov, V. S., and Francou, B.: A 25000-year tropical climate history from Bolivian ice cores, Science, 282, 1858-1864, https://doi.org/10.1126/science.282.5395.1858, 1998.

Thompson, L. G., Yao, T., Mosley-Thompson, E., Davis, M. E., Henderson, K. A., and Lin, P. N.: A high-resolution millennial record of the South Asian monsoon from Himalayan ice cores, Science, 289, 1916-1919, https://doi.org/10.1126/science.289.5486.1916, 2000.

Thompson, L. G., Mosley-Thompson, E., Davis, M. E., Lin, P. N., Henderson, K. A., Cole-Dai, J., and Liu, K. B.: Late glacial stage and Holocene tropical ice core records from Huascaran, Peru, Science, 269, 46-50, https://doi.org/10.1126/science.269.5220.46, 1995.

Thompson, L. G., Mosley-Thompson, E., Davis, M. E., Henderson, K. A., Brecher, H. H., Zagorodnov, V. S., and Beer, J.: Kilimanjaro ice core records: evidence of Holocene climate change in tropical Africa, Science, 298, 589-593, https://doi.org/10.1126/science.1073198, 2002.

Thompson, L. G., Mosley-Thompson, E., Brecher, H., Davis, M., León, B., Les, D., Lin, P.-N., Mashiotta, T., and Mountain, K.: Abrupt tropical climate change: Past and present, P. Natl. Acad. Sci. USA, 103, 10536–10543, https://doi.org/10.1073/pnas.0603900103, 2006a.

Thompson, L. G., Tandong, Y., Davis, M. E., Mosley-Thompson, E., Mashiotta, T. A., Lin, P. N., and Zagorodnov, V. S.: Holocene climate variability archived in the Puruogangri ice cap on the central Tibetan Plateau, Ann. Glaciol., 43, 61-69, https://doi.org/10.3189/172756406781812357, 2006b.

Thompson, L. G., Yao, T., Davis, M. E., Mosley-Thompson, E., Wu, G., Porter, S. E., and Kenny, D. V.: Ice core records of climate variability on the Third Pole with emphasis on the Guliya ice cap,

Formatted: Default Paragraph Font, Font color: Black

Formatted: Normal, Centered, Border: Top: (No border), Bottom: (No border), Left: (No border), Right: (No border), Between : (No border), Tab stops: 3.25", Centered + 6.5", Right, Position: Horizontal: Left, Relative to: Column, Vertical: In line, Relative to: Margin, Wrap Around

Formatted: Font color: Black

western Kunlun Mountains, Quaternary Sci. Rev., 188, 1-14, https://doi.org/10.1016/j.quascirev.2018.03.003, 2018.

Thompson, L. G., Yao, T.-D., Davis, M. E., Mosley-Thompson, E., Synal, H.-A., Wu, G., Bolzan, J. F., Kutuzov, S., Beaudon, E., Sierra-Hernández, M. R., and Beer, J.: Ice core evidence for an orbital-scale climate transition on the Northwest Tibetan Plateau, Quaternary Sci. Rev., 324, 108443, https://doi.org/10.1016/j.quascirev.2023.108443, 2024.

Thornhill, G., Collins, W., Olivié, D., Skeie, R. B., Archibald, A., Bauer, S., Checa-Garcia, R., Fiedler, S., Folberth, G., Gjermundsen, A., Horowitz, L., Lamarque, J.-F., Michou, M., Mulcahy, J., Nabat, P., Naik, V., O'Connor, F. M., Paulot, F., Schulz, M., Scott, C. E., Séférian, R., Smith, C., Takemura, T., Tilmes, S., Tsigaridis, K., and Weber, J: Climate-driven chemistry and aerosol feedbacks in CMIP6 Earth system models, Atmos. Chem. Phys., 21, 1105–1126. https://doi.org/10.5194/acp-21-1105-2021, 2021.

Timmreck, C., Lorenz, S. J., Crowley, T. J., Kinne, S., Raddatz, T. J., Thomas, M. A., and Jungclaus, J. H.: Limited temperature response to the very large AD 1258 volcanic eruption, Geophys. Res. Lett., 36, https://doi.org/10.1029/2009GL040083, 2009.

Timmreck, C., Mann, G. W., Aquila, V., Hommel, R., Lee, L. A., Schmidt, A., Brühl, C., Carn, S., Chin, M., Dhomse, S. S., Diehl, T., English, J. M., Mills, M. J., Neely, R., Sheng, J., Toohey, M., and Weisenstein, D.: The Interactive Stratospheric Aerosol Model Intercomparison Project (ISA-MIP): motivation and experimental design, Geosci. Model Dev., 11, 2581–2608, https://doi.org/10.5194/gmd-11-2581-2018, 2018.

Tomchovska, I., Pavia, F. J., Adkins, J. F., Berelson, W. M., Quinan, M. P., and Farley, K. A.: Fractionation during sediment winnowing drives divergent mass accumulation rates derived from ^{230}Th and ^{3}He on the Cocos Ridge, Geochim. Cosmochim. Ac., 395, 149-165, https://doi.org/10.1016/j.gca.2025.02.021, 2025.

Toohey, M., and Sigl, M.: Volcanic stratospheric sulfur injections and aerosol optical depth from 500 BCE to 1900 CE, Earth Syst. Sci. Data, 9, 809-831, https://doi.org/10.5194/essd-9-809-2017, 2017.

Toohey, M., Stevens, B., Schmidt, H., and Timmreck, C.: Easy Volcanic Aerosol (EVA v1.0): an idealized forcing generator for climate simulations, Geosci. Model Dev., 9, 4049-4070, https://doi.org/10.5194/gmd-9-4049-2016, 2016.

Toohey, M., Kruger, K., Schmidt, H., Timmreck, C., Sigl, M., Stoffel, M., and Wilson, R.: Disproportionately strong climate forcing from extratropical explosive volcanic eruptions, Nat. Geosci., 12, 100-107, https://doi.org/10.1038/s41561-018-0286-2, 2019.

Toole, D. A., Siegel, D. A., and Doney, S. C.: A light-driven, one-dimensional dimethylsulfide biogeochemical cycling model for the Sargasso Sea, J. Geophys. Res. Biogeo., 113, https://doi.org/10.1029/2007JG000426, 2008.

Torre, G., Gaiero, D. M., Coppo, R., Cosentino, N. J., Goldstein, S. L., De Vleeschouwer, F., Le Roux, G., Bolge, L., Kiro, Y., and Oliveira Sawakuchi, A.: Unravelling late Quaternary atmospheric circulation in the Southern Hemisphere through the provenance of Pampean loess, Earth-Sci. Rev., 232, 104143, https://doi.org/10.1016/j.earscirev.2022.104143, 2022.

Toth, T. D., Zhang, J., Campbell, J. R., Reid, J. S., Shi, Y., Johnson, R. S., Smirnov, A., Vaughan, M. A., and Winker, D. M.: Investigating enhanced Aqua MODIS aerosol optical depth retrievals over the mid-to-high latitude Southern Oceans through intercomparison with co-located CALIOP, MAN, and AERONET data sets, J. Geophys. Res.-Atmos., 118, 4700–4714, https://doi.org/10.1002/jgrd.50311, 2013.

Tsigaridis, K., Daskalakis, N., Kanakidou, M., Adams, P. J., Artaxo, P., Bahadur, R., Balkanski, Y., Bauer, S. E., Bellouin, N., Benedetti, A., Bergman, T., Berntsen, T. K., Beukes, J. P., Bian, H., Carslaw, K. S., Chin, M., Curci, G., Diehl, T., Easter, R. C., Ghan, S. J., Gong, S. L., Hodzic, A., Hoyle, C. R., Iversen, T., Jathar, S., Jimenez, J. L., Kaiser, J. W., Kirkevåg, A., Koch, D., Kokkola, H., H Lee, Y., Lin, G., Liu, X., Luo, G., Ma, X., Mann, G. W., Mihalopoulos, N., Morcrette, J. J., Müller, J. F., Myhre, G., Myriokefalitakis, S., Ng, N. L., O'donnell, D., Penner, J.

Formatted: Default Paragraph Font, Font color: Black

Formatted: Normal, Centered, Border: Top: (No border), Bottom: (No border), Left: (No border), Right: (No border), Between : (No border), Tab stops: 3.25", Centered + 6.5", Right, Position: Horizontal: Left, Relative to: Column, Vertical: In line, Relative to: Margin, Wrap Around

Formatted: Font color: Black

E., Pozzoli, L., Pringle, K. J., Russell, L. M., Schulz, M., Sciare, J., Seland, Shindell, D. T., Sillman, S., Skeie, R. B., Spracklen, D., Stavrakou, T., Steenrod, S. D., Takemura, T., Tiitta, P., Tilmes, S., Tost, H., Van Noije, T., Van Zyl, P. G., Von Salzen, K., Yu, F., Wang, Z., Wang, Z., Zaveri, R. A., Zhang, H., Zhang, K., Zhang, Q., and Zhang, X.: The AeroCom evaluation and intercomparison of organic aerosol in global models, Atmos. Chem. Phys., 14, 10845–10895, https://doi.org/10.5194/acp-14-10845-2014, 2014.

Tsigaridis, K., and Kanakidou, M.: The Present and Future of Secondary Organic Aerosol Direct Forcing on Climate, Current Climate Change Reports, 4, 84–98, https://doi.org/10.1007/s40641-018-0092-3, 2018.

Újvári, G., Klötzli, U., Stevens, T., Svensson, A., Ludwig, P., Vennemann, T., Gier, S., Horschinegg, M., Palcsu, L., Hippler, D., Kovács, J., Di Biagio, C., and Formenti, P.: Greenland Ice Core Record of Last Glacial Dust Sources and Atmospheric Circulation, J. Geophys. Res.-Atmos., 127, e2022JD036597, https://doi.org/10.1029/2022JD036597, 2022.

Unger, N.: Global Climate Forcing by Criteria Air Pollutants, Annual Review of Environment and Resources, 37, 1-24, https://doi.org/10.1146/annurev-environ-082310-100824, 2012.

Urbanski, S.P. (2013). Combustion efficiency and emission factors for wildfire-season fires in mixed conifer forests of the northern Rocky Mountains, US. Atmospheric Chemistry and Physics, 13, 7241–7262. https://doi.org/10.5194/acp-13-7241-2013

Vachula, R. S., Karp, A. T., Denis, E. H., Balascio, N. L., Canuel, E. A., and Huang, Y.: Spatially calibrating polycyclic aromatic hydrocarbons (PAHs) as proxies of area burned by vegetation fires: Insights from comparisons of historical data and sedimentary PAH fluxes, Palaeogeogr. Palaeocl., 596, 110995, https://doi.org/10.1016/j.palaeo.2022.110995, 2022a.

Vachula, R. S., Sheppard, R. Y., and Cheung, A. H.: Preservation biases are pervasive in Holocene paleofire records, Palaeogeogr. Palaeocl., 602, 111165, https://doi.org/10.1016/j.palaeo.2022.111165, 2022b.

Vachula, R. S.: A meta-analytical approach to understanding the charcoal source area problem, Palaeogeogr. Palaeocl., 562, 110111, https://doi.org/10.1016/j.palaeo.2020.110111, 2021.

Van Damme, M., Clarisse, L., Heald, C. L., Hurtmans, D., Ngadi, Y., Clerbaux, C., Dolman, A. J., Erisman, J. W., and Coheur, P. F.: Global distributions, time series and error characterization of atmospheric ammonia (NH_3) from IASI satellite observations, Atmos. Chem. Phys., 14, 2905–2922, https://doi.org/10.5194/acp-14-2905-2014, 2014.

van der Does, M., Brummer, G.-J. A., van Crimpen, F. C. J., Korte, L. F., Mahowald, N. M., Merkel, U., Yu, H., Zuidema, P., and Stuut, J.-B. W.: Tropical rains controlling deposition of Saharan dust across the North Atlantic Ocean, Geophys. Res. Lett., 47, e2019GL086867, https://doi.org/10.1029/2019GL086867, 2020.

Van Der Kaars, S., and De Deckker, P.: A Late Quaternary pollen record from deep-sea core Fr10/95, GC17 offshore Cape Range Peninsula, northwestern Western Australia, Rev. Palaeobot. Palyno., 120, 17–39, https://doi.org/10.1016/S0034-6667(02)00075-1, 2002.

van der Werf, G. R., Randerson, J. T., Giglio, L., Collatz, G. J., Kasibhatla, P. S., and Arellano Jr., A. F. : Interannual variability in global biomass burning emissions from 1997-2004, Atmos. Chem. Phys., 6, 3423–3441, https://doi.org/10.5194/acp-6-3423–2006, 2006.

van der Werf, G. R., Randerson, J. T., Giglio, L., Leeuwen, T. T. Van, Chen, Y, Collatz, G. J, Yokelson, R. J, and Kasibhatla, P. S: Global fire emissions estimates during 1997-2016, 9, 697–720, https://doi.org/10.5194/essd-9-697-2017, 2017.

van der Werf, G. R., Dempewolf, J., Trigg, S., Randerson, J., Kasibhatla, P., Giglio, L., Murdiyarso, D., Peters, W., Morton, D. C., Collatz, G., Dolman, A., and DeFries, R. S.: Climate regulation of fire emissions and deforestation in equatorial Asia, P. Natl. Acad. Sci. USA, 105, 20350–20355, https://doi.org/10.1073/pnas.0803375105, 2008.

van der Werf, G. R., Peters, W., van Leeuwen, T. T., and Giglio, L.: What could have caused pre-industrial biomass burning emissions to exceed current rates?, Clim. Past, 9, 289–306, https://doi.org/10.5194/cp-9-289-2013, 2013.

Formatted: Default Paragraph Font, Font color: Black

Formatted: Normal, Centered, Border: Top: (No border), Bottom: (No border), Left: (No border), Right: (No border), Between : (No border), Tab stops: 3.25", Centered + 6.5", Right, Position: Horizontal: Left, Relative to: Column, Vertical: In line, Relative to: Margin, Wrap Around

Formatted: Font color: Black

Van Dijk, E., Jungclaus, J., Sigl, M., Timmreck, C., and Krüger, K.: High-frequency climate forcing causes prolonged cold periods in the Holocene, Commun. Earth Environ., 5, 242, https://doi.org/10.1038/s43247-024-01380-0, 2024.

van Marle, M. J. E., Kloster, S., Magi, B. I., Marlon, J. R., Daniau, A. L., Field, R. D., Arneth, A., Forrest, M., Hantson, S., Kehrwald, N. M., Knorr, W., Lasslop, G., Li, F., Mangeon, S., Yue, C., Kaiser, J. W., and van der Werf, G. R.: Historic global biomass burning emissions for CMIP6 (BB4CMIP) based on merging satellite observations with proxies and fire models (1750–2015), Geosci. Model Dev., 10, 3329–3357, https://doi.org/10.5194/gmd-10-3329-2017, 2017.

van Wagtendonk, J. W., and Lutz, J. A.: Fire Regime Attributes of Wildland Fires in Yosemite National Park, USA, Fire Ecol., 3, 34–52, https://doi.org/10.4996/fireecology.0302034, 2007.

Varlas, G., Marinou, E., Gialitaki, A., Siomos, N., Tsarpalis, K., Kalivitis, N., Solomos, S., Tsekeri, A., Spyrou, C., Tsichla, M., Kampouri, A., Vervatis, V., Giannakaki, E., Amiridis, V., Mihalopoulos, N., Papadopoulos, A., and Katsafados, P.: Assessing Sea-State Effects on Sea-Salt Aerosol Modeling in the Lower Atmosphere Using Lidar and In-Situ Measurements, Remote Sensing, 13, 614. https://doi.org/10.3390/rs13040614, 2021.

Venugopal, A. U., Bhatti, Y. A., Morgenstern, O., Williams, J., Edkins, N., Hardacre, C., Jones, A., and Revell, L. E.: Constraining the Uncertainty Associated With Sea Salt Aerosol Parameterizations in Global Models Using Nudged UKESM1-AMIP Simulations, J. Geophys. Res.-Atmos., 130, e2024JD041643, https://doi.org/10.1029/2024JD041643, 2025.

Veraverbeke, S., Rogers, B. M., Goulden, M. L., Jandt, R. R., Miller, C. E., Wiggins, E. B., and Randerson, J. T.: Lightning as a major driver of recent large fire years in North American boreal forests, Nat. Clim. Change, 7, 529-534, https://doi.org/10.1038/nclimate3329, 2017.

Veretennikova, E. E., Kuryina, I. V., Dyukarev, E. A., Golovatskaya, E. A., and Smirnov, S. V.: Geochemical Features of Peat Deposits at Oligotrophic Bogs in the Southern Taiga Subzone of West Siberia. Geochem. Int.+, 59, 618–631, https://doi.org/10.1134/S0016702921050098, 2021.

Verkerk, M., Aubry, T. J., Smith, C., Hopcroft, P. O., Sigl, M., Tierney, J. E., Anchukaitis, K., Osman, M., Schmidt, A., and Toohey, M.: Using reduced-complexity volcanic aerosol and climate models to produce large ensemble simulations of Holocene temperature, Clim. Past, 21, 1755-1778, https://doi.org/10.5194/cp-21-1755-2025, 2025.

Visioni, D.: Personal Communication, 2026.

Volvakh, N. E., Kurbanov, R. N., Zykina, V. S., Murray, A. S., Stevens, T., Költringer, C. A., Volvakh, A. O., Malikov, D. G., Taratunina, N. A., and Buylaert, J.-P.: First high-resolution luminescence dating of loess in Western Siberia, Quat. Geochronol., 73, 101377, https://doi.org/10.1016/j.quageo.2022.101377, 2022.

Wade, D. C., Vidal, C. M., Abraham, N. L., Dhomse, S., Griffiths, P. T., Keeble, J., Mann, G., Marshall, L., Schmidt, A., and Archibald, A. T.: Reconciling the climate and ozone response to the 1257 CE Mount Samalas eruption, P. Natl. Acad. Sci. USA, 117, 26651-26659, https://doi.org/10.1073/pnas.1919807117, 2020.

Wahl, E., E. Zorita, and A. Hoell, 2022: The Kalman Filter as Post-Processor for Analog Data–Model Assimilation in Paleoclimate Reconstruction. J. Climate, 35, 5501–5518, https://doi.org/10.1175/JCLI-D-21-0454.1.

Wan, J. S., Hamilton, D. S., and Mahowald, N. M.: Importance of Uncertainties in the Spatial Distribution of Preindustrial Wildfires for Estimating Aerosol Radiative Forcing, Geophys. Res. Lett., 48, e2020GL089758, https://doi.org/10.1029/2020GL089758, 2021.

Wang, X., Sultana, C. M., Trueblood, J., Hill, T. C. J., Malfatti, F., Lee, C., Laskina, O., Moore, K. A., Beall, C. M., McCluskey, C. S., Cornwell, G. C., Zhou, Y., Cox, J. L., Pendergraft, M. A., Santander, M. V., Bertram, T. H., Cappa, C. D., Azam, F., DeMott, P. J., Grassian, V. H., and Prather, K. A.: Microbial control of sea spray aerosol composition: A tale of two blooms, ACS Central Science, 1(3), 124–131, https://doi.org/10.1021/acscentsci.5b00148, 2015.

Formatted: Default Paragraph Font, Font color: Black

Formatted: Normal, Centered, Border: Top: (No border), Bottom: (No border), Left: (No border), Right: (No border), Between : (No border), Tab stops: 3.25", Centered + 6.5", Right, Position: Horizontal: Left, Relative to: Column, Vertical: In line, Relative to: Margin, Wrap Around

Formatted: Font color: Black

Wang, Z., Chappellaz, J., Park, K., and Mak, J. E.: Large Variations in Southern Hemisphere Biomass Burning During the Last 650 Years, Science, 330, 1663-1666, https://doi.org/10.1126/science.1197257, 2010.

Wang, S. S.-C., Qian, Y., Leung, L. R., and Zhang, Y.: Interpreting machine learning prediction of fire emissions and comparison with FireMIP process-based models, Atmos. Chem. Phys., 22, 3445–3468, https://doi.org/10.5194/acp-22-3445-2022, 2022.

Ward, D. S., Kloster, S., Mahowald, N. M., Rogers, B. M., Randerson, J. T., and Hess, P. G.: The changing radiative forcing of fires: global model estimates for past, present and future, Atmos. Chem. Phys., 12, 10857-10886, 10.5194/acp-12-10857-2012, 2012.

Weber, J., Archer-Nicholls, S., Abraham, N. L., Shin, Y. M., Griffiths, P., Grosvenor, D. P., Scott, C. E., and Archibald, A. T.: Chemistry-driven changes strongly influence climate forcing from vegetation emissions, Nat. Commun., 13, https://doi.org/10.1038/s41467-022-34944-9, 2022.

Weinzierl, B., Ansmann, A., Prospero, J., Althausen, D., Benker, N., Chouza, F., Dollner, M., Farrell, D., Fomba, W., Freudenthaler, V., Gasteiger, J., Groß, S., Haarig, M., Heinold, B., Kandler, K., Kristensen, T., Mayol-Bracero, O., Müller, T., Reitebuch, O., Sauer, D., Schäfler, A., Schepanski, K., Spanu, A., Tegen, I., Toledano, C., and Walser, A.: The Saharan Aerosol Long-range Transport and Aerosol-Cloud Interaction Experiment (SALTRACE): overview and selected highlights, B. Am. Meteorol. Soc., 98, 1427-1451, https://doi.org/10.1175/BAMS-D-15-00142.1, 2017.

Wendl, I. A., Eichler, A., Isaksson, E., Martma, T., and Schwikowski, M.: 800-year ice-core record of nitrogen deposition in Svalbard linked to ocean productivity and biogenic emissions, Atmos. Chem. Phys., 15, 7287–7300, https://doi.org/10.5194/acp-15-7287-2015, 2015.

Werner, M., Tegen, I., Harrison, S. P., Kohfeld, K. E., Prentice, I. C., Balkanski, Y., Rodhe, H., and Roelandt, C.: Seasonal and interannual variability of the mineral dust cycle under present and glacial climate conditions, J. Geophys. Res.-Atmos., 107, AAC 2-1, https://doi.org/10.1029/2002JD002365, 2002.

Wilkinson, M. D., Dumontier, M., Aalbersberg, Ij. J., Appleton, G., Axton, M., Baak, A., Blomberg, N., Boiten, J.-W., Da Silva Santos, L. B., Bourne, P. E., Bouwman, J., Brookes, A. J., Clark, T., Crosas, M., Dillo, I., Dumon, O., Edmunds, S., Evelo, C. T., Finkers, R., Gonzalez-Beltran, A., Gray, A. J. G., Groth, P., Goble, C., Grethe, J. S., Heringa, J., 'T Hoen, P. A. C., Hooft, R., Kuhn, T., Kok, R., Kok, J., Lusher, S. J., Martone, M. E., Mons, A., Packer, A. L., Persson, B., Rocca-Serra, P., Roos, M., Van Schaik, R., Sansone, S.-A., Schultes, E., Sengstag, T., Slater, T., Strawn, G., Swertz, M. A., Thompson, M., Van Der Lei, J., Van Mulligen, E., Velterop, J., Waagmeester, A., Wittenburg, P., Wolstencroft, K., Zhao, J., and Mons, B.: The FAIR Guiding Principles for scientific data management and stewardship, Sci. Data, 3, 160018, https://doi.org/10.1038/sdata.2016.18, 2016.

Williams, A. P., Abatzoglou, J. T., Gershunov, A., Guzman-Morales, J., Bishop, D. A., Balch, J. K., and Lettenmaier, D. P.: Observed Impacts of Anthropogenic Climate Change on Wildfire in California, Earth's Future, 7, 892-910, https://doi.org/10.1029/2019EF001210, 2019.

Wilson, R., Anchukaitis, K., Briffa, K. R., Buntgen, U., Cook, E., D'Arrigo, R., Davi, N., Esper, J., Frank, D., Gunnarson, B., Hegerl, G., Helama, S., Klesse, S., Krusic, P. J., Linderholm, H. W., Myglan, V., Osborn, T. J., Rydval, M., Schneider, L., Schurer, A., Wiles, G., Zhang, P., and Zorita, E.: Last millennium northern hemisphere summer temperatures from tree rings: Part I: The long term context, Quaternary Sci. Rev., 134, 1-18, https://doi.org/10.1016/j.quascirev.2015.12.005, 2016.

Winckler, G., Anderson, R. F., Fleisher, M. Q., McGee, D. and Mahowald, N.: Covariant glacial-interglacial dust fluxes in the Equatorial Pacific and Antarctica, Science, 320, 93-96, https://doi.org/10.1126/science.1150595, 2008.

Winckler, G., Anderson, R. F., and Schlosser, P.: Equatorial Pacific productivity and dust flux during the Mid-Pleistocene Climate Transition, Paleoceanography, 20, https://doi.org/10.1029/2005PA001177, 2005.

Formatted: Default Paragraph Font, Font color: Black

Formatted: Normal, Centered, Border: Top: (No border), Bottom: (No border), Left: (No border), Right: (No border), Between : (No border), Tab stops: 3.25", Centered + 6.5", Right, Position: Horizontal: Left, Relative to: Column, Vertical: In line, Relative to: Margin, Wrap Around

Formatted: Font color: Black

Wolff, E. W., Rankin, A. M., and Röthlisberger, R.: An ice core indicator of Antarctic sea ice production?, Geophys. Res. Lett., 30, https://doi.org/10.1029/2003GL018454, 2003.
Wolff, E. W., Burke, A., Crick, L., Doyle, E. A., Innes, H. M., Mahony, S. H., Rae, J. W. B., Severi, M., and Sparks, R. S. J.: Frequency of large volcanic eruptions over the past 200000 years, Clim. Past, 19, 23-33, https://doi.org/10.5194/cp-19-23-2023, 2023.
Wullenweber, N., Lange, A., Rozanov, A., and von Savigny, C.: On the phenomenon of the blue sun, Clim. Past, 17, 969-983, https://doi.org/10.5194/cp-17-969-2021, 2021.
Xi, X., Sokolik, I. N.: Quantifying the anthropogenic dust emission from agricultural land use and desiccation of the Aral Sea in Central Asia, J. Geophys. Res.-Atmos., 121, 12270-12281, https://doi.org/10.1002/2016JD025556, 2016.
Xie, R. C., and Marcantonio, F.: Deglacial dust provenance changes in the Eastern Equatorial Pacific and implications for ITCZ movement, Earth Planet. Sc. Lett., 317–318, 386–395, https://doi.org/10.1016/j.epsl.2011.11.014, 2012.
Xu, L., and Penner, J. E.: Global simulations of nitrate and ammonium aerosols and their radiative effects, Atmos. Chem. Phys., 12, 9479–9504, https://doi.org/10.5194/acp-12-9479-2012, 2012.
Yan, Y., Xu, X., Xin, X., Yang, G., Wang, X., Yan, R., and Chen, B.: Effect of vegetation coverage on aeolian dust accumulation in a semiarid steppe of northern China, Catena, 87, 351–356, https://doi.org/10.1016/j.catena.2011.07.002, 2011.
Yang, X., Frey, M. M., Rhodes, R. H., Norris, S. J., Brooks, I. M., Anderson, P. S., Nishimura, K., Jones, A. E., and Wolff, E. W.: Sea salt aerosol production via sublimating wind-blown saline snow particles over sea ice: Parameterizations and relevant microphysical mechanisms, Atmos. Chem. Phys., 19, 8407–8424, https://doi.org/10.5194/acp-19-8407-2019, 2019.
Yang, Z., and Ludlow, F.: Climatic and societal impacts of volcanic eruptions in the Western Han Dynasty (206 BCE–8 CE): a comparative study., Clim. Past, 21, 2061-2081, https://doi.org/10.5194/cp-21-2061-2025, 2025.
Yao, F., Livneh, B., Rajagopalan, B., Wang, J., Crétaux, J., Wada, Y., Berge-Nguyen, M.: Satellites reveal widespread decline in global lake water storage, Science, 380, 743-749, https://doi.org/10.1126/science.abo2812, 2023.
Yu, Y., and Ginoux, P.: Enhanced dust emission following large wildfires due to vegetation disturbance, Nat. Geoscie., 15, 878-884, https://doi.org/10.1038/s41561-022-01046-6, 2022.
Yu, P., Portmann, R. W., Peng, Y., Liu, C.-C., Zhu, Y., Asher, E., Bai, Z., Lu, Y., Bian, J., Mills, M., Schmidt, A., Rosenlof, K. H., and Toon, O. B.: Radiative Forcing From the 2014–2022 Volcanic and Wildfire Injections, Geophys. Res. Lett., 50, e2023GL103791, https://doi.org/10.1029/2023GL103791, 2023.
Zan, J., Maher, B. A., Fang, X., Stevens, T., Ning, W., Wu, F., Yang, Y., Kang, J., and Hu, Z.: Global Dust Impacts on Biogeochemical Cycles and Climate, Nature Reviews Earth and Environment, 6, 789–807, https://doi.org/10.1038/s43017-025-00734-2, 2025.
Zangrando, R., Zanella, V., Karroca, O., Barbaro, E., Kehrwald, N. M., Battistel, D., Morabito, E., Gambaro, A., and Barbante, C.: Dissolved organic matter in the deep TALDICE ice core: A nano-UPLC-nano-ESI-HRMS method, Sci. Total Environ., 700, https://doi.org/10.1016/j.scitotenv.2019.134432, 2020.
Zender, C. S., Bian, H., and Newman, D.: Mineral Dust Entrainment and Deposition (DEAD) model: Description and 1990s dust climatology, J. Geophys. Res.-Atmos., 108, 4416, https://doi.org/10.1029/2002JD002775, 2003.
Zennaro, P., Kehrwald, N., McConnell, J. R., Schüpbach, S., Maselli, O. J., Marlon, J., Vallelonga, P., Leuenberger, D., Zangrando, R., Spolaor, A., Borrotti, M., Barbaro, E., Gambaro, A., and Barbante, C.: Fire in ice: two millennia of boreal forest fire history from the Greenland NEEM ice core, Clim. Past, 10, 1905-1924, https://doi.org/10.5194/cp-10-1905-2014, 2014.
Zhang, B., and Liu, P.: Reconstructed Black Carbon Emissions from 1750 to 2010 using Ice Core Records and Inverse modeling (V1), Harvard Dataverse [dataset], https://doi.org/10.7910/DVN/KB0ESS, 2024.

Formatted: Default Paragraph Font, Font color: Black

Formatted: Normal, Centered, Border: Top: (No border), Bottom: (No border), Left: (No border), Right: (No border), Between : (No border), Tab stops: 3.25", Centered + 6.5", Right, Position: Horizontal: Left, Relative to: Column, Vertical: In line, Relative to: Margin, Wrap Around

Formatted: Font color: Black

Zhang, B., Chellman, N. J., Kaplan, J. O., Mickley, L. J., Ito, T., Wang, X., Wensman, S. M., McCrimmon, D., Steffensen, J. P., McConnell, J. R., and Liu, P.: Improved biomass burning emissions from, 1750 to 2010 using ice core records and inverse modeling, Nat. Commun., 15, 3651, https://doi.org/10.1038/s41467-024-47864-7, 2024.

Zhang, Y., Mahowald, N., Scanza, R. A., Journet, E., Desboeufs, K., Albani, S., Kok, J. F., Zhuang, G., Chen, Y., Cohen, D. D., Paytan, A., Patey, M. D., Achterberg, E. P., Engelbrecht, J. P., and Fomba, K. W.: Modeling the global emission, transport and deposition of trace elements associated with mineral dust, Biogeosciences, 12(19), https://doi.org/10.5194/bg-12-5771-2015, 2015.

Zhu, F., Emile-Geay, J., Hakim, G. J., King, J., and Anchukaitis, K. J.: Resolving the Differences in the Simulated and Reconstructed Temperature Response to Volcanism, Geophys. Res. Lett., 47, e2019GL086908, https://doi.org/10.1029/2019GL086908, 2020.

Zhuo, Z. H., Fuglestvedt, H. F., Toohey, M., and Krüger, K.: Initial atmospheric conditions control transport of volcanic volatiles, forcing and impacts, Atmos. Chem. Phys., 24, 6233-6249, https://doi.org/10.5194/acp-24-6233-2024, 2024.

Zoëga, T., Storelvmo, T., and Krüger, K.: Arctic warming from a high-latitude effusive volcanic eruption, Sci. Rep.-UK, 15, 14653, https://doi.org/10.1038/s41598-025-98811-5, 2025a.

Zoëga, T., Storelvmo, T., and Krüger, K.: Climate state dependent response to very large Icelandic effusive volcanic eruptions, Geophys. Res. Lett., 52, e2025GL114638, https://doi.org/10.1029/2025GL114638, 2025b.

Zuo, H., Tan, Z., Han, Y. M., Mao, L., Zheng, S., Zhang, Q., Wang, M., and Li, S.: Record of polycyclic aromatic hydrocarbons (PAHs) from prehistoric sediments and human activity in the Lubei plain of China, Sci. Rep.-UK, 15, 7347, https://doi.org/10.1038/s41598-025-91885-1, 2025.

Formatted: Default Paragraph Font, Font color: Black

Formatted: Normal, Centered, Border: Top: (No border), Bottom: (No border), Left: (No border), Right: (No border), Between : (No border), Tab stops: 3.25", Centered + 6.5", Right, Position: Horizontal: Left, Relative to: Column, Vertical: In line, Relative to: Margin, Wrap Around

Formatted: Font color: Black

Page 35: [1] Deleted **Natalie M. Mahowald** **11/17/26 1:35:00 PM**